UNIVERSITY OF CALIFORNIA, SAN DIEGO

Direct Measurements of Marine Aerosols to Examine the Influence of Biological Activity, Anthropogenic Emissions, and Secondary Processing on Particle Chemistry

A dissertation submitted in partial satisfaction of the requirements for the degree Doctor of Philosophy

in

Oceanography

by

Cassandra Jayne Gaston

Committee in Charge:

Professor Kimberly A. Prather, Chair
Professor Farooq Azam
Professor Brian P. Palenik
Professor Lynn M. Russell
Professor Mark H. Thiemens

2012

The dissertation of Cassandra Jayne Gaston is approved, and it is acceptable in quality and form for publication on microfilm and electronically:

Chair

University of California, San Diego

2012

Epigraph

What the results of these investigations will be the future will tell; but whatever they may be, and to whatever this principle may lead, I shall be sufficiently recompensed if later it will be admitted that I have contributed a share, however small, to the advancement of science.

Nikola Tesla

The atmosphere has no walls.

Kimberly Prather

Whether the scientists like it or not, the mark of science is the determinate of the world to come and scientists therefore have a special responsibility for the political consequences of their work. Whether the politicians like it or not, their decisions and actions will be far worse than futile if they do not take account of technological change, and this can only be done through understanding of the nature of scientific discovery and its applications.

Roger Revelle

There's a divinity that shapes our ends,
Rough-hew them how we will.

Hamlet, Act V, Scene II

Table of Contents

List of Figures

List of Tables

Acknowledgements

First, and foremost, I would like to acknowledge my thesis advisor Prof. Kim Prather. I first met Kim when I took her course in atmospheric chemistry while I was an undergraduate at UCSD. I remember thinking at the time that I admired her enthusiasm for science and her dedication to a field of science that is so crucial to our everyday lives. As a thesis advisor, Kim has provided me with a tremendous amount of support both in my professional as well as my personal life. I see Kim as my "academic mom" as she has provided me with encouragement every step of the way and has trusted me to take instruments out on several field studies, including a month-long shipboard study. As I have looked back at the numerous goals I had when I started my PhD. I have come to realize that Kim has given me the opportunity to fulfill all of these goals. I can't thank her enough for her belief in me and the opportunities that she has given me to fulfill my dreams. She has also inspired me to continue on in academia and hopefully pursue a faculty position. I hope that I continue to collaborate with her well-after my graduate studies have ended. I also must thank her husband Joe Mayer who has taught me so much about the history of the instruments, the practical aspects of the mass spectrometers we develop and use in the Prather lab, and who has taught me several machining skills that will no doubt be helpful beyond graduate school. I have thoroughly enjoyed my experiences working with both of them.

I would also like to acknowledge each of my committee members: Profs. Lynn Russell, Brian Palenik, Farooq Azam, and Mark Thiemens. I have had the pleasure of working with several of my committee members on several different sets of

measurements. Each of my committee members has provided me with advice that has helped strengthen the work contained within my thesis and several of them have also provided recommendations for me for fellowships and postdoctoral positions. I cannot thank them enough for their encouragement and hope to collaborate with each one of them in future projects. I have also had the pleasure of collaborating with Prof. Tim Bertram who has encouraged me to accept a postdoctoral position with Prof. Joel Thornton and expand my expertise of atmospheric chemistry. Prof. Bertram has been a source of guidance for me as I began to delve more into heterogeneous reactions in the ambient environment. Several collaborators also served as mentors for me during CalNex. Tim Bates and Trish Quinn at NOAA, PMEL provided me with a tremendous amount of guidance and support during the field campaign and have been fantastic to collaborate with on manuscripts. I must thank Tim for generously taking us to his winery prior to CalNex and giving us all a tasting, I plan to have a lot more Eight Bells wine in my future. Tim also put up with my constant requests to use the "sea sweep" during CalNex to characterize primary sea spray aerosol. I look forward to collaborating more with both of them, which will only be facilitated by the fact that I will be moving up to Seattle after my graduate work. Drew Hamilton was also a fantastic person to get to know during CalNex. His endless tales of life at sea kept me constantly entertained during the cruise. I also got to learn a lot about sea spray aerosol from Bill Keene while on CalNex. Bill also provided me with a lot of advice and guidance on choosing a suitable postdoc and on applying for postdoc fellowships. I am also grateful to Chris Cappa for providing me with guidance after the CalNex cruise that aided in my analysis of this data set. I hope to collaborate with him on future projects.

I also must thank my academic family, the entire Prather group. It has been an absolute pleasure to get to know each and every single person that has joined this group. None of the accomplishments that are made both in the lab and field would be possible if we all didn't work together and help each other; I am truly grateful for all of the help they have provided me. I first have to acknowledge Hiroshi Furutani, who shared a strong passion for marine aerosols as well. Working with him and bouncing ideas off of him during my first year was an incredibly rewarding experience that set the stage for the rest of my experience in the Prather group. I am very grateful to his words of encouragement that only Hiroshi could bestow such as "You can do it!", "Are you serious?", and "You gonna do it" when I thought something wasn't possible. I have continued to collaborate with him on several projects including those discussed in this dissertation. I hope to continue those collaborations and am so happy for him and his family. Andy Ault and Kerri Pratt were both incredible to work with and to learn from. Kerri taught me how to analyze data, operate SLY, helped me with my first paper, and instilled confidence in my capabilities. Kerri and I have also formed a strong friendship that I hope will continue to grow over the years. She has been a real inspiration and I have no doubt that she will have an incredibly successful career. Andy taught me how to operate and tune the instruments, how to use the mobile lab, and took me on my first two field studies. It has been a true pleasure to have someone like Andy as a friend that I can talk to about life and that I can also bounce ideas off of. Our mutual interest in all things marine will no doubt lead to further collaborations that I look forward to in the future. Lindsay Hatch has been an incredible friend to me during our time in graduate school. Lindsay has helped edit almost all of my chapters and for that I am truly grateful. She has also been a

great friend and constantly keeps me laughing with her quick wit. Liz Fitzgerald, aka Liz Nelson, has been an absolute pleasure to work with. She has helped keep my balanced during my most stressful points in grad school. I have worked on several field campaigns with Melanie Zauscher and have been inspired by her incredible work ethic. Melanie also has an incredibly generous heart and it has been a true pleasure to get to know her. Jessie Creamean and I have worked extremely well together. Jessie has been a great friend who never fails to amuse me and has also been a great workout buddy. Doug "Plushenko" Collins is extremely focused, was wonderful to take out on a field campaign out on the SIO Pier, and is apparently quite the ice skater. I also had the pleasure of taking Jack Cahill on his first field study as well. Jack is a great meat 'n potatoes kind of guy who never fails to amuse me with his Fred Flintstone style meals. I have also learned a lot of Matlab and data analysis tricks from Jack. Kaitlyn Suski is another graduate student that I had the pleasure of mentoring when she first joined the group. Kaitlyn is a hard and dedicated worker who will no doubt have a successful graduate career. Alberto Cazorla is a postdoc in our lab who has taught me a lot about Matlab, programming, and new analysis tools to better process and understand our data sets. I thoroughly enjoy Alberto's personality and am impressed by his work ethic. Luis Cuadra-Rodriguiez is also a new postdoc in our lab. Luis gives hard working a new definition and is always willing to go above and beyond to get things done. Luis is also a great friend and an overall good person. I know he will be extremely successful in anything he does. Tim Guasco is also another postdoc that I have had the pleasure of interacting with. His unique personality and vast expertise makes him one of my favorite people to interact with in the lab. I will never tire of his PBR hat that is a staple of his daily wardrobe. I

have also had the pleasure of interacting with other new members of the group including Matt Ruppel, Defeng Zhao, Camille Sultana, and Chris Lee. I wish them all luck in their future endeavors. In addition to the Prather lab, I would also like to thank the staff at Scripps. Christian McDonald is in charge of the SIO Pier and has constantly put trust in me to utilize it as a sampling platform for several of the projects detailed. Josh Reeves, Becky Burrola, and Denise Darling are graduate student coordinators and staff that have all made my life in graduate school much easier. They have provided me with a lot of help and support during my time in grad school.

Finally, I have to thank my friends and family. My parents Chip and Judy have always been supportive of my decisions and dreams. As a kid, I was sick with rheumatoid arthritis; however, my parents did their absolute best to take care of me and to make sure that I led as normal of a life as I could. At one point, they were faced with a decision to have several of my joints replaced which would have made me bound to a wheelchair for the rest of my life. Instead, they choose to put faith into physical therapy and other medicinal therapies that turned out to be very successful. Their decisions have shaped my life for the best, and I will always be grateful for all of the sacrifices they have made in order to give me the best life possible. I know they will be extremely proud to have a doctor in the family. My sister Jaki has also been extremely loving, kind, and is probably the funniest person that I have ever met. She has always given me the push that I need to make good decisions throughout my life. Finally, I have to thank my husband, Oscar Guerrero. Oscar has always supported my dreams and decisions. He has provided me with the love and support that I have needed to complete my graduate studies. He

also constantly tells me how proud he is of me. I feel extremely blessed to have met such a wonderful person and look forward to what the rest of our future holds for us.

Chapter 2 is reproduced with permission from the American Geophysical Union: Gaston, C.J., Furutani, H., Guazzotti, S.A., Coffee, K.R., Bates, T.S., Quinn, P.K., Aluwihare, L.I., Mitchell, B.G., Prather, K.A. Unique ocean-derived particles serve as a proxy for changes in ocean chemistry. *Journal of Geophysical Research-[Atmospheres]*. 2011, 116, D18310, doi:10.1029/2010JD015289. Copyright 2011, American Geophysical Union. The dissertation author was the primary investigator and author of this paper.

Chapter 3 is in preparation for submission to *Proceedings of the National Academy of Sciences*: Gaston, C.J., Furutani, H., Guazzotti, S.A., Coffee, K.R., Bates, T.S., Quinn, P.K., Jung, J., Uematsu, M, Prather, K.A. Direct ejection of particle phase sulfur species from the ocean to the atmosphere. The dissertation author was the primary investigator and author of this paper.

Chapter 4 is in preparation for submission to *Environmental Science & Technology*: Gaston, C.J., Furutani, H., Charrier, J.G., Palenik, B.P., Aluwihare, L.I., Prather, K.A. The effect of biological activity on the single-particle chemistry of sea spray aerosols generated by bubble bursting natural and artificial seawater solutions. The dissertation author was the primary investigator and author of this paper.

Chapter 5 is in preparation for submission to *Journal of Geophysical Research*: Gaston, C.J., Quinn, P.K., Bates, T.S., Prather, K.A. The impact of shipping,

agricultural, and urban emissions on single particle chemistry observed aboard the R/V Atlantis during CalNex. The dissertation author was the primary investigator and author of this paper.

Chapter 6 is in preparation for submission to *Environmental Science & Technology*: Gaston, C.J., Ault, A.P., Zauscher, M.D., Furutani, H., Cahill, J.F., Collins, D.B., Suski, K.J., Prather, K.A. Changes in the single-particle composition of ship emissions in California: Impact of stricter regulations on shipping emissions. The dissertation author was the primary investigator and author of this paper.

Chapter 7 is reproduced with permission from the American Chemical Society: Gaston, C.J., Pratt, K.A., Qin, X., Prather, K.A. Real-time detection and mixing state of methanesulfonate in single particles at an inland urban location during a phytoplankton bloom. *Environmental Science & Technology*. 2010, 44, 1566-1572. Copyright 2010, American Chemical Society. The dissertation author was the primary investigator and author of this paper.

Vita

2005	B.S. in Biology, University of California, San Diego
2005	B.A. in Environmental Chemistry, University of California, San Diego
2003-2004	Teaching Assistant, Department of Biology, University of California, San Diego
2006-2012	Graduate Student Assistant, Scripps Institution of Oceanography, University of California, San Diego
2012	Ph.D. in Oceanography, University of California, San Diego

Publications

Zauscher, M.D., Y. Wang, M.J.K. Moore, **C.J. Gaston**, K.A. Prather. The mixing state and aging of biomass burning aerosols during the 2007 San Diego wildfires. 2012, In preparation.

Creamean, J.M., K.A. Pratt, A.P. Ault, X. Qin, **C.J. Gaston**, K.A. Prather. Inter-annual comparison of ambient, single-particle mixing state in Riverside, CA. 2012, In preparation.

Gaston, C.J., T.P. Riedel, J.A. Thornton, T.H. Bertram, N. Wagner, S.S. Brown, E. Williams, P.K. Quinn, T.S. Bates, K.A. Prather. Real-time observations of heterogeneous chemistry on ambient individual sea spray particles aboard the R/V Atlantis during CalNex. 2012, In preparation.

Gaston, C.J., A.P. Ault, M.D. Zauscher, H. Furutani, J.F. Cahill, D.B. Collins, K.J. Suski, K.A. Prather. Changes in the single-particle composition of ship emissions in California: Impact of stricter regulations on shipping emissions. 2012, In preparation.

Gaston, C.J., H. Furutani, J.G. Charrier, B.P. Palenik, L.I. Aluwihare, K.A. Prather. The effect of biological activity on the single-particle chemistry of sea spray aerosols generated by bubble bursting natural and artificial seawater solutions. 2012, In preparation.

Gaston, C.J., P.K. Quinn, T.S. Bates, K.A. Prather. The impact of shipping, agricultural, and urban emissions on single particle chemistry observed aboard the R/V Atlantis during CalNex**.** 2012, In preparation.

Gaston, C.J., H. Furutani, S.A. Guazzotti, K.R. Coffee, T.S. Bates, P.K. Quinn, J. Jung, M. Uematsu, K.A. Prather. Direct ejection of particle phase sulfur species from the ocean to the atmosphere. 2012, In preparation.

Cappa, C.D., T. Onasch, P. Massoli, T.S. Bates, **C.J. Gaston**, J. Hakala, K. Hayden, K.R. Kolesar, D. Mellon, S.-M. Li, I. Nuaaman, K. Prather, P.K. Quinn, C. Song, R. Subramanian, A. Vlasenko, D. Worsnop, R. Zaveri. On the magnitude of absorption enhancements due to mixing state of black carbon. 2012, Submitted to *Science*.

Riedel, T.P., T.H. Bertram, O.S. Ryder, S. Liu, D.A. Day, L.M. Russell, **C.J. Gaston**, K.A. Prather, J.A. Thornton. Direct N_2O_5 Reactivity Measurements at a Polluted Coastal Site. *Atmos. Chem. Phys. Discuss.*, 2011. 11: 31911-31935.

Gaston, C.J., H. Furutani, S.A. Guazzotti, K.R. Coffee, T.S. Bates, P.K. Quinn, L.I. Aluwihare, B.G. Mitchell, K.A. Prather. Unique ocean-derived particles serve as a proxy for changes in ocean chemistry. *Journal of Geophysical Research-[Atmospheres]*. 2011. 116 (D18310): doi: 10.1029/2010JD015289.

Ault, A.P., C.R. Williams, A.B. White, P.J. Neiman, J.M. Creamean, **C.J. Gaston**, F.M. Ralph, K.A. Prather. Detection of Asian dust in California orographic precipitation. *Journal of Geophysical Research-[Atmospheres]*. 2011. 116 (D16205): doi:10.1029/2010JD015351.

Urbano, R., B. Palenik, **C.J. Gaston,** K.A. Prather. Detection and phylogenetic analysis of coastal bioaerosols using culture dependent and independent techniques. *Biogeosciences*. 2010. 8: 301-309.

Pratt, K.A., C.H. Twohy, S.M. Murphy, R.C. Moffett, A.J. Heymsfield, **C.J. Gaston**, P.J. DeMott, P.R. Field, T.R. Henn, D.C. Rogers, M.K. Gilles, J.H. Seinfeld, K.A. Prather. Observation of playa salts as nuclei in orographic wave clouds. *Journal of Geophysical Research-[Atmospheres]*. 2010. 115 (D15301): doi:10.1029/2009JD013606.

Ault, A.P., **C.J. Gaston**, Y. Wang, G. Dominguez, M.H. Thiemens, K.A. Prather. Characterization of the single particle mixing state of individual ship plume events measured at the Port of Los Angeles. *Environmental Science & Technology*. 2010. 44(6): 1954-1961.

Gaston, C.J., K.A. Pratt, X. Qin, K.A. Prather. Real-time detection and mixing state of methanesulfonate in single particles at an inland urban location during a phytoplankton bloom. *Environmental Science & Technology*. 2010. 44(6): 1566-1572.

Fields of Study

Major Field: Oceanography

Studies in Atmospheric Chemistry
Professor Kimberly A. Prather

ABSTRACT OF THE DISSERTATION

Direct Measurements of Marine Aerosols to Examine the Influence of Biological Activity, Anthropogenic Emissions, and Secondary Processing on Particle Chemistry

by

Cassandra Jayne Gaston

Doctor of Philosophy in Oceanography

University of California, San Diego, 2012

Professor Kimberly A. Prather, Chair

Aerosols influence global climate directly by scattering and absorbing incoming solar radiation and indirectly by initiating cloud droplet and ice crystal formation; both particle size and chemical composition play a role in these impacts. Particle size and composition constantly evolve due to atmospheric processing. The physicochemical properties of marine aerosols, including sea spray and anthropogenic emissions, are of particular interest since oceans cover over 70% of the Earth's surface. This dissertation aims to probe the role of oceanic biological activity, anthropogenic emissions, and subsequent atmospheric processing on marine particle chemistry by measuring the size-resolved chemistry of individual ambient marine aerosols and laboratory-generated particles using aerosol time-of-flight mass spectrometry (ATOFMS).

The impact of biological activity on the mixing-state of sea spray particles was examined by adding biologically-derived organic material and/or phytoplankton cells to seawater then generating particles through bubble bursting. Unique particles characterized by organics, Mg^{2+} and/or Ca^{2+} were detected during these experiments as well as in the ambient atmosphere during periods of elevated biological activity. Additionally, elemental sulfur ions were also detected in ambient marine particles in regions of elevated biological activity at night. These particles were successfully reproduced from bubble bursting experiments suggesting that these particles are directly ejected from the ocean.

In addition to sea spray aerosol, the particle chemistry of marine aerosols from anthropogenic sources was also examined during shipboard measurements made during CalNex along the California coast. Soot was dominant in Southern California while organics characterized the particle chemistry in the Sacramento area highlighting regional differences in anthropogenic emissions in California. Further, measurements made at the Port of Los Angeles and those made on the Scripps Pier showed a decline in emissions from ships combusting residual fuel compared to earlier measurements; these results are in compliance with recent regulations requiring ships to combust low sulfur fuel when approaching the California coast. Finally, during the Study of Organic Aerosols in Riverside, CA (SOAR), the dimethyl sulfide (DMS) oxidation product methanesulfonic acid (MSA) was detected in anthropogenic particle types, and was elevated in vanadium-containing emissions characteristic of residual fuel combustion suggesting that

anthropogenic particles can enhance the atmospheric processing of marine biogenic emissions.

Chapter 1

1. Introduction

1.1 Importance of Atmospheric Aerosols

Defined as a solid or liquid suspended in a gas, atmospheric aerosols contribute to air pollution, adverse effects on human health, and global climate change [*Gauderman et al.*, 2000; *Pope and Dockery*, 2006; *Poschl*, 2005]. Particles also scatter and absorb solar and terrestrial radiation contributing to the aerosol direct effect [*Forster et al.*, 2007; *Poschl*, 2005], and further serve as nuclei for the formation of cloud droplets and ice crystals constituting the aerosol indirect effect [*Forster et al.*, 2007; *Kohler*, 1936; *Lohmann and Feichter*, 2005; *Poschl*, 2005]. In addition to microphysical effects, aerosols also play a role in altering the lifetime [*Albrecht*, 1989] and radiative properties of clouds [*Twomey*, 1977] in addition to altering precipitation frequency and intensity [*Rosenfeld et al.*, 2008]. The radiative impact of aerosols on global climate is uncertain and represents the greatest challenge in our ability to accurately forecast future temperature rises due to climate change [*Forster et al.*, 2007], highlighting the need for additional studies probing the physicochemical properties of aerosols and their impacts on human health and climate.

Two key properties that shape the lifetime, as well as the health and climatic impacts, of aerosols are particle size and chemical composition. Depending on these properties, aerosol lifetime in the atmosphere is anywhere from seconds to up to about a month [*Raes et al.*, 2000]. Particles are emitted from natural sources (e.g. biogenic emissions and the ocean) and anthropogenic sources (e.g. emissions from cars and ships).

Particle size spans several orders of magnitude from several nanometers up to 10 μm [*Poschl*, 2005; *Seinfeld and Pandis*, 2006]; the size of aerosols depends on the particle formation mechanism, source, and interactions in the atmosphere. Particles nucleated from the clustering of gas molecules are found in the smallest size range known as the nucleation mode (> 10 nm in size), particles emitted from anthropogenic sources are typically submicron (< 1 μm) encompassing the Aitken size mode (~10-100 nm) and part of the accumulation mode (~100 nm-2 μm) while particles originating from mechanical processes such as the ejection of sea salt from the ocean are typically supermicron (> 1 μm) encompassing part of the accumulation mode and the coarse mode (~2 μm to several μm) [*Noble and Prather*, 1996; *Poschl*, 2005; *Seinfeld and Pandis*, 2006]. The chemical composition is also dependent on the source of the particles and is highly complex including inorganic components (e.g. ammonium, sulfate, nitrate, metals, minerals found in dust particles, and sea salts found in sea spray, etc.) and organic constituents (e.g. carboxylic acids, humic substances, aromatics, alkanes, alkenes, amines, polysaccharides, etc.) [*Jacobson et al.*, 2000; *Murphy et al.*, 2006; *Noble and Prather*, 1996; *Russell et al.*, 2011; *Silva and Prather*, 2000]. Despite insights from laboratory and ambient measurements and recent advances in measurement techniques, much remains unknown about the chemical composition of aerosols particularly regarding the composition of the organic component of aerosols and the chemical mixing-state of aerosols (e.g. whether chemical components are associated with a single particle, which is known as an internal mixture, or whether different components are found on different aerosol particles, which is known as an external mixture). Knowledge of the chemical mixing-state is important because mixing-state affects the water uptake, heterogeneous reactivity, and cloud

nucleating properties of single aerosol particles [*Poschl*, 2005]. In addition to understanding the physicochemical properties of particles directly emitted from different sources, also known as primary aerosols, it is important to also note that particle size and composition evolve over time due to secondary processes, which are processes that occur in the atmosphere subsequent to emission; secondary processes include gas-particle partitioning, heterogeneous reactions, aqueous phase processing, etc. [*Poschl*, 2005].

In terms of health impacts, smaller particles, particularly ultrafine particles (< 0.1 μm), have more severe health effects due to their ability to penetrate deeper into the respiratory system [*Bernstein et al.*, 2004; *Gauderman et al.*, 2000; *Pope and Dockery*, 2006]. Chemical composition further influences aerosol toxicity, for example, the presence of transition metals and polycyclic aromatic hydrocarbons (PAHs) in particles contributes greatly to their toxicity [*Bernstein et al.*, 2004; *Campen et al.*, 2001; *Fang et al.*, 2008; *Pinkerton et al.*, 2004; *Pope and Dockery*, 2006; *Sunderman*, 2001]. Particle size and chemical composition also influence both the aerosol direct and indirect effects. Particle size affects aerosol optical properties since light scattering efficiency is greatest for particle diameters of the same order of magnitude as solar and terrestrial radiation wavelengths [*Poschl*, 2005; *Quinn et al.*, 2005]; further, smaller particles are also less efficient as cloud nuclei [*Lohmann and Feichter*, 2005; *McFiggans et al.*, 2006; *Poschl*, 2005; *Quinn et al.*, 2008]. Aerosol mixing-state also impacts the aerosol direct effect, particularly for black carbon (soot) and other carbonaceous aerosol. Models and measurements have shown that soot internally mixed with secondary species such as organic carbon, sulfate, and nitrate has a greater warming potential than freshly emitted

soot containing no secondary species [*Jacobson*, 2000; *Moffet and Prather*, 2009; *Schnaiter et al.*, 2005]. In addition to soot, the role of organics in influencing the aerosol direct effect has recently become of great interest. Higher mass concentrations of non-refractory organic aerosol have been associated with less water uptake and reduced scattering of solar radiation [*Massoli et al.*, 2009; *Quinn et al.*, 2005]; however, the extent of this effect depends on whether the organic material is oxidized or more hydrocarbon-like [*Massoli et al.*, 2009; *Saxena et al.*, 1995]. Particle chemistry also influences the cloud forming potential of aerosols. For example, high mass fractions of hydrocarbon-like organics, which are highly water insoluble, have been shown to decrease the ability of particles to act as nuclei for cloud droplets [*Quinn et al.*, 2008]; however, the addition of small amounts of soluble material, such as sulfate, to particles that are water insoluble has been found to greatly increase the cloud forming potential of aerosols [*Roberts et al.*, 2002]. In sum, particle size and composition play crucial roles in determining their health impacts and in shaping aerosol-cloud interactions, which represents the greatest challenge in our ability to accurately forecast future temperature rises due to climate change [*Forster et al.*, 2007].

1.2 Measurement Techniques Used to Characterize Aerosols

Aerosol particles span several orders of magnitude, are composed of complex mixtures containing ~10^2-10^{15} molecules per particle, and are constantly evolving in time due to atmospheric processing [*Finlayson-Pitts and Pitts*, 2000; *Pratt and Prather*, 2011a]. As such, analyzing the physicochemical properties of atmospheric aerosols represents a significant challenge; several reviews have recently been published pointing

out these challenges while highlighting several techniques currently used to address these challenges [*Hoffmann et al.*, 2011; *McMurray*, 2000; *Pratt and Prather*, 2011a; *Pratt and Prather*, 2011b; *Sullivan and Prather*, 2005]. The on-line technique that is the focus of the measurements included in this dissertation is the aerosol time-of-flight mass spectrometer (ATOFMS).

1.2.1 Real-Time Measurements of Size-Resolved Composition

The ATOFMS makes real-time measurements of the aerodynamic size and chemical composition of individual particles between 0.2-3 μm aerodynamic diameter [*Gard et al.*, 1997; *Prather et al.*, 1994]. A schematic of the ATOFMS is shown in Figure 1.1. The ATOFMS operates by sampling particles at atmospheric pressure through a converging nozzle inlet where they enter a differentially pumped vacuum region; the pressure drop causes the particles to be accelerated to a size-dependent terminal velocity. Each particle passes through two continuous wave lasers (532 nm) separated by a known distance producing scattered light signals, which are detected by two photomultiplier tube detectors. The time required to traverse these two lasers is correlated to the terminal velocity of the particle; the velocity is converted to an aerodynamic diameter by calibrating with polystyrene latex spheres (PSLs) of a known size. The transit time and light signals are also used to trigger a third pulsed laser passing through the ion source region of a time-of-flight mass spectrometer. When each sized particle arrives in the ion source region, a pulsed UV laser fires to induce laser desorption/ionization, producing positive and negative ion mass spectra for each particle. The resulting positive and negative ions are analyzed by a dual-polarity time-

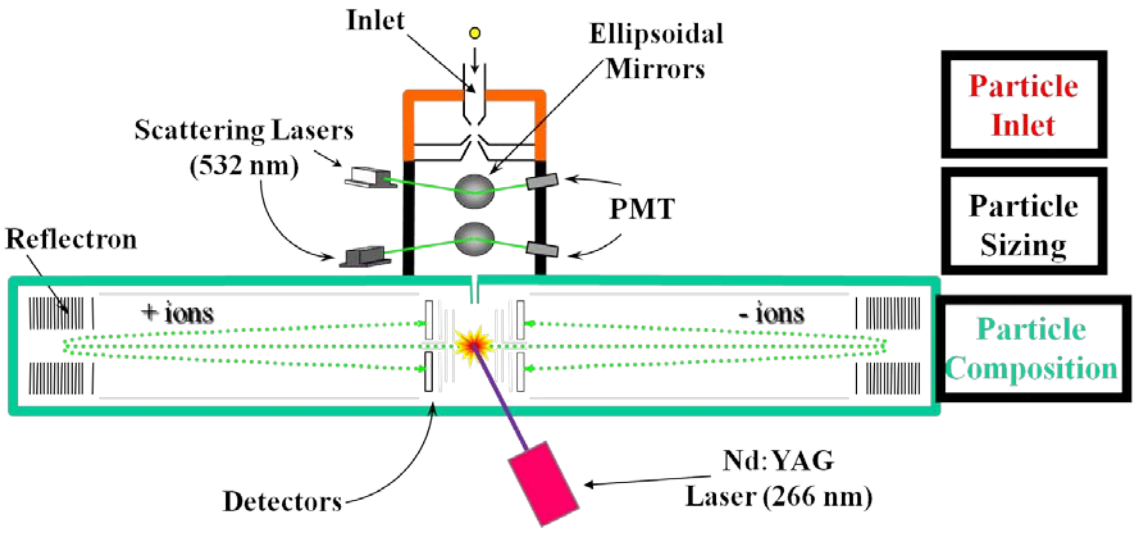

Figure 1.1: Schematic of the nozzle inlet ATOFMS adapted from *Gard et al.*, 1997.

of-flight mass spectrometer. The mass spectra show the chemical associations within each particle and can be coupled with the size information to derive size-resolved composition distributions of particles. Positive ion spectra provide insight into particle source (e.g. sea salt vs. ship emissions, etc) while negative ion particle age (e.g. reacted versus fresh sea salt) [*Fergenson et al.*, 2001; *Gard et al.*, 1998; *Guazzotti et al.*, 2001; *Song et al.*, 1999] including the acquisition of secondary species acquired during atmospheric processing, such as sulfates and nitrates.

The single particle mass spectra generated by this technique are imported into Matlab using a software toolkit [*Allen*, 2002], and an adaptive neural network (ART-2a) is used to group particles based on the mass spectral peaks and intensities into distinct "clusters" indicative of particle sources and chemistry [*Fergenson et al.*, 2001; *Song et al.*, 1999]. Typically the top 50 clusters are representative of ~80-90% of the particle population. Submicron (0.2-1.0 μm) and supermicron (1.0-3.0 μm) particles are typically analyzed separately because previous ATOFMS studies have demonstrated that the largest differences in chemical composition occur at 1 μm [*Noble and Prather*, 1996] and separate analysis allows more subtle distinctions to be observed. In addition to characterizing particle types, the temporal and size profiles of individual chemical species can be probed by selecting a threshold value for a specific ion peak area for the chemical species selected. This has been done to probe temporal trends and mixing-states of compounds such as oxalic acid [*Sullivan and Prather*, 2007]. For the work shown in this dissertation, ATOFMS measurements of marine aerosols from both laboratory experiments and ambient measurements are presented.

1.3 Marine Aerosols

Marine aerosols are of great interest because oceans cover over 70% of the Earth's surface, hence, understanding the physicochemical properties of marine aerosols and the transformations they undergo during secondary processing is essential for reducing the uncertainty regarding the impact of aerosols on climate [*Forster et al.*, 2007; *Raes et al.*, 2000]. The oceans are globally one of the largest sources of natural aerosols with estimates of sea salt mass fluxes on the order of ~10^{16} g/yr; however, the overall number flux is quite low [*O'Dowd and De Leeuw*, 2007; *Raes et al.*, 2000]. Clouds in marine environments have a tremendous global impact on climate, particularly in the subtropics, where the marine stratocumulus deck has been estimated to provide more radiative cooling than the radiative forcing associated with a double of $CO_{2(g)}$ [*Stevens et al.*, 2003]. Another reason for the great interest in marine aerosols is that marine environments are characterized by low number concentrations of background particles, typically 300-600 particles/cm^3 [*Fitzgerald*, 1991; *O'Dowd and De Leeuw*, 2007; *O'Dowd et al.*, 1997], making them extremely sensitive to perturbations in aerosol number concentrations [*Slingo*, 1990]. Perturbations to background marine conditions typically lead to increases in aerosol number concentrations causing increases in cloud droplet number concentrations (CDNC), which altered the cloud microphysics of marine stratocumulus clouds resulting in increased cloud optical thickness, decreased cloud effective radius, increased cloud lifetime, and potentially suppress the formation of precipitation [*Albrecht*, 1989; *Baker*, 1997; *Hobbs et al.*, 2000; *Hudson et al.*, 2000; *Russell et al.*, 1999; *Twohy et al.*, 2005; *Twomey*, 1977]. Further, oceans represent a dark

surface with a low albedo, hence, even subtle changes in cloud microphysics over the oceans can have a large impact on the aerosol indirect effect [*Baker*, 1997; *Slingo*, 1990]. The following sections will detail the physicochemical properties of marine aerosols, which are comprised of both natural sea spray aerosol, consisting of sea salt and biologically-produced organic material, in addition to anthropogenic emissions.

1.4 Characteristics of Natural Sea Spray Aerosol

1.4.1 Production Mechanism

Sea spray particles are directly emitted to the atmosphere primarily from air bubbles formed by breaking waves [*O'Dowd and De Leeuw*, 2007]. Bursting bubbles form jet drops, which result from the breakup of the vertical jet of water that forms after the bubble cavity collapses, and the more numerous film drops, which result from the collapse of the thin film surrounding the bubble [*Blanchard and Woodcock*, 1957; *Cipriano and Blanchard*, 1981; *Clarke et al.*, 2006]. Wind speed plays a key role in the production mechanism by enhancing jet drop formation for wind speeds > 5m/s [*Leck et al.*, 2002]. Enhanced wind speeds also increase whitecap production [*Monahan et al.*, 1983] resulting in the increased production of sea spray aerosol. The chemical composition of sea spray is proposed to depend on the distribution of jet and film drops; sea salt, primarily NaCl, is thought to result primarily from jet drops while film drops are thought to produce particles significantly enriched in organic material [*Cipriano and Blanchard*, 1981; *Leck et al.*, 2002]. This is because the bubble surface is thought to act as a hydrophobic interface that scavenges surface active material including organic

matter and marine organisms causing them to adsorb to the bubble surface and become incorporated into sea spray aerosol upon the collapse of the bubble [*Blanchard*, 1964; *Blanchard*, 1989; *Blanchard and Syzdek*, 1970; *Blanchard and Syzdek*, 1972; *Tseng et al.*, 1992]. The proposed differences in sea spray composition based on the formation of jet and film droplets highlights the need for laboratory studies to accurately reproduce the formation mechanism of sea spray in order for comparisons to ambient sea spray aerosol to be made. Recent laboratory measurements have shown that bubble bursting and plunging jets are superior aerosol generation techniques for accurately reproducing the physicochemical properties of sea spray aerosol compared to atomization, which has been frequently used in previous experiments to generate sea spray aerosol. These two techniques are more suitable for producing sea spray aerosol because these techniques scavenge organic material unlike the atomization technique [*Fuentes et al.*, 2010a; *Wise et al.*, 2009]. Further work is being done to develop and improve upon current sea spray aerosol generation techniques in order to accurately reproduce sea spray aerosols.

1.4.2 Size Distributions of Sea Spray Aerosol

Size distribution measurements of primary sea spray aerosol have recently been made during bubble bursting and plunging jet experiments. Overall, these laboratory-generated size distributions are dominated by a large mode in number concentration at ~80-100 nm; some laboratory experiments have also shown other minor size modes including a small Aitken mode peaking at ~45 nm, which is thought to predominately contain organic material, and a mode at ~300 nm that is thought to result from wind shear at the air-sea interface, which forces rising bubbles to shatter at the interface [*Fuentes et*

al., 2010b; *Martensson et al.*, 2003; *O'Dowd and De Leeuw*, 2007; *Sellegri et al.*, 2006; *Tyree et al.*, 2007]. Particle number size distributions also extend out to the coarse mode, where most of the sea salt mass resides. In the ambient marine atmosphere, similar number size distributions are also observed; however, these distributions undergo a shift to a bimodal number size distribution with a distinct minimum, known as the Hoppel minimum, at ~100 nm due to the activation and subsequent cloud processing of particles at this particle size [*Hoppel et al.*, 1990]. This is not observed in laboratory experiments, which probe the size distributions of freshly produced sea spray aerosol. In addition to primary sea spray aerosol produced from bubble bursting, ambient studies have also detected nucleation mode particles that have coincided with elevated biological activity in the ocean, changes in season, changes in tidal flux, and the evaporation of fog [*Leck and Bigg*, 1999; *Leck and Bigg*, 2010; *Meskhidze and Nenes*, 2006; *O'Dowd et al.*, 1998; *Wiedensohler et al.*, 1996]. The proposed composition of these particles as well as the role of biological activity in determining sea spray aerosol composition is discussed below.

1.4.3 Chemical Composition of Sea Spray Aerosol: The Effect of Biological Activity

Biological activity has been proposed to influence the chemical composition of sea spray aerosols through both primary and secondary emissions. These emissions can lead to changes in the physicochemical properties and, more importantly, the number concentrations of marine aerosols, potentially altering the radiative properties of clouds in the marine environment. However, linking changes in oceanic biological activity to changes in the atmosphere has been challenging, particularly for ambient measurements.

Probably the most common tracer of biological activity used is chlorophyll *a*, which is a proxy for phytoplankton biomass. Several studies have noted trends between chlorophyll-*a* concentrations, cloud microphysics, and aerosol optical depth [*Cropp et al.*, 2005; *Kruger and Grabl*, 2011; *Meskhidze and Nenes*, 2006; *Sorooshian et al.*, 2009]; however, many of these links have been difficult to make due to contributions from anthropogenic emissions. Another challenge stems from attempts to compare chlorophyll *a* concentrations with dimethyl sulfide (DMS), a gas formed from the enzymatic cleavage of phytoplankton-derived dimethylsulfoniopropionate (DMSP) thought to play a key role in shaping the physicochemical properties of sea spray aerosol and, potentially, CDNC in the marine environment, as discussed below [*Bates et al.*, 1992; *Charlson et al.*, 1987]. Difficulties with this comparison arise from the fact that the production of DMS is highly species specific [*Keller et al.*, 1989], and DMS is subjected to complex biological and ecological processes [*Bates et al.*, 1994; *Leck et al.*, 1990]; as such, DMS can be poorly correlated with total phytoplankton biomass (e.g. chlorophyll *a* concentrations) [*Bates et al.*, 1989; *Bates et al.*, 1994; *Leck et al.*, 1990]. Despite these challenges, several field and laboratory studies have provided compelling evidence that ocean biota directly and indirectly impact both the physicochemical properties of sea spray aerosols in addition to cloud formation and microphysics in the marine environment.

The first marine biogenic compound proposed to impact climate through the production of new particles is DMS [*Bates et al.*, 1992; *Charlson et al.*, 1987]. Once in the atmosphere, DMS is oxidized primarily via OH radicals to form sulfur-containing compounds (e.g. sulfuric acid, methanesulfonic acid, etc) [*Andreae*, 1990; *Andreae and*

Crutzen, 1997; *Ayers and Gillett*, 2000; *Barnes et al.*, 2006; *Bates et al.*, 1994; *Bates et al.*, 1992; *Charlson et al.*, 1987; *Hopkins et al.*, 2008; *Ooki et al.*, 2003]. Organosulfur compounds such as methanesulfonic acid (MSA) and sulfuric acid partition onto pre-existing compounds [*Barnes et al.*, 2006; *Hopkins et al.*, 2008]. Sulfuric acid can also undergo homogeneous binary nucleation with water vapor to form new particles that could then grow to sizes large enough to act as CCN potentially providing a direct link between marine biological activity, the radiative properties of clouds, and climate [*Andreae*, 1990; *Barnes et al.*, 2006; *Bates et al.*, 1994; *Charlson et al.*, 1987; *Hopkins et al.*, 2008; *Ooki et al.*, 2003]. Several observations of new particle formation from sulfuric acid derived from DMS have been made [*Clarke et al.*, 1998; *Ferek et al.*, 1995; *Weber et al.*, 1995]. However, binary nucleation from DMS-derived sulfuric acid has only been found to occur during suitable conditions, such as when aerosol surface area is incredibly low to limit condensational losses of sulfuric acid to particles or during humid conditions found at evaporating cloud edges and is thus, highly improbable under most conditions [*Clarke et al.*, 1999; *Pirjola et al.*, 2000]. It has been recently proposed that instead of participating in new particle formation, DMS oxidation products influence clouds and climate in the marine environment by condensing onto primary sea spray aerosol and newly formed particles from other sources causing these particles to grow into sizes able to activate into cloud droplets [*Leck and Bigg*, 2005b; *Leck and Bigg*, 2007; *O'Dowd et al.*, 2004; *Quinn and Bates*, 2011]. Another recently proposed source for the nucleation of new particles is the oxidation of biogenically-produced iodine gas ($I_{2(g)}$); however, this process has been found to be limited to coastal environments and cannot explain new particle formation in open ocean environments [*O'Dowd et al.*, 1998;

O'Dowd and Hoffmann, 2005]. Recent evidence has suggested that newly formed particles associated with biological activity could result from an increased number flux of particles from a primary ocean source rather than from nucleation of new particles from gas-phase compounds.

Although prior observations of an organic contribution to sea spray aerosol have been made, the ambient observations of *O'Dowd et al.* [2004] were the first to suggest that biologically-derived organic material directly ejected from the ocean could be the key source of newly formed submicron sea spray aerosol responsible for linking oceanic biological activity to cloud formation and changes in cloud microphysics over the marine environment. Since then, a number of publications have highlighted the influence of biological activity on the chemical composition of marine aerosols through the enrichment of organic material, particularly in the smallest particles [*Bigg*, 2007; *Bigg and Leck*, 2008; *Cavalli et al.*, 2004; *Facchini et al.*, 2008a; *Hawkins and Russell*, 2010b; *Keene et al.*, 2007; *Leck and Bigg*, 2005a; *Leck and Bigg*, 2005b; *Leck and Bigg*, 2008; *Ovadnevaite et al.*, 2011; *Russell et al.*, 2010]. Marine organics are primarily water-insoluble material, largely composed of polysaccharides with contributions from proteins and lipids [*Ceburnis et al.*, 2008; *Facchini et al.*, 2008b; *Hawkins and Russell*, 2010b; *Kuznetsova et al.*, 2005; *Rinaldi et al.*, 2010; *Russell et al.*, 2010] derived from whole and fragmented cells, and exopolymeric secretions (EPS) or microgels. EPS constitutes ~10% of the dissolved organic material (DOM) pool (7×10^{16} gC) [*Chin et al.*, 1998; *Orellana et al.*, 2007; *Orellana and Verdugo*, 2003; *Verdugo et al.*, 2008] that, unlike most DOM, is bioavailable making EPS one of the most significant contributors to the

global carbon cycle [*Verdugo et al.*, 2008]. EPS or microgels are the result of gel assembly/dispersion equilibria from dissolved polymers, namely polysaccharides, proteins, and lipids [*Chin et al.*, 1998; *Verdugo et al.*, 2004; *Wells*, 1998]. The polymer network of these microgels has been shown to be stabilized through ionic bonding with divalent cations (Ca^{2+}, Mg^{2+}) [*Chin et al.*, 1998; *Verdugo et al.*, 2004; *Wells*, 1998]. Hence, in addition to being a source of organic carbon, atmospheric enrichment of inorganic ions associated with EPS could also occur in the marine environment; however, in contrast to the observed enrichment of organic material, enrichment of inorganic ions in sea spray aerosol compared to bulk seawater has been difficult to discern particularly in ambient measurements. The detection of EPS in the atmosphere has been highlighted in previous publications [*Bigg and Leck*, 2001; *Leck and Bigg*, 2005a; *Leck and Bigg*, 2005b; *Leck et al.*, 2002; *Posfai et al.*, 2003]. Recent evidence has shown that EPS is subject to atmospheric processing, namely, a breakdown in the polymer network via UV-photolysis [*Orellana and Verdugo*, 2003]. A recent study by *Leck and Bigg* [2010] has suggested that this breakdown results in the formation of particles ~40 nm and smaller in diameter that appear to be nucleation events, but are not. In addition to primary emissions, organics associated with biological activity have been found to contribute to secondary organic marine aerosol in addition to potentially causing nucleation events in the remote marine atmosphere. One example of the formation of secondary organic aerosol from marine biogenic emissions is the formation of oxalate in marine aerosols from the cloud processing of biogenically-produced glyoxal [*Rinaldi et al.*, 2011]. Additionally, biogenic amines have been shown to contribute to marine aerosol and, when co-emitted with MSA, have been suggested to lead to the nucleation of new

particles [*Facchini et al.*, 2008a; *Sorooshian et al.*, 2009]. The study by *Meskhidze and Nenes* [2006] hypothesized that emission of gaseous isoprene from marine phytoplankton led to nucleation events capable of altering the radiative impact of clouds over the Southern Ocean.

1.5 Characteristics of Anthropogenic Contributions to Marine Aerosols

1.5.1 Continental Outflow

As mentioned previously, in addition to sea spray aerosol, anthropogenic emissions shape aerosol-cloud-climate interactions in the marine environment. Continental emissions are advected out over the ocean contributing to marine aerosol and impacting the aerosol direct and indirect effects over the ocean. Although anthropogenic sources exert a stronger influence in coastal regions, anthropogenic particles, such as soot, have been detected even in remote marine regions [*Posfai et al.*, 1999]. The physicochemical properties of continental outflow on the marine environment are very regional with contributions from biomass burning, fossil fuel combustion, agricultural emissions, etc. An additional contribution to marine aerosol with a continental origin is mineral dust with strong contributions from Asia and Africa to the Pacific and Atlantic Oceans [*Bates et al.*, 2004; *Huebert et al.*, 2003]. These dust particles are thought to deposit key trace elements (e.g. Fe) to the ocean potentially stimulating the growth of marine phytoplankton [*Jickells et al.*, 2005]. Anthropogenic sulfate, formed from the oxidation of $SO_{2(g)}$ mainly produced from fossil fuel, coal, and biofuel combustion, is a large contributor to marine aerosols found to significantly increase CDNC, altering the

radiative properties of clouds over the marine environment [*Charlson et al.*, 1992; *Hawkins et al.*, 2010; *Leaitch et al.*, 1992; *Novakov et al.*, 1994; *Quinn and Bates*, 2005]. Contributions of sulfate from ships are discussed below.

Biomass burning emissions have been found to contribute significantly to marine aerosols contributing both soot and organic carbon, namely alkanes and alcohols including the biomass burning tracer levoglucosan [*Hawkins and Russell*, 2010a; *Hegg et al.*, 2010]. A study of these emissions along the California coast found that biomass burning aerosol contributed to the aerosol indirect effect and increased the cooling effect of marine stratocumulus near the coast while resulting in a decrease in cloud cover providing a warming effect further away from the coast [*Brioude et al.*, 2009]. Soot from biomass burning was found to significantly contribute to marine aerosol along the African coast and Indian subcontinent contributing to an increase in radiative absorption by aerosols compared to background marine conditions in these regions [*Guazzotti et al.*, 2003; *Quinn and Bates*, 2005]. Soot from diesel truck and ship emissions from ports also contribute to marine aerosol [*Ault et al.*, 2010]. Particulate organic matter from continental outflow has also been found to be a significant contributor to marine aerosol, particularly off the NE United States coast [*Quinn and Bates*, 2005]. Alkanes and carboxylic acids emitted during combustion have been found to contribute to marine regions [*Hawkins et al.*, 2010; *Russell et al.*, 2011; *Russell et al.*, 2009]. Particulate organics emitted from anthropogenic sources have been shown to alter the light scattering properties of marine aerosols and their ability to nucleate cloud droplets, particularly

when this organic material is hydrocarbon-like (i.e. alkanes) [*Kaku et al.*, 2006; *Massoli et al.*, 2009; *Quinn et al.*, 2005; *Quinn et al.*, 2008].

1.5.2 Ship Emissions

The most ubiquitous anthropogenic contribution to marine aerosols is ships emissions. Ship emissions represent the highest source of pollution per ton of fuel consumed [*Corbett and Fischbeck*, 1997; *Eyring et al.*, 2010] producing ~1.2-1.6 Tg particulate matter/yr [*Corbett and Koehler*, 2003; *Eyring et al.*, 2010], with most of these emissions occurring within 400 km of coastal regions [*Corbett and Fischbeck*, 1997; *Corbett et al.*, 1999]. The physicochemical properties of particles emitted from ships are dependent on whether ships are combusting high sulfur residual oil or cleaner distillate fuels; due to the low cost, ~70-80% of commercial ships combust high sulfur residual fuel oil [*Corbett and Fischbeck*, 1997]. Particles from ships contain pollutants such as black carbon (soot), organics, sulfate, and transition metals, particularly Fe, V, and Ni [*Agrawal et al.*, 2008; *Ault et al.*, 2010; *Ault et al.*, 2009; *Healy et al.*, 2009; *Murphy et al.*, 2009], with residual fuel combustion producing higher concentrations of these pollutants [*Lack et al.*, 2011; *Lack et al.*, 2009]. Marine vessels burning residual fuel oil tend to produce more particles capable of forming cloud droplets due to increased number and mass concentrations of sulfate and organic aerosols [*Hudson et al.*, 2000; *Lack et al.*, 2011; *Lack et al.*, 2009; *Langley et al.*, 2010; *Russell et al.*, 2000]. In fact, up to 17-39% of the anthropogenic indirect effect is thought to be due to the effect of ship emissions, primarily from the combustion of residual fuel oil, on clouds over the ocean [*Eyring et al.*, 2010; *Hudson et al.*, 2000]. Combustion of marine distillate fuel tends to

produce fewer particles, and due to the lack of sulfate associated with these particles, emissions from ships combusting marine distillate fuel are less likely to activate into cloud droplets; however, these emissions have been found to exert a larger influence on the aerosol direct effect [*Lack et al.*, 2011; *Lack et al.*, 2009].

1.6 Secondary Processing and Aging of Marine Aerosols

Secondary processing of marine aerosols through the oxidation of organics, heterogeneous uptake of reactive gases onto particles, and aqueous phase processing, particularly in cloud droplets, with biogenic (e.g. isoprene, DMS oxidation products, etc.) and anthropogenic gases ($NO_{x(g)}$, $SO_{2(g)}$, etc.) leads to the addition of particulate organic material, sulfate, methanesulfonate, and nitrate to marine aerosols. The addition of these secondary species, particularly sulfate and nitrate, can add soluble material that alter the cloud activation properties of marine aerosols, especially those emitted from anthropogenic sources such as soot [*Furutani et al.*, 2008]. This section will point out examples of some of the most important and prevalent aging processes pertaining to marine aerosols and is by no means exhaustive. As mentioned in section 1.4.3, organic compounds emitted in the gas phase from biogenic and anthropogenic sources can contribute secondary particulate matter to marine aerosols. One example, already mentioned, is the formation of biogenic oxalate in marine aerosols from the aqueous phase processing of glyoxal in cloud droplets [*Rinaldi et al.*, 2011]. In addition to the contribution of secondary organic material, another process relevant for the marine atmosphere is the proposed oxidation of primary organic matter ejected from the ocean to form oxygenated organic aerosol that is more likely to take up water and participate in

cloud droplet formation [*Ceburnis et al.*, 2008; *Ellison et al.*, 1999]. In addition to organic material, secondary processing also contributes heavily to the formation of particulate sulfate in marine aerosols. DMS oxidation chemistry was mentioned in section 1.4.3 as a means of contributing particulate sulfate; however, anthropogenic emissions of $SO_{2(g)}$ from continental and ship emissions can also lead to the formation of sulfate in marine aerosols [*Capaldo et al.*, 1999]. Although this process can occur via heterogeneous uptake onto particles, the dominant formation mechanism of sulfate is aqueous processing generally occurring in cloud droplets [*Lelieveld and Heintzenberg*, 1992]; this process is thought to be the main mechanism leading to the formation of a bimodal size distribution and the Hoppel minimum [*Hoppel et al.*, 1990]. Transition metals, such as Fe, have been found to catalyze the formation of sulfate during aqueous processing; metals that are most efficient at this process are emitted from combustion sources, including ship emissions in the marine environment, rather than mineral dust particles [*Alexander et al.*, 2009; *Ault et al.*, 2010; *Deguillaume et al.*, 2005]. The catalysis of sulfur oxidation by transition metals has also been suggested to occur for DMS oxidation products suggesting that anthropogenic emissions may play a role in the atmospheric processing of marine biogenic emissions [*Key et al.*, 2008]; this is a largely unexplored topic that will be addressed, in part, in this dissertation. Perhaps the most prevalent reaction observed in the ambient marine atmosphere is the heterogeneous displacement of chloride on sea spray particles by reactive gases, namely nitrogen oxides such as $HNO_{3(g)}$ and $N_2O_{5(g)}$ [*Chang et al.*, 2011; *Gard et al.*, 1998; *Quinn and Bates*, 2005]. The reaction results in the formation of $HCl_{(g)}$, $ClNO_{2(g)}$, and particulate nitrate in sea spray particles [*Behnke et al.*, 1997; *Finlayson-Pitts et al.*, 1989]; $HCl_{(g)}$ has been

shown to react with alkaline particles such as mineral dust [*Sullivan et al.*, 2007] while $ClNO_{2(g)}$ is photolyzed during the day producing the reactive Cl radical, which can alter ozone production [*Keene et al.*, 1990]. The heterogeneous uptake of $N_2O_{5(g)}$ has generated considerable interest recently for several reasons, mainly that the reaction leads to the formation of particulate nitrate, which is poorly accounted for in current global climate models that factor in aerosol composition [*Forster et al.*, 2007]. The reaction is thought to decrease global NO_x concentrations by ~50% annually [*Dentener and Crutzen*, 1993], which influences the production of tropospheric ozone and the lifetime of methane, two key greenhouse gases [*Forster et al.*, 2007; *Shindell et al.*, 2009].

1.7 Key Remaining Questions

Despite recent advances in our understanding of marine aerosols made by both ambient and laboratory measurements, many questions remain regarding the role of biological activity, anthropogenic emissions, and atmospheric processing in shaping aerosol-cloud-climate interactions in the marine environment. Some of these questions are presented below:

1. Can real-time measurements between oceanic proxies for biological activity and changes in sea spray chemistry be established?
2. In addition to DMS oxidation products, does biological activity contribute any other sulfur-containing particle types and/or compounds to sea spray aerosol?
3. How does biological activity alter the mixing-state of individual sea spray particles?

4. How do continental outflow and ship emissions influence the single-particle chemistry of marine aerosols?

5. How does the single-particle mixing-state of shipping emissions differ for ships combusting marine residual fuel and ships combusting high sulfur residual fuel oil?

6. How do marine biogenic emissions interact with anthropogenic emissions? Can anthropogenic emissions alter the atmospheric processing of marine biogenic emissions?

1.8 Synopsis of the Dissertation

The remaining chapters of this dissertation attempt to address these questions through real-time measurements of size-resolved particle mixing-state made for both ambient and laboratory-generated marine aerosols. Chapter 2 of this dissertation shows the presence of unique ocean-derived particles that track chlorophyll *a* and atmospheric DMS concentrations in real-time. These unique particles contain internal mixtures of Mg^{2+} and/or Ca^{2+}, K^{+}, and organic carbon that are externally mixed from sea salt particles. Chapter 3 discusses the nighttime detection of particulate, elemental sulfur in regions of elevated biological activity. These particles were found to be directly ejected from the ocean and are not formed from DMS oxidation products. Chapter 4 shows how the single-particle mixing-state of particles generated from bubble bursting experiments changes as biologically-derived organic matter and/or phytoplankton cells are added to artificial seawater solutions; these results were compared to particles generated by bubbling natural seawater solutions. Particle types produced by these experiments were

found to match ambient particles detected during coastal and shipboard studies. Chapter 5 highlights differences in the single-particle mixing-state of anthropogenic emissions observed along the California coast during the CalNex field campaign. Soot internally mixed with organics was the dominate particle type in Southern California while organics dominated the particle chemistry in the Sacramento area, particularly after new particle formation events. Further, most carbonaceous particle types were internally mixed with sulfate in Southern California, particularly when emissions came from the Ports of Los Angeles and Long Beach. As discussed in Chapter 6 of this dissertation, measurements during CalNex and those made on the Scripps Pier showed a decline in the number concentrations of vanadium-containing particles characteristic of emissions from ships combusting residual fuel compared to earlier measurements. Ship emissions from the Port of Los Angeles and the Scripps Pier in 2009 were also associated with less sulfate and sulfuric acid compared to earlier measurements. These results are in compliance with recent regulations requiring ships to combust low sulfur fuel when approaching the California coast. These results highlight regional and temporal differences in anthropogenic aerosols along the California coast. Finally, Chapter 7 probes interactions between marine biogenic and anthropogenic emissions during the Study of Organic Aerosols in Riverside, CA (SOAR) campaign. During a red tide bloom off the coast of Southern California, the DMS oxidation product methanesulfonic acid (MSA) was found to be internally mixed with anthropogenic particles including ship emissions and biomass burning particles. Particles that were internally mixed with vanadium contained elevated levels of MSA suggesting that anthropogenic, metal-containing particles can catalyze the atmospheric processing of marine biogenic emissions. Overall, the contents of this

dissertation provide insights into the role of biological activity, anthropogenic emissions, and subsequent atmospheric processing on the size-resolved mixing-state of marine aerosols.

1.9 Acknowledgements

Andrew Ault is acknowledged for helping edit this chapter.

1.10 References

Agrawal, H., Q.G.J. Malloy, W.A. Welch, J.W. Miller, and D.R. Cocker (2008), In-use gaseous and particulate matter emissions from a modern ocean going container vessel, *Atmos. Environ., 42* (21), 5504-5510.

Albrecht, B.A. (1989), Aerosols, Cloud Microphysics, and Fractional Cloudiness, *Science, 245* (4923), 1227-1230.

Alexander, B., R.J. Park, D.J. Jacob, and S. Gong (2009), Transition metal-catalyzed oxidation of atmospheric sulfur: Global implications for the sulfur budget, *J. Geophys. Res., 114* (D02309), doi:10.1029/2008JD010486.

Allen, J.O. (2002), YAADA software toolkit to analyze single-particle mass spectral data: Reference manual version 1.1, *Arizona State University*, http://www.yaada.org.

Andreae, M.O. (1990), Ocean-atmosphere interactions in the global biogeochemical sulfur cycle, *Mar. Chem., 30* (1-3), 1-29.

Andreae, M.O., and P.J. Crutzen (1997), Atmospheric aerosols: Biogeochemical sources and role in atmospheric chemistry, *Science, 276* (5315), 1052-1058.

Ault, A.P., C.J. Gaston, Y. Wang, G. Dominguez, M.H. Thiemens, and K.A. Prather (2010), Characterization of the single particle mixing state of individual ship plume events measured at the Port of Los Angeles, *Environ. Sci. Tech., 44* (6), 1954-1961.

Ault, A.P., M.J. Moore, H. Furutani, and K.A. Prather (2009), Impact of emissions from the Los Angeles port region on San Diego air quality during regional transport events, *Environ. Sci. Tech., 43* (10), 3500-3506.

Ayers, G.P., and R.W. Gillett (2000), DMS and its oxidation products in the remote marine atmosphere: implications for climate and atmospheric chemistry, *J. Sea Res., 43* (3-4), 275-286.

Baker, M.B. (1997), Cloud microphysics and climate, *Science, 276* (5315), 1072-1078.

Barnes, I., J. Hjorth, and N. Mihalopoulos (2006), Dimethyl sulfide and dimethyl sulfoxide and their oxidation in the atmosphere, *Chem. Rev., 106* (3), 940-975.

Bates, T.S., A.D. Clarke, V.N. Kapustin, J.E. Johnson, and R.J. Charlson (1989), Oceanic dimethylsulfide and marine aerosol: Difficulties associated with assessing their covariance, *Glob. Biogeochem. Cy., 3* (4), 299-304.

Bates, T.S., R.P. Kiene, G.V. Wolfe, P.A. Matrai, F.P. Chavez, K.R. Buck, B.W. Blomquist, and R.L. Cuhel (1994), The cycling of sulfur in surface seawater of the northeast Pacific, *J. Geophys. Res.-[Oceans]*, *99* (C4), 7835-7843.

Bates, T.S., B.K. Lamb, A. Guenther, J. Dignon, and R.E. Stoiber (1992), Sulfur emissions to the atmosphere from natural sources, *J. Atmos. Chem.*, *14* (1-4), 315-337.

Bates, T.S., P.K. Quinn, D.J. Coffman, D.S. Covert, T.L. Miller, J.E. Johnson, G.R. Carmichael, I. Uno, S.A. Guazzotti, D.A. Sodeman, K.A. Prather, M. Rivera, L.M. Russell, and J.T. Merrill (2004), Marine boundary layer dust and pollutant transport associated with the passage of a frontal system over eastern Asia, *J. Geophys. Res.-[Atmos.]*, *109* (D19S19), doi:10.1029/2003JD004094.

Behnke, W., C. George, V. Scheer, and C. Zetzsch (1997), Production and decay of $ClNO_2$ from the reaction of gaseous N_2O_5 with NaCl solution: Bulk and aerosol experiments, *J. Geophys. Res.-[Atmos.]*, *102* (D3), 3795-3804.

Bernstein, J.A., N. Alexis, C. Barnes, I.L. Bernstein, J.A. Bernstein, A. Nel, D. Peden, D. Diaz-Sanchez, S.M. Tarlo, and P.B. Williams (2004), Health effects of air pollution, *Journal of Allergy and Clinical Immunology*, *114* (5), 1116-1123.

Bigg, E.K. (2007), Sources, nature and influence on climate of marine airborne particles, *Environ. Chem.*, *4* (3), 155-161.

Bigg, E.K., and C. Leck (2001), Cloud-active particles over the central Arctic Ocean, *J. Geophys. Res.-[Atmos.]*, *106* (D23), 32155-32166.

Bigg, E.K., and C. Leck (2008), The composition of fragments of bubbles bursting at the ocean surface, *J. Geophys. Res.*, *113*, D11209, doi:10.1029/2007JD009078.

Blanchard, D.C. (1964), Sea-to-air transport of surface active material, *Science*, *146* (364), 396-397.

Blanchard, D.C. (1989), The ejection of drops from the sea and their enrichment with bacteria and other materials: A review, *Estuaries*, *12* (3), 127-137.

Blanchard, D.C., and L. Syzdek (1970), Mechanism for water-to-air transfer and concentration of bacteria, *Science*, *170* (3958), 626-628.

Blanchard, D.C., and L.D. Syzdek (1972), Concentration of bacteria in jet drops from bursting bubbles, *J. Geophys. Res.*, *77* (27), 5087-5099.

Blanchard, D.C., and A.H. Woodcock (1957), Bubble formation and modification in the sea and its meteorological significance, *Tellus*, *9* (2), 145-158.

Brioude, J., O.R. Cooper, G. Feinfeld, M. Trainer, S.R. Freitas, D. Kowal, J.R. Ayers, E. Prins, P. Minnis, S.A. McKeen, G.J. Frost, and E.-Y. Hsie (2009), Effect of biomass burning on marine stratocumulus clouds off the California coast, *Atmos. Chem. Phys.*, *9*, 8841-8856.

Campen, M.J., J.P. Nolan, M.C.J. Schladweiler, U.P. Kodavanti, P.A. Evansky, D.L. Costa, and W.P. Watkinson (2001), Cardiovascular and thermoregulatory effects of inhaled PM-associated transition metals: A potential interaction between nickel and vanadium sulfate, *Toxicological Sciences*, *64* (2), 243-252.

Capaldo, K., J.J. Corbett, P. Kasibhatla, P. Fischbeck, and S.N. Pandis (1999), Effects of ship emissions on sulphur cycling and radiative climate forcing over the ocean, *Nature*, *400* (6746), 743-746.

Cavalli, F., M.C. Facchini, S. Decesari, M. Mircea, L. Emblico, S. Fuzzi, D. Ceburnis, Y.J. Yoon, C.D. O'Dowd, J.P. Putaud, and A. Dell'Acqua (2004), Advances in characterization of size-resolved organic matter in marine aerosol over the North Atlantic, *J. Geophys. Res.-[Atmos.]*, *109*, D24215, doi:10.1029/2004JD005137.

Ceburnis, D., C.D. O'Dowd, G.S. Jennings, M.C. Facchini, L. Emblico, S. Decesari, S. Fuzzi, and J. Sakalys (2008), Marine aerosol chemistry gradients: Elucidating primary and secondary processes and fluxes, *Geophys. Res. Lett.*, *35* (7), L07804, doi:10.1029/2008GL033462.

Chang, W.L., P.V. Bhave, S.S. Brown, N. Riemer, J. Stutz, and D. Dabdub (2011), Heterogeneous atmospheric chemistry, ambient measurements, and model calculations of N_2O_5: A review, *Aerosol Sci. Tech.*, *45* (6), 665-695.

Charlson, R.J., J.E. Lovelock, M.O. Andreae, and S.G. Warren (1987), Oceanic phytoplankton, atmospheric sulfur, cloud albedo and climate, *Nature*, *326* (6114), 655-661.

Charlson, R.J., S.E. Schwartz, J.M. Hales, R.D. Cess, J.A. Coakley, J.E. Hansen, and D.J. Hofmann (1992), Climate forcing by anthropogenic aerosols, *Science*, *255*, 423-430.

Chin, W.C., M.V. Orellana, and P. Verdugo (1998), Spontaneous assembly of marine dissolved organic matter into polymer gels, *Nature*, *391* (6667), 568-572.

Cipriano, R.J., and D.C. Blanchard (1981), Bubble and aerosol spectra produced by a laboratory 'breaking wave', *J. Geophys. Res.*, *86* (C9), 8085-8092.

Clarke, A.D., D. Davis, V.N. Kapustin, F. Eisele, G. Chen, I. Paluch, D. Lenschow, A.R. Bandy, D. Thornton, K. Moore, L. Mauldin, D. Tanner, M. Litchy, C. M.A., J. Collins, and G. Albercook (1998), Particle nucleation in the tropical boundary layer and its coupling to marine sulfur sources, *Science*, *282*, 89-92.

Clarke, A.D., V.N. Kapustin, F.L. Eisele, R.J. Weber, and P.H. McMurray (1999), Particle production near marine clouds: Sulfuric acid and predictions from classical binary nucleation, *Geophys. Res. Lett.*, *26* (16), 2425-2428.

Clarke, A.D., S.R. Owens, and J.C. Zhou (2006), An ultrafine sea-salt flux from breaking waves: Implications for cloud condensation nuclei in the remote marine atmosphere, *J. Geophys. Res.-[Atmos.]*, *111* (D6), D06202, doi:10.1029/2005JD006565.

Corbett, J.J., and P. Fischbeck (1997), Emissions from ships, *Science*, *278* (5339), 823-824.

Corbett, J.J., P.S. Fishbeck, and S.N. Pandis (1999), Global nitrogen and sulphur inventories for oceangoing ships, *J. Geophys. Res.*, *104* (3), 3457-3470.

Corbett, J.J., and H.W. Koehler (2003), Updated emissions from ocean shipping, *J. Geophys. Res.-[Atmos.]*, *108* (D20), 4650, doi:10.1029/2003JD003751.

Cropp, R.A., A.J. Gabric, G.H. McTainsh, R.D. Braddock, and N. Tindale (2005), Coupling between ocean biota and atmospheric aerosols: Dust, dimethylsulphide, or artifact? *Glob. Biogeochem. Cy.*, *19*, GB4002, doi:10.1029/2004GB002436.

Deguillaume, L., M. Leriche, K. Desboeufs, G. Mailhot, C. George, and N. Chaumerliac (2005), Transition metals in atmospheric liquid phases: Sources, reactivity, and sensitive parameters, *Chem. Rev.*, *105* (9), 3388-3431.

Dentener, F.J., and P.J. Crutzen (1993), Reaction of N_2O_5 on tropospheric aerosols: Impact on the global distributions of NO_x, O_3, and OH, *J. Geophys. Res.*, *98* (D4), 7149-7163.

Ellison, G.B., A.F. Tuck, and V. Vaida (1999), Atmospheric processing of organic aerosols, *J. Geophys. Res.-[Atmos.]*, *104* (D9), 11633-11641.

Eyring, V., I.S.A. Isaksen, T. Berntsen, W.J. Collins, J.J. Corbett, O. Endresen, R.G. Grainger, J. Moldanova, H. Schlager, and D.S. Stevenson (2010), Transport impacts on atmosphere and climate: Shipping, *Atmos Environ*, *44*, 4735-4771.

Facchini, M.C., S. Decesari, M. Rinaldi, C. Carbone, E. Finessi, M. Mircea, S. Fuzzi, F. Moretti, E. Tagliavini, D. Ceburnis, and C.D. O'Dowd (2008a), Important source

of marine secondary organic aerosol from biogenic amines, *Environ. Sci. Tech.*, *42* (24), 9116-9121.

Facchini, M.C., M. Rinaldi, S. Decesari, C. Carbone, E. Finessi, M. Mircea, S. Fuzzi, D. Ceburnis, R. Flanagan, E.D. Nilsson, G. de Leeuw, M. Martino, J. Woeltjen, and C.D. O'Dowd (2008b), Primary submicron marine aerosol dominated by insoluble organic colloids and aggregates, *Geophys. Res. Lett.*, *35*, L17814, doi:10.1029/2008GL034210.

Fang, S.C., E.A. Eisen, J.M. Cavallari, M.A. Mittleman, and D.C. Christiani (2008), Acute changes in vascular function among welders exposed to metal-rich particulate matter, *Epidemiology*, *19* (2), 217-225.

Ferek, R.J., P.V. Hobbs, L.F. Radke, and J.A. Herring (1995), Dimethyl sulfide in the arctic atmosphere, *J. Geophys. Res.*, *100* (D12), 26093-26104.

Fergenson, D.P., X.H. Song, Z. Ramadan, J.O. Allen, L.S. Hughes, G.R. Cass, P.K. Hopke, and K.A. Prather (2001), Quantification of ATOFMS data by multivariate methods, *Anal. Chem.*, *73* (15), 3535-3541.

Finlayson-Pitts, B.J., M.J. Ezell, and J.N. Pitts Jr. (1989), Formation of chemically active chlorine compounds by reactions of atmospheric NaCl particles with gaseous N_2O_5 and $ClONO_2$, *Nature*, *337*, 241-244.

Finlayson-Pitts, B.J., and J.N. Pitts, *Chemistry of the upper and lower atmosphere: Theory, experiments and applications*, Academic Press, San Diego, 2000.

Fitzgerald, J.W. (1991), Marine aerosols: A review, *Atmos. Environ. A-Gen. Topics*, *25* (3-4), 533-545.

Forster, P., V. Ramaswamy, P. Artaxo, T. Berntsen, R. Betts, D.W. Fahey, J. Haywood, J. Lean, D.C. Lowe, G. Myhre, J. Nganga, R. Prinn, G. Raga, M. Schulz, and R. Van Dorland, Changes in Atmospheric Constituents and in Radiative Forcing, in *Climate Change 2007: The Physical Science Basis. Contribution of Working Group I to the Fourth Assessment Report of the Intergovernmental Panel on Climate Change*, edited by S. Solomon, D. Qin, M. Manning, Z. Chen, M. Marquis, K.B. Averyt, M. Tignor, and H.L. Miller, Cambridge University Press, Cambridge, United Kingdom and New York, NY, USA, 2007.

Fuentes, E., H. Coe, D. Green, G. de Leeuw, and G. McFiggans (2010a), Laboratory-generated primary marine aerosol via bubble-bursting and atomization, *Atmos. Meas. Tech.*, *3* (1), 141-162.

Fuentes, E., H. Coe, D. Green, G. de Leeuw, and G. McFiggans (2010b), On the impacts of phytoplankton-derived organic matter on the properties of the primary marine aerosol - Part 1: Source fluxes, *Atmos. Chem. Phys.*, *10* (19), 9295-9317.

Furutani, H., M. Dall'osto, G.C. Roberts, and K.A. Prather (2008), Assessment of the relative importance of atmospheric aging on CCN activity derived from field observations, *Atmos. Environ.*, *42* (13), 3130-3142.

Gard, E., J.E. Mayer, B.D. Morrical, T. Dienes, D.P. Fergenson, and K.A. Prather (1997), Real-time analysis of individual atmospheric aerosol particles: Design and performance of a portable ATOFMS, *Anal. Chem.*, *69* (20), 4083-4091.

Gard, E.E., M.J. Kleeman, D.S. Gross, L.S. Hughes, J.O. Allen, B.D. Morrical, D.P. Fergenson, T. Dienes, M.E. Galli, R.J. Johnson, G.R. Cass, and K.A. Prather (1998), Direct observation of heterogeneous chemistry in the atmosphere, *Science, 279* (5354), 1184-1187.

Gauderman, W.J., R. McConnell, F. Gilliland, S. London, D. Thomas, E. Avol, H. Vora, K. Berhane, E.B. Rappaport, F. Lurmann, H.G. Margolis, and J. Peters (2000), Association between air pollution and lung function growth in southern California children, *American Journal of Respiratory and Critical Care Medicine*, *162* (4), 1383-1390.

Guazzotti, S.A., K.R. Coffee, and K.A. Prather (2001), Continuous measurements of size-resolved particle chemistry during INDOEX-Intensive Field Phase 99, *J. Geophys. Res.-[Atmos.]*, *106* (D22), 28607-28627.

Guazzotti, S.A., D.T. Suess, K.R. Coffee, P.K. Quinn, T.S. Bates, A. Wisthaler, A. Hansel, W.P. Ball, R.R. Dickerson, C. Neususs, P.J. Crutzen, and K.A. Prather (2003), Characterization of carbonaceous aerosols outflow from India and Arabia: Biomass/biofuel burning and fossil fuel combustion, *J. Geophys. Res.-[Atmos.]*, *108* (D15), 4485, doi:10.1029/2002JD003277.

Hawkins, L.N., and L.M. Russell (2010a), Oxidation of ketone groups in transported biomass burning aerosol from the 2008 Northern California Lightening Series fires, *Atmos Environ*, *44*, 4142-4154.

Hawkins, L.N., and L.M. Russell (2010b), Polysaccharides, proteins, and phytoplankton fragments: Four chemically distinct types of marine primary organic aerosol classified by single particle spectromicroscopy, *Advances in Meteorology*, doi:10.1155/2010/612132.

Hawkins, L.N., L.M. Russell, D.S. Covert, P.K. Quinn, and T.S. Bates (2010), Carboxylic acids, sulfates, and organosulfates in processed continental organic

aerosol over the southeast Pacific Ocean during VOCALS-REx 2008, *J. Geophys. Res.-[Atmos.]*, *115*, D13201, doi:10.1029/2009JD013276.

Healy, R.M., I.P. O'Connor, S. Hellebust, A. Allanic, J.R. Sodeau, and J.C. Wenger (2009), Characterization of single particles from in-port ship emissions, *Atmos Environ*, *43*, 6408-6414.

Hegg, D.A., D.S. Covert, H.H. Jonsson, and R.K. Woods (2010), The contribution of anthropogenic aerosols to aerosol light-scattering and CCN activity in the California coastal zone, *Atmos. Chem. Phys.*, *10*, 7341-7351.

Hobbs, P.V., T.J. Garrett, R.J. Ferek, S.R. Strader, D.A. Hegg, G.M. Frick, W.A. Hoppel, R.F. Gasparovic, L.M. Russell, D.W. Johnson, C.D. O'Dowd, P.A. Durkee, K.E. Nielsen, and G. Innis (2000), Emissions from ships with respect to their effects on clouds, *Journal of Atmospheric Sciences*, *57*, 2570-2590.

Hoffmann, T., R.-J. Huang, and M. Kalberer (2011), Atmospheric analytical chemistry, *Anal. Chem.*, *83*, 4696-4666.

Hopkins, R.J., Y. Desyaterik, A.V. Tivanski, R.A. Zaveri, C.M. Berkowitz, T. Tyliszczak, M.K. Gilles, and A. Laskin (2008), Chemical speciation of sulfur in marine cloud droplets and particles: Analysis of individual particles from the marine boundary layer over the California Current, *J. Geophys. Res.-[Atmos.]*, *113* (D4), D04209, doi:10.1029/2007JD008954.

Hoppel, W.A., J.W. Fitzgerald, G.M. Frick, R.E. Larson, and E.J. Mack (1990), Aerosol Size Distributions and Optical-Properties Found in the Marine Boundary-Layer over the Atlantic-Ocean, *J. Geophys. Res.-[Atmos.]*, *95* (D4), 3659-3686.

Hudson, J.G., T.J. Garrett, P.V. Hobbs, S.R. Strader, Y. Xie, and S.S. Yum (2000), Cloud condensation nuclei and ship tracks, *Journal of Atmospheric Sciences*, *57*, 2696-2706.

Huebert, B.J., T. Bates, P.B. Russell, G.Y. Shi, Y.J. Kim, K. Kawamura, G. Carmichael, and T. Nakajima (2003), An overview of ACE-Asia: Strategies for quantifying the relationships between Asian aerosols and their climatic impacts, *J. Geophys. Res.-[Atmos.]*, *108* (D23), 8633, doi:10.1029/2003JD003550.

Jacobson, M.C., H.C. Hansson, K.J. Noone, and R.J. Charlson (2000), Organic atmospheric aerosols: Review and state of the science, *Reviews of Geophysics*, *38* (2), 267-294.

Jacobson, M.Z. (2000), A physically-based treatment of elemental carbon optics: Implications for global direct forcing of aerosols, *Geophys. Res. Lett.*, *27* (2), 217-220.

Jickells, T.D., Z.S. An, K.K. Andersen, A.R. Baker, G. Bergametti, N. Brooks, J.J. Cao, P.W. Boyd, R.A. Duce, K.A. Hunter, H. Kawahata, N. Kubilay, J. laRoche, P.S. Liss, N. Mahowald, J.M. Prospero, A.J. Ridgwell, I. Tegen, and R. Torres (2005), Global iron connections between desert dust, ocean biogeochemistry, and climate, *Science, 308* (5718), 67-71.

Kaku, K.C., D.A. Hegg, D.S. Covert, J.L. Santarpia, H. Jonsson, G. Buzorius, and D.R. Collins (2006), Organics in the Northeastern Pacific and their impacts on aerosol hygroscopicity in the subsaturated and supersaturated regimes, *Atmos. Chem. Phys., 6*, 4101-4115.

Keene, W.C., H. Maring, J.R. Maben, D.J. Kieber, A.A.P. Pszenny, E.E. Dahl, M.A. Izaguirre, A.J. Davis, M.S. Long, X.L. Zhou, L. Smoydzin, and R. Sander (2007), Chemical and physical characteristics of nascent aerosols produced by bursting bubbles at a model air-sea interface, *J. Geophys. Res.-[Atmos.], 112* (D21), D21202, doi:10.1029/2007JD008464.

Keene, W.C., A.A.P. Pszenny, D.J. Jacob, R.A. Duce, J.N. Galloway, J.J. Schultz-Tokos, H. Sievering, and J.F. Boatman (1990), The geochemical cycling of reactive chlorine through the marine troposphere, *Glob. Biogeochem. Cy., 4* (4), 407-430.

Keller, M.D., W. Bellows, K., and R.L. Guillard, Dimethyl sulfide production in marine phytoplankton, in *Biogenic Sulfur in the Environment*, edited by E.S. Saltzman, and W.J. Cooper, pp. 167-182, American Chemical Society, Washington, D.C., 1989.

Key, J.M., N. Paulk, and A.M. Johansen (2008), Photochemistry of iron in simulated crustal aerosols with dimethyl sulfide oxidation products, *Environ. Sci. Tech., 42* (1), 133-139.

Kohler, H. (1936), The nucleus in and the growth of hygroscopic droplets., *Transactions of the Faraday Society, 32* (2), 1152-1161.

Kruger, O., and H. Grabl (2011), Southern Ocean phytoplankton increases cloud albedo and reduces precipitation, *Geophys. Res. Lett., 38*, L08809, doi:10.1029/2011GL047116.

Kuznetsova, M., C. Lee, and J. Aller (2005), Characterization of the proteinaceous matter in marine aerosols, *Mar. Chem., 96* (3-4), 359-377.

Lack, D.A., C.D. Cappa, J. Langridge, R. Bahreini, G. Buffaloe, C. Brock, K. Cerully, D. Coffman, K. Hayden, J. Holloway, B. Lerner, P. Massoli, S.-M. Li, R. McLaren, A.M. Middlebrook, R. Moore, A. Nenes, I. Nuaaman, T.B. Onasch, J. Peischl, A. Perring, P.K. Quinn, T. Ryerson, J.P. Schwartz, R. Spackman, S.C. Wofsy, D.

Worsnop, B. Xiang, and E. Williams (2011), Impact of fuel quality regulation and speed reductions on shipping emissions: Implications for climate and air quality, *Environ. Sci. Tech.*, *45* (20), 9052-9060.

Lack, D.A., J.J. Corbett, T. Onasch, B. Lerner, P. Massoli, P.K. Quinn, T.S. Bates, D.S. Covert, D. Coffman, B. Sierau, S. Herndon, J. Allan, T. Baynard, E. Lovejoy, A.R. Ravishankara, and E. Williams (2009), Particulate emissions from commercial shipping: Chemical, physical, and optical properties, *J. Geophys. Res.-[Atmos.]*, *114*, D00F04, doi:10.1029/2008JD011300.

Langley, L., W.R. Leaitch, U. Lohmann, N.C. Shantz, and D. Worsnop (2010), Contributions from DMS and ship emissions to CCN observed over the summertime North Pacific, *Atmos. Chem. Phys.*, *10*, 1287-1314.

Leaitch, W.R., G.A. Isaac, J.W. Strapp, C.M. Banic, and H.A. Wiebe (1992), The Relationship between Cloud Droplet Number Concentrations and Anthropogenic Pollution - Observations and Climatic Implications, *J. Geophys. Res.-[Atmos.]*, *97* (D2), 2463-2474.

Leck, C., and E.K. Bigg (1999), Aerosol production over remote marine areas: A new route, *Geophys. Res. Lett.*, *26* (23), 3577-3580.

Leck, C., and E.K. Bigg (2005a), Biogenic particles in the surface microlayer and overlaying atmosphere in the central Arctic Ocean during summer, *Tellus Ser. B*, *57* (4), 305-316.

Leck, C., and E.K. Bigg (2005b), Source and evolution of the marine aerosol: A new perspective, *Geophys. Res. Lett.*, *32* (19), L19803, doi:10.1029/2005GL023651.

Leck, C., and E.K. Bigg (2007), A modified aerosol–cloud–climate feedback hypothesis, *Environ. Chem.*, *4*, 400-403.

Leck, C., and E.K. Bigg (2008), Comparison of sources and nature of the tropical aerosol with the summer high Arctic aerosol, *Tellus*, *60B*, 118-126.

Leck, C., and E.K. Bigg (2010), New particle formation of marine biological origin, *Aerosol Sci. Tech.*, *44* (7), 570-577.

Leck, C., U. Larsson, L.E. Bagander, S. Johansson, and S. Hajdu (1990), Dimethyl sulfide in the Baltic Sea - Annual variability in relation to biological activity, *J. Geophys. Res.-[Oceans]*, *95* (C3), 3353-3363.

Leck, C., M. Norman, E.K. Bigg, and R. Hillamo (2002), Chemical composition and sources of the high Arctic aerosol relevant for cloud formation, *J. Geophys. Res.-[Atmos.]*, *107* (D12), 4135, doi:10.1029/2001JD001463.

Lelieveld, J., and J. Heintzenberg (1992), Sulfate cooling effect on climate through in-cloud processing of anthropogenic SO_2, *Science, 258*, 117-120.

Lohmann, U., and J. Feichter (2005), Global indirect aerosol effects: A review, *Atmos. Chem. Phys., 5*, 715-737.

Martensson, E.M., E.D. Nilsson, G. de Leeuw, L.H. Cohen, and H.C. Hansson (2003), Laboratory simulations and parameterization of the primary marine aerosol production, *J. Geophys. Res.-[Atmos.], 108* (D9), doi:10.1029/2002JD002263.

Massoli, P., T.S. Bates, P.K. Quinn, D.A. Lack, T. Baynard, B.M. Lerner, S.C. Tucker, J. Brioude, A. Stohl, and E.J. Williams (2009), Aerosol optical and hygroscopic properties during TexAQS-GoMACCS 2006 and their impact on aerosol direct radiative forcing, *J. Geophys. Res.-[Atmos.], 114*, D00F07, doi:10.1029/2008JD011604.

McFiggans, G., P. Artaxo, U. Baltensperger, H. Coe, M.C. Facchini, G. Feingold, S. Fuzzi, M. Gysel, A. Laaksonen, U. Lohmann, T.F. Mentel, D.M. Murphy, C.D. O'Dowd, J.R. Snider, and E. Weingartner (2006), The effect of physical and chemical aerosol properties on warm cloud droplet activation, *Atmos. Chem. Phys., 6*, 2593-2649.

McMurray, P.H. (2000), A review of atmospheric aerosol measurements, *Atmos Environ, 34*, 1959-1999.

Meskhidze, N., and A. Nenes (2006), Phytoplankton and cloudiness in the Southern Ocean, *Science, 314* (5804), 1419-1423.

Middlebrook, A.M., D.M. Murphy, and D.S. Thomson (1998), Observations of organic material in individual marine particles at Cape Grim during the First Aerosol Characterization Experiment (ACE 1), *J. Geophys. Res.-[Atmos.], 103* (D13), 16475-16483.

Moffet, R.C., and K.A. Prather (2009), In-situ measurements of the mixing state and optical properties of soot with implications for radiative forcing estimates, *PNAS, 106* (29), 11872-11877.

Monahan, E.C., C.W. Fairall, K.L. Davidson, and P.J. Boyle (1983), Observed interrelations between 10m winds, ocean whitecaps and marine aerosols, *Quarterly Journal of the Royal Meteorological Society, 109* (460), 379-392.

Murphy, D.M., D.J. Cziczo, K.D. Froyd, P.K. Hudson, B.M. Matthew, A.M. Middlebrook, R.E. Peltier, A. Sullivan, D.S. Thomson, and R.J. Weber (2006),

Single-particle mass spectrometry of tropospheric aerosol particles, *J. Geophys. Res.-[Atmos.]*, *111* (D23), D23S32, doi:10.1029/2006JD007340.

Murphy, S.M.A., H.; Sorooshian, A.; Padro, L. T.; Gates, S.W. H.; Hersey, W. A.; Jung, H.; Miller, J. W.; Cocker, D. R., and A.J. Nenes, H. H.; Flagan, R. C.; Seinfeld, J. H. (2009), Comprehensive simultaneous shipboard and airborne characterization of exhaust from a modern container ship at sea., *Environ. Sci. Tech.*, *43* (13), 4626-4640.

Noble, C.A., and K.A. Prather (1996), Real-time measurement of correlated size and composition profiles of individual atmospheric aerosol particles, *Environ. Sci. Tech.*, *30* (9), 2667-2680.

Novakov, T., C. Rivera-Carpio, J.E. Penner, and C.F. Rogers (1994), The effect of anthropogenic sulfate aerosols on marine cloud droplet concentrations, *Tellus, 46B*, 132-141.

O'Dowd, C.D., and G. De Leeuw (2007), Marine aerosol production: a review of the current knowledge, *Phil. Trans. A, 365* (1856), 1753-1774.

O'Dowd, C.D., M.C. Facchini, F. Cavalli, D. Ceburnis, M. Mircea, S. Decesari, S. Fuzzi, Y.J. Yoon, and J.P. Putaud (2004), Biogenically driven organic contribution to marine aerosol, *Nature, 431* (7009), 676-680.

O'Dowd, C.D., M. Geever, M.K. Hill, M.H. Smith, and S.G. Jennings (1998), New particle formation: Nucleation rates and spatial scales in the clean marine coastal environment, *Geophys. Res. Lett.*, *25* (10), 1661-1664.

O'Dowd, C.D., and T. Hoffmann (2005), Coastal new particle formation: A review of the current state-of-the-art, *Environ. Chem.*, *2*, 245-255.

O'Dowd, C.D., M.H. Smith, I.E. Consterdine, and J.A. Lowe (1997), Marine aerosol, sea-salt, and the marine sulphur cycle: A short review, *Atmos. Environ.*, *31* (1), 73-80.

Ooki, A., K. Miura, and M. Uematsu (2003), The increase of biogenic sulfate aerosol and particle number in marine atmosphere over the northwestern North Pacific, *J. Oceanogr.*, *59* (6), 799-807.

Orellana, M.V., and P. Verdugo (2003), Ultraviolet radiation blocks the organic carbon exchange between the dissolved phase and the gel phase in the ocean, *Limnol. Oceangr.*, *48* (4), 1618-1623.

Ovadnevaite, J., C. O'Dowd, M. Dall'Osto, D. Ceburnis, D.R. Worsnop, and H. Berresheim (2011), Detecting high contributions of primary organic matter to marine aerosol: A case study, *Geophys. Res. Lett.*, *38*, L02807, doi:10.1029/2010GL046083.

Pinkerton, K.E., Y.M. Zhou, S.V. Teague, J.L. Peake, R.C. Walther, I.M. Kennedy, V.J. Leppert, and A.E. Aust (2004), Reduced lung cell proliferation following short-term exposure to ultrafine soot and iron particles in neonatal rats: Key to impaired lung growth? *Inhalation Toxicology, 16*, 73-81.

Pirjola, L., C.D. O'Dowd, I.M. Brooks, and M. Kulmala (2000), Can new particle formation occur in the clean marine boundary layer? *J. Geophys. Res.*, *105* (D21), 26531-26546.

Pope, C.A., and D.W. Dockery (2006), Health effects of fine particulate air pollution: Lines that connect, *Journal of the Air & Waste Management Association, 56* (6), 709-742.

Poschl, U. (2005), Atmospheric aerosols: Composition, transformation, climate and health effects, *Angewandte Chemie-International Edition*, *44* (46), 7520-7540.

Posfai, M., J.R. Anderson, P.R. Buseck, and H. Sievering (1999), Soot and sulfate aerosol particles in the remote marine troposphere, *J. Geophys. Res.-[Atmos.]*, *104* (D17), 21685-21693.

Posfai, M., J. Li, J.R. Anderson, and P.R. Buseck (2003), Aerosol bacteria over the southern ocean during ACE-1, *Atmos. Res.*, *66* (4), 231-240.

Prather, K.A., T. Nordmeyer, and K. Salt (1994), Real-Time Characterization of Individual Aerosol-Particles Using Time-of-Flight Mass-Spectrometry, *Anal. Chem.*, *66* (9), 1403-1407.

Pratt, K.A., and K.A. Prather (2011a), Mass spectrometry of atmospheric aerosols—Recent developments and applications. Part I: Off-line mass spectrometry techniques, *Mass Spectrometry Reviews*, DOI 10.1002/mas.20330.

Pratt, K.A., and K.A. Prather (2011b), Mass spectrometry of atmospheric aerosols—Recent developments and applications. Part II: On-line mass spectrometry techniques, *Mass Spectrometry Reviews*, DOI 10.1002/mas.20330.

Quinn, P.K., and T.S. Bates (2005), Regional aerosol properties: Comparisons of boundary layer measurements from ACE 1, ACE 2, Aerosols99, INDOEX, ACE Asia, TARFOX, and NEAQS, *J. Geophys. Res.*, *110* (D14202), doi:10.1029/2004JD004755.

Quinn, P.K., and T.S. Bates (2011), The case against climate regulation via oceanic phytoplankton sulfur emissions, *Nature, 480*, 51-56.

Quinn, P.K., T.S. Bates, T. Baynard, A.D. Clarke, T.B. Onasch, W. Wang, M.J. Rood, E. Andrews, J. Allan, C.M. Carrico, D. Coffman, and D. Worsnop (2005), Impact of particulate organic matter on the relative humidity dependence of light scattering: A simplified parameterization, *Geophys. Res. Lett.*, *32* (22), L22809, doi:10.1029/2005GL024322.

Quinn, P.K., T.S. Bates, D.J. Coffman, and D.S. Covert (2008), Influence of particle size and chemistry on the cloud nucleating properties of aerosols, *Atmos. Chem. Phys.*, *8* (4), 1029-1042.

Raes, F., R. Van Dingenen, E. Vignati, J. Wilson, J.P. Putaud, J.H. Seinfeld, and P. Adams (2000), Formation and cycling of aerosols in the global troposphere, *Atmos. Environ.*, *34* (25), 4215-4240.

Rinaldi, M., S. Decesari, C. Carbone, E. Finessi, S. Fuzzi, D. Ceburnis, C.D. O'Dowd, J. Sciare, J.P. Burrows, M. Vrekoussis, B. Ervens, K. Tsigaridis, and M.C. Facchini (2011), Evidence of a natural marine source of oxalic acid and a possible link to glyoxal, *J. Geophys. Res.*, *116*, D16204, doi:10.1029/2011JD015659.

Rinaldi, M., S. Decesari, D. Finessi, L. Giulianelli, C. Carbone, S. Fuzzi, C.D. O'Dowd, D. Ceburnis, and M.C. Facchini (2010), Primary and secondary organic marine aerosol and oceanic biological activity: Recent results and new perspectives for future studies, *Advances in Meteorology*, doi:10.1155/2010/310682.

Roberts, G.C., P. Artaxo, J.C. Zhou, E. Swietlicki, and M.O. Andreae (2002), Sensitivity of CCN spectra on chemical and physical properties of aerosol: A case study from the Amazon Basin, *J. Geophys. Res.-[Atmos.]*, *107* (D20), 8070, doi:10.1029/2001JD000583.

Rosenfeld, D., U. Lohmann, G.B. Raga, C.D. O'Dowd, M. Kulmala, S. Fuzzi, A. Reissell, and M.O. Andreae (2008), Flood or drought: How do aerosols affect precipitation? *Science*, *321* (5894), 1309-1313.

Russell, L.M., R. Bahadur, and P.J. Ziemann (2011), Identifying organic aerosol sources by comparing functional group composition in chamber and atmospheric particles, *PNAS*, doi:10.1073/pnas.1006461108.

Russell, L.M., L.N. Hawkins, A.A. Frossard, P.K. Quinn, and T.S. Bates (2010), Carbohydrate-like composition of submicron atmospheric particles and their production from ocean bubble bursting, *PNAS*, *107* (15), 6652-6657.

Russell, L.M., K.J. Noone, R.J. Ferek, R.A. Pockalny, R.C. Flagan, and J.H. Seinfeld (2000), Combustion organic aerosol as cloud condensation nuclei in ship tracks, *American Meteorological Society*, 2591-2606.

Russell, L.M., J.H. Seinfeld, R.C. Flagan, R.J. Ferek, D.A. Hegg, P.V. Hobbs, W. Wobrock, A.I. Flossmann, C.D. O'Dowd, K.E. Nielsen, and P.A. Durkee (1999), Aerosol dynamics in ship tracks, *J. Geophys. Res.-[Atmos.]*, *104* (D24), 31077-31095.

Russell, L.M., S. Takahama, S. Liu, L.N. Hawkins, D.S. Covert, P.K. Quinn, and T.S. Bates (2009), Oxygenated fraction and mass of organic aerosol from direct emission and atmospheric processing measured on the R/V Ronald Brown during TEXAQS/GoMACCS 2006, *J. Geophys. Res.-[Atmos.]*, *114*, D00F05, doi:10.1029/2008JD011275.

Saxena, P., L.M. Hildemann, P.H. McMurry, and J.H. Seinfeld (1995), Organics Alter Hygroscopic Behavior of Atmospheric Particles, *J. Geophys. Res.-[Atmos.]*, *100* (D9), 18755-18770.

Schnaiter, M., C. Linke, O. Mohler, K.H. Naumann, H. Saathoff, R. Wagner, U. Schurath, and B. Wehner (2005), Absorption amplification of black carbon internally mixed with secondary organic aerosol, *J. Geophys. Res.-[Atmos.]*, *110* (D19), D19204, doi:10.1029/2005JD006046.

Seinfeld, J.H., and S.N. Pandis, *Atmospheric Chemistry and Physics*, John Wiley & Sons, Inc., Hoboken, New Jersey, 2006.

Sellegri, K., C.D. O'Dowd, Y.J. Yoon, S.G. Jennings, and G. de Leeuw (2006), Surfactants and submicron sea spray generation, *J. Geophys. Res.-[Atmos.]*, *111* (D22), doi:10.1029/2005JD006658.

Shindell, D.T., G. Faluvegi, D.M. Koch, G.A. Schmidt, N. Unger, and S.E. Bauer (2009), Improved attribution of climate forcing to emissions, *Science*, *326* (5953), 716-718.

Silva, P.J., and K.A. Prather (2000), Interpretation of mass spectra from organic compounds in aerosol time-of-flight mass spectrometry, *Anal. Chem.*, *72* (15), 3553-3562.

Slingo, A. (1990), Sensitivity of the Earth's radiation budget to changes in low clouds, *Nature*, *343* (6253), 49-51.

Song, X.H., P.K. Hopke, D.P. Fergenson, and K.A. Prather (1999), Classification of single particles analyzed by ATOFMS using an artificial neural network, ART-2a, *Anal. Chem.*, *71* (4), 860-865.

Sorooshian, A., L.T. Padro, A. Nenes, G. Feingold, A. McComiskey, S.P. Hersey, H. Gates, H.H. Jonsson, S.D. Miller, G.L. Stephens, R.C. Flagan, and J.H. Seinfeld (2009), On the link between ocean biota emissions, aerosol, and maritime clouds:

Airborne, ground, and satellite measurements off the coast of California, *Glob. Biogeochem. Cy.*, *23*, GB4007, doi:10.1029/2009GB003464.

Stevens, B., D. Lenschow, G. Vali, H. Gerber, A.R. Bandy, B. Blomquist, J.-L. Brenguier, C.S. Bretherton, F. Burnet, T. Campos, S. Chai, I. Faloona, D. Friesen, S. Haimov, K. Laursen, D.K. Lilly, S.M. Loehrer, S.P. Malinowski, B. Morley, M.D. Petters, D.C. Rogers, L.M. Russell, V. Savic-Jovcic, J.R. Snider, D. Straub, M.J. Szumowski, H. Takagi, D. Thornton, M. Tschudi, C. Twohy, M. Wetzel, and M.C. van Zanten (2003), Dynamics and chemistry of marine stratocumulus: DYCOMS-II, *American Meteorological Society*, 579-593.

Sullivan, R.C., S.A. Guazzotti, D.A. Sodeman, Y. Tang, G.R. Carmichael, and K.A. Prather (2007), Mineral dust is a sink for chlorine in the marine boundary layer, *Atmos Environ*, *41*, 7166-7179.

Sullivan, R.C., and K.A. Prather (2005), Recent advances in our understanding of atmospheric chemistry and climate made possible by on-line aerosol analysis instrumentation, *Anal. Chem.*, *77* (12), 3861-3885.

Sullivan, R.C., and K.A. Prather (2007), Investigations of the diurnal cycle and mixing state of oxalic acid in individual particles in Asian aerosol outflow, *Environ. Sci. Tech.*, *41* (23), 8062-8069.

Sunderman, F.W. (2001), Review: Nasal toxicity, carcinogenicity, and olfactory uptake of metals, *Annals of Clinical and Laboratory Science*, *31* (1), 3-24.

Tseng, R.-S., J.T. Viechnicki, R.A. Skop, and J.W. Brown (1992), Sea-to-air transfer of surface-active organic compounds by bursting bubbles, *J. Geophys. Res.*, *97* (C4), 5201-5206.

Twohy, C.H., M.D. Petters, J.R. Snider, B. Stevens, W. Tahnk, M. Wetzel, L. Russell, and F. Burnet (2005), Evaluation of the aerosol indirect effect in marine stratocumulus clouds: Droplet number, size, liquid water path, and radiative impact, *J. Geophys. Res.-[Atmos.]*, *110* (D8), doi:10.1029/2004JD005116.

Twomey, S. (1977), The influence of pollution on the shortwave albedo of clouds, *J. Atmos. Sci.*, *34* (7), 1149-1152.

Tyree, C.A., V.M. Hellion, O.A. Alexandrova, and J.O. Allen (2007), Foam droplets generated from natural and artificial seawaters, *J. Geophys. Res.-[Atmos.]*, *112*, D12204, doi:10.1029/2006JD007729.

Verdugo, P., A.L. Alldredge, F. Azam, D.L. Kirchman, U. Passow, and P.H. Santschi (2004), The oceanic gel phase: a bridge in the DOM-POM continuum, *Mar. Chem.*, *92* (1-4), 67-85.

Weber, R.J., P.H. McMurray, F.L. Eisele, and D.J. Tanner (1995), Measurement of expected nucleation precursor species and 3-500-nm diameter particles at Mauna Loa Observatory, Hawaii, *J. Atmos. Sci.*, *52* (12), 2242-2257.

Wells, M.L. (1998), Marine colloids: A neglected dimension, *Nature, 391*, 530-531.

Wiedensohler, A., D.S. Covert, E. Swietlicki, P. Aalto, J. Heintzenberg, and C. Leck (1996), Occurrence of an ultrafine particle mode less than 20 nm in diameter in the marine boundary layer during Arctic summer and autumn, *Tellus Ser. B, 48* (2), 213-222.

Wise, M.E., E.J. Freney, C.A. Tyree, J.O. Allen, S.T. Martin, L.M. Russell, and P.R. Buseck (2009), Hygroscopic behavior and liquid-layer composition of aerosol particles generated from natural and artificial seawater, *J. Geophys. Res.-[Atmos.]*, *114*, D03201, doi:10.1029/2008JD010449.

Chapter 2

2. Unique Ocean-Derived Particles Serve as a Proxy for Changes in Ocean Chemistry

2.1 Synopsis

Oceans represent a significant natural source of gases and particles to the atmosphere. Relative to gas phase compounds, less is known regarding the influence of changes in biological activity in the ocean on the chemistry of sea spray aerosols produced in marine environments. To gain insight into the influence of ocean biology and chemistry on atmospheric aerosol chemistry, simultaneous real-time measurements were made of atmospheric aerosol size and chemical mixing-state, gas phase dimethyl sulfide (DMS), as well as seawater DMS and chlorophyll *a*. In three different marine environments with elevated chlorophyll *a* and DMS, unique Mg particles were detected containing Mg^{2+}, Ca^{2+}, K^{+}, and organic carbon. These particles were segregated from sea salt particles highlighting that two subpopulations within the sea spray were being ejected from the ocean. Strong temporal correlations were observed between these unique ocean-derived particles and freshly emitted sea salt particles (R^2 = 0.86), particularly as wind speed increased to at least 10 m/s, and atmospheric DMS (R^2 = 0.76). Time series correlations between ocean measurements and atmospheric aerosol chemistry suggest that chlorophyll *a* and DMS serve as indicators of changes in the chemistry of the ocean, most likely an increase in organic material, which is directly reflected in the single particle mixing-state. This is the first time such *real-time* correlations are shown between

ocean chemistry and atmospheric aerosol mixing-state. The reasons behind these observed changes in aerosol chemistry are critical for understanding the heterogeneous reactivity, water uptake, and cloud forming potential of sea spray aerosols.

2.2 Introduction

Aerosols influence global climate directly by scattering and absorbing incoming solar radiation and indirectly by acting as cloud condensation nuclei (CCN) [*Lohmann and Feichter*, 2005; *Poschl*, 2005]. The size and chemical composition of aerosols influence whether particles can act as CCN and participate in cloud droplet formation [*McFiggans et al.*, 2006; *Quinn et al.*, 2008]. In the marine environment, biological activity has been proposed to change the chemical composition of marine aerosols through secondary oxidation reactions involving the gaseous compound dimethyl sulfide (DMS) formed from the enzymatic cleavage of phytoplankton-derived dimethylsulfoniopropionate (DMSP) [*Andreae and Crutzen*, 1997; *Bates et al.*, 1992] and, more recently, by changing the chemical composition of primary sea spray aerosol [*O'Dowd et al.*, 2004]. Sea spray particles are directly emitted to the atmosphere primarily from air bubbles formed by breaking waves [*O'Dowd and De Leeuw*, 2007]. Bursting bubbles result in the formation of jet drops, which result from the breakup of the vertical jet of water that forms after the bubble cavity collapses, and the more numerous film drops, which result from the collapse of the thin film surrounding the bubble [*Blanchard and Woodcock*, 1957]. Bubble bursting can be enhanced by high wind velocities that increase whitecap production [*Monahan et al.*, 1983] and by the impact of raindrops on the ocean surface [*Marks*, 1990]. In addition to sea salt, organic material

produced by marine biota can be ejected to the atmosphere from the bubble bursting mechanism. As bubbles rise in the water column, they can scavenge surface active material including organic matter and marine organisms, which become enriched in ejected sea spray particles compared to bulk seawater [*Aller et al.*, 2005; *Blanchard*, 1964; *Blanchard and Syzdek*, 1970; *Cloke et al.*, 1991; *Duce and Hoffman*, 1976; *Zhou et al.*, 1998]. Oceanic biological activity provides a source of both organisms as well as organic material to the ocean [*Aluwihare and Repeta*, 1999; *Passow*, 2002; *Zhou et al.*, 1998], and thus can directly impact the chemical composition of sea spray particles. A number of publications highlight the influence of biological activity on the chemical composition of marine aerosols through the enrichment of organic material, particularly in submicron particles [*Bigg*, 2007; *Bigg and Leck*, 2001; *Bigg and Leck*, 2008; *Blanchard*, 1964; *Cavalli et al.*, 2004; *Duce and Hoffman*, 1976; *Facchini et al.*, 2008; *Keene et al.*, 2007; *Leck and Bigg*, 2005a; *Leck and Bigg*, 2005b; *Leck and Bigg*, 2008; *Leck et al.*, 2002; *Mayol-Bracero et al.*, 2001; *Middlebrook et al.*, 1998; *Novakov et al.*, 1997; *O'Dowd et al.*, 2004; *Oppo et al.*, 1999; *Russell et al.*, 2010; *Yoon et al.*, 2007]. Primary organic material resulting from bubble bursting is water insoluble in nature [*Ceburnis et al.*, 2008; *Leck and Bigg*, 2005a; *Facchini et al.*, 2008]. These primary organic particles are proposed to grow large enough to act as CCN through the condensation of DMS oxidation products potentially linking marine biota, sea spray aerosol, clouds, and climate [*Leck and Bigg*, 2005a; *Leck and Bigg*, 2005b; *Leck and Bigg*, 2007].

Exopolymeric secretions (EPS) represent one large source of organic material in the ocean. EPS constitutes ~10% of the dissolved organic material (DOM) pool (7×10^{16} gC) [*Chin et al.*, 1998; *Orellana et al.*, 2007; *Orellana and Verdugo*, 2003; *Verdugo et al.*, 2008] that, unlike most DOM, is bioavailable making EPS one of the most significant contributors to the global carbon cycle [*Verdugo et al.*, 2008]. EPS or microgels are the result of gel assembly/dispersion equilibria from dissolved polymers (namely polysaccharides, proteins, and lipids) [*Chin et al.*, 1998; *Verdugo et al.*, 2004; *Wells*, 1998]. The polymer network of these microgels has been shown to be stabilized through ionic bonding with the use of divalent cations (Ca^{2+}, Mg^{2+}) [*Chin et al.*, 1998; *Verdugo et al.*, 2004; *Wells*, 1998]; the detection of EPS in the atmosphere has been highlighted in previous publications [*Bigg and Leck*, 2001; *Bigg and Leck*, 2008; *Leck and Bigg*, 2005a; *Leck and Bigg*, 2005b; *Leck and Bigg*, 2008; *Leck et al.*, 2002]. Hence, in addition to being a source of organic carbon, atmospheric enrichment of inorganic ions associated with EPS could also occur in the marine environment. However, in contrast to the observed enrichment of organic material, enrichment of inorganic ions in sea spray aerosol compared to bulk seawater has been difficult to discern particularly in ambient measurements. The lack of conclusive evidence stems primarily from the inability of measurement methods to distinguish between inorganic ions directly ejected in marine particles versus input into the ocean from inorganic ions in atmospheric aerosols such as dust [*Duce and Hoffman*, 1976; *Hoffman et al.*, 1980]. Hence, without being able to directly determine the origin of the particles (i.e. ocean vs. atmosphere), it is impossible to positively correlate changes in inorganic constituents in atmospheric aerosols with changes in ocean chemistry induced by biological activity.

Understanding how ocean-derived organic compounds and inorganic ions are distributed within individual sea spray particles (i.e. whether they are internally or externally mixed with other chemical compounds) is a requirement for properly assessing the heterogeneous reactivity, water uptake, and cloud nucleating abilities of marine-derived particles. Bulk, filter-based techniques collect chemical information over a relatively broad size range and provide an average picture of the ambient aerosol that may not be representative of any individual particles within the aerosol population. *O'Dowd et al.* [2004] hypothesized that the manner in which submicron organic material was mixed with sea spray aerosol would greatly impact the cloud droplet number concentration that could potentially be formed over the ocean during periods of high biological activity. Single-particle techniques elucidate the chemical mixing-state of individual particles. However, these measurements have been extremely scarce in marine environments. Electron microscopy has been used in marine environments to detect both single particles composed of organic material and bacteria in the absence of sea salt as well as sea salt particles associated with surface active EPS [*Bigg and Leck*, 2001; *Bigg and Leck*, 2008; *Leck and Bigg*, 2005a; *Leck and Bigg*, 2005b; *Leck and Bigg*, 2008; *Leck et al.*, 2002; *Posfai et al.*, 2003]; real-time single particle mass spectrometry observed the presence of organic material internally mixed with sea salt particles [*Middlebrook et al.*, 1998]. No previous studies have simultaneously probed *real-time* changes in single particle chemistry and changes in ocean chemistry with high time resolution.

Aerosol time-of-flight mass spectrometry (ATOFMS) measurements of marine aerosols were conducted during three field campaigns in the eastern Pacific Ocean,

Indian Ocean, and the western Pacific Ocean. ATOFMS can be used to differentiate between particle sources (e.g. marine versus continental) and particle age (reacted versus fresh sea salt) [*Guazzotti et al.*, 2001] as well as determine the chemical mixing-state (e.g. organics internally or externally mixed with sea salt) of individual particles in real-time [*Noble and Prather*, 1996]. Observations of marine aerosols in all of these campaigns reveal unique chemical fingerprints of ocean-derived particles during time periods influenced by increased levels of phytoplankton biomass (chlorophyll *a*) and/or DMS concentrations. The ocean-derived individual particles described herein are characterized by an enrichment of Mg^{2+} and/or Ca^{2+}, and organic carbon with K^{+}. We hypothesize that the detection of these particles in the marine atmosphere serves as a proxy for changes in ocean chemistry. The atmospheric implications of these findings are discussed.

2.3 Experimental

2.3.1 Single-Particle Measurements Using Aerosol Time-of-Flight Mass Spectrometry

ATOFMS measurements were made aboard the NOAA RV Ronald H. Brown during the Indian Ocean Experiment (INDOEX) in March 1999 [*Lelieveld et al.*, 2001] and the Asian Pacific Regional Aerosol Characterization Experiment (ACE-Asia) from March-April 2001 [*Huebert et al.*, 2003]. Ground-based measurements were made during the Cloud Indirect Effects Experiment (CIFEX) at the coastal site Trinidad Head, CA in April 2004. The sampling inlet for all three studies was heated to control relative humidity (RH) at 55% [*Bates et al.*, 2004]. The details of each of these campaigns can be found in Table 2.1 and the cruise tracks of ACE-Asia and INDOEX can be found in

Figure 2.1. ATOFMS makes real-time measurements of the aerodynamic size and chemical composition of individual particles between 0.2-3 um diameter. A full description of the instrument has been given previously [*Gard et al.*, 1997; *Prather et al.*, 1994]. Briefly, aerosols are continuously pulled by vacuum into the instrument through a nozzle inlet and interface region, which collimates the particles into a narrow beam. Each particle passes through two continuous wave lasers (532 nm) separated by a known distance, producing scattered light signals, which are detected by two photomultiplier tube detectors. The time taken for each particle to traverse between the laser beams provides a measure of the aerodynamic diameter of each particle. The transit time and light signals are also used to trigger a third pulsed laser passing through the ion source region of a time-of-flight mass spectrometer. When each sized particle arrives in the ion source region, a pulsed UV laser fires to induce laser desorption/ionization, producing positive and negative ion mass spectra for each particle. The mass spectra show the chemical associations within each particle and can be coupled with the size information to derive size-resolved composition distributions of particles. Size-resolved chemical composition was monitored continuously and subsequently averaged into 1-hour time bins; data is presented in this paper as day of year (DOY).

The single particle mass spectra generated by this technique were imported into Matlab (The MathWorks, Inc.) using a software toolkit, YAADA [*Allen*, 2002]. An adaptive neural network (ART-2a), was used to classify particles based on the mass spectral peaks and intensities into distinct “clusters” indicative of particle sources and chemistry [*Noble and Prather*, 1996; *Song et al.*, 1999]. Each ion peak assignment

Table 2.1: Details of the INDOEX, ACE-Asia, and CIFEX field campaigns.

Campaign	Ocean Basin	Platform	Latitude	Longitude	Date	Inlet RH
INDOEX	Indian Ocean	Ship	6.07 N to 12.7 S	75 E to 72.03 E	Mar. 1999	55%
ACE-Asia	Pacific Ocean	Ship	39.4 N to 30.5 N	173.92 E to 126.14 E	Mar.-Apr. 2001	55%
CIFEX	Pacific Ocean	Ground	41.05 N	124.15 W	Mar.-Apr. 2004	55%

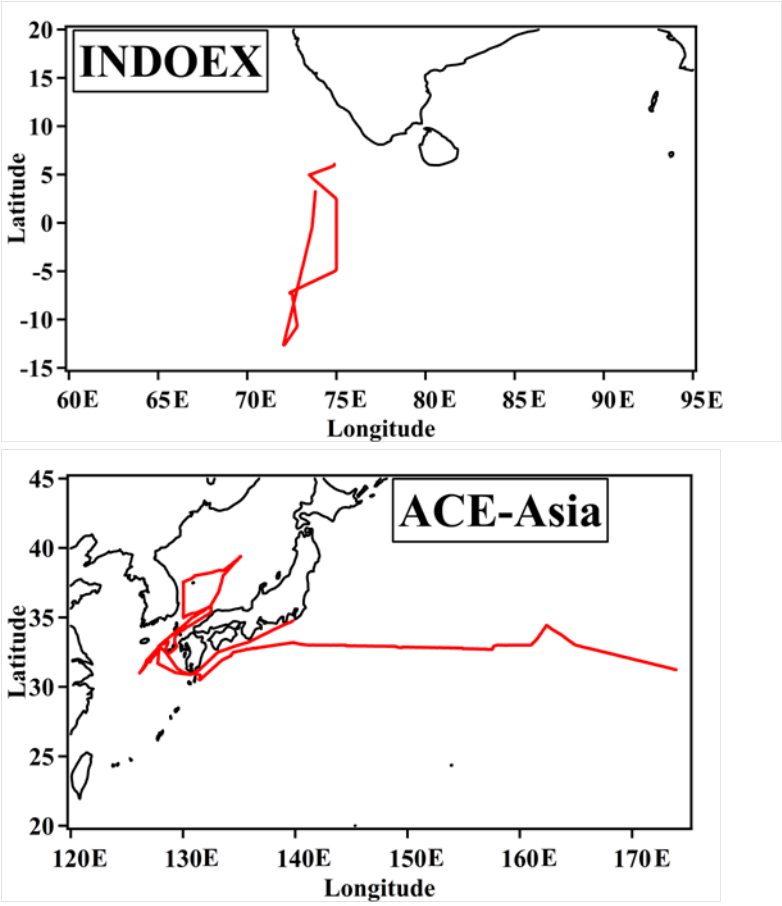

Figure 2.1: Cruise tracks for INDOEX and ACE-Asia.

presented in this paper corresponds to the most likely ion produced at a given mass-to-charge (*m/z*) (see Table 2.2). Particle types described in this paper are defined by characteristic ion peaks and/or possible sources and do not reflect all of the compounds present within a particular particle class.

2.3.2 Laboratory Bubble Bursting Experiments

Natural seawater was collected on June 15, 2005 at the Scripps Institution of Oceanography pier and immediately used to generate sea spray aerosol particles in the laboratory. The collected seawater sample was divided into two aliquots and particle generation was performed either by atomizing or bubbling the seawater solution. The details of the apparatus used to generate sea spray aerosol through bubble bursting can be found in Moore et al. [2011]. Briefly, the apparatus consisted of a glass jar (ID ~ 70 mm, height~120 mm), L-shaped glass tube with a fritted glass head (size of frit: ID = 5 mm, L = 10 mm, maximum pore size = 25-50 um), and gas dispersion tube for particle carrier flow. Approximately 150 mL of seawater was added to the glass jar and the fritted glass bubbler head was placed approximately 15 mm below the surface of the seawater. A tube used to disperse the carrier gas was placed about 25 mm above the surface of the seawater sample. Flow to the fritted glass bubbler head and carrier gas dispersion tube was regulated by mass flow controllers at 0.04 lpm and 1.0 lpm, respectively. For the atomizing generation method, ~150 mL of seawater was used; the tip of the atomizer spraying head, where sample seawater was aspirated, was placed about 10-15 mm below the surface of the seawater. To maintain the aspiration of seawater and subsequent atomizing, a flow rate of 1.1 lpm was used in this experiment. The particle concentration

Table 2.2: Assignments of ion peaks for a given mass-to-charge.

Mass-to-Charge	Assignment
12	C^+
15	CH_3^+
19	H_3O^+
23	Na^+
24,25,26	Mg^+ (includes isotopes)
27	Al^+, $C_2H_3^+$, CHN^+
30	NO^+
36	C_3^+
39	K^+, $C_3H_3^+$
40	Ca^+
41	$C_3H_5^+$, $Na{\cdot}H_2O^+$
43	$C_2H_3O^+$
50	$C_4H_2^+$
56	Fe^+, CaO^+
57	$CaOH^+$, $K(H_2O)^+$
59	$Na{\cdot}(H_2O)_2^+$
62	Na_2O^+
63	Na_2OH^+, $C_5H_3^+$
75	$K{\cdot}(H_2O)_2^+$
77	$Na{\cdot}(H_2O)_3^+$, $C_6H_5^+$
81,83	Na_2Cl^+ (includes isotopes)
91	$C_7H_7^+$
95	$Na{\cdot}(H_2O)_4^+$

was reduced by subtracting 1.08 lpm of the atomizer output flow leaving only 0.02 lpm of the sample gas stream to reach the flow tube for further drying. This modification also produced a particle concentration similar to that generated by bubbling and was done to avoid coincidence errors in the ATOFMS where one particle causes the first light scattering signal and a different, faster particle, causes the second light scattering signal.

The generated sea spray droplets were then introduced to a glass flow tube (ID = 48 mm, L=1500 mm) where RH was kept low (RH ~1-3% for atomizing and ~13-15% for bubbling) by the co-infusion of dry nitrogen gas (RH ~0%, 10 lpm for atomizing and 5 lpm for bubbling). The residence time of the gas stream in the flow tube was about 20-30 seconds, which was long enough to dry the liquid sea spray droplets. About 1 lpm of the airflow from the output of the flow tube was introduced to the ATOFMS. The excess sample flow was monitored by a RH/temperature sensor (HMP-237, Vaisala, Helsinki, Finland). Nitrogen gas was provided by a liquid nitrogen tank throughout the experiment and was filtered through a HEPA filter (HEPA capsule, Pall, NY, USA) to remove any particles. The temperature of the nitrogen gas was kept constant (25°C) by passing the gas through a temperature-regulated water bath. All experiments were conducted at room temperature.

2.3.3 Chlorophyll *a* and DMS Measurements

Measurements of DMS (seawater and atmospheric) were made during the ACE-Asia and INDOEX field campaigns; chlorophyll *a* was only measured during INDOEX. Chlorophyll *a* is a proxy for phytoplankton biomass. As stated earlier, DMS is produced from the enzymatic cleavage of DMSP. It should be noted that the production of DMS is

highly species specific [*Keller et al.*, 1989] and, as such, DMS concentrations are correlated with biological activity over large regional scales; however, DMS is typically poorly correlated with total phytoplankton biomass on smaller regional scales [*Bates et al.*, 1994; *Leck et al.*, 1990]. DMS concentrations also depend on complex biological and ecological processes [*Bates et al.*, 1994; *Leck et al.*, 1990] causing DMS to be a non-conservative tracer of biological activity.

Ambient air and seawater were analyzed for DMS concentrations using an automated collection/purge and trap system [*Bates et al.*, 2000; *Cooper and Saltzman*, 1993]. Air samples were pulled through a Teflon filter and tubing to the analytical system where 0.1 lpm of the 4 lpm flow were pulled through a KI solution in the analytical system to eliminate oxidant interferences. The air sample volume ranged from 0.5 to 1.5 L depending on the DMS concentration. Seawater samples were collected from the ship's seawater pumping system, which had an inlet located near the ship's bow at a depth of approximately 4 m. The samples were purged with hydrogen at 0.08 lpm for 5 min. Water vapor in either the air or purged seawater sample stream was removed by passing the flow through a -25°C Teflon tube filled with silanized glass wool. DMS was then trapped in a -25°C Teflon tube filled with Tenax. At the end of the sampling/purge period, the coolant was pushed away from the trap and the trap was electrically heated allowing DMS to desorb onto a DB-1 mega-bore fused silica column where the sulfur compounds were separated isothermally at 50°C and quantified with a sulfur chemiluminesence detector. System blanks were below detection limit. Water samples are reported in units of nanomoles/liter (nM). Air samples are reported in units

of parts-per-trillion by volume (ppt). The mixing ratios were calculated at standard temperature (25°C) and pressure (1013 mbar) such that 1 nanomole/m^3 equals 24.5 ppt.

Continuous chlorophyll *a* measurements were made using a Turner 10-AU-005 fluorometer with a flow-cell. The distilled water blank (generally 4 mV) was subtracted from the remaining data (millivolt readings from 4 to 3000). The detection limit (instrument resolution above zero) was 0.02 ug/L.

2.4 Results and Discussion

2.4.1 Chemical Composition of Particles in a Marine Environment

ATOFMS can be used to distinguish between the relative proportions of fresh and reacted sea salt particles in marine environments based on their characteristic mass spectra [*Gard et al.*, 1998]. Representative mass spectra of reacted and fresh sea salt particles taken from the CIFEX field campaign are shown in Figure 2.2. In addition to an intense sodium peak ($^{23}Na^+$), fresh, unreacted sea salt particle spectra contain intense chloride ions ($^{81, 83}Na_2Cl^+$, $^{35, 37}Cl^-$, $^{93, 95, 97}NaCl_2^-$, etc.) in addition to smaller ion peaks from minor constituents such as $^{24}Mg^+$, $^{39}K^+$, $^{40}Ca^+$, etc. Reacted sea salt contains secondary components including nitrate ($^{108}Na_2NO_3^+$, $^{46}NO_2^-$, $^{62}NO_3^-$) and sulfate ($^{165}Na_3SO_4^+$, $^{97}HSO_4^-$) formed by reactions of sea salt with acidic gases such as $HNO_{3(g)}$ and $H_2SO_{4(g)}$, which heterogeneously displace chloride [*Gard et al.*, 1998]. As such, distinctions between fresh and reacted particle types described herein are defined based on the relative intensities of chloride and nitrate peaks with fresh sea salt having more intense chloride peaks and reacted sea salt having more intense nitrate ion peaks.

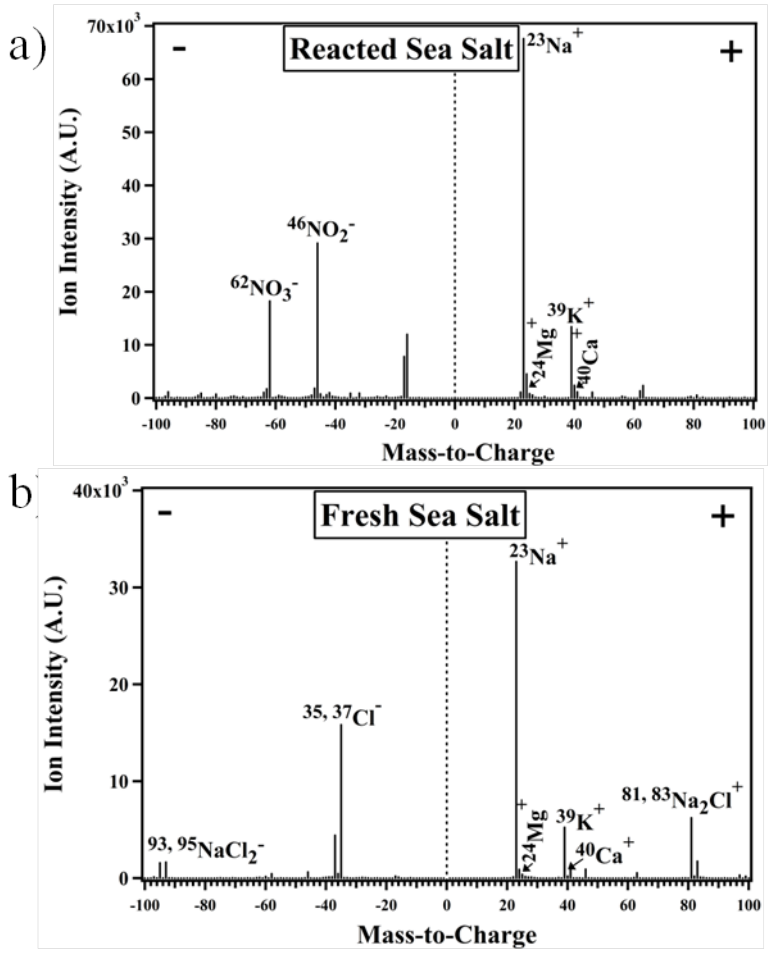

Figure 2.2: Mass spectra of individual particles representative of (a) reacted and (b) fresh sea salt.

Reacted sea salt occurs in marine regions with low wind speed as a background marine particle type and is typically not temporally correlated with freshly emitted sea salt particles.

2.4.2 Chemical Composition of Particles in Regions with Elevated DMS and/or Chlorophyll *a*

In addition to the fresh and reacted sea salt particles described above, particles measured in marine environments with elevated DMS and/or chlorophyll *a* revealed a unique and ubiquitous mass spectral signature containing Mg^{2+}, Ca^{2+}, K^{+}, and organic carbon [*Coffee*, 2002]. It is important to note that these particles have not been detected in non-marine environments. Their mass spectra contain intense peaks due to $^{24}Mg^{+}$ and/or $^{40}Ca^{+}$ as well as $^{39}K^{+}$ and less intense organic ions (e.g. $^{27}C_2H_3^{+}$, $^{29}C_2H_5^{+}$, $^{41}C_3H_5^{+}$, $^{43}C_2H_3O^{+}$, $^{50}C_4H_2^{+}$) (see Figure 2.3a and 2.3b for example mass spectra from INDOEX). Many of these particles lacked negative ion spectra even when a heated inlet was used to control RH at 55% [*Bates et al.*, 2004] during all three field campaigns. Using laser desorption/ionization as the ionization technique, a lack of negative ion spectra indicates the presence of particle-phase water [*Neubauer et al.*, 1997; *Neubauer et al.*, 1998]. In contrast, sea salt particles typically produced both positive and negative ion spectra at the same RH, indicating that these unique particles have hygroscopic properties that differ from pure sea salt. Since Mg was often observed as the most intense ion in these ocean-derived particles, we refer to these particles herein as Mg-type particles. The mass spectral characteristics used to define the Mg-type particles (e.g. intense ion signal from

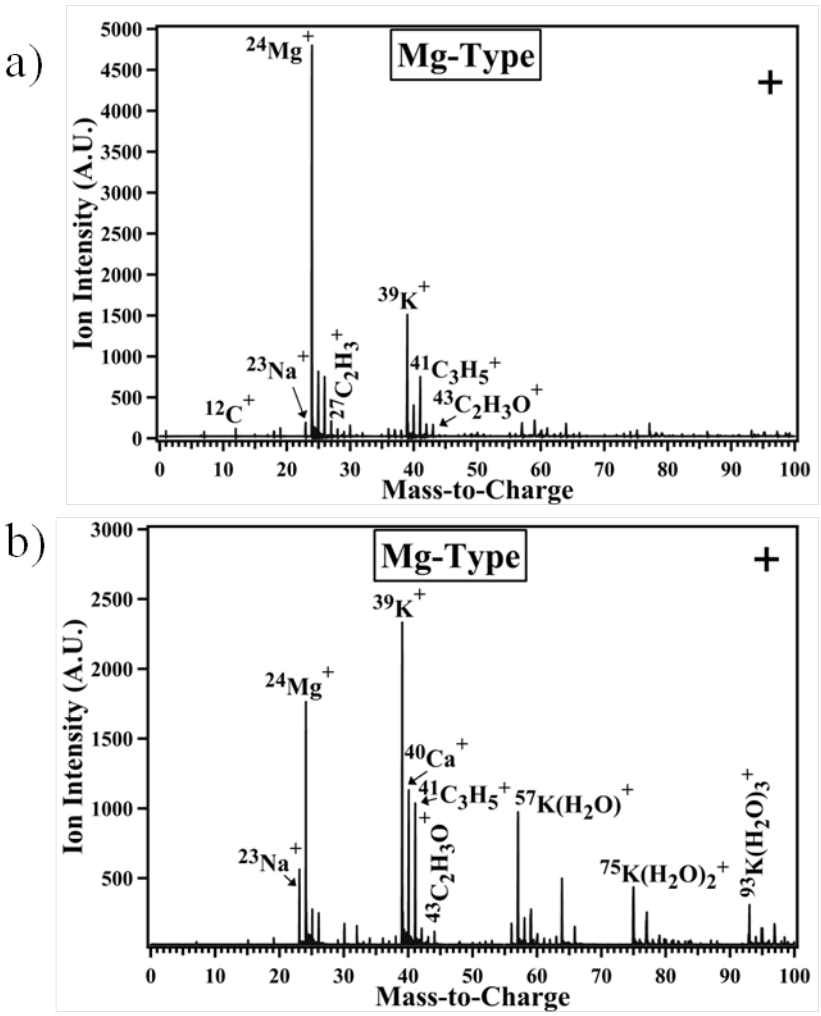

Figure 2.3: Top (a) and bottom (b) panel show mass spectra of individual representative Mg-type particles containing $^{24}Mg^+$, $^{39}K^+$, $^{40}Ca^+$, and organic carbon.

$^{24}Mg^{+}$ and/or $^{40}Ca^{+}$ as well as $^{39}K^{+}$, lower intensity ion signals from organic carbon peaks, and a lack of negative ion spectra) were common across all three field campaigns.

The Mg-type particles observed in marine environments are chemically distinct from sea salt and continental sources such as dust. In sea salt particles, the dominant peak is typically $^{23}Na^{+}$ rather than $^{24}Mg^{+}$ (see Figure 2.2b) [*Gross et al.*, 2000; *Guazzotti et al.*, 2001] due to the higher concentration of Na^{+} in seawater and also due to the lower ionization potential of Na versus Mg (5.14 eV versus 7.65 eV) [*Lide*, 2009] [*Gross et al.*, 2000]. However, the ratio of $^{23}Na^{+}$ to $^{24}Mg^{+}$ present in the Mg-type particles is reversed indicating that these particles represent a distinct aerosol population. Most Mg-containing dust particles also produce $^{27}Al^{+}$ and $^{56}Fe^{+}$ along with silicate peaks in the negative ion spectra [*Silva et al.*, 2000] (see Figure 2.4 for comparison). These peaks are absent from these marine Mg-type particles.

Further evidence that Mg-type and sea salt particles represent distinct sea spray aerosol populations is shown during CIFEX where Mg-type particles were enhanced in smaller particle sizes compared to sea salt particles. ATOFMS has known transmission biases based on the inlet design that affect the raw number size distribution obtained with the instrument [*Allen et al.*, 2000; *Dall'Osto et al.*, 2006]; however, number concentrations obtained from ATOFMS can be corrected using a scaling factor derived from a sizing instrument such as an aerodynamic particle sizer (APS) to obtain accurate particle counts for discrete size bins [*Qin et al.*, 2006]. Since the lower limit of the APS is 0.5 um, ATOFMS counts are only scaled down to this size even though the nozzle inlet ATOFMS can analyze particles down to 0.2 um. Figure 2.5 shows scaled particle

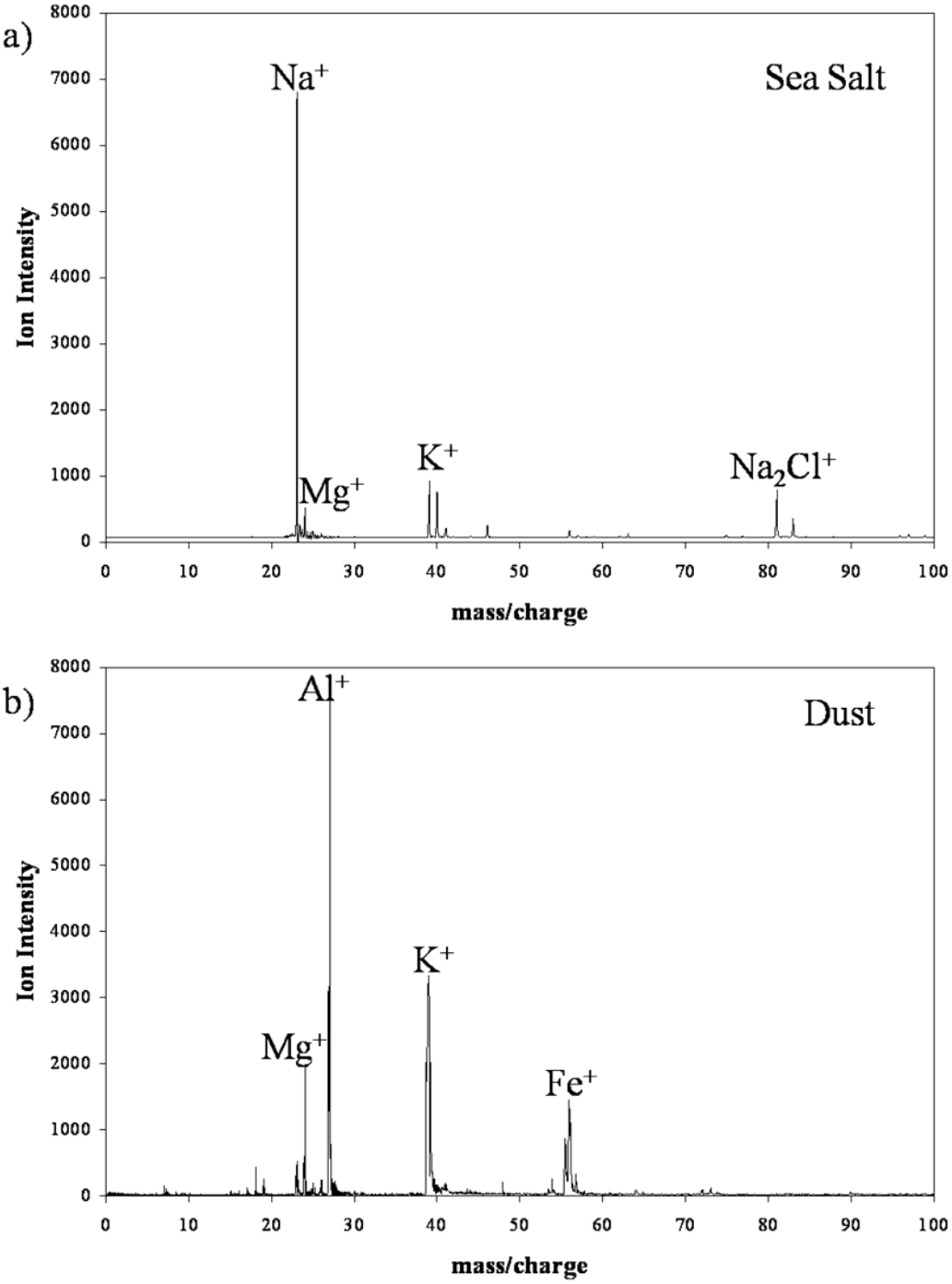

Figure 2.4: Positive ion mass spectra of representative (a) sea salt and (b) dust particles.

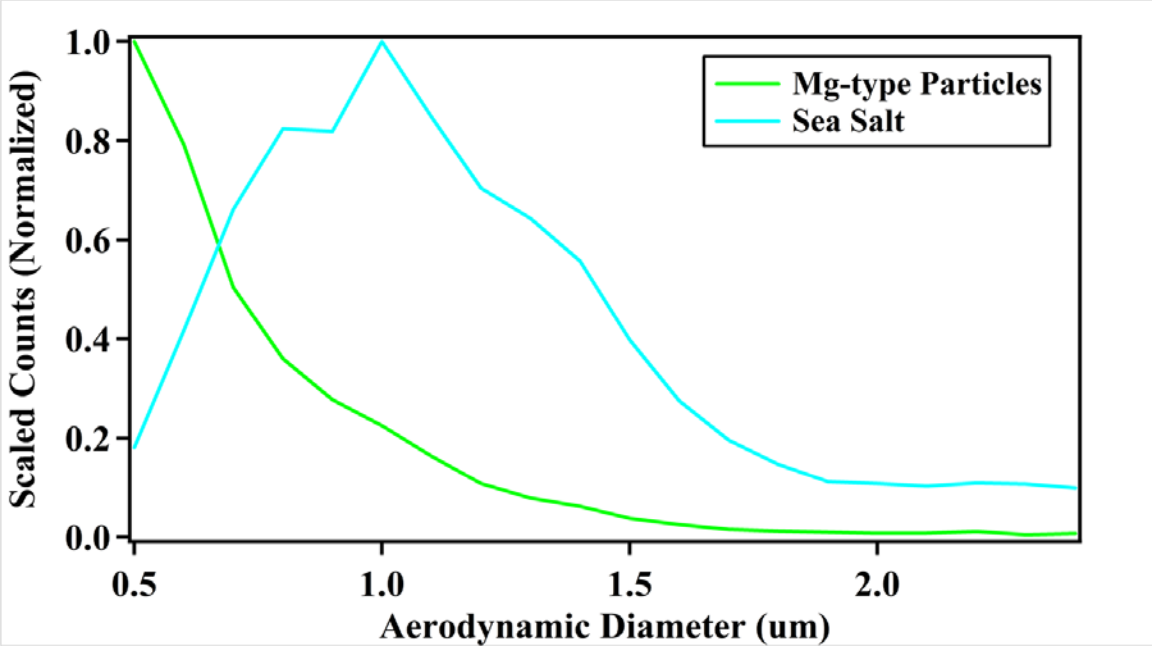

Figure 2.5: Number size distributions for Mg-type (green line) and sea salt (blue line) particles sampled at 55% RH during CIFEX. Particle counts have been scaled using an aerodynamic particle sizer (APS) to account for transmission biases in the ATOFMS. Particle counts have been normalized to total counts per size bin to show the relative fractions of scaled counts per size.

number counts normalized to the total particle counts per size range taken over several days during CIFEX for the two different particle types. As shown, sea salt particles peak in the supermicron size mode while Mg-type particles peak in the submicron size mode. We note that the observation of the Mg-type particles in smaller sizes compared to sea salt was observed for CIFEX; however, some variability in this result is expected for other studies. The enhancement in Mg-type particles in smaller sizes depends on conditions that affect the formation of this particle type such as wind speed; further research will be done to verify these results for differing oceanic and meteorological conditions.

The particle types described in this paper contain intense inorganic peaks (e.g. Mg^{2+}, Ca^{2+}, K^{+}); however, in the ATOFMS, the presence of inorganic ions in low relative abundance (< 1-2%) along with water can suppress ion signal intensities particularly for some organic compounds, making the particles appear mostly inorganic [*Gross et al.*, 2000]. Thus, it is likely that the overall increase in absolute Mg^{2+} mass from these particles is quite small and the particles contain a significant amount of organic material. Further support for this is given during the North Atlantic Marine Boundary Layer Experiment (NAMBLEX) [*Heard et al.*, 2006] when Mg-type particles detected using ATOFMS and high organic mass concentrations detected by aerosol mass spectrometry (AMS) were observed simultaneously in a pristine marine region at Mace Head [*Dall'Osto et al.*, 2005]. In these same marine regions where Mg-type particles are present, the number of total submicron particles that scatter light but are not chemically analyzed by ATOFMS increases. At this juncture, we can only hypothesize that these

particles are composed of long chain hydrophobic organic species that do not absorb the 266 nm radiation. Overall, these observations suggest that the Mg-type particles detected online by the ATOFMS could serve as a proxy for an increase in carbonaceous material in the ocean in the dissolved and particulate phase, that are transferred to the atmosphere through bubble bursting.

2.4.3 Evidence of an Oceanic Source for Mg-type Particles

If the Mg-type particles represent fresh, oceanic emissions rather than continental emissions, they should be temporally correlated with fresh sea salt particles. Measurements carried out during the CIFEX field campaign in Trinidad Head on the northern California coast exhibited relatively clean marine background sampling conditions over several days allowing for direct comparison between fresh sea salt and Mg-type particles. Before the campaign began, a rain event occurred on DOY 90 causing the percentage of reacted sea salt (indicated by the presence of nitrate ions) to decrease from 70-90% of the sea salt particles to 20%, whereas fresh sea salt increased to ~60% and a subsequent increase in the percentage of Mg-type particles also occurred. The increase in Mg and fresh sea salt particles mostly likely occurred because of an enhancement in the bubble bursting mechanism induced by high winds (reaching up to ~20 m/s) [*Monahan et al.*, 1983] and raindrops impacting the ocean surface [*Marks*, 1990]. To further probe whether a primary, oceanic source was responsible for the detection of Mg-type particles, the time series of Mg-type particles, fresh sea salt, reacted sea salt, and wind speed was compared for DOY 104-114 (Figure 2.6a). As shown in Figure 2.6, the time-series of the Mg-type particles were strongly correlated (R^2 = 0.86)

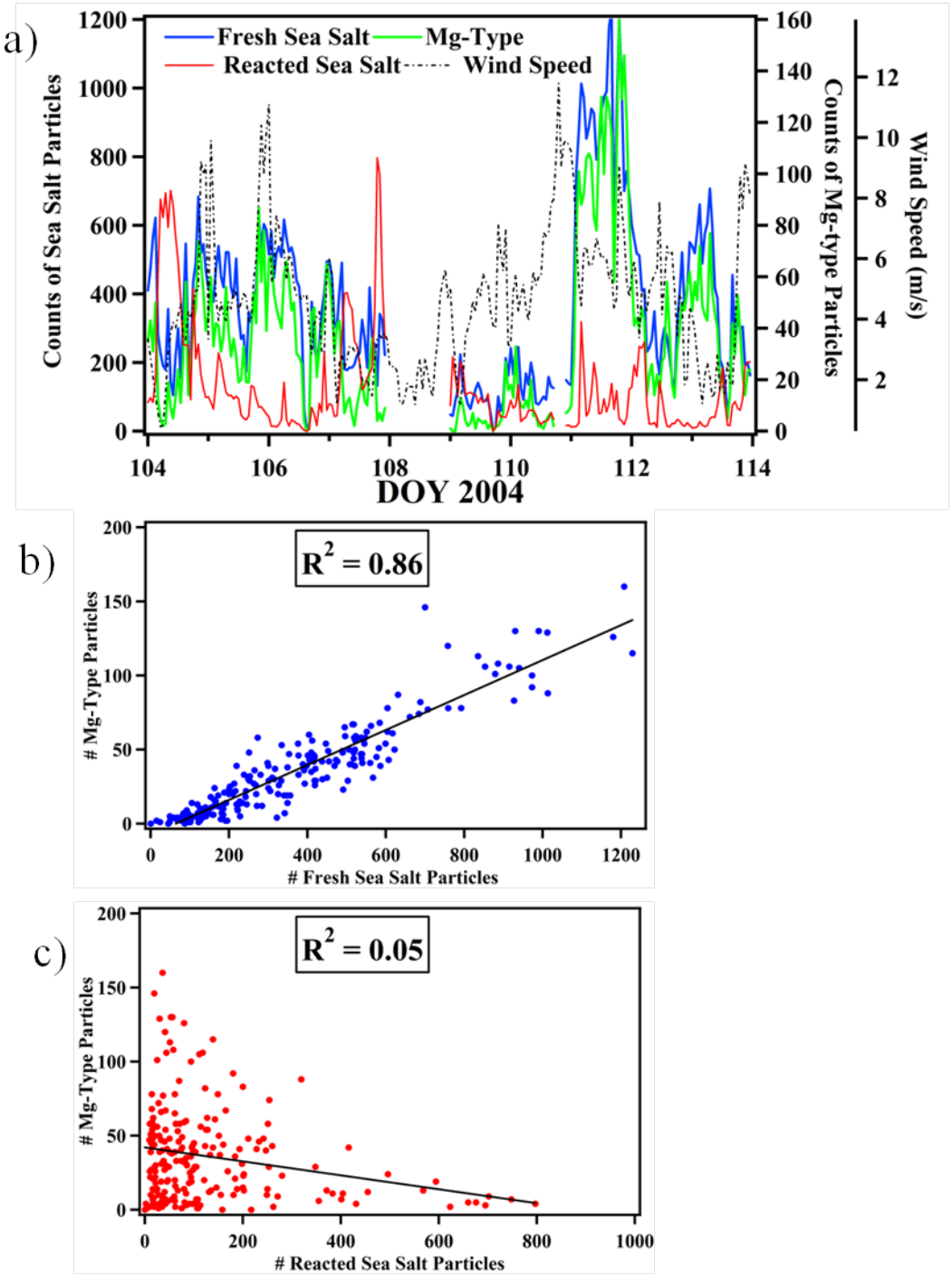

Figure 2.6: (a) Hourly time series of ATOFMS measurements showing the evolution of fresh, unreacted sea salt particles (blue line), Mg-type particles (green line), reacted sea salt particles (red line), and wind speed (black dotted line) during CIFEX. Scatter p lots of particle counts show correlations between (b) Mg-type and freshly ejected sea salt particles and (c) Mg-type and reacted (background) sea salt particles.

with that of freshly ejected sea salt particles (Figure 2.6b) particularly as the wind speed increased to at least 10 m/s; conversely, Mg-type particles were not correlated with reacted sea salt particles (R^2 = 0.05) (Figure 2.6c) or with dust particles (R^2 = 0.04) suggesting that Mg-type particles represent freshly emitted particles from the ocean via bubble bursting.

2.4.4 Temporal Correlations of Mg-type Particles with DMS and Chlorophyll *a*

During the INDOEX field campaign, measurements of atmospheric and seawater DMS and chlorophyll *a* concentrations were made concurrently with ATOFMS measurements. Figure 2.7 shows a time-series of changes in Mg-type particles, dust particles, atmospheric DMS, and chlorophyll *a* as a function of cruise track during INDOEX. As the ship passed through the Intertropical Convergence Zone (ITCZ) and moved into the southern Indian Ocean, higher levels of chlorophyll *a* were observed in addition to high concentrations of DMS, both atmospheric and oceanic (see Figure 2.7) [*Kumar et al.*, 2002; *Shenoy et al.*, 2002]. Continental particle types were not transported across the ITCZ [*Norman et al.*, 2003], as shown in Figure 2.7, where the percentage of dust particles reached zero at the southern-most point of the cruise. Overall, these observations suggest that particles encountered in the southern Indian Ocean were exclusively of marine origin. During the beginning of the cruise on DOY 74-76, fresh sea salt constituted up to ~60% of the particles; however, Mg-type particles were typically < 1% of the detected particles highlighting the observation that Mg-type particles are not always present in marine environments. Mg-type particles increased from 0% of the particles north of the ITCZ up to 14% of the particles south of the ITCZ

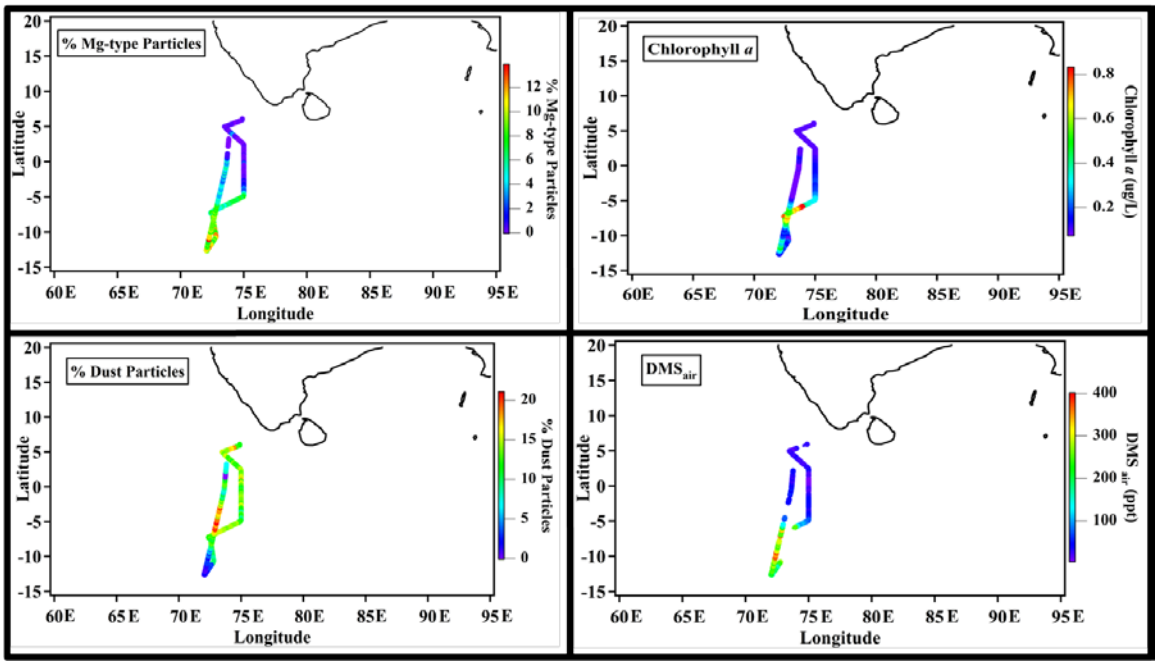

Figure 2.7: Percentages of Mg-type particles (upper left panel), chlorophyll a concentrations (upper right panel), dust particles (lower left panel), and atmospheric DMS concentrations (lower right panel) as a function of cruise position during INDOEX.

during periods when wind speeds increased up to 12 m/s (see Figure 2.8) and as atmospheric DMS and chlorophyll *a* concentrations rose. Interestingly, unique S-ions were also detected in the southern Indian Ocean during periods of elevated Mg-type particles. This unique particle type will be the subject of a future publication by our group (C.J. Gaston et al., manuscript in preparation, 2011a). Figure 2.9 shows the correlations between Mg-type particles and dust observed by ATOFMS, atmospheric DMS, and chlorophyll *a*. Mg-type particles were found to be anti-correlated with dust particles supporting their marine rather than continental origin. Mg-type particles were found to have a strong, positive correlation with atmospheric DMS ($R^2 = 0.76$), a positive correlation with seawater DMS ($R^2 = 0.48$), and a weak positive correlation with chlorophyll *a* ($R^2 = 0.25$). Similar correlations between atmospheric DMS and Mg-type particles ($R^2 = 0.54$) were also observed during ACE-Asia in 2001 on DOY 82-84 when clean marine conditions were encountered, as indicated by air mass back-trajectories and low radon concentrations [*Bates et al.*, 2004]. Chlorophyll *a* was not measured during ACE-Asia. Overall, these correlations between Mg-type particles, atmospheric DMS, and chlorophyll *a* concentrations suggest that the Mg-type particles are detected due to changes in ocean chemistry associated with biological activity.

2.4.5 Laboratory Investigations of Ocean-Derived Particles via Bubble Bursting

In order to better understand the differences in marine particle signatures observed in the ambient measurements, laboratory investigations were performed. Figure 2.10 shows the percentages of the different particle types formed by bubbling and atomization generation methods, using the same seawater sample collected at the Scripps

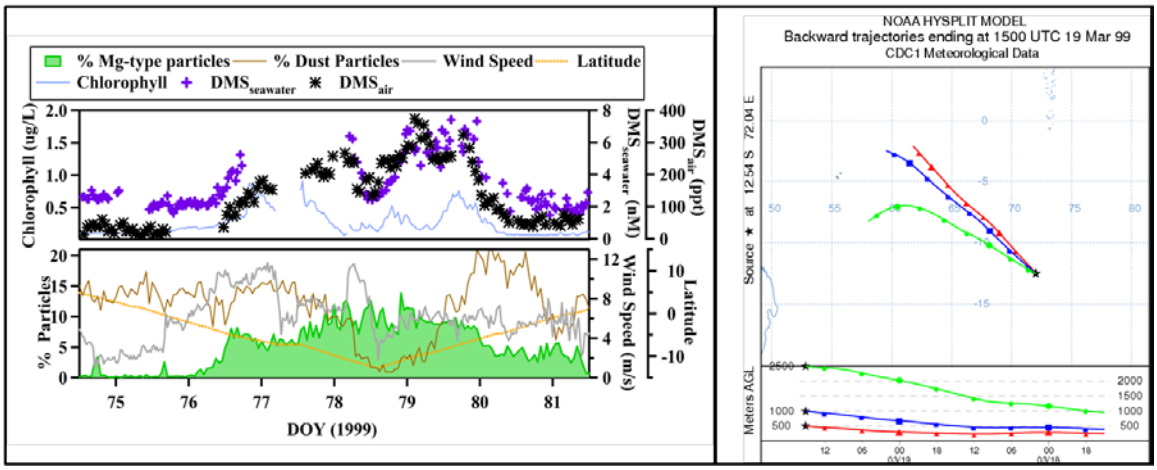

Figure 2.8: Left panel shows one hour resolution time series of Mg-type particles (green), dust particles (brown line), wind speed (grey line), atmospheric DMS concentrations (black asterisks), seawater DMS concentrations (purple crosses), chlorophyll (blue line), and latitude (dotted orange line) observed during the INDOEX cruise aboard the RV Ronald Brown. Right panel shows a representative 48-hour HYSPLIT back trajectory during the INDOEX cruise taken at 2500 m (green line), 1000 m (blue line), and 500 m (red line).

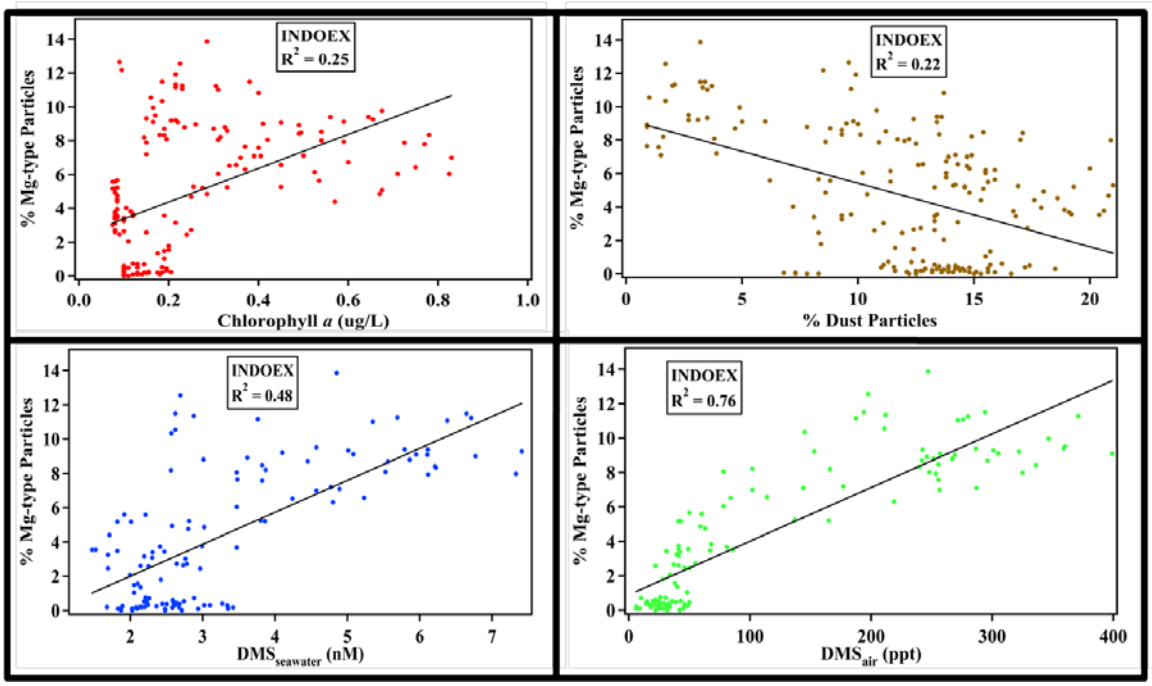

Figure 2.9: Correlation plots between Mg-type particles and chlorophyll *a* concentrations (upper left panel), Mg-type particles and dust particles (upper right panel), Mg-type particles and seawater DMS concentrations (lower left panel), and Mg-type particles and atmospheric DMS concentrations (lower right panel) measured during INDOEX.

Institution of Oceanography pier. While sea salt is formed using both methods, the main difference is the enhancement in the percentage of Mg-type particles (light and dark green traces) when the seawater was bubbled (Figure 2.10a) rather than atomized (Figure 2.10b). This agrees with previous findings that the physicochemical properties of sea spray aerosol depend on the aerosol generation technique [*Fuentes et al.*, 2010a]. The likely explanation for the increase in Mg-type particles when seawater is bubbled rather than atomized is that bubbles scavenge organic material along with any associated inorganic ions causing these compounds to be enriched in individual particles produced when the bubbles burst. Additional laboratory studies have been conducted to further characterize the single particle composition of sea spray aerosol using ATOFMS and are the focus of a future publication by our group (C.J. Gaston et al., manuscript in preparation, 2011b). While these laboratory studies demonstrate that Mg-type particles can be produced by bubble bursting using this particular set-up, this laboratory set-up may not be representative of the full complexity of sea spray aerosol generation under ambient oceanic conditions. Current efforts are underway in our group to test how different sea spray generation methods affect the chemistry of wave and bubble generated sea spray aerosols.

2.4.6 Impact of Chemical Segregation on Single-Particle Mixing-State

The term chemical fractionation in marine aerosols typically describes the situation where certain chemical compounds exhibit higher concentrations relative to Na within atmospheric aerosols compared to the same ratio of ions in bulk ocean water [*Duce and Hoffman*, 1976; *Hoffman and Duce*, 1972]. While the transfer and enrichment

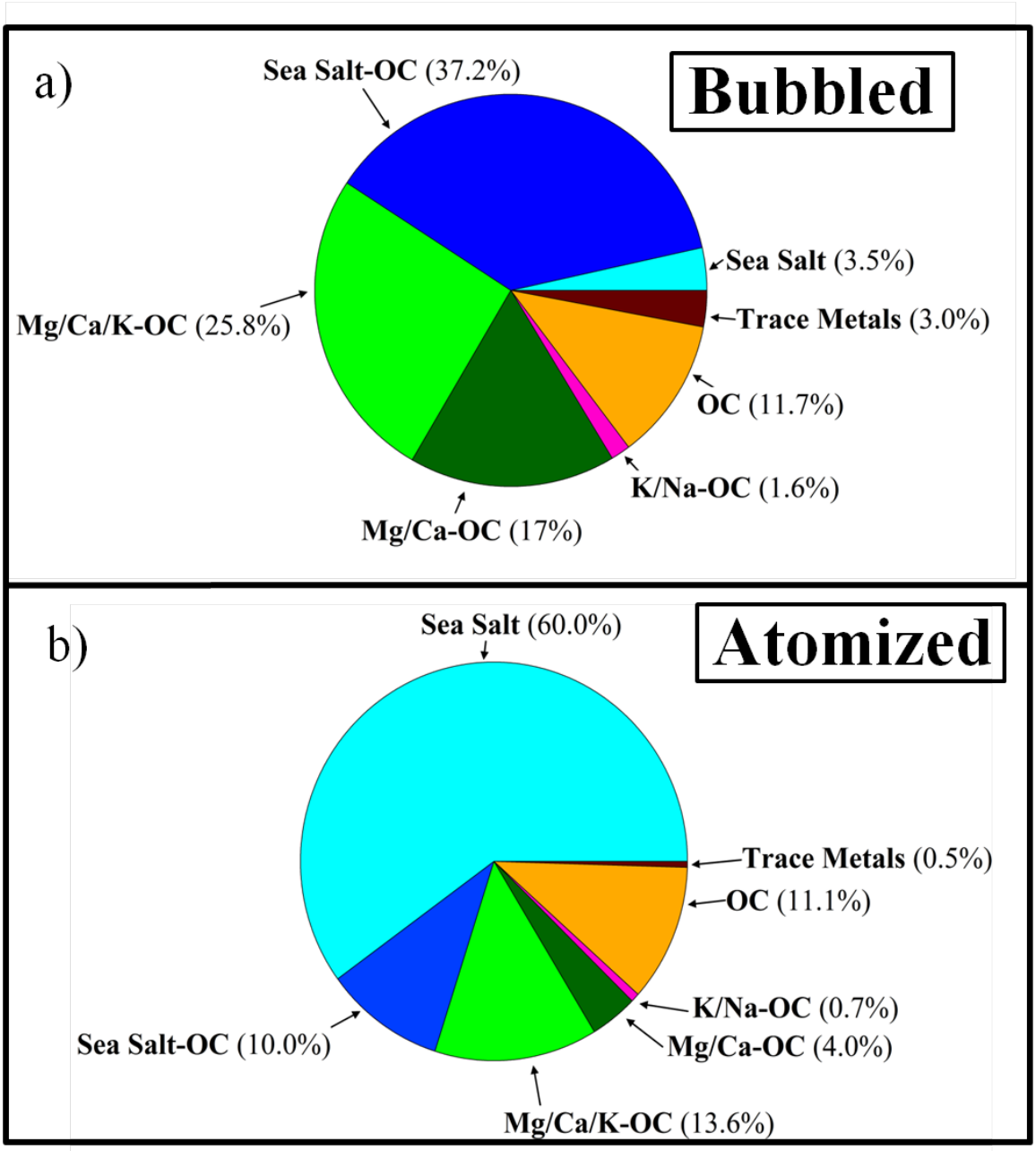

Figure 2.10: Differences in particle chemistry of (a) bubbled and (b) atomized natural seawater collected from the surface of the ocean at the Scripps Institution of Oceanography pier.

of organic material is well documented [*Blanchard*, 1964; *Duce and Hoffman*, 1976], uncertainty remains regarding the enrichment of inorganic ions (i.e. Mg^{2+}, Ca^{2+}) owing to the difficulty in distinguishing between marine, continental, and anthropogenic sources (e.g. Mg associated with organics and biological material vs. Mg in soil dust vs. Mg in sea salt) [*Duce and Hoffman*, 1976; *Hoffman and Duce*, 1977; *Hoffman et al.*, 1980]. One of the primary goals of this study is to use a single particle technique to probe whether chemical segregation of organic and inorganic ions occurs during the bubble bursting process.

One question that arises is whether the unique Mg signature could be due to chemical fractionation occurring in the instrument. Fractional recrystallization has been postulated to occur when sea spray particles are dried out causing compounds with different solubilities to recrystallize and shatter creating particles with inorganic concentrations that differ from bulk seawater [*Mouri et al.*, 1997; *Mouri and Okada*, 1993]. While composition dependent chemical fractionation within the instrument is possible, it is highly unlikely due to the following reasons. First, the sampling mast for these studies was conditioned to 55% RH and in the standard ATOFMS nozzle inlet used for these studies, the particles undergo minimal evaporation as they are only under vacuum for < 1 ms before they are analyzed; hence, chemical fractionation due to efflorescence within the instrument is an unlikely explanation for the presence of these particle types. Second, if segregation were occurring for sea salt particles in the single particle mass spectrometer, then Mg-type particles should be present during all time periods in marine environments when sea salt particles are detected; as discussed, this is

not the case particularly during INDOEX when Mg-type particles increased only as chlorophyll *a* and DMS concentrations increased. This observation is consistent with other studies. Finally, laboratory investigations show that Mg-type particles were significantly enhanced when seawater was bubbled rather than atomized. If chemical fractionation were occurring within the instrument, then similar percentages of Mg-type particles should have been detected regardless of the aerosol generation technique used.

Instead, we hypothesize that distinct sea spray particle populations at the single particle level form, as ocean-derived Mg-type and fresh sea salt in different particle populations, when changes in ocean chemistry occur. Single particle analysis provides direct insight into the presence of these individual populations, information that is not apparent from techniques that average the composition of sea spray particles into a single average chemical composition (see Figure 2.11). Different sea spray aerosol populations have been shown by electron microscopy where organic-rich particles lacking sea salt were detected [*Bigg and Leck*, 2001; *Leck and Bigg*, 2005a; *Leck and Bigg*, 2005b; *Leck and Bigg*, 2008; *Leck et al.*, 2002]. However, this study is the first to show real-time temporal correlations between changes in ocean chemistry (i.e. DMS and chlorophyll *a*) with changes in the mixing-state of sea spray aerosols. It is important to understand the factors leading to these chemical differences as they will impact the heterogeneous reactivity, water uptake, and cloud forming abilities of sea spray aerosols.

2.4.7 Potential Sources of Mg-type Particles

The Mg-type particles could result from EPS, cell debris or fragments, viruses, bacteria, or organics released by lysed cells. As stated previously, divalent cations such

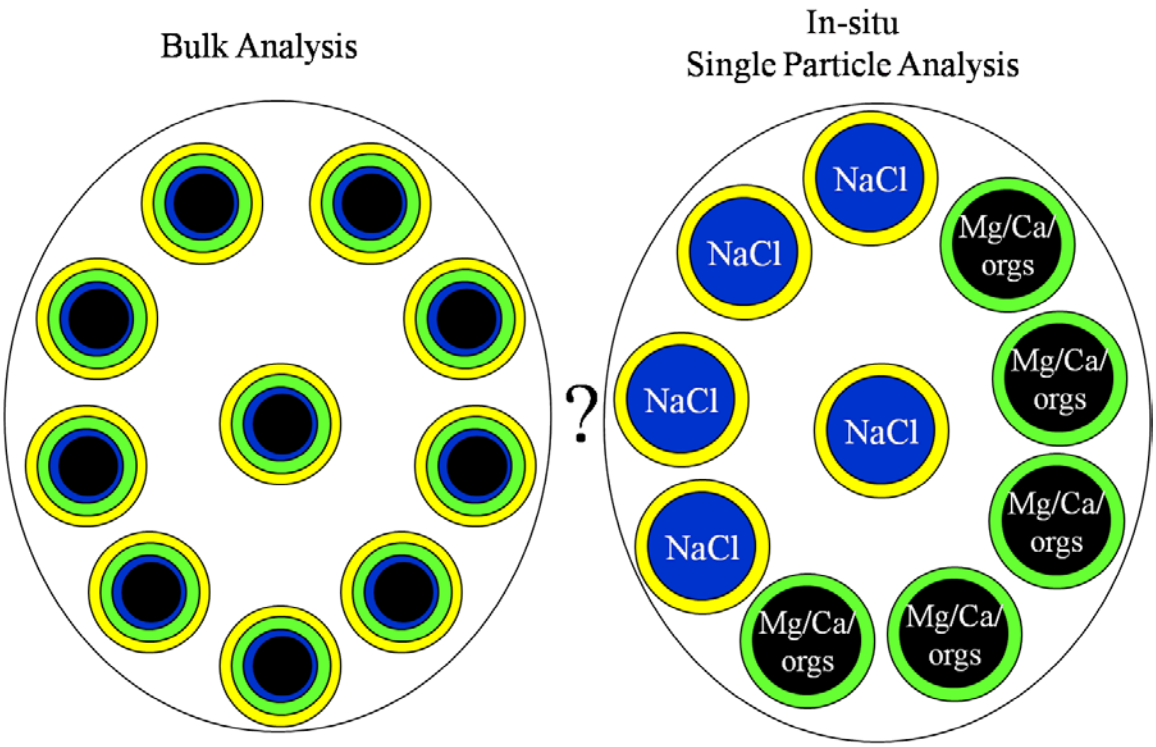

Figure 2.11: Traditional filter (bulk) analysis shows the same seawater and air concentrations of Mg^{2+}, Ca^{2+}, and K^{+} by assuming all particles have the exact same composition (left). Single particle analysis can reveal distinctions in sea spray aerosol populations (right).

as Mg^{2+} and Ca^{2+} have been shown to facilitate the formation of microgels [*Chin et al.*, 1998; *Verdugo et al.*, 2004; *Wells*, 1998] and, thus, could be responsible for the detection of Mg-type particles by ATOFMS. If the origin of the Mg-type particles is due to the association of Mg^{2+} with organic material, then periods with enhanced organic material in the ocean, such as when ocean biota is present, could enhance the detection of this particle type. The bubble bursting process is known to lyse cells [*Cherry and Hulle, 1995*] potentially releasing organics and/or chlorophyll *a* into the water column that could be the source of enhanced organic material and Mg^{2+} in the particle phase. Furthermore, Mg^{2+} has been shown to deprotonate and associate with the polar head groups of surface active fatty acids creating a particle interface rich in Mg^{2+} and organics [*Casillas-Ituarte et al.*, 2010]. The Mg-type particles detected by ATOFMS could, thus, primarily reflect an organic-rich particle coating when water insoluble organic material is present in sea spray aerosols. While the exact mechanism and source of the Mg-type particles are unknown, it is clear that chemical segregation appears to be occurring during the bubble bursting process in areas with increased organic material.

2.5 Conclusions

Unique ocean-derived particle types enriched in organic carbon and Mg^{2+} and/or Ca^{2+} were detected by ATOFMS in marine environments. These particles were observed to increase during periods of elevated DMS and/or phytoplankton biomass, as measured by chlorophyll *a* concentrations, suggesting that the observation of these particles accompanies changes in ocean chemistry due to biological activity providing an unambiguous link between changes in ocean chemistry and sea spray aerosol chemistry.

The Mg-type particles were externally mixed from sea salt particles providing evidence of chemical segregation occurring at the single-particle level, which is in agreement with other off-line electron microscopy single sea spray particle measurements including those of Bigg and Leck [2008]. The characteristic spectra of these particle types can be reproduced experimentally by bubbling seawater solutions. The bubbling mechanism is known to scavenge organic material and microorganisms from the water column resulting in enriched levels of organic material in sea spray aerosol relative to bulk seawater. It is likely that the Mg-type particles are associated with the scavenged organic material and/or microorganisms. Potential sources for these particles include microgels stabilized by divalent cations (e.g. Ca^{2+} and Mg^{2+}), structural changes in sea spray aerosol due to the presence of surface active fatty acids bound to Mg^{2+}, cell debris or fragments, viruses, bacteria, or organics released by lysed cells. Future research will be conducted to directly link these Mg-type particles to particular organic compounds including EPS, primary production, and particular phytoplankton species. Measurements of marine aerosols have demonstrated a peak in number concentration at sizes of ~0.1 um and below [*Fuentes et al.*, 2010a; *Fuentes et al.*, 2010b; *Martensson et al.*, 2003; *Sellegri et al.*, 2006; *Tyree et al.*, 2007]. Particle measurements presented in this paper have a lower limit of 0.2 um; however, the Mg-type particles described herein most likely extend to smaller sizes. We also hypothesize that the Mg-type particles described herein serve as a proxy for the production of particulate organic carbon in single particles associated with biological activity, which has also been shown to contribute to particles < 0.2 um [*Bigg and Leck*, 2001; *Bigg and Leck*, 2008; *Leck and Bigg*, 2005a; *Leck and Bigg*, 2005b; *Leck and Bigg*, 2008; *Leck et al.*, 2002]. Current efforts are underway in our group to determine the

lower size limit of this unique particle type. If the enhanced Mg in these particles is due to organic and Mg^{2+} enrichment particle interface, this has implications for reactivity, hygroscopicity, optical properties, and ice and cloud nucleating abilities, which will be quite different from traditional sea salt particles. These findings provide further support for how changes in ocean chemistry induced by biological processes can impact particle chemistry and, possibly, cloud formation.

2.6 Acknowledgements

The authors thank Profs. L. M. Russell, V. Ramanathan, R. von Glasow, P. Crutzen, F. Azam, and Dr. G. Poon for valuable discussions and help in editing this manuscript. We also thank J. Holecek, M. Spencer, and D. Sodeman for data collection. The authors acknowledge the National Science Foundation #0296170, National Science Foundation #1038028, and NOAA for the funding to conduct this research. Support for B. G. Mitchell was provided by NASA SIMBIOS and NOAA. Support for C. J. Gaston was provided by Pacific Northwest National Laboratory through the Aerosol Chemistry and Climate Institute. NOAA/ESRL/GMD provided wind speed data for CIFEX. L. E. Hatch is acknowledged for help with editing this manuscript. The authors would also like to thank anonymous reviewers for their suggestions and comments.

Chapter 2 is reproduced with permission from the American Geophysical Union: Gaston, C.J., Furutani, H., Guazzotti, S.A., Coffee, K.R., Bates, T.S., Quinn, P.K., Aluwihare, L.I., Mitchell, B.G., Prather, K.A. Unique ocean-derived particles serve as a proxy for changes in ocean chemistry. *Journal of Geophysical Research-[Atmospheres]*. 2011, 116, D18310, doi:10.1029/2010JD015289.

Geophysical Union. The dissertation author was the primary investigator and author of this paper.

2.7 References

Allen, J.O. (2002), YAADA software toolkit to analyze single-particle mass spectral data: Reference manual version 1.1, *Arizona State University*, http://www.yaada.org.

Allen, J.O., D.P. Fergenson, E.E. Gard, L.S. Hughes, B.D. Morrical, M.J. Kleeman, D.S. Gross, M.E. Galli, K.A. Prather, and G.R. Cass (2000), Particle detection efficiencies of aerosol time of flight mass spectrometers under ambient sampling conditions, *Environ. Sci. Tech., 34* (1), 211-217.

Aller, J.Y., M.R. Kuznetsova, C.J. Jahns, and P.F. Kemp (2005), The sea surface microlayer as a source of viral and bacterial enrichment in marine aerosols, *J. Aerosol Sci., 36* (5-6), 801-812.

Aluwihare, L.I., and D.J. Repeta (1999), A comparison of the chemical characteristics of oceanic DOM and extracellular DOM produced by marine algae, *Mar. Ecol. Prog. Ser., 186*, 105-117.

Andreae, M.O., and P.J. Crutzen (1997), Atmospheric aerosols: Biogeochemical sources and role in atmospheric chemistry, *Science, 276* (5315), 1052-1058.

Bates, T.S., R.P. Kiene, G.V. Wolfe, P.A. Matrai, F.P. Chavez, K.R. Buck, B.W. Blomquist, and R.L. Cuhel (1994), The cycling of sulfur in surface seawater of the northeast Pacific, *J. Geophys. Res.-[Oceans], 99* (C4), 7835-7843.

Bates, T.S., B.K. Lamb, A. Guenther, J. Dignon, and R.E. Stoiber (1992), Sulfur emissions to the atmosphere from natural sources, *J. Atmos. Chem., 14* (1-4), 315-337.

Bates, T.S., P.K. Quinn, D.J. Coffman, D.S. Covert, T.L. Miller, J.E. Johnson, G.R. Carmichael, I. Uno, S.A. Guazzotti, D.A. Sodeman, K.A. Prather, M. Rivera, L.M. Russell, and J.T. Merrill (2004), Marine boundary layer dust and pollutant transport associated with the passage of a frontal system over eastern Asia, *J. Geophys. Res.-[Atmos.], 109* (D19S19), doi:10.1029/2003JD004094.

Bates, T.S., P.K. Quinn, D.S. Covert, D.J. Coffman, J.E. Johnson, and A. Wiedensohler (2000), Aerosol physical properties and processes in the lower marine boundary layer: a comparison of shipboard sub-micron data from ACE-1 and ACE-2, *Tellus Ser. B, 52* (2), 258-272.

Bigg, E.K. (2007), Sources, nature and influence on climate of marine airborne particles, *Environ. Chem.*, *4* (3), 155-161.

Bigg, E.K., and C. Leck (2001), Cloud-active particles over the central Arctic Ocean, *J. Geophys. Res.-[Atmos.]*, *106* (D23), 32155-32166.

Bigg, E.K., and C. Leck (2008), The composition of fragments of bubbles bursting at the ocean surface, *J. Geophys. Res.*, *113*, D11209, doi:10.1029/2007JD009078.

Blanchard, D.C. (1964), Sea-to-air transport of surface active material, *Science*, *146* (364), 396-397.

Blanchard, D.C., and L. Syzdek (1970), Mechanism for water-to-air transfer and concentration of bacteria, *Science*, *170* (3958), 626-628.

Blanchard, D.C., and A.H. Woodcock (1957), Bubble formation and modification in the sea and its meteorological significance, *Tellus*, *9* (2), 145-158.

Casillas-Ituarte, N.N., K.M. Callahan, C.Y. Tang, X.K. Chen, M. Roeselová, D.J. Tobias, and H.C. Allen (2010), Surface organization of aqueous $MgCl_2$ and application to atmospheric marine aerosol chemistry, *PNAS*, *107* (15), 6616-6621.

Cavalli, F., M.C. Facchini, S. Decesari, M. Mircea, L. Emblico, S. Fuzzi, D. Ceburnis, Y.J. Yoon, C.D. O'Dowd, J.P. Putaud, and A. Dell'Acqua (2004), Advances in characterization of size-resolved organic matter in marine aerosol over the North Atlantic, *J. Geophys. Res.-[Atmos.]*, *109*, D24215, doi:10.1029/2004JD005137.

Ceburnis, D., C.D. O'Dowd, G.S. Jennings, M.C. Facchini, L. Emblico, S. Decesari, S. Fuzzi, and J. Sakalys (2008), Marine aerosol chemistry gradients: Elucidating primary and secondary processes and fluxes, *Geophys. Res. Lett.*, *35* (7), L07804, doi:10.1029/2008GL033462.

Cherry, R.S. and C.T. Hulle (1995), Cell death in the thin films of bursting bubbles, *Biotech. Prog.*, *8* (1), 11-18.

Chin, W.C., M.V. Orellana, and P. Verdugo (1998), Spontaneous assembly of marine dissolved organic matter into polymer gels, *Nature*, *391* (6667), 568-572.

Cloke, J., W.A. Mckay, and P.S. Liss (1991), Laboratory investigations into the effect of marine organic material on the sea-salt aerosol generated by bubble bursting, *Mar. Chem.*, *34* (1-2), 77-95.

Coffee, K.R. (2002), Single particle characterization of soil and dust particulate matter in the urban and marine environments, PhD. Thesis, Depart. of Chem., Univ. of California, Riverside.

Cooper, D.J., and E.S. Saltzman (1993), Measurements of atmospheric dimethylsulfide, hydrogen sulfide, and carbon disulfide during Gte Cite-3, *J. Geophys. Res.-[Atmos.]*, *98* (D12), 23397-23409.

Dall'Osto, M., R.M. Harrison, D.C.S. Beddows, E.J. Freney, M.R. Heal, and R.J. Donovan (2006), Single-particle detection efficiencies of aerosol time-of-flight mass spectrometry during the North Atlantic marine boundary layer experiment, *Environ. Sci. Tech.*, *40* (16), 5029-5035.

Dall'Osto, M., R.M. Harrison, H. Furutani, K.A. Prather, H. Coe, and J.D. Allan (2005), Studies of aerosol at a coastal site using two aerosol mass spectrometry instruments and identification of biogenic particle types, *Atmos. Chem. Phys. Discuss.*, *5*, 10799-10383.

Duce, R.A., and E.J. Hoffman (1976), Chemical fractionation at the air-sea interface, *Ann. Rev. Earth Planet. Sci.*, *4*, 187-228.

Facchini, M.C., M. Rinaldi, S. Decesari, C. Carbone, E. Finessi, M. Mircea, S. Fuzzi, D. Ceburnis, R. Flanagan, E.D. Nilsson, G. de Leeuw, M. Martino, J. Woeltjen, and C.D. O'Dowd (2008), Primary submicron marine aerosol dominated by insoluble organic colloids and aggregates, *Geophys. Res. Lett.*, *35*, L17814, doi:10.1029/2008GL034210.

Fuentes, E., H. Coe, D. Green, G. de Leeuw, and G. McFiggans (2010a), Laboratory-generated primary marine aerosol via bubble-bursting and atomization, *Atmos. Meas. Tech.*, *3* (1), 141-162.

Fuentes, E., H. Coe, D. Green, G. de Leeuw, and G. McFiggans (2010b), On the impacts of phytoplankton-derived organic matter on the properties of the primary marine aerosol - Part 1: Source fluxes, *Atmos. Chem. Phys.*, *10* (19), 9295-9317.

Gard, E., J.E. Mayer, B.D. Morrical, T. Dienes, D.P. Fergenson, and K.A. Prather (1997), Real-time analysis of individual atmospheric aerosol particles: Design and performance of a portable ATOFMS, *Anal. Chem.*, *69* (20), 4083-4091.

Gard, E.E., M.J. Kleeman, D.S. Gross, L.S. Hughes, J.O. Allen, B.D. Morrical, D.P. Fergenson, T. Dienes, M.E. Galli, R.J. Johnson, G.R. Cass, and K.A. Prather (1998), Direct observation of heterogeneous chemistry in the atmosphere, *Science*, *279* (5354), 1184-1187.

Gross, D.S., M.E. Galli, P.J. Silva, and K.A. Prather (2000), Relative sensitivity factors for alkali metal and ammonium cations in single particle aerosol time-of-flight mass spectra, *Anal. Chem., 72* (2), 416-422.

Guazzotti, S.A., K.R. Coffee, and K.A. Prather (2001), Continuous measurements of size-resolved particle chemistry during INDOEX-Intensive Field Phase 99, *J. Geophys. Res.-[Atmos.], 106* (D22), 28607-28627.

Heard, D.E., K.A. Read, J. Methven, S. Al-Haider, W.J. Bloss, G.P. Johnson, M.J. Pilling, P.W. Seakins, S.C. Smith, R. Sommariva, J.C. Stanton, T.J. Still, T. Ingham, B. Brooks, G. de Leeuw, A.V. Jackson, J.B. McQuaid, R. Morgan, M.H. Smith, L.J. Carpenter, N. Carslaw, J. Hamilton, J.R. Hopkins, J.D. Lee, A.C. Lewis, R.M. Purvis, D.J. Wevill, N. Brough, T. Green, G. Mills, S.A. Penkett, J.M.C. Plane, A. Saiz-Lopez, D. Worton, P.S. Monks, Z. Fleming, A.R. Rickard, M.R. Alfarra, J.D. Allan, K. Bower, H. Coe, M. Cubison, M. Flynn, G. McFiggans, M. Gallagher, E.G. Norton, C.D. O'Dowd, J. Shillito, D. Topping, G. Vaughan, P. Williams, M. Bitter, S.M. Ball, R.L. Jones, I.M. Povey, S. O'Doherty, P.G. Simmonds, A. Allen, R.P. Kinnersley, D.C.S. Beddows, M. Dall'Osto, R.M. Harrison, R.J. Donovan, M.R. Heal, S.G. Jennings, C. Noone, and G. Spain (2006), The North Atlantic Marine Boundary Layer Experiment (NAMBLEX). Overview of the campaign held at Mace Head, Ireland, in summer 2002, *Atmos. Chem. Phys., 6*, 2241-2272.

Hoffman, E.J., and R.A. Duce (1977), Alkali and alkaline-earth metal chemistry of marine aerosols generated in laboratory with natural seawaters, *Atmos. Environ., 11* (4), 367-372.

Hoffman, E.J., G.L. Hoffman, and R.A. Duce (1980), Particle-size dependence of alkali and alkaline-earth metal enrichment in marine aerosols from Bermuda, *J. Geophys. Res., 85* (C10), 5499-5502.

Hoffman, G.L., and R.A. Duce (1972), Consideration of chemical fractionation of alkali and alkaline-earth metals in Hawaiian marine atmosphere, *J. Geophys. Res., 77* (27), 5161-5169.

Huebert, B.J., T. Bates, P.B. Russell, G.Y. Shi, Y.J. Kim, K. Kawamura, G. Carmichael, and T. Nakajima (2003), An overview of ACE-Asia: Strategies for quantifying the relationships between Asian aerosols and their climatic impacts, *J. Geophys. Res.-[Atmos.], 108* (D23), 8633, doi:10.1029/2003JD003550.

Keller, M.D., W. Bellows, K., and R.L. Guillard, Dimethyl sulfide production in marine phytoplankton, in *Biogenic Sulfur in the Environment*, edited by E.S. Saltzman,

and W.J. Cooper, pp. 167-182, American Chemical Society, Washington, D.C., 1989.

Keene, W.C., H. Maring, J.R. Maben, D.J. Kieber, A.A.P. Pszenny, E.E. Dahl, M.A. Izaguirre, A.J. Davis, M.S. Long, X.L. Zhou, L. Smoydzin, and R. Sander (2007), Chemical and physical characteristics of nascent aerosols produced by bursting bubbles at a model air-sea interface, *J. Geophys. Res.-[Atmos.]*, *112* (D21), D21202, doi:10.1029/2007JD008464.

Kumar, M.D., D.M. Shenoy, V.V.S.S. Sarma, M.D. George, and M. Dandekar (2002), Export fluxes of dimethylsulfoniopropionate and its break down gases at the air-sea interface, *Geophys. Res. Lett.*, *29* (2), 1021, doi:10.1029/2001GL013967.

Leck, C., and E.K. Bigg (2005a), Biogenic particles in the surface microlayer and overlaying atmosphere in the central Arctic Ocean during summer, *Tellus Ser. B*, *57* (4), 305-316.

Leck, C., and E.K. Bigg (2005b), Source and evolution of the marine aerosol: A new perspective, *Geophys. Res. Lett.*, *32* (19), L19803, doi:10.1029/2005GL023651.

Leck, C., and E.K. Bigg (2007), A modified aerosol–cloud–climate feedback hypothesis, *Environ. Chem.*, *4*, 400-403.

Leck, C., and E.K. Bigg (2008), Comparison of sources and nature of the tropical aerosol with the summer high Arctic aerosol, *Tellus, 60B*, 118-126.

Leck, C., U. Larsson, L.E. Bagander, S. Johansson, and S. Hajdu (1990), Dimethyl sulfide in the Baltic Sea - Annual variability in relation to biological activity, *J. Geophys. Res.-[Oceans]*, *95* (C3), 3353-3363.

Leck, C., M. Norman, E.K. Bigg, and R. Hillamo (2002), Chemical composition and sources of the high Arctic aerosol relevant for cloud formation, *J. Geophys. Res.-[Atmos.]*, *107* (D12), 4135, doi:10.1029/2001JD001463.

Lelieveld, J., P.J. Crutzen, V. Ramanathan, M.O. Andreae, C.A.M. Brenninkmeijer, T. Campos, G.R. Cass, R.R. Dickerson, H. Fischer, J.A. de Gouw, A. Hansel, A. Jefferson, D. Kley, A.T.J. de Laat, S. Lal, M.G. Lawrence, J.M. Lobert, O.L. Mayol-Bracero, A.P. Mitra, T. Novakov, S.J. Oltmans, K.A. Prather, T. Reiner, H. Rodhe, H.A. Scheeren, D. Sikka, and J. Williams (2001), The Indian Ocean Experiment: Widespread air pollution from South and Southeast Asia, *Science*, *291* (5506), 1031-1036.

Lide, D.R., (Ed.) (2009), *CRC Handbook of Chemistry and Physics*, CRC Press/Taylor and Francis, Boca Raton, FL.

Lohmann, U., and J. Feichter (2005), Global indirect aerosol effects: A review, *Atmos. Chem. Phys.*, *5*, 715-737.

Marks, R. (1990), Preliminary investigations on the influence of rain on the production, concentration, and vertical distribution of sea salt aerosol, *J. Geophys. Res.*, *95* (22), 22299-22304.

Martensson, E.M., E.D. Nilsson, G. de Leeuw, L.H. Cohen, and H.C. Hansson (2003), Laboratory simulations and parameterization of the primary marine aerosol production, *J. Geophys. Res.-[Atmos.]*, *108* (D9), doi:10.1029/2002JD002263.

Mayol-Bracero, O.L., O. Rosario, C.E. Corrigan, R. Morales, I. Torres, and V. Perez (2001), Chemical characterization of submicron organic aerosols in the tropical trade winds of the Caribbean using gas chromatography/mass spectrometry, *Atmos. Environ.*, *35* (10), 1735-1745.

McFiggans, G., P. Artaxo, U. Baltensperger, H. Coe, M.C. Facchini, G. Feingold, S. Fuzzi, M. Gysel, A. Laaksonen, U. Lohmann, T.F. Mentel, D.M. Murphy, C.D. O'Dowd, J.R. Snider, and E. Weingartner (2006), The effect of physical and chemical aerosol properties on warm cloud droplet activation, *Atmos. Chem. Phys.*, *6*, 2593-2649.

Middlebrook, A.M., D.M. Murphy, and D.S. Thomson (1998), Observations of organic material in individual marine particles at Cape Grim during the First Aerosol Characterization Experiment (ACE 1), *J. Geophys. Res.-[Atmos.]*, *103* (D13), 16475-16483.

Monahan, E.C., C.W. Fairall, K.L. Davidson, and P.J. Boyle (1983), Observed interrelations between 10m winds, ocean whitecaps and marine aerosols, *Q. J. Roy. Meteor. Soc.*, *109* (460), 379-392.

Moore, M.J.K., H. Furatani, G.C. Roberts, R.C. Moffet, M.K. Giles, B. Palenik, and K.A. Prather (2011), Effect of organic compounds on cloud condensation nuclei (CCN) activity of sea spray aerosol produced by bubble bursting, *Atmos. Environ.*, Accepted.

Mouri, H., I. Nagao, K. Okada, S. Koga, and H. Tanaka (1997), Elemental compositions of individual aerosol particles collected over the Southern Ocean: A case study, *Atmos. Res.*, *43*, 183-195.

Mouri, H., and K. Okada (1993), Shattering and modification of sea-salt particles in the marine atmosphere, *Geophys. Res. Lett., 20* (1), 49-52.

Neubauer, K.R., M.V. Johnston, and A.S. Wexler (1997), On-line analysis of aqueous aerosols by laser desorption ionization, *Int. J. Mass Spectrom., 163* (1-2), 29-37.

Neubauer, K.R., M.V. Johnston, and A.S. Wexler (1998), Humidity effects on the mass spectra of single aerosol particles, *Atmos. Environ., 32* (14-15), 2521-2529.

Noble, C.A., and K.A. Prather (1996), Real-time measurement of correlated size and composition profiles of individual atmospheric aerosol particles, *Environ. Sci. Tech., 30* (9), 2667-2680.

Norman, M., C. Leck, and H. Rodhe (2003), Differences across the ITCZ in the chemical characteristics of the Indian Ocean MBL aerosol during INDOEX, *Atmos. Chem. Phys., 3*, 563-579.

Novakov, T., C.E. Corrigan, J.E. Penner, C.C. Chuang, O. Rosario, and O.L.M. Bracero (1997), Organic aerosols in the Caribbean trade winds: A natural source? *J. Geophys. Res.-[Atmos.], 102* (D17), 21307-21313.

O'Dowd, C.D., and G. De Leeuw (2007), Marine aerosol production: a review of the current knowledge, *Phil. Trans. A, 365* (1856), 1753-1774.

O'Dowd, C.D., M.C. Facchini, F. Cavalli, D. Ceburnis, M. Mircea, S. Decesari, S. Fuzzi, Y.J. Yoon, and J.P. Putaud (2004), Biogenically driven organic contribution to marine aerosol, *Nature, 431* (7009), 676-680.

Oppo, C., S. Bellandi, N.D. Innocenti, A.M. Stortini, G. Loglio, E. Schiavuta, and R. Cini (1999), Surfactant components of marine organic matter as agents for biogeochemical fractionation and pollutant transport via marine aerosols, *Mar. Chem., 63* (3-4), 235-253.

Orellana, M.V., T.W. Peterson, A.H. Diercks, S. Donohoe, P. Verdugo, and G. van den Engh (2007), Marine microgels: Optical and proteomic fingerprints, *Mar. Chem., 105*, 229-239.

Orellana, M.V., and P. Verdugo (2003), Ultraviolet radiation blocks the organic carbon exchange between the dissolved phase and the gel phase in the ocean, *Limnol. Oceangr., 48* (4), 1618-1623.

Passow, U. (2002), Production of transparent exopolymer particles (TEP) by phyto- and bacterioplankton, *Mar. Ecol. Prog. Ser., 236*, 1-12.

Poschl, U. (2005), Atmospheric aerosols: Composition, transformation, climate and health effects, *Angewandte Chemie-International Edition*, *44* (46), 7520-7540.

Posfai, M., J. Li, J.R. Anderson, and P.R. Buseck (2003), Aerosol bacteria over the southern ocean during ACE-1, *Atmos. Res.*, *66* (4), 231-240.

Prather, K.A., T. Nordmeyer, and K. Salt (1994), Real-time characterization of individual aerosol-particles using time-of-flight mass-spectrometry, *Anal. Chem.*, *66* (9), 1403-1407.

Qin, X.Y., P.V. Bhave, and K.A. Prather (2006), Comparison of two methods for obtaining quantitative mass concentrations from aerosol time-of-flight mass spectrometry measurements, *Anal. Chem.*, *78* (17), 6169-6178.

Quinn, P.K., T.S. Bates, D.J. Coffman, and D.S. Covert (2008), Influence of particle size and chemistry on the cloud nucleating properties of aerosols, *Atmos. Chem. Phys.*, *8* (4), 1029-1042.

Russell, L.M., L.N. Hawkins, A.A. Frossard, P.K. Quinn, and T.S. Bates (2010), Carbohydrate-like composition of submicron atmospheric particles and their production from ocean bubble bursting, *PNAS*, *107* (15), 6652-6657.

Sellegri, K., C.D. O'Dowd, Y.J. Yoon, S.G. Jennings, and G. de Leeuw (2006), Surfactants and submicron sea spray generation, *J. Geophys. Res.-[Atmos.]*, *111* (D22), doi:10.1029/2005JD006658.

Shenoy, D.M., S. Joseph, M.D. Kumar, and M.D. George (2002), Control and interannual variability of dimethyl sulfide in the Indian Ocean, *J. Geophys. Res.-[Atmos.]*, *107* (D19), 8008, doi:10.1029/2001JD000371.

Silva, P.J., R.A. Carlin, and K.A. Prather (2000), Single particle analysis of suspended soil dust from Southern California, *Atmos. Environ.*, *34*, 1811-1820.

Song, X.H., P.K. Hopke, D.P. Fergenson, and K.A. Prather (1999), Classification of single particles analyzed by ATOFMS using an artificial neural network, ART-2a, *Anal. Chem.*, *71* (4), 860-865.

Tyree, C.A., V.M. Hellion, O.A. Alexandrova, and J.O. Allen (2007), Foam droplets generated from natural and artificial seawaters, *J. Geophys. Res.-[Atmos.]*, *112*, D12204, doi:10.1029/2006JD007729.

Verdugo, P., A.L. Alldredge, F. Azam, D.L. Kirchman, U. Passow, and P.H. Santschi (2004), The oceanic gel phase: a bridge in the DOM-POM continuum, *Mar. Chem., 92* (1-4), 67-85.

Verdugo, P., M.V. Orellana, W.C. Chin, T.W. Peterson, G. van den Engh, R. Benner, and J.I. Hedges (2008), Marine biopolymer self-assembly: implications for carbon cycling in the ocean, *Faraday Discuss., 139*, 393-398.

Wells, M.L. (1998), Marine colloids: A neglected dimension, *Nature, 391*, 530-531.

Yoon, Y.J., D. Ceburnis, F. Cavalli, O. Jourdan, J.P. Putaud, M.C. Facchini, S. Decesari, S. Fuzzi, K. Sellegri, S.G. Jennings, and C.D. O'Dowd (2007), Seasonal characteristics of the physicochemical properties of North Atlantic marine atmospheric aerosols, *J. Geophys. Res.-[Atmos.]*, *112* (D4), D04206, doi:1O.1029/2005JD007044.

Zhou, J., K. Mopper, and U. Passow (1998), The role of surface-active carbohydrates in the formation of transparent exopolymer particles by bubble adsorption of seawater, *Limnol. Oceangr., 43* (8), 1860-1871.

Chapter 3

3. Direct Ejection of Particle Phase Sulfur Species from the Ocean to the Atmosphere

3.1 Synopsis

The influence of biological activity in the ocean on the chemical composition of sea spray, clouds, and climate remains poorly understood. The production and transfer of gas phase dimethyl sulfide (DMS) from the ocean to the atmosphere represents a well-documented biogenic process that influences both particle chemistry and number concentrations, as well as cloud formation processes in marine environments. However, the direct transfer of biogenic sulfur in the particle phase from the ocean to the atmosphere represents an area that remains largely unexplored. Here we show evidence for the direct ejection of oceanic particles containing elemental sulfur ions ($^{32}S^{+}$, $^{64}S_2^{+}$) into the marine atmosphere in seven different marine environments, as documented with on-line single particle mass spectrometry measurements. In studies with coupled ocean-atmosphere measurements, seawater chlorophyll concentrations were elevated in the same locations, suggesting a link between these S-rich particles and biological activity. Interestingly, these particles only appeared at night and comprised up to ~67% of the detected aerosol number fraction, primarily in the supermicron size range. These S-rich particles were detected along the California coast, across the northern and southern Pacific Oceans, and in the southern Indian Ocean, highlighting their global significance. Generation of primary sea spray from seawater obtained off the coast of southern

California confirm that these sulfur-containing particles are indeed being directly ejected from the ocean, adding a new and potentially important pathway for global sulfur cycling induced by marine biota.

3.2 Introduction

Aerosols influence global climate directly by scattering and absorbing incoming solar radiation and indirectly by acting as cloud condensation and ice nuclei; both particle size and composition play key roles that shape the radiative properties of aerosols [*Lohmann and Feichter*, 2005; *Poschl*, 2005]. In the marine environment, sulfur-containing compounds, namely sulfate, are key components of sea spray aerosols influencing both the aerosol direct and indirect effects [*Fitzgerald*, 1991]. Understanding the production of sulfur-containing compounds via the marine sulfur cycle is, therefore, important for understanding the radiative properties of sea spray aerosols [*O'Dowd et al.*, 1997]. Primary sea spray aerosol, consisting of both sea salt and biologically-produced organic material, is emitted from the ocean to the atmosphere via bursting bubbles generated from breaking waves [*O'Dowd and De Leeuw*, 2007]. Primary emissions contribute sea salt sulfate to sea spray aerosol; however, most sulfur-containing compounds found in sea spray aerosol derive from secondary sources, generated from gas-to-particle processes. In the marine atmosphere, most of the secondary sulfur-containing compounds are formed from biogenic gases such as dimethyl sulfide (DMS) produced by the enzymatic cleavage of the phytoplankton-excreted product dimethylsulfoniopropionate (DMSP). Once in the atmosphere, DMS is oxidized to form sulfur-containing compounds (e.g. sulfuric acid, methanesulfonic acid, etc), which can

either condense onto pre-existing particles or nucleate new particles potentially impacting both particle chemistry and number concentrations in the marine environment [*Barnes et al.*, 2006; *Charlson et al.*, 1987; *O'Dowd and De Leeuw*, 2007; *O'Dowd et al.*, 1997]. In addition to DMS, the biogenic marine sulfur cycle contributes additional reduced gas-phase species to the atmosphere such as methanethiol (CH_3SH), carbon disulfide (CS_2), carbonyl sulfide (OCS), and hydrogen sulfide (H_2S) that can potentially contribute secondary sulfur-containing compounds to sea spray [*Andreae*, 1990; *Kettle et al.*, 2001]. Marine biogenic sulfur has, thus, been found to contribute secondary sulfur-containing compounds to marine aerosols; however, it is unknown whether biogenic sulfur species can be directly emitted on primary marine particles.

Herein, we present real-time, single-particle measurements during seven field campaigns conducted in different marine environments; these measurements revealed the presence of unique sulfur species in the particle phase that were not formed by standard DMS oxidation chemical pathways. Shipboard measurements were conducted during the Indian Ocean Experiment (INDOEX) from January-March 1999 [*Lelieveld et al.*, 2001], the Asian Pacific Regional Aerosol Characterization Experiment (ACE-Asia) from March-April 2001 [*Huebert et al.*, 2003], the California Cooperative Oceanic Fisheries Investigation (CalCOFI) in November 2004 [*Furutani et al.*, 2008], the South Pacific Ocean Research Activity (SORA) field campaign from January-March 2009 (http://www.jamstec.go.jp/j/jamstec_news/sora2009/index.html), and the CalNex field campaign from May-June 2010 (http://www.esrl.noaa.gov/csd/calnex/). Ground-based measurements were conducted during the Cloud Indirect Effects Experiments (CIFEX) at

a coastal site in Trinidad Head, CA in April 2004 and on the Scripps Institution of Oceanography (SIO) pier from August-October 2009. Table 3.1 provides experimental details for all seven field campaigns including the start and stop dates, the latitudinal and longitudinal ranges, the relative humidity (RH) of the sampled aerosol, the ocean basin the study took place in, and the research platform the measurements were performed on. Figure 3.1 shows the locations where these unique sulfur species were detected in addition to the percentage detected during the shipboard studies as a function of cruise track; S-type particles were found to represent between ~5-67% of detected particles, by number, highlighting the importance and high abundance of these unique particles in marine environments.

3.3 Methods

Measurements were conducted using ATOFMS during seven different field campaigns in marine environments. The relative humidity (RH) of the sampled aerosol during four of the studies (INDOEX, ACE-Asia, CIFEX, and CalNex) was controlled to 55% using a heated inlet [*Bates et al.*, 2004]; during the SIO Pier 2009 and SORA campaigns, the RH was maintained at 15-30% using one silica gel drier. The RH of the sampled aerosol was not conditioned during the CalCOFI field campaign. The standard nozzle inlet ATOFMS [*Gard et al.*, 1997], which sizes and chemically analyzes particles in the 0.2-3 μm size range, was used for all field campaigns except for SORA, where an ATOFMS using an aerodynamic lens inlet was operated in the 0.1-2.0 μm size range [*Su et al.*, 2004]. The operating principles of the ATOFMS have been previously described [*Gard et al.*, 1997; *Su et al.*, 2004]. Briefly, atmospheric particles are pulled into a

Table 3.1: Experimental conditions during the seven field campaigns used to characterize the S-type particles described in the manuscript.

Campaign	Ocean Basin	Platform	Latitude	Longitude	Date	Inlet RH
INDOEX	Indian Ocean	Ship	6.07 N to 12.7 S	75 E to 72.03 E	Mar. 1999	55%
ACE-Asia	Pacific Ocean	Ship	39.4 N to 30.5 N	173.92 E to 126.14 E	Mar.-Apr. 2001	55%
CalCOFI	Pacific Ocean	Ship	35.1 to 29.8 N	124.3 to 117.2 W	Nov. 2004	Ambient
CIFEX	Pacific Ocean	Ground	41.05 N	124.15 W	Mar.-Apr. 2004	55%
SORA 2009	N. & S. Pacific Ocean	Ship	41.4 N to 56.3 S	141.2 E to 66 W	Jan.-Apr. 2009	15-30%
SIO Pier 2009	Pacific Ocean	Ground	32.87 N	117.25 W	Aug.-Oct. 2009	15-30%
CalNex	Pacific Ocean	Ship	38.6 to 32.6 N	123 to 117.1 W	May-Jun. 2010	55%

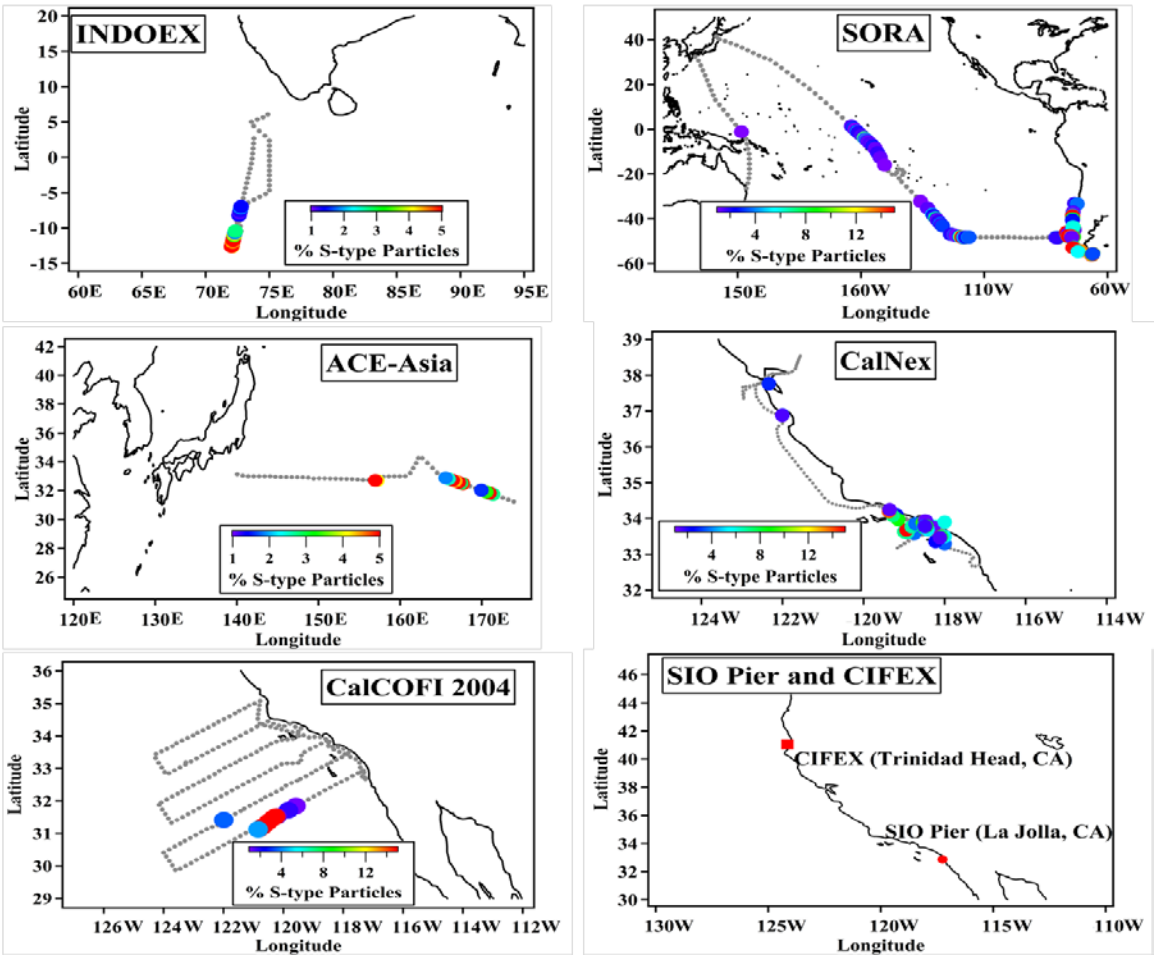

Figure 3.1: Percentages of S-type particles (colored dots) are shown as a function of cruise track (grey dots) for the INDOEX, ACE-Asia, CalCOFI, SORA, and CalNex field campaigns. The locations of the ground-based CIFEX and SIO Pier campaigns are also shown (bottom, right panel).

vacuum chamber though the sampling inlet. Particles enter the light scattering region consisting of two continuous wave (532 nm) scattering lasers where the time taken to traverse the laser beams is recorded giving the terminal velocity of the particle, which is used to calculate the aerodynamic diameter of the particle. The transit time is also used to fire a Q-switched Nd:YAG laser that desorbs and ionizes the particles simultaneously creating positive and negative ions, which are analyzed in a dual-polarity time-of-flight mass spectrometer. Mass spectra are imported into Matlab (The MathWorks, Inc.) using a software toolkit, YAADA [*Allen,* 2002], and clustered together based on similarities in ion peaks and ion intensity using an adaptive-resonance neural network (ART-2a) [*Song et al.,* 1999]. Each ion peak assignment presented in this paper corresponds to the most likely ion produced at a given mass-to-charge (*m/z*). Size resolved chemical composition was monitored continuously and subsequently averaged in 1-hour time bins for the data presented in this paper.

3.4 Results and Discussion

3.4.1 Characteristics of Sulfur-Containing Particles

Real-time, single-particle measurements using an aerosol time-of-flight mass spectrometer (ATOFMS) [*Gard et al.,* 1997] measured sulfur ions (*m/z* $^{32}S^+$ and $^{64}S_2^+$) [*Coffee,* 2002] in particles unique to marine environments. As shown in Figure 3.2a, the sulfur-rich particles (S-type particles) are characterized by a $^{64}S_2^+$ peak that is more intense than the $^{32}S^+$ peak; additional peaks shown in Figure 3.2a include $^{30}NO^+$, which could be due to the presence of marine nitrogen species, and less intense peaks from inorganic ions ($^{23}Na^+$, $^{24}Mg^+$, $^{39}K^+$, $^{40}Ca^+$) and organic ions ($^{12}C^+$, $^{27}C_2H_3^+$, $^{43}C_2H_3O^+$)

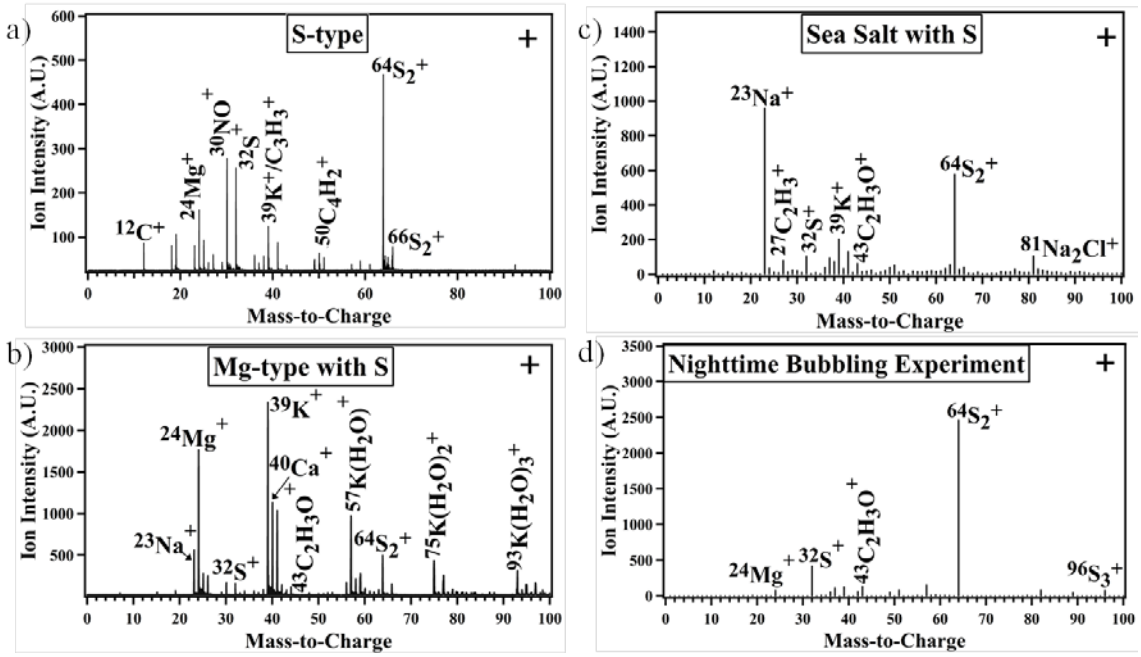

Figure 3.2: Representative average mass spectra of (a) S-type particles containing intense elemental sulfur ions ($^{32}S^+$, $^{64}S_2^+$), (b) a Mg-type particle internally mixed with elemental sulfur ions, (c) a sea salt particle internally mixed with elemental sulfur ions, and (d) an S-type particle observed during a nighttime bubble bursting experiment conducted during CalNex onboard the R/V Atlantis.

typical of marine-derived particles measured by ATOFMS [*Gaston et al.*, 2011]. It is also possible that the ion peak at *m/z* +64 could be due to SO_2^+, however, this can be ruled out by examining the relative isotopic abundance pattern for the ion peaks *m/z* +64, +65, +66, and +68, which matches S_2^+ but not SO_2^+. Another unique feature of these particles is the lack of negative ion spectra on the majority of S-type particles indicating the presence of tightly bound particle phase water, which suppresses negative ions produced by laser desorption/ionization [*Neubauer et al.*, 1997; *Neubauer et al.*, 1998].

Common sulfur-containing compounds do not account for the observed elemental sulfur ions. While ATOFMS studies frequently detect sulfur-containing species in the marine environment including sulfate, sulfite, hydroxymethanesulfonate, and methanesulfonate, these species are detected as negative ions at $^{97}HSO_4^-$, $^{80}SO_3^-$, $^{111}CH_3SO_4^-$ and $^{95}CH_3SO_3^-$, respectively [*Gaston et al.*, 2010; *Silva and Prather*, 2000; *Whiteaker and Prather*, 2003], and do not produce positive sulfur ions (see Figure 3.3). Figure 3.3 shows a comparison of spectra containing sulfate and MSA while the bottom panel shows a mass spectrum of the S-type particles described in this manuscript. The appearance of elemental sulfur ions ($^{32}S^+$, $^{64}S_2^+$) cannot be explained by the fragmentation of other S-containing species commonly found in sea spray aerosols such as methanesulfonate (MSA) ($^{95}CH_3SO_3^-$) or sulfate ($^{97}HSO_4^-$) [*Gaston et al.*, 2010]. It is thus likely these sulfur ions arise from a reduced form of sulfur. To test this hypothesis, sulfur-containing standards commonly found in the ocean including the amino acids cysteine and methionine, glutathione (oxidized and reduced), dimethyl sulfide (DMS), dimethylsulfoniopropionate (DMSP), which is the precursor for DMS, elemental sulfur,

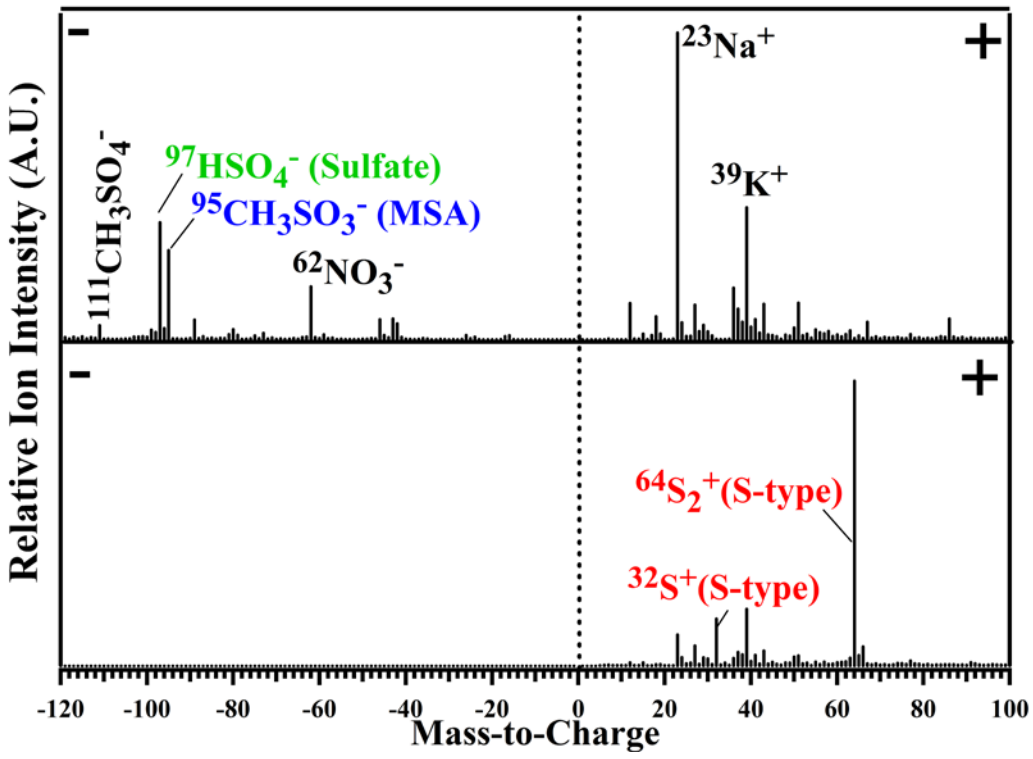

Figure 3.3: Comparison of representative mass spectra of particles containing methanesulfonate (MSA) and sulfate (top panel) and the S-type particles described in the manuscript (bottom panel).

and a saturated hydrogen sulfide solution were chemically analyzed. Cysteine, methionine, glutathione (oxidized and reduced), and DMS were obtained from Sigma Aldrich and were at least 97% pure. DMSP was obtained from Research Plus, Inc. Elemental sulfur (99.5% purity) was obtained from Acros Organic. A saturated solution of hydrogen sulfide containing 0.4 g hydrogen sulfide (99.5% purity) in 100mL water was obtained from Ricca Chemical Company. Solutions of ~25mg of each compound in ~150mL of milli-Q water (> 18.2 MΩ) were prepared. The point of these standards was to obtain qualitative information regarding the elemental sulfur ions detected by ATOFMS. The solutions were then atomized using a custom-made set-up and the generated particles were dried to a relative humidity of < 10% using two diffusion silica gel driers. The dried particles were then chemically analyzed using ATOFMS; at least 100 particles were analyzed for each compound. Figure 3.4 shows representative spectra of each of the standard compounds used. Only the elemental sulfur standard and the hydrogen sulfide solution, which precipitates elemental sulfur due to the reaction of $H_2S_{(g)}$ with dissolved oxygen in water, reproduced the elemental sulfur ion peaks ($^{32}S^+$ and $^{64}S_2^+$) found in ambient spectra. This provides strong evidence that the S-type particles arise from compounds containing a reduced form of sulfur, including organic sulfur-containing compounds, rather than oxidized sulfur compounds. In contrast to ambient S-particles, the spectra produced by both standards also produced sulfur peaks in the negative ion spectra (see Figure 3.4). One possible explanation is that ambient S-type particles are associated with other species (e.g. Mg^{2+})/particle types that retain water more than the particles generated from standards in the lab; however, further studies are required to confirm this hypothesis.

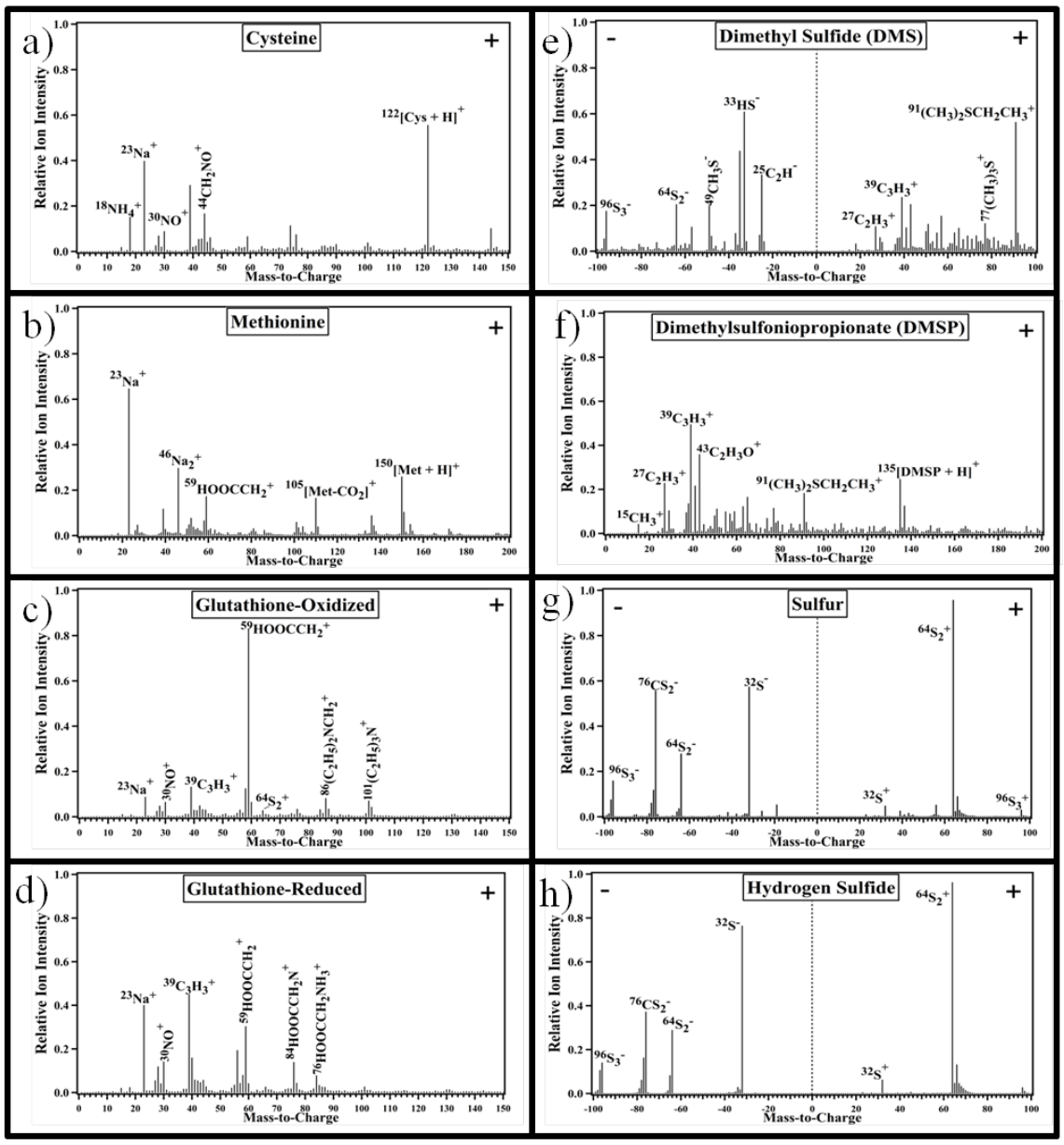

Figure 3.4: Representative mass spectra of (a) cysteine, (b) methionine, glutathione (c) oxidized and (d) reduced, (e) DMS, (f) DMSP, (g) elemental sulfur, and (h) hydrogen sulfide. Spectra only showing positive ions produced no negative ion spectra.

3.4.2 Evidence for the Primary Formation of S-type Particles

In addition to their associations with S-type particles, sulfur ions were also found internally mixed on other particle types (Figures 3.2b-c). Low intensity sulfur peaks were frequently internally mixed with Mg-type particles containing intense $^{24}Mg^+$ and/or $^{40}Ca^+$ (Figure 3.2b), which have also been shown to be produced in marine regions with elevated chlorophyll *a* [*Gaston et al.*, 2011]. Mg-type particles were found to be strongly bound to particulate water and, as such typically lack negative negative ion spectra at 55% RH [*Gaston et al.*, 2011]; thus, association of sulfur ions with this particle type could explain the lack of negative ion spectra observed for S-type particles. Sulfur ions were also occasionally found on sea salt particles ($^{23}Na^+$) (Figure 3.2c). To probe whether these S ions were enriched on the particle surface or not, the ratio of $^{24}Mg^+/^{32}S^+$, $^{24}Mg^+/^{64}S_2^+$, $^{23}Na^+/^{32}S^+$ and $^{23}Na^+/^{64}S_2^+$ were compared for different total ion intensities ("low", "medium", and "high"). Using laser desorption/ionization, ion peaks that are more intense at lower total ion intensities and lower laser fluencies have been shown to be concentrated on the particle surface [*Zelenyuk et al.*, 2008]. As shown in Figure 3.5, the ratios of $^{23}Na^+$ and $^{24}Mg^+$ to $^{32}S^+$ and $^{64}S_2^+$ were lower at lower total ion intensities suggesting that $^{32}S^+$ and $^{64}S_2^+$ are found on the surface of the particles. The fact that sulfur ions were found exclusively on primary, ocean-derived particle types (e.g. sea salt, Mg-type particles), even though particle types from other sources (e.g. soot, organic carbon, etc.) were present in the same air masses, supports the hypothesis that sulfur was directly ejected from the ocean in the particulate phase as opposed to forming in the atmosphere and partitioning to the particles from the gas phase. This was confirmed by

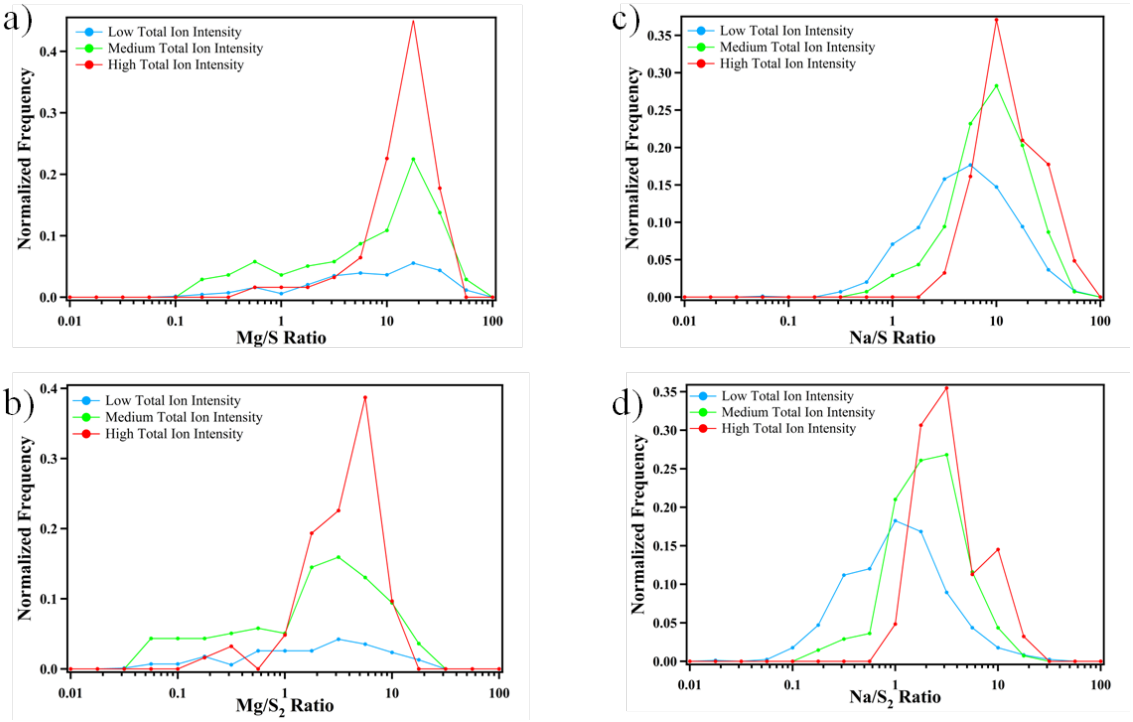

Figure 3.5: Ratios of $^{24}Mg^{+}/^{32}S^{+}$, $^{24}Mg^{+}/^{64}S_2^{+}$, $^{23}Na^{+}/^{32}S^{+}$ and $^{23}Na^{+}/^{64}S_2^{+}$ for individual particles observed during INDOEX.

bubble bursting experiments conducted during the CalNex cruise. A large-scale bubbler was deployed in the ocean during various points of the cruise including during the day and night to generate primary sea spray particles [*Keene et al.*, 2007], which were sampled directly by the instrumentation onboard the ship including the ATOFMS. Figure 3.2d shows a representative spectrum of an S-type particle, which contains similar peaks to ambient S-type particles (Figure 3.2a) such as $^{24}Mg^{+}$ and $^{43}C_2H_3O^{+}$. These S-type particles were only produced during nighttime bubbling experiments, consistent with the ambient observations as discussed below. These experiments support the assignment of this particle type as being produced from a primary rather than secondary oceanic source. Further evidence for a primary oceanic source is given by the fact that during all of the studies investigated, S-type particles were typically observed as wind speeds reached, on average, at least 5-10 m/s. In fact, S-type particles, representing ~12% of the detected particles by number, peaked during CIFEX when a storm occurred, resulting in strong winds (up to 20 m/s) and rain (see Figure 3.6), both of which increase the production of primary sea spray aerosol [*Gaston et al.*, 2011; *Marks*, 1990; *Monahan et al.*, 1983].

3.4.3 Linking Marine Biological Activity and the Detection of S-type Particles

The production of S-type particles illustrates another previously unreported example of the impact of marine biological activity on the composition of sea spray aerosol. As shown in Figure 3.1 and Table 3.1, S-type particles have primarily been observed during studies in the California Current, which is a highly productive upwelling environment. In fact, during CalNex, a red tide bloom of *L. polyedrum*, an organism found to contribute marine biogenic sulfur to the particle phase [*Gaston et al.*, 2010], was

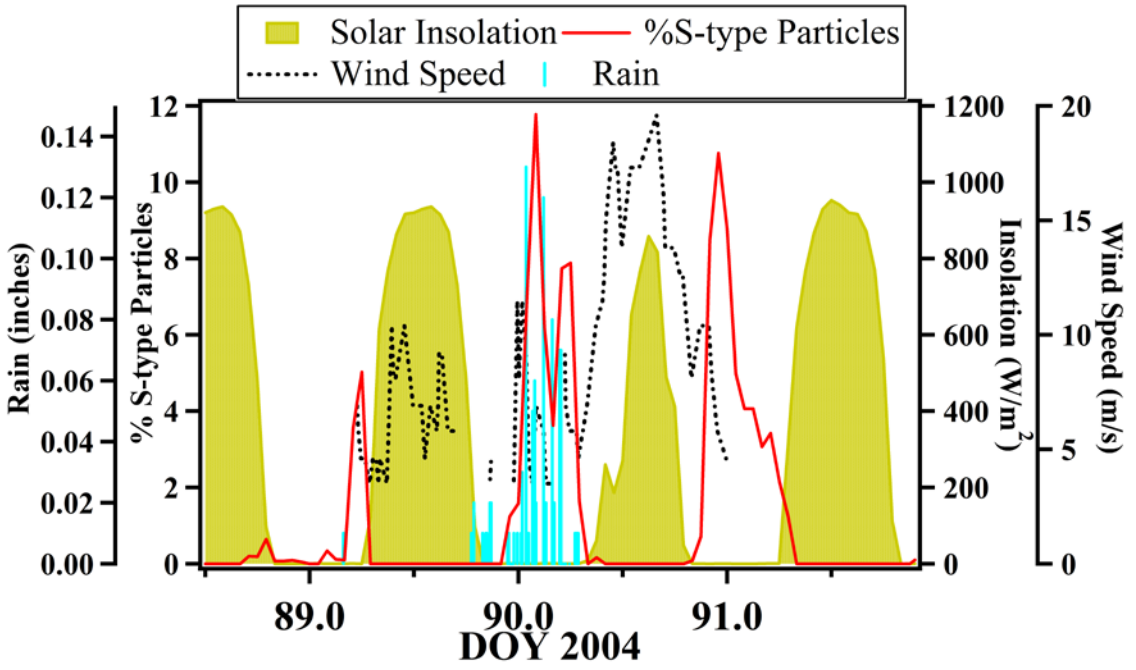

Figure 3.6: Temporal profile of S-type particles (red line), solar insolation (solid yellow), wind speed (dashed black line), and rain (blue lines) during CIFEX.

observed suggesting a link between enhanced levels of DMS producers and the observed S-type particles. Additional evidence for this link was also observed in the Indian Ocean during INDOEX where S-type particles were observed at the southern-most point of the cruise (see Figures 3.1 and 3.7a), below the Intertropical Convergence Zone (ITCZ). Continental particle types were not transported across the ITCZ, and thus did not occur during the period with elevated S-type particles, supporting the hypothesis that the S particles were ocean-derived [*Gaston et al.*, 2011]. It should be noted that in addition to S-type particles, biogenic Mg-type particles, including Mg-type particles internally mixed with elemental S ions, were also elevated in the southern Indian Ocean [*Gaston et al.*, 2011], supporting a biological source of these S-containing particles. As shown in Figure 3.8a, chlorophyll *a* levels, a proxy for phytoplankton biomass and DMS were also elevated in these same southern waters [*Gaston et al.*, 2011; *Kumar et al.*, 2002]. Furthermore, DMS and DMSP were also found in the particle phase during INDOEX highlighting the direct export of biogenic marine sulfur during this campaign [*Kumar et al.*, 2002]. Lastly, evidence for the link between biological activity and S-type particles was also observed on a much larger regional scale across the northern and southern Pacific Ocean during the SORA campaign. Figure 3.8b shows S-type particles detected during SORA as a function of the cruise track and chlorophyll *a* concentrations as measured by the MODIS satellite. S-type particles were primarily detected in regions of elevated chlorophyll *a* concentrations such as eastern boundary currents where upwelling occurs (e.g. eastern tropical Pacific), again highlighting the link between this unique particle type and biological activity.

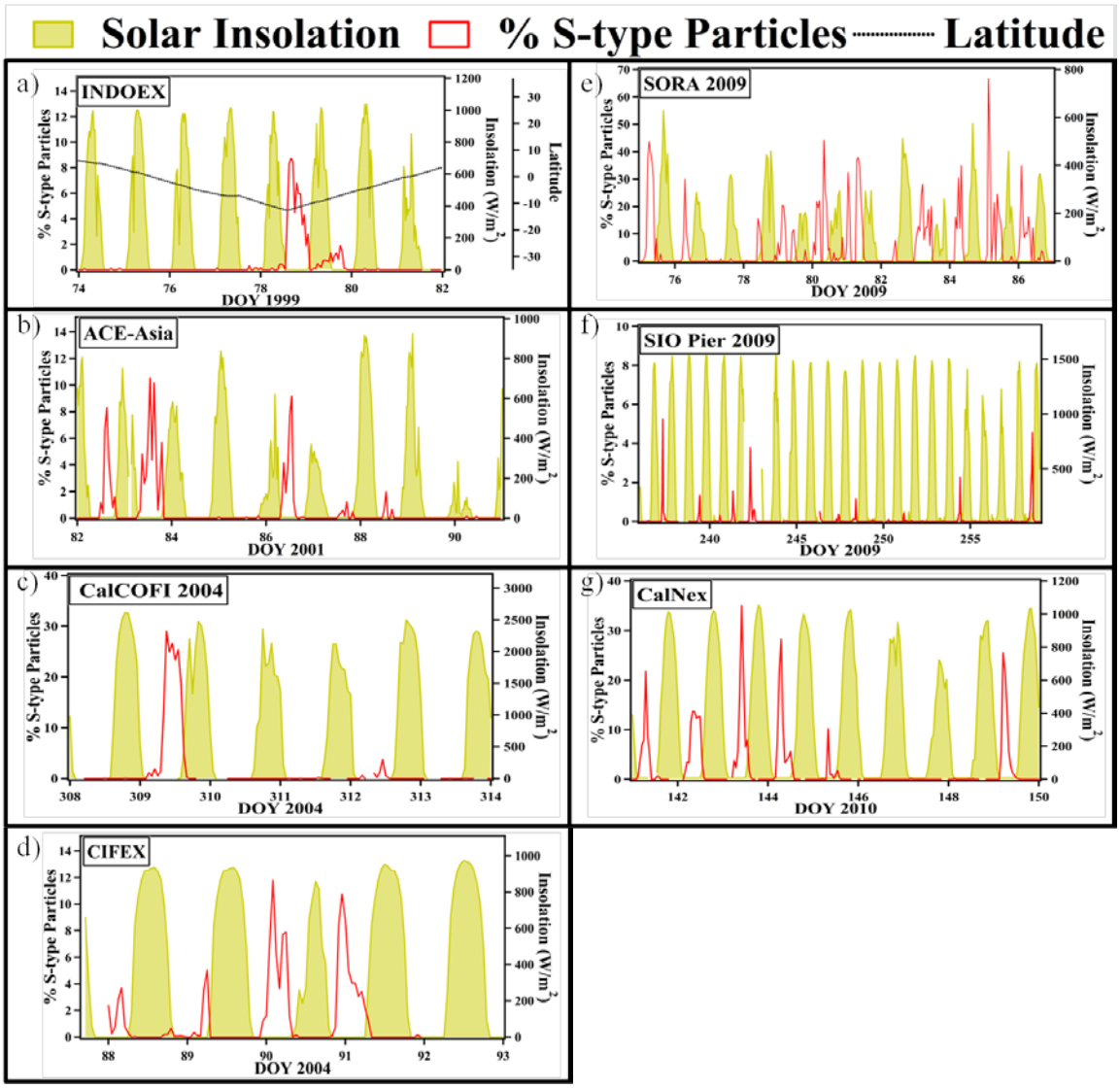

Figure 3.7: Hourly time series of ATOFMS measurements of S-type particles (red line) and solar insolation (solid yellow) during (a) INDOEX, (b) ACE-Asia, (c) CalCOFI 2004, (d) CIFEX, (e) SORA 2009, (f) Pier 2009, and (g) CalNex. Solar insolation data for DOY 242-243 during the Pier 2009 (f) field campaign is missing.

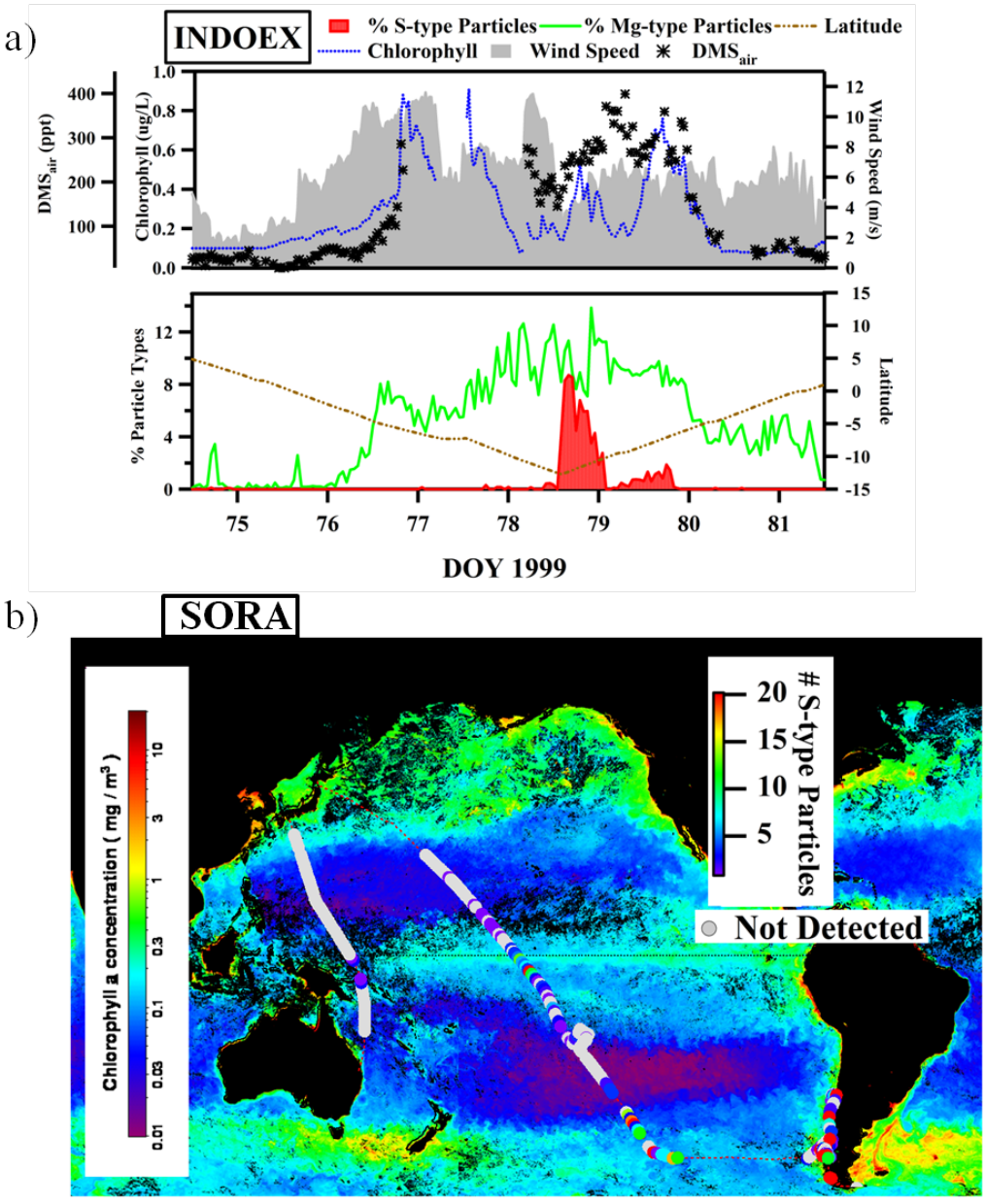

Figure 3.8: (a) Measurements of S-type particles (solid red), Mg-type particles (green line), wind speed (solid grey), chlorophyll (dotted blue line), and atmospheric DMS (black asterisks) during the INDOEX campaign. (b) Measurements of S-type particles (colored dots) and chlorophyll concentrations (colored gradient over the oceans) during the 99 day SORA 2009 cruise from Japan to South America. S-type particles are shown for data averaged over 4 hours.

3.4.4 Diurnal Profiles of S-type Particles

The observed diurnal behavior of this particle type, shown in Figure 3.7, provides additional constraints on the sources and formation mechanisms of S-type particles. The percentage of detected S-type particles typically exhibits a nocturnal maximum that decreases either before sunrise or ~1-2 hours after solar insolation rises (Figure 3.7). Due to the rapid loss of this particle type with the increase of solar radiation, the diurnal profile of S-type particles is most likely due to photolytic destruction; this destruction mechanism is also supported by the fact that the S ions appear to be enriched at the particle surface where photolysis is most likely to occur. Another potential explanation for the diurnal profile of this particle type could be diel changes, which occur in many biological processes. For example, light sensitive zooplankton are known to vertically migrate toward the surface ocean at night resulting in increased predation of species such as marine bacteria at night [*Dacey and Wakeham*, 1986] resulting in the release of intracellular biogenic sulfur to the water column at night. Further studies are being conducted to address the nighttime production mechanism leading to these unique S-containing particles.

3.4.5 Possible Sources of S-type Particles

S-type particles could result from elemental sulfur produced by marine bacteria, proteins and peptides containing disulfide bridges produced by marine bacteria and viruses, and sulfur-containing compounds resulting from reactions involving H_2S dissolved in seawater. Once formed in the surface ocean, $H_2S_{(aq)}$ dissociates to form $HS^-_{(aq)}$ and $S^{2-}_{(aq)}$, the sum of all three species are herein referred to as total dissolved sulfides

(TDS) [*Cutter et al.*, 1999]. In addition to being produced from the hydrolysis of carbonyl sulfide, TDS is also commonly produced in the surface ocean by marine algae [*Cutter et al.*, 1999; *Walsh et al.*, 1994]. As such, TDS is derived from marine biological activity and is observed to track chlorophyll *a* concentrations [*Cutter and Krahforst*, 1988; *Radford-Knoery and Cutter*, 1994] providing further evidence that S-type particles, which also tracked proxies for marine biological activity, could derive from TDS. The diurnal profile of S-type particles provides additional evidence that the production of this particle type could be from TDS, which also exhibit a maximum at night and a minimum during the daytime due to photodecomposition leading to the rapid oxidation and loss of TDS in the surface ocean [*Andreae*, 1990; *Cutter and Krahforst*, 1988; *Pos et al.*, 1997; *Radford-Knoery and Cutter*, 1994]. TDS is subjected to sulfur oxidation by marine bacteria leading to the formation of particulate elemental sulfur globules [*Brune*, 1989; *Steudel*, 1996], which are in the 1-3 μm size range. These globules are polysulfides composed of long chain S molecules ending in carbon-containing moieties ($R\text{-}S_n\text{-}R$) [*Brune*, 1989; *Prange et al.*, 1999; *Steudel*, 1996]. The size distribution of the S-type particles detected by the ATOFMS peaked at ~1.5 μm in Figure 3.9, which shows scaled aerodynamic particle size distributions. ATOFMS has known transmission biases based on the inlet design that affect the raw size distribution obtained with the instrument [*Allen et al.*, 2000; *Dall'Osto et al.*, 2006]; however, number concentrations obtained from ATOFMS can be corrected using a scaling factor derived from a sizing instrument such as an aerodynamic particle sizer (APS) to obtain accurate particle counts for discrete size bins [*Qin et al.*, 2006]. This was done to obtain the size distributions shown in Figure 3.9. For comparison, the scaled size profile of sea salt, not internally mixed with S ions

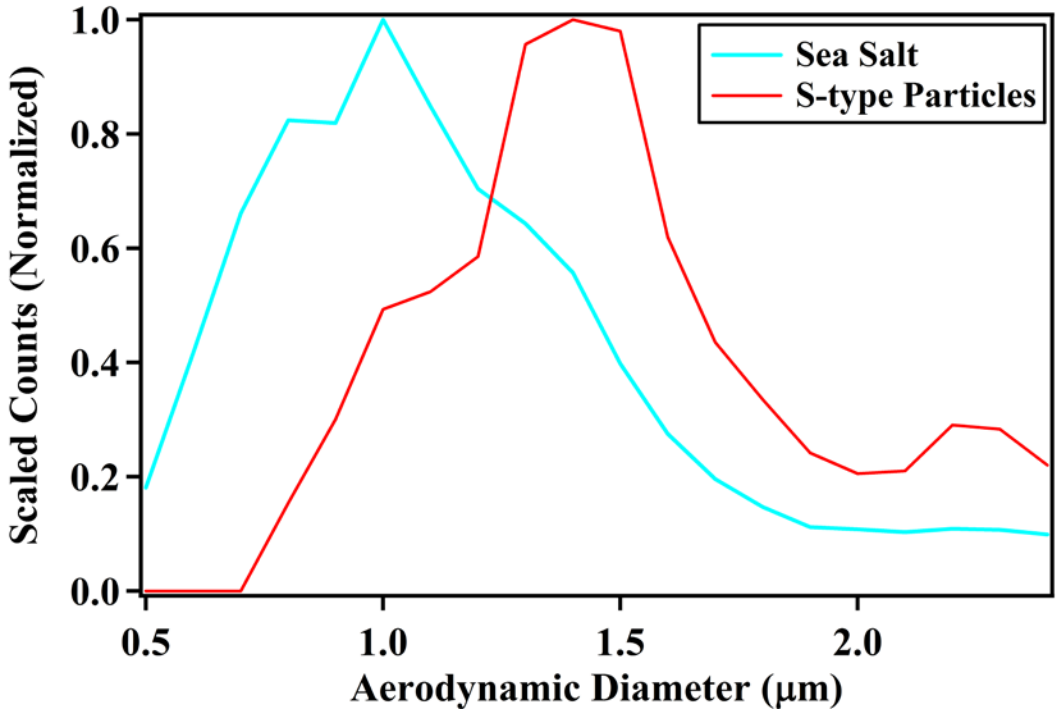

Figure 3.9: Size distributions for S-type (red line) and fresh sea salt (blue line) particles. Particle counts have been scaled using an aerodynamic particle sizer (APS) to account for transmission biases in the ATOFMS. Particle counts have been normalized to total counts per size bin to show the relative fractions of scaled counts per size. Fresh sea salt particles are not internally mixed with S ions in this case.

is shown in Figure 3.9. The S-type particles are clearly enhanced in the coarse mode and are found in larger particle sizes than sea salt particles. The size range of the S-particles is consistent with previous measurements of elemental sulfur globules produced by sulfur oxidizing bacteria. This size range is also consistent with S-containing compounds associated with whole marine bacteria themselves, which are typically ~0.3-1.0 μm in diameter [*Azam and Hodson*, 1977]. Notably, Mouri *et al.* [1995] also detected giant sulfur particles (1-1.5 μm radii) during a cruise in the equatorial Pacific; however, since these particles were detected off-line and the speciation of the sulfur detected was not obtained, the source and composition of these particles remain unknown [*Mouri et al.*, 1995]. Other possible sources include biogenic compounds containing disulfide bonds formed between cysteine molecules, proteins, and/or organic sulfur compounds found in/or surrounding marine microorganisms.

3.6 Conclusions

The importance of sulfur cycling in the marine atmosphere has been shown to occur mainly through the contribution of secondary sulfate and methanesulfonate to sea spray aerosols [*Barnes et al.*, 2006; *Charlson et al.*, 1987; *O'Dowd et al.*, 1997]; however, the results presented herein reveal a new nighttime ejection process for sulfur in the particulate form from the ocean to the marine atmosphere. As highlighted in Figures 3.1 and 3.7, S-type particles have been observed off the California coast (CalCOFI, CIFEX, SIO Pier, and CalNex), across the northern Pacific Ocean (ACE-Asia, SORA), in the southern Pacific Ocean (SORA), and in the southern Indian Ocean (INDOEX). Particles containing molecules with reduced forms of sulfur were detected by ATOFMS

resulting from primary oceanic emissions to the atmosphere, and showing a strong diurnal cycle with concentrations peaking at night likely due to photolytic destruction of this particle type during the day. The detection of these particles was linked with elevated indicators of biological activity including Mg-type particles and chlorophyll *a* concentrations. These observations provide evidence for the formation of S-type particles from biologically-derived compounds including surface ocean TDS, sulfur-containing proteins and peptides, etc. The sulfur particles described herein could influence not only marine aerosol chemistry, but also gas-phase chemistry in the marine atmosphere. Depending on the chemical form, this reduced sulfur could oxidize to form $SO_{2(g)}$ [*Hills et al.*, 1987], an important precursor of particulate sulfate and sulfuric acid, which can lead to new particle formation under certain conditions [*Clarke et al.*, 1998; *Clarke et al.*, 1999]. The detection of particulate compounds containing reduced sulfur in regions of elevated chlorophyll *a* concentrations highlights that S-type particles described herein result from biological activity in the ocean providing evidence for a new route for emission of sulfur to the atmosphere.

3.7 Acknowledgements

PNNL is acknowledged for support of C.J. Gaston. K. Suski, J. Cahill, and D. Collins are thanked for help with measurements during the SIO pier field campaign. C. McDonald is acknowledged for use of the SIO pier for measurements. M. Spencer and J. Holecek are thanked for carrying out measurements during the CIFEX field campaign. D. Sodeman is thanked for assisting with measurements during ACE-Asia. D. Hamilton

and D. Coffman are acknowledged for assistance during the ACE-Asia, INDOEX, and CalNex field measurements.

Chapter 3 is in preparation for submission to *Proceedings of the National Academy of Sciences*: Gaston, C.J., Furutani, H., Guazzotti, S.A., Coffee, K.R., Bates, T.S., Quinn, P.K., Jung, J., Uematsu, M, Prather, K.A. Direct ejection of particle phase sulfur species from the ocean to the atmosphere. The dissertation author was the primary investigator and author of this paper.

3.8 References

Allen, J.O. (2002), YAADA software toolkit to analyze single-particle mass spectral data: Reference manual version 1.1, *Arizona State University*, http://www.yaada.org.

Allen, J.O., D.P. Fergenson, E.E. Gard, L.S. Hughes, B.D. Morrical, M.J. Kleeman, D.S. Gross, M.E. Galli, K.A. Prather, and G.R. Cass (2000), Particle detection efficiencies of aerosol time of flight mass spectrometers under ambient sampling conditions, *Environ. Sci. Tech., 34* (1), 211-217.

Andreae, M.O. (1990), Ocean-atmosphere interactions in the global biogeochemical sulfur cycle, *Mar. Chem., 30* (1-3), 1-29.

Azam, F., and R.E. Hodson (1977), Size distribution and activity of marine microheterotrophs, *Limnol. Oceangr., 22* (3), 492-501.

Barnes, I., J. Hjorth, and N. Mihalopoulos (2006), Dimethyl sulfide and dimethyl sulfoxide and their oxidation in the atmosphere, *Chem. Rev., 106* (3), 940-975.

Bates, T.S., P.K. Quinn, D.J. Coffman, D.S. Covert, T.L. Miller, J.E. Johnson, G.R. Carmichael, I. Uno, S.A. Guazzotti, D.A. Sodeman, K.A. Prather, M. Rivera, L.M. Russell, and J.T. Merrill (2004), Marine boundary layer dust and pollutant transport associated with the passage of a frontal system over eastern Asia, *J. Geophys. Res.-[Atmos.], 109* (D19S19), doi:10.1029/2003JD004094.

Brune, D.C. (1989), Sulfur oxidation by phototrophic bacteria, *Biochimica et Biophysica Acta*, *975*, 189-221.

Charlson, R.J., J.E. Lovelock, M.O. Andreae, and S.G. Warren (1987), Oceanic phytoplankton, atmospheric sulfur, cloud albedo and climate, *Nature*, *326* (6114), 655-661.

Clarke, A.D., D. Davis, V.N. Kapustin, F. Eisele, G. Chen, I. Paluch, D. Lenschow, A.R. Bandy, D. Thornton, K. Moore, L. Mauldin, D. Tanner, M. Litchy, C. M.A., J. Collins, and G. Albercook (1998), Particle nucleation in the tropical boundary layer and its coupling to marine sulfur sources, *Science*, *282*, 89-92.

Clarke, A.D., V.N. Kapustin, F.L. Eisele, R.J. Weber, and P.H. McMurray (1999), Particle production near marine clouds: Sulfuric acid and predictions from classical binary nucleation, *Geophys. Res. Lett., 26* (16), 2425-2428.

Coffee, K.R. (2002), Single particle characterization of soil and dust particulate matter in the urban and marine environments, Department of Chemistry, University of California, Riverside, Riverside, CA.

Cutter, G.A., and C.F. Krahforst (1988), Sulfide in surface waters of the western Atlantic Ocean, *Geophys. Res. Lett.*, *15* (2), 1393-1396.

Cutter, G.A., R.A. Walsh, and C. Silva del Echos (1999), Production and speciation of hydrogen sulfide in surface waters of the high latitude North Atlantic Ocean, *Deep Sea Res.II*, *46*, 991-1010.

Dacey, J.W.H., and S.G. Wakeham (1986), Oceanic dimethylsulfide - Production during zooplankton grazing on phytoplankton, *Science*, *233* (4770), 1314-1316.

Dall'Osto, M., R.M. Harrison, D.C.S. Beddows, E.J. Freney, M.R. Heal, and R.J. Donovan (2006), Single-particle detection efficiencies of aerosol time-of-flight mass spectrometry during the North Atlantic marine boundary layer experiment, *Environ. Sci. Tech.*, *40* (16), 5029-5035.

Fitzgerald, J.W. (1991), Marine aerosols: A review, *Atmos. Environ. A-Gen. Topics*, *25* (3-4), 533-545.

Furutani, H., M. Dall'osto, G.C. Roberts, and K.A. Prather (2008), Assessment of the relative importance of atmospheric aging on CCN activity derived from field observations, *Atmos. Environ.*, *42* (13), 3130-3142.

Gard, E., J.E. Mayer, B.D. Morrical, T. Dienes, D.P. Fergenson, and K.A. Prather (1997), Real-time analysis of individual atmospheric aerosol particles: Design and performance of a portable ATOFMS, *Anal. Chem.*, *69* (20), 4083-4091.

Gaston, C.J., H. Furutani, S.A. Guazzotti, K.R. Coffee, T.S. Bates, P.K. Quinn, L.I. Aluwihare, B.G. Mitchell, and K.A. Prather (2011), Unique ocean-derived particles serve as a proxy for changes in ocean chemistry, *J. Geophys. Res.-[Atmos.]*, *116*, D18310, doi:10.1029/2010JD015289.

Gaston, C.J., K.A. Pratt, X.Y. Qin, and K.A. Prather (2010), Real-time detection and mixing state of methanesulfonate in single particles at an inland urban location during a phytoplankton bloom, *Environ. Sci. Tech.*, *44* (5), 1566-1572.

Hills, A.J., R.J. Cicerone, J.G. Calvert, and J.W. Birks (1987), Kinetics of the Reactions of S_2 with O, O_2, O_3, N_2O, NO, and NO_2, *Journal of Physical Chemistry*, *91* (5), 1199-1204.

Huebert, B.J., T. Bates, P.B. Russell, G.Y. Shi, Y.J. Kim, K. Kawamura, G. Carmichael, and T. Nakajima (2003), An overview of ACE-Asia: Strategies for quantifying

the relationships between Asian aerosols and their climatic impacts, *J. Geophys. Res.-[Atmos.]*, *108* (D23), 8633, doi:10.1029/2003JD003550.

Keene, W.C., H. Maring, J.R. Maben, D.J. Kieber, A.A.P. Pszenny, E.E. Dahl, M.A. Izaguirre, A.J. Davis, M.S. Long, X.L. Zhou, L. Smoydzin, and R. Sander (2007), Chemical and physical characteristics of nascent aerosols produced by bursting bubbles at a model air-sea interface, *J. Geophys. Res.-[Atmos.]*, *112* (D21), D21202, doi:10.1029/2007JD008464.

Kettle, A.J., T.S. Rhee, M. von Hobe, A. Poulton, J. Aiken, and M.O. Andreae (2001), Assessing the flux of different volatile sulfur gases from the ocean to the atmosphere, *J Geophys Res-Atmos*, *106* (D11), 12193-12209.

Kumar, M.D., D.M. Shenoy, V.V.S.S. Sarma, M.D. George, and M. Dandekar (2002), Export fluxes of dimethylsulfoniopropionate and its break down gases at the air-sea interface, *Geophys. Res. Lett.*, *29* (2), 1021, doi:10.1029/2001GL013967.

Lelieveld, J., P.J. Crutzen, V. Ramanathan, M.O. Andreae, C.A.M. Brenninkmeijer, T. Campos, G.R. Cass, R.R. Dickerson, H. Fischer, J.A. de Gouw, A. Hansel, A. Jefferson, D. Kley, A.T.J. de Laat, S. Lal, M.G. Lawrence, J.M. Lobert, O.L. Mayol-Bracero, A.P. Mitra, T. Novakov, S.J. Oltmans, K.A. Prather, T. Reiner, H. Rodhe, H.A. Scheeren, D. Sikka, and J. Williams (2001), The Indian Ocean Experiment: Widespread air pollution from South and Southeast Asia, *Science*, *291* (5506), 1031-1036.

Lohmann, U., and J. Feichter (2005), Global indirect aerosol effects: A review, *Atmos. Chem. Phys.*, *5*, 715-737.

Marks, R. (1990), Preliminary investigations on the influence of rain on the production, concentration, and vertical distribution of sea salt aerosol, *J. Geophys. Res.*, *95* (22), 22299-22304.

Monahan, E.C., C.W. Fairall, K.L. Davidson, and P.J. Boyle (1983), Observed interrelations between 10m winds, ocean whitecaps and marine aerosols, *Quarterly Journal of the Royal Meteorological Society*, *109* (460), 379-392.

Mouri, H., K. Okada, and S. Takahashi (1995), Giant sulfur-dominant particles in remote marine boundary layer, *Geophys. Res. Lett.*, *22* (5), 595-598.

Neubauer, K.R., M.V. Johnston, and A.S. Wexler (1997), On-line analysis of aqueous aerosols by laser desorption ionization, *International Journal of Mass Spectrometry and Ion Processes*, *163* (1-2), 29-37.

Neubauer, K.R., M.V. Johnston, and A.S. Wexler (1998), Humidity effects on the mass spectra of single aerosol particles, *Atmos. Environ.*, *32* (14-15), 2521-2529.

O'Dowd, C.D., and G. De Leeuw (2007), Marine aerosol production: a review of the current knowledge, *Phil. Trans. A, 365* (1856), 1753-1774.

O'Dowd, C.D., M.H. Smith, I.E. Consterdine, and J.A. Lowe (1997), Marine aerosol, sea-salt, and the marine sulphur cycle: A short review, *Atmos. Environ., 31* (1), 73-80.

Pos, W.S., P.J. Milne, D.D. Riemer, and R.G. Zika (1997), Photoinduced oxidation of H_2S species: A sink for sulfide in seawater, *J. Geophys. Res., 102* (D11), 12,831-12,837.

Poschl, U. (2005), Atmospheric aerosols: Composition, transformation, climate and health effects, *Angewandte Chemie-International Edition, 44* (46), 7520-7540.

Prange, A., I. Arzberger, C. Engemann, H. Modrow, O. Schumann, H.G. Truper, R. Steudel, C. Dahl, and J. Hormes (1999), In situ analysis of sulfur in the sulfur globules of phototrophic sulfur bacteria by X-ray absorption near edge spectroscopy, *Biochimica et Biophysica Acta, 1428*, 446-454.

Qin, X.Y., P.V. Bhave, and K.A. Prather (2006), Comparison of two methods for obtaining quantitative mass concentrations from aerosol time-of-flight mass spectrometry measurements, *Anal. Chem., 78* (17), 6169-6178.

Radford-Knoery, J., and G.A. Cutter (1994), Biogeochemistry of dissolved hydrogen sulfide species and carbonyl sulfide in the western North Atlantic Ocean, *Geochimica et Cosmochimica Acta, 58* (24), 5421-5431.

Silva, P.J., and K.A. Prather (2000), Interpretation of mass spectra from organic compounds in aerosol time-of-flight mass spectrometry, *Anal. Chem., 72* (15), 3553-3562.

Song, X.H., P.K. Hopke, D.P. Fergenson, and K.A. Prather (1999), Classification of single particles analyzed by ATOFMS using an artificial neural network, ART-2a, *Anal. Chem., 71* (4), 860-865.

Steudel, R. (1996), Mechanism for the formation of elemental sulfur from aqueous sulfide in chemical and microbiological desulfurization processes, *Ind. Eng. Chem. Res., 35*, 1417-1423.

Su, Y.X., M.F. Sipin, H. Furutani, and K.A. Prather (2004), Development and characterization of an aerosol time-of-flight mass spectrometer with increased detection efficiency, *Anal. Chem., 76* (3), 712-719.

Walsh, R.S., G.A. Cutter, W.M. Dunstan, J. Radfordknoery, and J.T. Elder (1994), The biogeochemistry of hydrogen-sulfide - Phytoplankton production in the surface ocean, *Limnol. Oceangr.*, *39* (4), 941-948.

Whiteaker, J.R., and K.A. Prather (2003), Hydroxymethanesulfonate as a tracer for fog processing of individual aerosol particles, *Atmos. Environ.*, *37* (8), 1033-1043.

Zelenyuk, A., J. Yang, C. Song, R.A. Zaveri, and D. Imre (2008), "Depth-profiling" and quantitative characterization of the size, composition, shape, density, and morphology of fine particles with SPLAT, a single-particle mass spectrometer, *J. Phys. Chem. A*, *112*, 669-677.

Chapter 4

4. The Effect of Biological Activity on the Single-Particle Chemistry of Sea Spray Aerosols Generated by Bubble Bursting Natural and Artificial Seawater Solutions

4.1 Synopsis

Sea spray, consisting of sea salt and biologically-produced organic material, is a globally significant contributor to atmospheric particulate matter. The role of biological activity in shaping sea spray aerosol mixing-state remains largely unexplored despite the fact that mixing-state plays a crucial role in affecting the reactivity and water uptake properties of particles. Here we present measurements of the size-resolved chemistry of individual sea spray particles generated by bubbling artificial seawater (ASW) then adding phytoplankton-derived dissolved organic material (DOM) or intact phytoplankton cells to elucidate the impact of biological material on aerosol mixing-state. Salts dominated the chemistry of ASW; however, when DOM was added, significant increases in organic material enriched in Mg^{2+}, Ca^{2+}, and/or K^{+} were observed while internally mixed potassium and phosphate representative of bioaerosols were observed when intact phytoplankton cells were added to ASW. Similar particle types were observed when natural seawater (NSW) was bubbled and have been observed in ambient measurements of sea spray particles highlighting the atmospheric significance of our findings. These results demonstrate the ability of biological activity to alter the single-particle chemistry

of sea spray particles, which has implications for the cloud nucleating properties of sea spray particles produced in biologically active waters.

4.2 Introduction

Aerosols influence global climate directly by scattering and absorbing incoming solar radiation and indirectly by initiating cloud droplet and ice crystal formation [*Kohler*, 1936; *Poschl*, 2005]; both particle size and chemical composition play a role in these impacts [*Quinn et al.*, 2008; *Swietlicki et al.*, 2008]. Since oceans cover over 70% of the Earth's surface, understanding the physicochemical properties of sea spray aerosols is essential for reducing the uncertainty regarding the impact of aerosols on climate [*IPCC*, 2007]. Sea spray aerosol is generated by bursting bubbles produced from breaking waves [*Woodcock et al.*, 1953]; the resulting aerosol mass is dominated by sea salts, primarily NaCl, similar in composition to that of bulk seawater [*Fitzgerald*, 1991]. In additional to sea salt, recent evidence has shown that in biologically-active waters, organic material is significantly enriched in sea spray aerosols, predominantly in the submicron size mode (< 1 μm) [*Meskhidze and Nenes*, 2006; *O'Dowd et al.*, 2004; *Rinaldi et al.*, 2010]. Marine organics are primarily water-insoluble material, largely composed of polysaccharides with contributions from proteins and lipids[*Facchini et al.*, 2008; *Kuznetsova et al.*, 2005; *Rinaldi et al.*, 2010; *Russell et al.*, 2010] derived from whole and fragmented cells, and exopolymeric secretions (EPS) or microgels [*Leck and Bigg*, 2005], which form from the spontaneous assembly of DOM [*Chin et al.*, 1998].

While these recent findings have shed light on how biological activity shapes the chemical composition of sea spray particles primarily from a bulk perspective, the

influence of biological activity on the distribution of inorganic and organic components across individual sea spray particles remains unknown. Understanding the complexity of sea spray aerosol mixing-state is crucial because chemical distinctions at the single-particle level affect the heterogeneous reactivity, cloud forming potential, and hygroscopicity of sea spray aerosol generated in biologically active waters. Electron microscopy studies have shown that a significant fraction of the organic material is assembled into microgels that are externally mixed from sea salts [*Bigg and Leck*, 2008; *Hawkins and Russell*, 2010; *Leck and Bigg*, 2005; *Leck and Bigg*, 2008]. Further, a recent study has shown that in addition to organic enrichment, inorganic ions, namely Mg^{2+}, associated with organic material are enriched in individual sea spray particles that are externally mixed from sea salt when biological activity is elevated [*Gaston et al.*, 2011]. However, single-particle studies of sea spray aerosols have also shown that most sea salt particles are internally mixed with organic material rather than externally mixed [*Middlebrook et al.*, 1998]. These contrasting results highlight the need for laboratory studies to discern how biological activity and differences in biological conditions (e.g. differences in phytoplankton species, differences in the amount of DOM, etc.) shape the mixing-state of organic and inorganic material in sea spray aerosol. This paper aims to characterize primary sea spray aerosol generated during controlled bubble bursting experiments using single-particle mass spectrometry to elucidate how inorganic and organic material was distributed among individual particles. The implications of these findings are discussed.

4.3 Methods

4.3.1 Aerosol Generation

Sea spray aerosol was generated using two different bubblers. Bubbler 1 and associated experimental conditions have been described previously [*Moore et al.*, 2011]; briefly, Bubbler 1 consists of an L-shaped, sintered glass bubbler with a grade C (25-50 μm) porosity frit submerged 2 cm in a ~200 mL seawater solution. A stainless steel tube sits 1 cm above the surface of the solution and is used to provide 1 lpm of sheath flow of dry nitrogen. Bubbler 2 consists of a circular (25 mm diameter) sintered glass bubbler with a grade A (145-174 μm) porosity frit that is located 11.92 cm below the seawater solution (see Figure 4.1 for a schematic of the experimental set up using Bubbler 2). The bubbler is placed in a glass bottle that allows for the containment of 500 mL of seawater. The bubble path length in this system is 11.92 cm, which may affect the amount of organic material observed from Bubbler 1 vs. Bubbler 2 since bubble rise distance is thought to play a role in the amount of organic material that gets scavenged by a rising bubble [*Duce and Hoffman*, 1976; *Keene et al.*, 2007]. However, Bubbler 1, which has a shorter bubble rise distance, has still been shown to concentrate organic material on particles compared to other aerosol generation techniques such as atomization [*Gaston et al.*, 2011; *Moore et al.*, 2011] and, thus, the results of these experiments can provide insight into the particle types observed from bubbling seawater solutions. To further probe the differences between the two bubblers, the sizes of bubbles generated from each bubbler were determined by image capture. As seen in Figure 4.2, the size distributions of bubbles generated by both bubblers were similar at ~1-4 mm in diameter. Conditions for experiments conducted with ASW and natural seawater (NSW) solutions are shown in

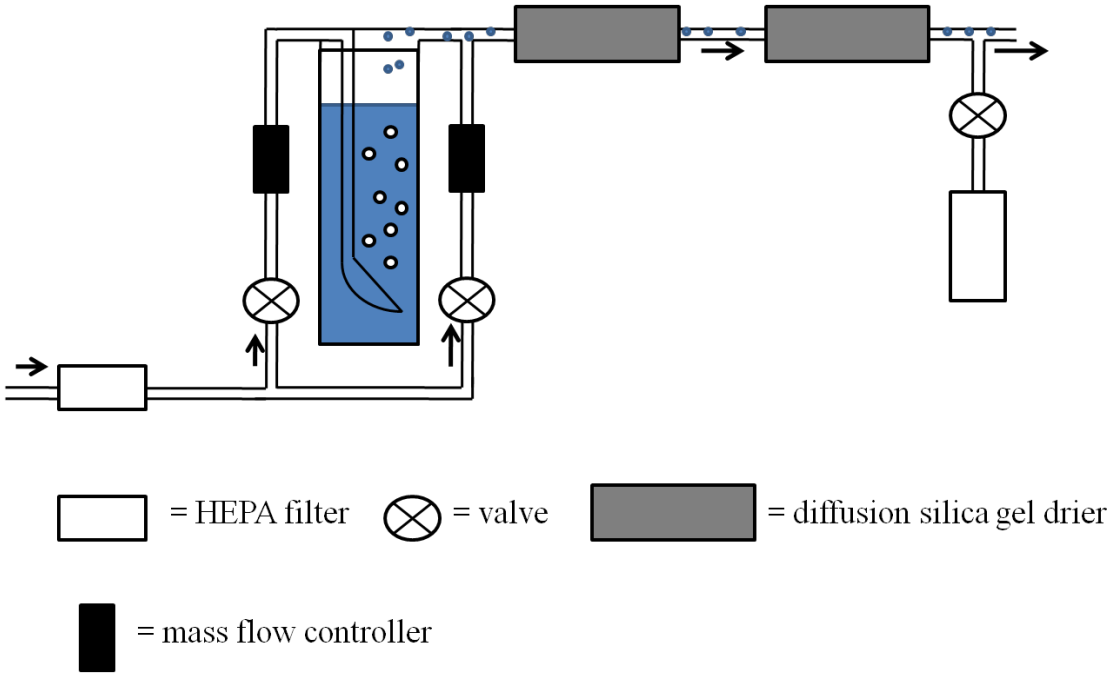

Figure 4.1: Schematic of the experimental set-up used to generate sea spray aerosol via bubble bursting.

a)

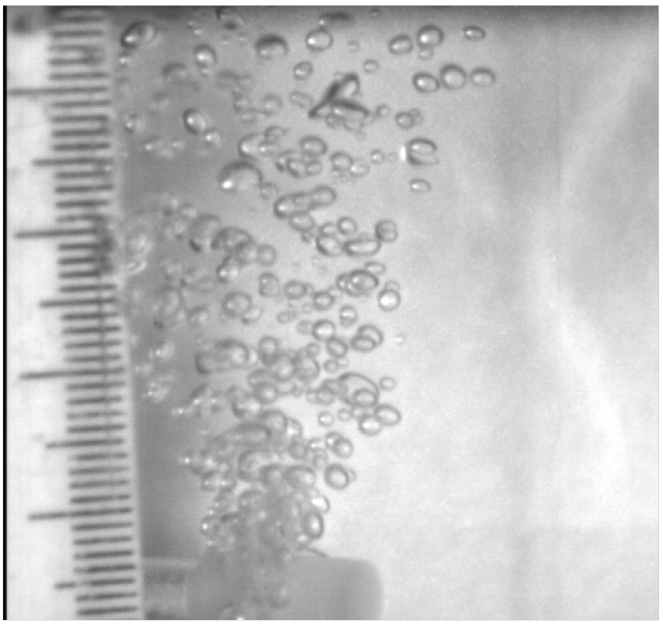

b)

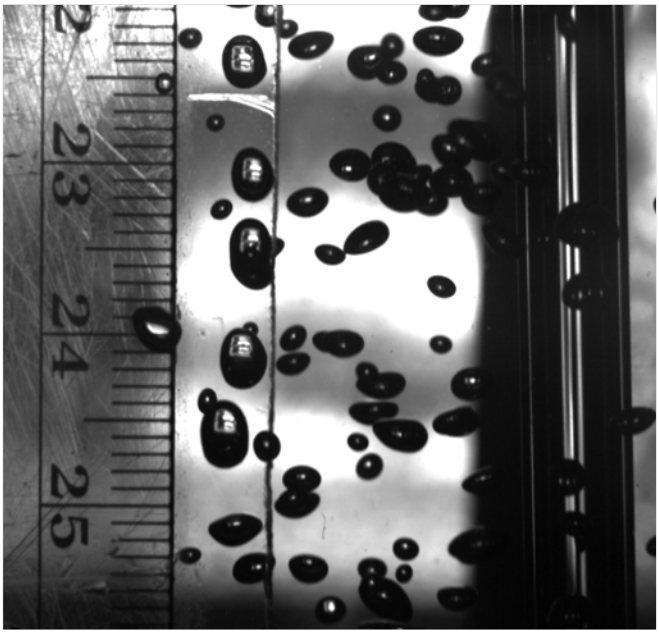

Figure 4.2: Image capture of bubbles generated from the two different bubblers used in this manuscript. Scales on the left side of the images are in centimeters. The top panel (a) shows bubbles generated from Bubbler 1 while the bottom panel (b) shows bubbles generated from Bubbler 2.

Table 4.1: Experimental conditions and particle detection efficiencies for experiments using artificial seawater and phytoplankton cultures. "Sub" denotes submicron particles while "super" denotes supermicron particles.

Experiment	Detected Particles	Hit Particles	% Hit	Bubbler
ASW Sub	15971	30	0.2	1
ASW Super	23592	2059	8.7	1
Filtered Cells Sub	17642	23	0.1	1
Filtered Cells Super	33532	1929	5.8	1
Chaetoceros Sub	33091	17	0.1	1
Chaetoceros Super	30228	1041	3.4	1
ASW Sub	3055	262	8.6	2
ASW Super	21472	4485	20.9	2
Filtered Cells Sub	1916	143	7.5	2
Filtered Cells Super	23036	4601	20.0	2
E. Huxleyi Sub	3141	167	5.3	2
E. Huxleyi Super	28446	5467	19.2	2
ASW Sub	30707	42	0.1	1
ASW Super	33720	1985	5.9	1
Filtered Cells Sub	30358	72	0.2	1
Filtered Cells Super	30770	1849	6.0	1
Synechococcus Sub	54190	228	0.4	1
Synechococcus Super	62508	5173	8.3	1
ASW Sub	2319	90	3.9	2
ASW Super	10674	2405	22.5	2
Tricho Sub	5165	57	1.1	2
Tricho Super	23475	2407	10.3	2

Table 4.2: Experimental conditions and particle detection efficiencies for experiments using natural seawater collected from the Scripps Pier. “Sub” denotes submicron particles while “super” denotes supermicron particles.

Experiment	Detected Particles	Hit Particles	% Hit	Bubbler
June, 2009 Sub	8587	462	5.4	2
June, 2009 Super	58011	12699	21.9	2
September, 2009 Sub	8164	169	2.1	2
September, 2009 Super	47603	6066	12.7	2

in Tables 4.1 and 4.2 including which bubbler was used. Also shown in these tables are how many particles were "hit" (optically detected/sized and subsequently chemically analyzed by the 266 nm YAG laser) and how many were "detected" (all particles that are optically detected by the scattering lasers including those that are not chemical analyzed by the 266 nm laser). While the different pore size and path-length used for the two bubbling set-ups may still result in differences in the percentages of particle types observed in this manuscript, our approach was to compare bubbling experiments using the same conditions. Bubbler 1 was initially used; however, Bubbler 2 was used primarily for later experiments since Bubbler 2 is composed of all glass components and can therefore be completely cleaned and combusted. Several studies are currently underway utilizing both wave tank and bubbling experiments to further probe the influence of the method of generating sea spray aerosols on the physicochemical properties of sea spray aerosol. Prior to all experiments, the bubbling glassware was rinsed with DI water, milli-q water (18.2 MΩ), methanol, acetone, and a final rinse of milli-q water. The glassware was then wrapped in tin foil and combusted at 450°C for 4 hours in a combustion oven similar to the protocol of *Moore et al.* [2011].

The experimental set-up and images of bubbles produced from Bubblers 1 and 2 are shown in Figures 4.1 and 4.2, respectively. A dry air flow is passed through a HEPA filter and split between the bubbler (0.5 lpm) and a dilution line (1.5-3.5 lpm depending on the instrumentation used) using a valve and mass flow controller between each line to control the flows. Most experiments were conducted using nitrogen to generate aerosol except for bubbling experiments conducted at the Scripps Institution of Oceanography

(SIO) pier where filtered air was used instead. The generated aerosol then passes through two diffusion silica gel driers prior to detection.

4.3.2 Seawater Samples and Phytoplankton Cultures

Natural seawater (NSW) samples were collected in June and September, 2009 from the end of the SIO Pier (32.87° N, 117.25° W). In order to interpret the resulting particle composition from bubbling NSW solutions, several control experiments were conducted using artificial seawater (ASW), which was designed to mimic the inorganic composition of seawater (e.g. 0.48 mol Na^+/kg, 0.0102 mol K^+/kg, 0.0546 mol Mg^{2+}/kg, 0.0105 mol Ca^{2+}/kg, 0.559 mol Cl^-/kg, 0.0288 mol SO_4^{2-}/kg, etc.) [*Sander et al.*, 2003]. Fresh ASW solutions were made before each experiment and three aliquots of each ASW solution were used to perform bubbling experiments using three different case studies: (1) ASW only; (2) ASW spiked with dissolved organic material (DOM), which was produced by passing a phytoplankton culture through a 0.2 μm Millipore filter to remove cellular material; (3) ASW spiked with intact marine organisms. Phytoplankton used in these experiments included diatoms (Chaetoceros), cyanobacteria (Synechococcus), coccolithophores (*E. huxleyi*), and Trichodesmium (Tricho); both the Chaetoceros and Synechococcus cultures were spiked with ~10 mM RbCl prior to bubbling intact cells, which is similar to the concentration of K^+ in seawater [*Sander et al.*, 2003]. Rb^+ can exchange with K^+ in cells [*Epstein et al.*, 1963; *Pyo et al.*, 2010]; the detection of Rb^+ ion peaks ($^{85,87}Rb^+$) in ASW solutions with phytoplankton cells was used to probe particle types associated with cell fragments and whole cells. These three case studies were used to differentiate the impact of DOM and whole cells on sea spray aerosol chemistry. The

different phytoplankton cultures used in these experiments are by no means exhaustive and only provide a first look at the role of phytoplankton diversity on sea spray aerosol chemistry. Future work will aim to expand the diversity of organisms used for sea spray generation experiments.

4.3.3 Aerosol Characterization

The size-resolved, single-particle mixing-state of generated aerosol in the 0.2-3 μm size range was characterized using aerosol time-of-flight mass spectrometry (ATOFMS), which has been previously described in detail [*Gard et al.*, 1997]. Briefly, particles enter through a converging nozzle inlet into a differentially pumped vacuum chamber causing the particles to be accelerated to their size-dependent terminal velocity. The particles then enter the sizing region of the instrument consisting of two continuous wave 532 nm lasers located at a fixed distance apart. The time required for each particle to traverse each beam is a function of the particle's terminal velocity and can be converted to aerodynamic diameter by calibration with polystyrene latex spheres of known sizes. Next, particles are simultaneously desorbed and ionized by a pulsed 266 nm Nd:YAG laser operating at ~1.0-1.2 mJ laser power creating both positive and negative ions, which are then analyzed in the dual polarity time-of-flight mass spectrometer. Mass spectra were imported into Matlab (The MathWorks, Inc.) using the YAADA software toolkit [*Allen*, 2002] and either clustered together based on similarities in ion peaks and ion intensity using an adaptive-resonance neural network (ART-2a) [*Song et al.*, 1999] or classified by hand if < 100 particles were analyzed. Mass spectral peak assignments refer to the most probable ion peak at a particular mass-to-charge (*m/z*).

Submicron (0.2-1.0 μm) and supermicron (1.0-3.0 μm) particles were analyzed separately; particle classifications are based on the most prevalent mass spectral peaks and do not reflect all species present in the particle.

4.4 Results and Discussion

4.4.1 Observed Particle Types

Figure 4.3 shows representative mass spectra of the different particle types observed during bubbling experiments (both natural and artificial). Shown in Figure 4.3a is a representative spectrum of sea salt particles, which contain intense sodium and chloride peaks ($^{23}Na^+$, $^{35,37}Cl^-$, $^{81,83}Na_2Cl^+$, $^{58}NaCl^-$, $^{93,95,97}NaCl_2^-$) as well as less intense magnesium ($^{24}Mg^+$), potassium ($^{39}K^+$), and calcium ($^{40}Ca^+$) peaks [*Gard et al.*, 1998; *Gaston et al.*, 2011; *Guazzotti et al.*, 2001]. In addition to sea salt, other inorganic types detected include other salts, such as KCl which are characterized by intense potassium, sodium, iron ($^{56}Fe^+$) and chloride peaks (see Figure 4.3b) in contrast to sea salt particles; these particles could represent a sea salt artifact. MgCl particles are characterized by intense Mg and chloride peaks (Figure 4.3c); these particles were separated from other salts due to the association of Mg-enriched spectra with biological activity as discussed below [*Gaston et al.*, 2011]. Trace metals are characterized by an intense $^{56}Fe^+$ peak with less intense peaks due to $^{39}K^+$ as well as $^{23}Na^+$; most trace metal particles lacked negative ion spectra; however, some contained phosphate and organic nitrogen (Figure 4.3d). Iron microcolloids have previously been detected in seawater and could account for detection of trace metals [*Wells and Goldberg*, 1992]; however, as discussed below, trace metals could also represent an artifact from ASW solutions.

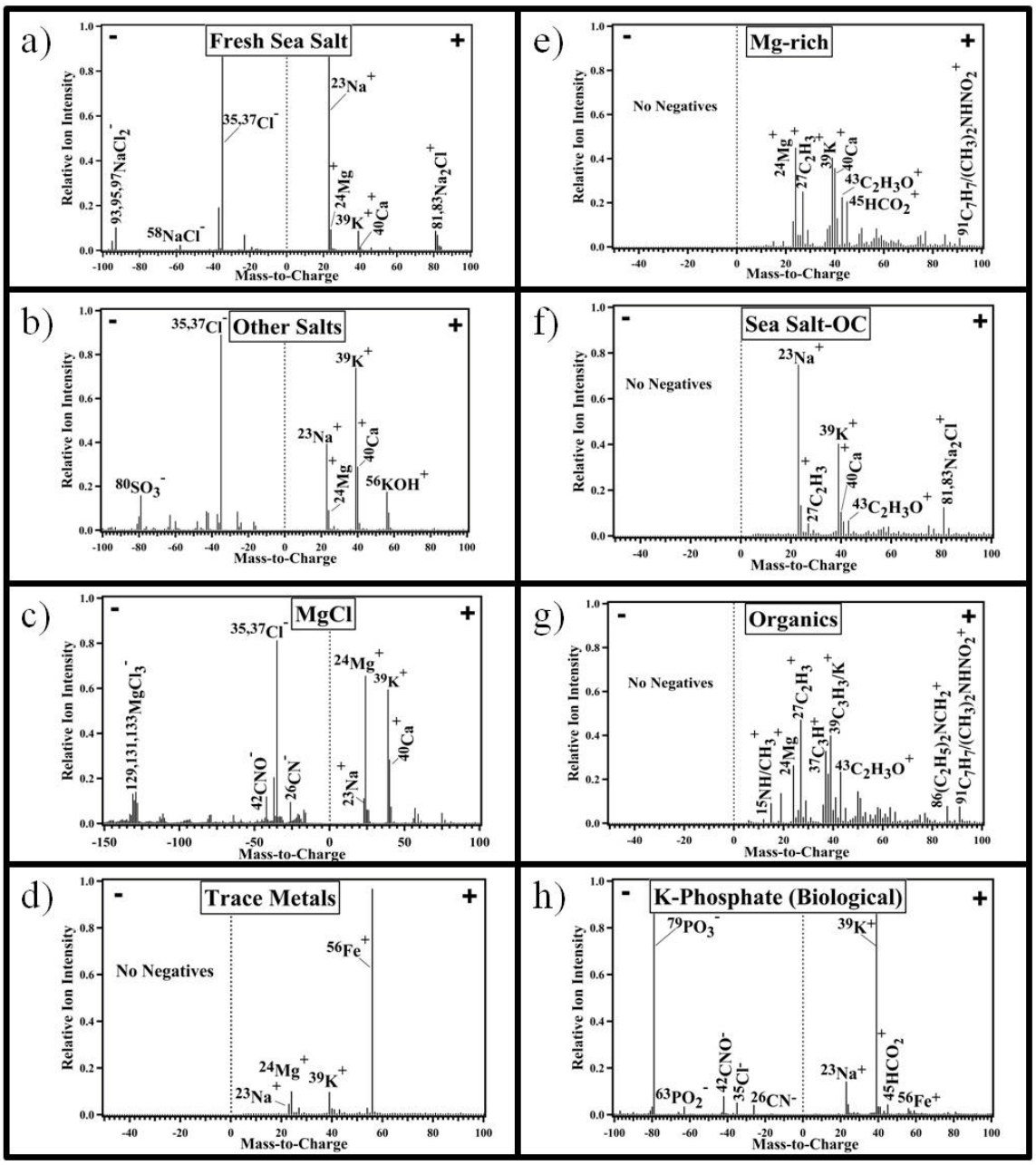

Figure 4.3: Representative mass spectra of particle types defined as (a) sea salt, (b) other salts, (c) MgCl, (d) trace metals, (e) Mg-rich, (f) sea salt-OC, (g) organics, and (h) K-phosphate. Each spectrum is divided into negative (left) and positive (right) ion peaks.

In addition to "purely" inorganic particle types, intense inorganic ion peaks were also observed internally mixed with organic carbon (OC); these particle types include Mg-rich (Mg/Ca/K/OC), K-rich (K/Ca/Mg/OC), and Ca-rich (Ca/Mg/OC) particles. Mg-rich particles were classified as Mg-type particles in a previous ambient study and are characterized by intense $^{24}Mg^+$, $^{40}Ca^+$ and $^{39}K^+$ ion peaks with $^{24}Mg^+$ being the most intense in addition to less intense organic ions (e.g. $^{27}C_2H_3^+$, $^{29}C_2H_5^+$, $^{41}C_3H_5^+$, $^{43}C_2H_3O^+$, $^{45}CH_2O^+$, $^{50}C_4H_2^+$) (Figure 4.3e).[*Gaston et al.*, 2011] It should be noted that in the ATOFMS, the presence of inorganic ions in low relative abundance (< 1-2%) along with water can suppress ion signal intensities particularly for some organic compounds, making the particles appear mostly inorganic [*Gaston et al.*, 2011; *Gross et al.*, 2000], thus, it is entirely possible that these particle types are primarily organic. K-rich and Ca-rich particles have similar particle signatures to Mg-rich particles; however, $^{39}K^+$ and $^{40}Ca^+$, respectively, were the most intense ion rather than $^{24}Mg^+$. Although the Mg-rich, K-rich, and Ca-rich particle types have similar characteristics, it should be noted that unlike Mg-rich particles which have been observed in the marine atmosphere during multiple field campaigns, Ca-rich particles were primarily observed during the Indian Ocean Experiment [*Gaston et al.*, 2011]; thus, these types were separated to elucidate if organics and/or whole cells from different phytoplankton might influence the detection of Mg-rich vs. Ca-rich vs. K-rich particle types. Mg- and Ca-rich particles typically lack negative ion spectra indicating the presence of appreciable particulate water [*Gaston et al.*, 2011; *Neubauer et al.*, 1997; *Neubauer et al.*, 1998]. However, on average ~23%, ~61%, and ~7% of Mg-rich, K-rich, and Ca-rich particles, respectively, produced negative ions, including organic nitrogen peaks ($^{26}CN^-$, $^{42}CNO^-$), which is most likely due

to the presence of amide bonds [*Silva and Prather*, 2000] that have been shown to contribute to primary marine aerosol [*Hawkins and Russell*, 2010; *Kuznetsova et al.*, 2005], in addition to chloride including MgCl clusters ($^{129,\ 131,\ 133}MgCl_3^-$) and lower intensity phosphate ($^{79}PO_3^-$) and organic peaks $^{59}CH_3COO^-$ and $^{71}C_3H_3OO^-$ that are most likely due to polysaccharides, which have been found to be abundant in sea spray aerosol and marine microgels [*Aluwihare and Repeta*, 1999; *Chin et al.*, 1998; *Russell et al.*, 2010].

Additionally, sea salt was also observed internally mixed with OC (Sea salt-OC) and characterized by the same ion peaks as sea salt particles; however, most of the sea salt-OC particles also lacked negative ion spectra indicating that organic material could alter the water uptake and retention properties of sea salt particles as noted in previous studies [*Wise et al.*, 2009; *Zelenyuk et al.*, 2007] (see Figure 4.3f). Sea salt-OC particles that did produce negative ion spectra contained phosphate and organic nitrogen in addition to chloride. Organics were also observed externally mixed from inorganic constituents. Organics contained intense organic carbon peaks and amines ($^{86}(C_2H_5)_2NCH_2^+$) [*Angelino et al.*, 2001] (Figure 4.3g). Amines have been shown to contribute significantly to secondary marine aerosol [*Facchini et al.*, 2008a]; however, the results of this work highlight that amines can contribute to primary marine aerosol. Of note, many of the organic particles as well as other particle types (sea salt-OC, Mg-rich, Ca-rich, K-rich) also contained a peak at *m/z* +91, which can be attributed to either amines ($^{91}(CH_3)_2NHNO_2^+$) [*Angelino et al.*, 2001] or aromatic/humic species ($^{91}C_7H_7^+$) [*Holecek et al.*, 2007; *Silva and Prather*, 2000]. Either peak assignment is plausible since

in addition to amines, both humic and aromatic compounds, phenols in particular, have been associated with marine aerosols [*Bahadur et al.*, 2010; *Facchini et al.*, 2008a; *Hawkins and Russell*, 2010; *Kuznetsova et al.*, 2005; *Russell et al.*, 2011]. Finally, K-phosphate particles characterized by an intense $^{39}K^{+}$ as well as $^{23}Na^{+}$ and organic carbon peaks in addition to intense phosphate peaks and less intense organic nitrogen and chloride peaks were also detected (see Figure 4.3h); these particles are thought to represent biological aerosols [*Holecek et al.*, 2007].

4.4.2 Artificial Seawater Experiments

The size-resolved composition of particles generated with ASW-only (first column), ASW and DOM (second column), and ASW and intact phytoplankton cells (last column) are shown in Figure 4.4; rows in Figure 4.4 show how the addition of DOM and intact cells from a specific phytoplankton species to aliquots of the ASW solution impacts the observed particle types. Different size ranges are shown in Figure 4.4 since some of the size bins only contained a few chemically detected particles, particularly in the smaller size ranges. Bins with less than 10 particles were excluded. Table 4.1 of the Supporting Information provides details regarding the conditions and particle detection efficiencies for each experiment. These experiments should be regarded as a first look into the role of DOM and phytoplankton diversity on sea spray aerosol chemistry as additional experiments using different phytoplankton cultures and different aerosol generation techniques should also be probed.

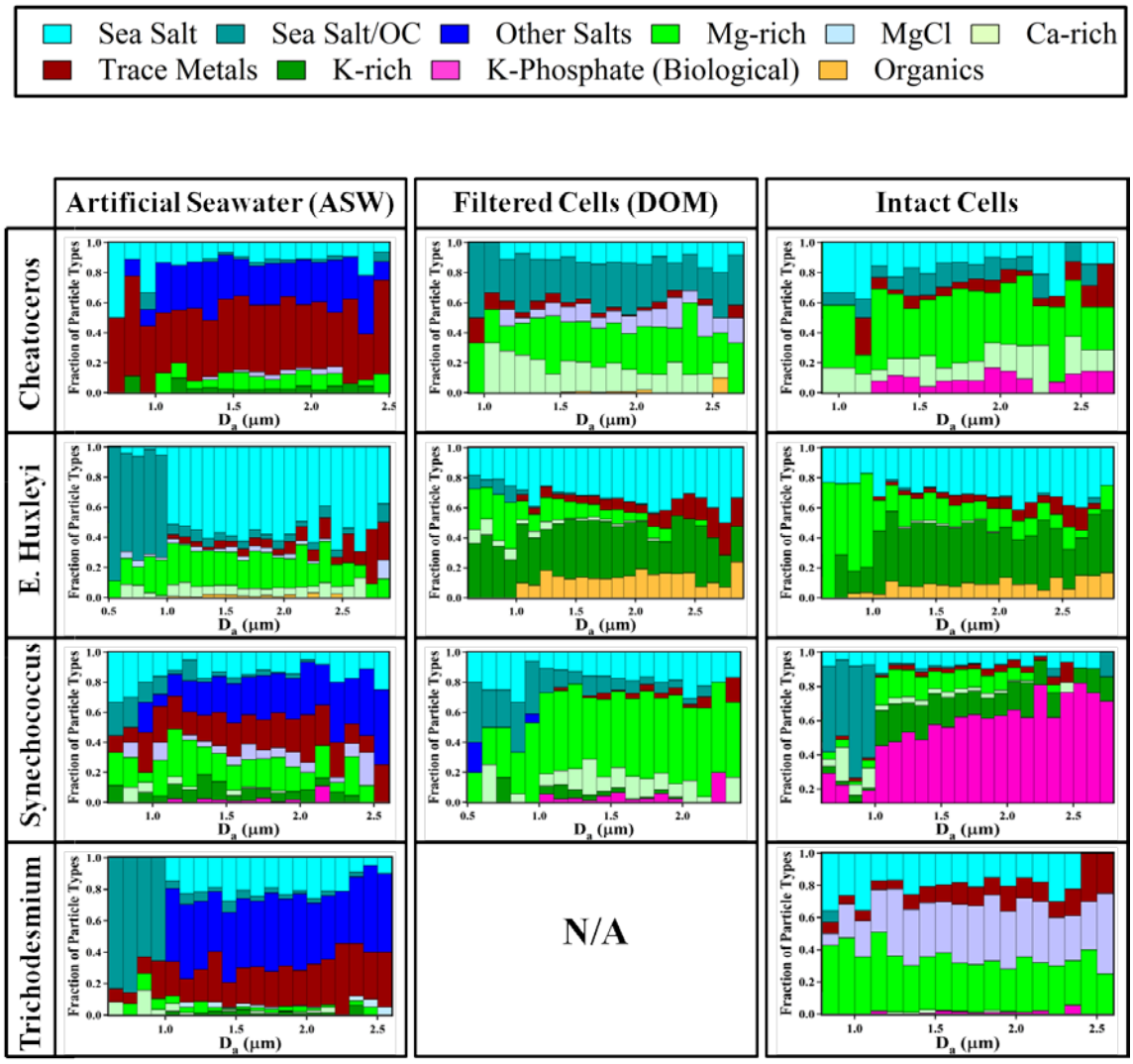

Figure 4.4: Fraction of major particle types observed from bubbling artificial seawater solutions (ASW) alone (first column), ASW containing organic material from filtered cells (DOM, second column), and ASW containing phytoplankton cells (third column). Particle types are plotted as a function of size in 0.1 μm size bins.

4.4.2.1 Case 1: ASW

As shown in the first column of Figure 4.4, bubbling ASW by itself produced mainly inorganic particle types with sea salt representing up to ~55% of the detected particles. In addition to sea salt, other inorganic types detected include other salts, representing up to ~44% of the detected particles by number while MgCl represented up to ~8% of the detected particles, and trace metals represented up to ~44% of the detected particles. It is very important to point out that a lot of these inorganic types contained inorganic contaminates, namely trace metals, and organic contamination, namely organic nitrogen. Further, organic particle types, namely sea salt-OC, were also observed, particularly in the submicron size fraction. As shown in the first column of Figure 4.4, differences in the percentage of the main particle types were observed for each of the different experiments likely because a new ASW solution was made before each experiment. The presence of particle types other than sea salt and the presence of peaks organic nitrogen and trace metals is likely due to the presence of trace contaminants found in artificial seawater solutions, which can be susceptible to organic (Rachel Chang and Jonathan Abbatt, personal communication) and trace metal contamination [*Bigg and Leck*, 2008]. The percentage of sea salt particles produced from ASW is probably underestimated by the ATOFMS since the absorption cross section for NaCl is quite low at 266 nm [*Dall'Osto et al.*, 2006] and, therefore, particles containing contaminants would be preferentially ionized and chemically analyzed. These observations highlight the caveats associated with using artificial seawater solutions due to the prevalence of both organic and inorganic contaminants. Since particles were generated via bubble bursting in these experiments, organic contaminants would be preferentially concentrated

in particles generated from ASW simply due to the generation method; other generation methods such as plunging jets should also be explored when producing particles from ASW. It is also important to point out the low percentage of detected submicron particles that are chemically analyzed by the ATOFMS for these experiments (~0.2-8.6%), which could also contribute to the higher percentage of organic containing particles detected in submicron particles generated with ASW (Table 4.1). As mentioned above, the missing particle type in this case is most likely sodium chloride, sea salt particles. Although different percentages of each particle type were observed for each ASW solution, the main point is that particles generated from just ASW serve as a baseline for comparing how particle chemistry change as filtered cells and intact cells are added to ASW solutions (as shown in each row in Figure 4.4).

4.4.2.2 Case 2: Effect of Adding DOM to ASW

As shown in the middle column of Figure 4.4, the addition of filtered cells (DOM) to ASW primarily resulted in an increase in organic particle types internally mixed with inorganic constituents. As shown in Figure 4.4, the addition of DOM to ASW primarily resulted in an increase in the percentage of sea salt-OC, Mg-, K-, and Ca-rich particles and organics detected. The increase in Mg-, K-, and Ca-rich particle types after the addition of DOM could be due to the fact that Mg^{2+} and Ca^{2+} facilitate microgel formation from DOM through ionic bonding [*Chin et al.*, 1998]. Additionally, cations such as Mg^{2+} have been shown to associate with the polar head groups of deprotonated surface active fatty acids creating a particle interface rich in Mg^{2+} and organics [*Casillas-Ituarte et al.*, 2010]; thus these particle types could primarily reflect an organic-rich

particle surface coating around sea spray aerosols. In addition to DOM, the filtered cells could also contain cellular fragments, microcolloids, and viruses, which could also affect the particle chemistry and account for the detection of Mg-, K-, and Ca-rich particle types [*Wells and Goldberg*, 1991; *Wells and Goldberg*, 1992]. Additional experiments are currently being conducted to confirm this hypothesis. As shown in Figure 4.4, sea salt-OC particles were primarily found in the submicron size mode while Mg-, K-, and Ca-rich particles were detected in both submicron and supermicron size modes. Further, differences in single-particle chemistry were observed when DOM from different phytoplankton was added to ASW possibly due to differences in the amount and type of organics excreted; however, it should be noted that the addition of DOM to ASW was not investigated for Trichodesmium cultures since limited amounts of Trichodesmium were available. Submicron particles generated by DOM from Chaetoceros were dominated by sea salt-OC, Mg-rich, and Ca-rich particles, which represented ~28%, ~27% and ~15%, respectively of the submicron particles; additional particle types observed in the supermicron size range included sea salt and MgCl particles. The highest percentage of Mg-rich particles (~53%) were generated using DOM from Synechococcus while the highest percentage of K-rich particles was detected in both the submicron and supermicron size range, representing ~35% of the detected particles, when sea spray aerosol was generated using DOM from *E. huxleyi*. The addition of DOM from *E. huxleyi* produced higher percentages of "pure" organics (~13%). Surprisingly, "purely" organic particle types were concentrated in supermicron rather than submicron sizes even though sea salt-OC, Mg-, K-, and Ca-rich particles were found in submicron sizes; the most likely explanation is that these particle types represent distinct aerosol populations

and that the organics present in sea salt-OC vs. Mg-, K-, and Ca-rich particles vs. “pure” organic particle types are, thus, likely different in composition.

4.4.2.3 Case 3: Effect of Adding Cells to ASW

The addition of phytoplankton cells to ASW had a similar result to adding DOM; however, additional particle types, notably K-phosphate particles, were also observed. The addition of Trichodesmium cells to ASW resulted in higher percentages of Mg-rich particles (~31% of detected particles) in addition to higher percentages of MgCl particles (~35% of detected particles) compared to ASW. Although MgCl is inorganic, it is possible that the increase in this particle type was due to the influence of biological activity, which has been shown to produce Mg-enriched spectra [*Gaston et al.*, 2011]. The addition of intact Chaetoceros and *E. huxleyi* namely resulted in an increase in both Mg-rich and K-rich particles, while Ca-rich particles were predominately associated with the addition of Chaetoceros. It is important to note that the number of particles that are scattered by not chemically detected by the ATOFMS increases, namely in the submicron size range, particularly when cells are added to ASW. The most likely explanation for this missing particle type are hydrocarbon-like organics, which absorb poorly at 266 nm radiation; further experiments are needed to prove this hypothesis. This is in agreement with ambient measurements of Mg-rich particles, which were detected concurrently with a missing submicron particle type thought to be hydrocarbon-like biogenically-produced organic material [*Gaston et al.*, 2011]. Further, as shown in Figure 4.4, elevated number concentrations of K-phosphate particles were observed when intact Synechococcus was added to ASW. K-phosphate particles only represented up to ~3% of particles generated

with DOM and ASW; however, this particle type represented ~60% of the detected supermicron particles when Synechococcus cells were added. This particle type has been previously attributed to cellular material in studies of rainwater samples and has been detected in single-particle studies aimed at characterizing bioaerosols [*Holecek et al.*, 2007]. Synechococcus cells are < 2 μm in diameter, which is within the detectable size range of the ATOFMS, unlike the other phytoplankton used for these experiments, which are on the order of several microns, suggesting that K-phosphate particles represent whole, intact Synechococcus cells.

As mentioned above, Chaetoceros and Synechococcus cultures were spiked with RbCl before they were used for experiments; Rb^+ can be exchanged for K^+ in the cell causing Rb^+ to be a unique tracer for cells and their fragments [*Epstein et al.*, 1963; *Pyo et al.*, 2010] (Figure 4.5 shows a representative mass spectrum of a particle internally mixed with Rb). Figure 4.6 shows the percentage of particle types internally mixed with (hatched colors) and without Rb^+ (solid colors) generated from bubbling ASW and intact cells. As shown in Figure 4.6, ~90% of detected K-phosphate particles, ~98% of detected Ca-rich particles, and ~52% of Mg-rich particles generated from bubbling ASW with Chaetoceros were internally mixed with Rb^+. Additionally, all detected Mg-rich particles, ~70% of K-rich particles, and ~27% of detected K-phosphate generated from bubbling ASW with Synechococcus were internally mixed with Rb^+. Further, the fact that no aerosols containing Rb ion peaks ($^{85,87}Rb^+$) were generated from solutions with ASW and DOM from Synechococcus and only ~4% of particles from ASW and DOM from Chaetoceros contained Rb, while ~39% and ~54% of particles generated from ASW

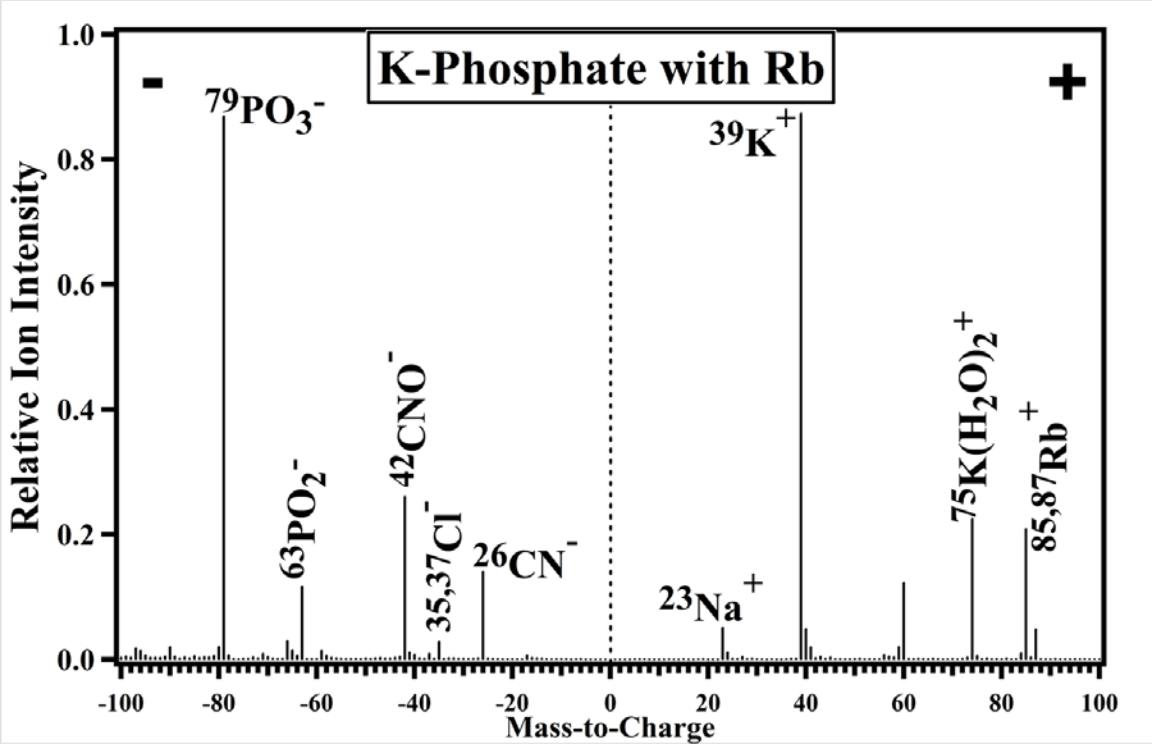

Figure 4.5: Representative mass spectrum of K-phosphate particles internally mixed with Rb^+ ion peaks.

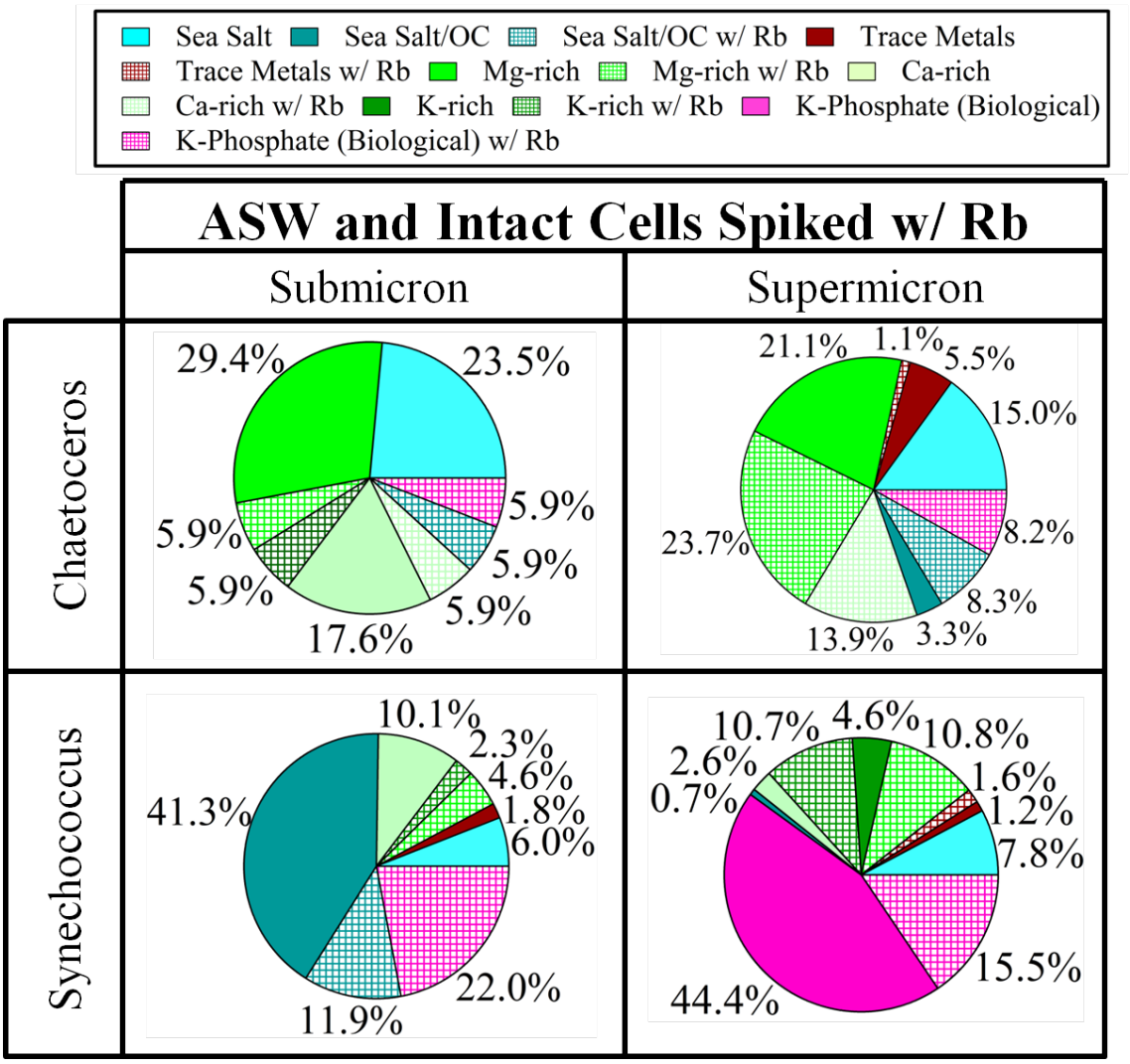

Figure 4.6: Pie charts of particle types generated from ASW and intact Chaetoceros (top panel) and Synechococcus (bottom panel). Particle types internally mixed with Rb^+ are hatched.

and intact Synechococcus and Chaetoceros cells, respectively, were internally mixed with Rb^+ suggests that Rb^+ was successfully taken up by the cells and that Rb^+ contamination from the culture solution was not observed. These results provide evidence that K-phosphate particles represent bioaerosols and also suggest that Mg-rich, K-rich, and Ca-rich particles are associated with cellular fragments and/or whole cells. The detection of Mg-rich, K-rich, and Ca-rich particles when DOM was added and when cells spiked with Rb^+ were added suggests that these particle types could represent organic coatings around sea salts and cells and/or cellular fragments.

In sum, the addition of filtered or intact cells to ASW resulted in a significant shift in particle chemistry from inorganic salt particle types and trace metals to particles characterized by organics internally mixed with inorganic ions (e.g. Mg-, K-, and Ca-rich particles) and sea salt internally mixed with OC. A missing particle type believed to be hydrocarbon-like organics that absorb poorly at 266 nm radiation is also prevalent particularly when cells are added to ASW solutions. In addition, K-phosphate particles representative of bioaerosols were detected when Synechococcus cells were added to ASW. These results also highlight the difficulties associated with generating sea spray aerosol from ASW solutions, namely due to the presence of contaminants. These results highlight the influence of biological activity on single-particle chemistry and can be used to probe differences in sea spray particles generated from natural seawater solutions.

4.4.3 Chemical Characteristics of Sea Spray Particles Generated from Natural Seawater

Bubbled NSW collected from the ocean surface off the SIO pier produced diverse sea spray particles that varied between the two collection months. NSW was collected twice on June 10 and on September 7, September 14, and September 21; no significant differences in the percentage of detected particle types were observed between the two experiments from NSW collected in June and between the three experiments from seawater collected in September, thus, the two June experiments and the three September experiments were combined for simplicity. Submicron and supermicron sea spray particles generated from NSW collected in June were dominated by sea salt (~56% and ~60%, respectively) as shown in the top panel of Figure 4.7. Additionally, MgCl represented ~18% of submicron and ~16% of supermicron particles while Mg-rich particles represented ~18% of submicron and ~8% of supermicron particles. K-rich particles constituted ~4% of submicron and ~9% of supermicron particles, while low percentages of organics, K-phosphate, and sea salt-OC particles were observed. In contrast, sea salt only constituted ~32% of submicron and ~23% of supermicron sea spray particles generated from NSW collected in September as shown in the bottom panel of Figure 4.7. Also shown in Figure 4.7, elevated percentages of sea salt-OC (~13% of submicron and ~18% of supermicron detected particles) and K-rich particles (~13% of submicron and ~6% of supermicron particles) were detected in September, while Ca-rich particles and trace metals were also detected in September but not in the June samples. The most notable difference between sea spray generated in June and September is the higher percentage of Mg-rich particles observed when particles were generated from

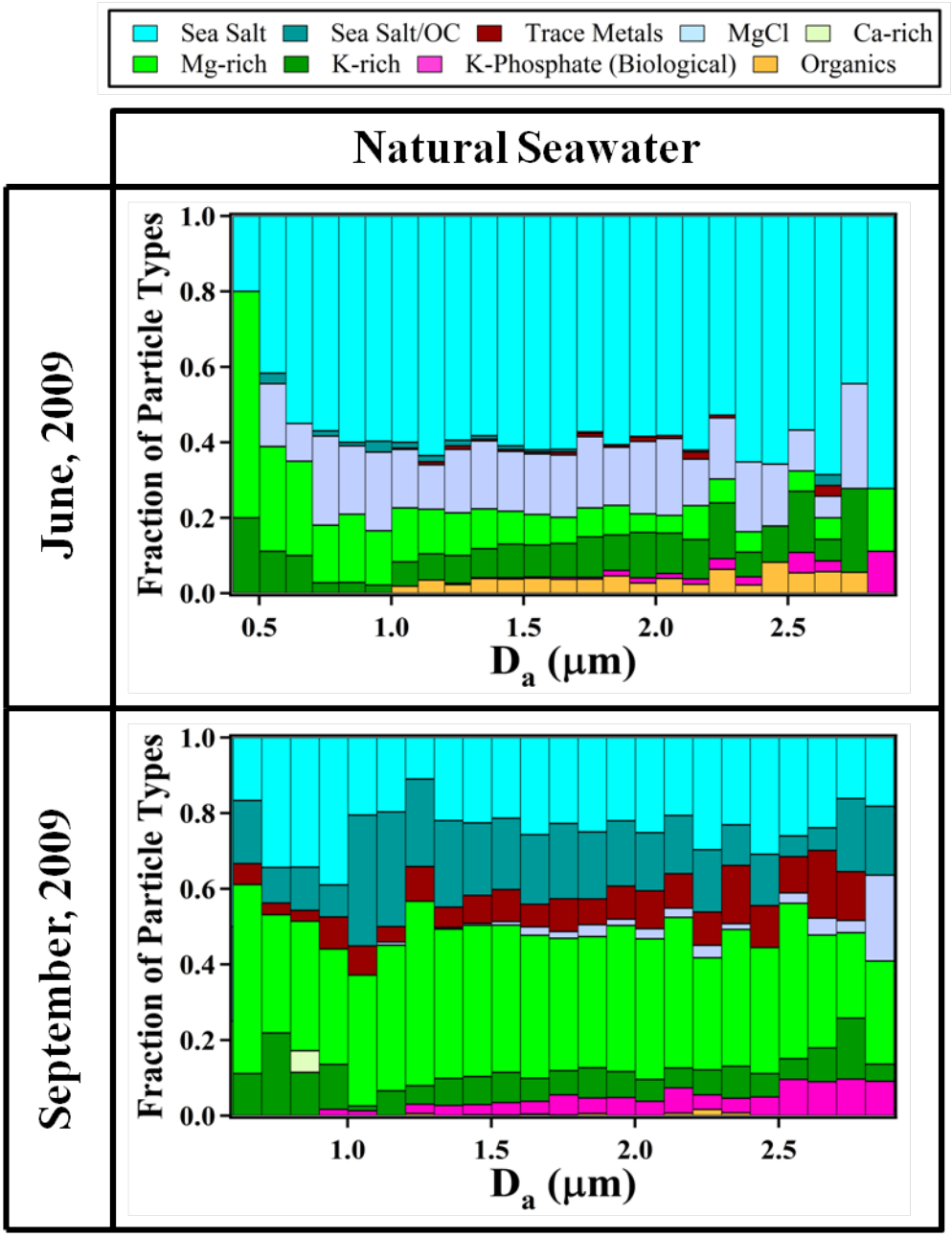

Figure 4.7: Fraction of major particle types observed from bubbling natural seawater (NSW) in June (top panel) and September (bottom panel) 2009. Particle types are plotted as a function of size in 0.1 μm size bins.

seawater collected in September: ~34% of submicron and ~38% of supermicron particles in contrast to ~18% of submicron and ~8% of supermicron particles detected in June, while the percentage of MgCl particles decreased to ~1% of the detected particles in September. Additionally, lower percentages of "pure" organics were observed in September (~0.3% particles in contrast to ~3% in June) suggesting that Mg^{2+} was associated with increased amounts of organic material in September than in June. Also of note, Table 4.2 shows that overall low percentages of submicron particles were chemically analyzed, and that this percentage decreased from ~5% in June to ~2% in September possibly due to the enhanced presence of submicron organics that do not interact well with 266 nm light.

The contrasting particle types observed in June and September could be due to differences in the amount of biological activity; however, similar chlorophyll *a* concentrations (~1 μg/L), which is a proxy for phytoplankton biomass, were observed at 3 m depth off the SIO Pier when the samples were taken in both June and September (http://www.sccoos.org/) suggesting that similar levels of biological activity were observed between the two months. The biological conditions (e.g. differences in phytoplankton species present, differences in the amount and/or composition of DOM present) rather than the overall amount of biological activity may have differed. Further, as shown in Table 4.2, the number of scattered particles that were not chemically detected was elevated in the September seawater samples, possibly due to the presence of elevated concentrations of organic material. Differences in biological conditions were observed between June and September with increased relative concentrations of zooplankton,

Table 4.3: Experimental conditions and particle detection efficiencies for experiments using natural seawater collected from the Scripps Pier. “Sub” denotes submicron particles while “super” denotes supermicron particles.

Experiment	Detected Particles	Hit Particles	% Hit	Bubbler
June, 2009 Sub	8587	462	5.4	2
June, 2009 Super	58011	12699	21.9	2
September, 2009 Sub	8164	169	2.1	2
September, 2009 Super	47603	6066	12.7	2

dinoflagellates, and detritus observed in September in contrast to increased concentrations of diatoms observed in June (http://www.sccoos.org/). Grazing of phytoplankton by zooplankton has been shown to increase the release of DOM to the surface ocean [*Lampert*, 1978], which, in addition to the increased amounts of detritus, could possibly explain the differences in sea spray aerosol chemistry produced from NSW collected in September and June. Further, previous work has shown that the type not the amount of DOM excreted from different organisms had a larger effect on the total flux as well as in the physicochemical properties of generated sea spray aerosol [*Fuentes et al.*, 2010; *Fuentes et al.*, 2011] suggesting an additional possibility that the observations in this study could be due to differences in the amount and/or composition of DOM in the surface ocean associated with differences in phytoplankton composition between the two months.

Overall, all of the particle types produced from bubbling NSW solutions were reproduced when ASW solutions were bubbled with DOM and phytoplankton cells with the exception of the other salts particle type, suggesting that this particle type is likely an artifact from using an ASW solution. The controlled experiments using ASW and phytoplankton cultures also provided insight into the differences observed from bubbling NSW solutions during two different months, possibly due to differences in biological conditions and ocean chemistry. These results highlight two main points: (1) the addition of DOM and intact cells result in significant shifts in the observed single-particle mixing-state compared to ASW and (2) the resulting single-particle mass spectral

fingerprints from the ASW experiments can be used to differentiate sea spray particles generated from NSW during different biological conditions.

4.4.4 Atmospheric Implications

While the bubbling experiments performed may not reflect the full complexity of sea spray aerosol generation under ambient conditions, several of the particle types detected by ATOFMS have been observed in the atmosphere during multiple field campaigns as well as in rainwater samples [*Gaston et al.*, 2011; *Hawkins and Russell*, 2010; *Holecek et al.*, 2007; *Middlebrook et al.*, 1998; *Russell et al.*, 2010] highlighting the atmospheric relevance of these findings. The majority of the organic material detected by ATOFMS was internally mixed with Mg^{2+}, Ca^{2+}, and K^{+} possibly due to the association of these cations with microgels. These trace ions in seawater have been shown to have water uptake and retention properties that differ from NaCl [*Cziczo et al.*, 1997; *Kelly and Wexler*, 2006; *Xiao et al.*, 2008] suggesting that the Mg-, K-, and Ca-rich particle types might have different hygroscopic properties from sea salt. Further evidence for this is shown by fact that most Mg-, K-, and Ca-rich particles lack negative ion spectra suggesting that more particulate water is associated with these types than with sea salt particles. Since these particle types are most likely associated with high amounts of organic material and possibly organic coatings, these findings are in agreement with previous studies, which have shown evidence for the production of hygroscopic organics from bubbling experiments [*Keene et al.*, 2007]. Marine organic material has also been shown to influence cloud droplet formation and sub-saturated water uptake [*Fuentes et al.*, 2011; *Moore et al.*, 2008]. Finally, internal mixtures of potassium with phosphate

and organic nitrogen were found to represent whole and/or fragments of marine bioaerosols, which have been shown to act as natural ice nuclei [*Knopf et al.*, 2011] further illustrating the climatic relevance of these findings. Our results provide a first look into how oceanic biological activity influences the single-particle chemistry of sea spray aerosols. Further experiments are necessary to determine the source and composition of missing particle types that increase as cellular material is added to seawater solutions. These initial experiments demonstrate the need for additional studies to probe the role of different phytoplankton cultures and aerosol generation methods in order to link changes in sea spray aerosol chemistry due to biological activity to changes in particle hygroscopicity, heterogeneous reactivity, and cloud nucleating properties in order to understand the role sea spray aerosols play on climate.

4.5 Acknowledgements

The authors would like to acknowledge the National Science Foundation #1038028 and the UC San Diego Chancellor's Interdisciplinary Collaboratory Fellowship. C.J.G. was funded through the Aerosol Chemistry and Climate Institute at Pacific Northwest National Laboratory. Kelly Roe is thanked for providing cultures of Trichodesmium. Christian McDonald is acknowledged for use of the SIO Pier and with assistance in setup. Dr. Grant Deane is thanked for characterizing the bubble size distributions from both bubblers. L.E. Hatch and J.M. Creamean are acknowledged for helpful comments and discussion.

Chapter 4 is in preparation for submission to *Environmental Science & Technology*: Gaston, C.J., Furutani, H., Charrier, J.G., Palenik, B.P., Aluwihare, L.I.,

Prather, K.A. The effect of biological activity on the single-particle chemistry of sea spray aerosols generated by bubble bursting natural and artificial seawater solutions. The dissertation author was the primary investigator and author of this paper.

4.6 References

Allen, J.O. (2002), YAADA software toolkit to analyze single-particle mass spectral data: Reference manual version 1.1, *Arizona State University*, http://www.yaada.org.

Aluwihare, L.I., and D.J. Repeta (1999), A comparison of the chemical characteristics of oceanic DOM and extracellular DOM produced by marine algae, *Mar. Ecol. Prog. Ser.*, *186*, 105-117.

Angelino, S., D.T. Suess, and K.A. Prather (2001), Formation of aerosol particles from reactions of secondary and tertiary alkylamines: Characterization by aerosol time-of-flight mass spectrometry, *Environ. Sci. Tech.*, *35* (15), 3130-3138.

Bahadur, R., T. Uplinger, L.M. Russell, B.C. Sive, S.S. Cliff, D.B. Millet, A. Goldstein, and T.S. Bates (2010), Phenol groups in Northeastern US submicrometer aerosol particles produced from seawater sources, *Environ. Sci. Tech.*, *44* (7), 2542-2548.

Bigg, E.K., and C. Leck (2008), The composition of fragments of bubbles bursting at the ocean surface, *J. Geophys. Res.*, *113*, D11209, doi:10.1029/2007JD009078.

Casillas-Ituarte, N.N., K.M. Callahan, C.Y. Tang, X.K. Chen, M. Roeselova, D.J. Tobias, and H.C. Allen (2010), Surface organization of aqueous $MgCl_2$ and application to atmospheric marine aerosol chemistry, *PNAS*, *107* (15), 6616-6621.

Chin, W.C., M.V. Orellana, and P. Verdugo (1998), Spontaneous assembly of marine dissolved organic matter into polymer gels, *Nature*, *391* (6667), 568-572.

Cziczo, D.J., J.B. Nowak, J.H. Hu, and J.P.D. Abbatt (1997), Infrared spectroscopy of model tropospheric aerosols as a function of relative humidity: Observation of deliquescence and crystallization, *J. Geophys. Res.-[Atmos.]*, *102* (D15), 18843-18850.

Dall'Osto, M., R.M. Harrison, D.C.S. Beddows, E.J. Freney, M.R. Heal, and R.J. Donovan (2006), Single-particle detection efficiencies of aerosol time-of-flight mass spectrometry during the North Atlantic marine boundary layer experiment, *Environ. Sci. Tech.*, *40* (16), 5029-5035.

Duce, R.A., and E.J. Hoffman (1976), Chemical fractionation at the air-sea interface, *Ann. Rev. Earth Planet. Sci.*, *4*, 187-228.

Epstein, E., O.E. Elzam, and D.W. Rains (1963), Resolution of dual mechanisms of potassium absorption by barley roots, *PNAS*, *49* (5), 684-692.

Facchini, M.C., S. Decesari, M. Rinaldi, C. Carbone, E. Finessi, M. Mircea, S. Fuzzi, F. Moretti, E. Tagliavini, D. Ceburnis, and C.D. O'Dowd (2008a), Important source of marine secondary organic aerosol from biogenic amines, *Environ. Sci. Tech.*, *42* (24), 9116-9121.

Facchini, M.C., M. Rinaldi, S. Decesari, C. Carbone, E. Finessi, M. Mircea, S. Fuzzi, D. Ceburnis, R. Flanagan, E.D. Nilsson, G. de Leeuw, M. Martino, J. Woeltjen, and C.D. O'Dowd (2008b), Primary submicron marine aerosol dominated by insoluble organic colloids and aggregates, *Geophys. Res. Lett.*, *35*, L17814, doi:10.1029/2008GL034210.

Fergenson, D.P., M.E. Pitesky, H.J. Tobias, P.T. Steele, G.A. Czerwieniec, S.C. Russell, C.B. Lebrilla, J.M. Horn, K.R. Coffee, A. Srivastava, S.P. Pillai, M.T.P. Shih, H.L. Hall, A.J. Ramponi, J.T. Chang, R.G. Langlois, P.L. Estacio, R.T. Hadley, M. Frank, and E.E. Gard (2004), Reagentless detection and classification of individual bioaerosol particles in seconds, *Anal. Chem.*, *76* (2), 373-378.

Fitzgerald, J.W. (1991), Marine aerosols: A review, *Atmos. Environ. A-Gen. Topics*, *25* (3-4), 533-545.

Forster, P., V. Ramaswamy, P. Artaxo, T. Berntsen, R. Betts, D.W. Fahey, J. Haywood, J. Lean, D.C. Lowe, G. Myhre, J. Nganga, R. Prinn, G. Raga, M. Schulz, and R. Van Dorland, Changes in Atmospheric Constituents and in Radiative Forcing, in *Climate Change 2007: The Physical Science Basis. Contribution of Working Group I to the Fourth Assessment Report of the Intergovernmental Panel on Climate Change*, edited by S. Solomon, D. Qin, M. Manning, Z. Chen, M. Marquis, K.B. Averyt, M. Tignor, and H.L. Miller, Cambridge University Press, Cambridge, United Kingdom and New York, NY, USA, 2007.

Fuentes, E., H. Coe, D. Green, G. de Leeuw, and G. McFiggans (2010), On the impacts of phytoplankton-derived organic matter on the properties of the primary marine aerosol - Part 1: Source fluxes, *Atmos. Chem. Phys.*, *10* (19), 9295-9317.

Fuentes, E., H. Coe, D. Green, and G. McFiggans (2011), On the impacts of phytoplankton-derived organic matter on the properties of primary marine aerosol - Part 2: Composition, hygroscopicity, and cloud condensation activity, *Atmos. Chem. Phys.*, *11*, 2585-2602.

Gard, E., J.E. Mayer, B.D. Morrical, T. Dienes, D.P. Fergenson, and K.A. Prather (1997), Real-time analysis of individual atmospheric aerosol particles: Design and performance of a portable ATOFMS, *Anal. Chem.*, *69* (20), 4083-4091.

Gard, E.E., M.J. Kleeman, D.S. Gross, L.S. Hughes, J.O. Allen, B.D. Morrical, D.P. Fergenson, T. Dienes, M.E. Galli, R.J. Johnson, G.R. Cass, and K.A. Prather

(1998), Direct observation of heterogeneous chemistry in the atmosphere, *Science*, *279* (5354), 1184-1187.

Gaston, C.J., H. Furutani, S.A. Guazzotti, K.R. Coffee, T.S. Bates, P.K. Quinn, L.I. Aluwihare, B.G. Mitchell, and K.A. Prather (2011), Unique ocean-derived particles serve as a proxy for changes in ocean chemistry, *J. Geophys. Res.-[Atmos.], 116*, D18310, doi:10.1029/2010JD015289.

Gross, D.S., M.E. Galli, P.J. Silva, and K.A. Prather (2000), Relative sensitivity factors for alkali metal and ammonium cations in single particle aerosol time-of-flight mass spectra, *Anal. Chem.*, *72* (2), 416-422.

Guazzotti, S.A., K.R. Coffee, and K.A. Prather (2001), Continuous measurements of size-resolved particle chemistry during INDOEX-Intensive Field Phase 99, *J. Geophys. Res.-[Atmos.]*, *106* (D22), 28607-28627.

Hawkins, L.N., and L.M. Russell (2010), Polysaccharides, proteins, and phytoplankton fragments: Four chemically distinct types of marine primary organic aerosol classified by single particle spectromicroscopy, *Advances in Meteorology*, doi:10.1155/2010/612132.

Holecek, J.C., M.T. Spencer, and K.A. Prather (2007), Analysis of rainwater samples: Comparison of single particle residues with ambient particle chemistry from the northeast Pacific and Indian oceans, *J. Geophys. Res.-[Atmos.]*, *112* (D22), doi:10.1029/2006JD008269.

Keene, W.C., H. Maring, J.R. Maben, D.J. Kieber, A.A.P. Pszenny, E.E. Dahl, M.A. Izaguirre, A.J. Davis, M.S. Long, X.L. Zhou, L. Smoydzin, and R. Sander (2007), Chemical and physical characteristics of nascent aerosols produced by bursting bubbles at a model air-sea interface, *J. Geophys. Res.-[Atmos.]*, *112* (D21), D21202, doi:10.1029/2007JD008464.

Kelly, J.T., and A.S. Wexler (2006), Water uptake by aerosol: Water activity in supersaturated potassium solutions and deliquescence as a function of temperature, *Atmos. Environ.*, *40* (24), 4450-4468.

Knopf, D.A., P.A. Alpert, B. Wang, and J.Y. Aller (2011), Stimulation of ice nucleation by marine diatoms, *Nature Geoscience*, *4* (2), 88-90.

Kohler, H. (1936), The nucleus in and the growth of hygroscopic droplets., *Transactions of the Faraday Society*, *32* (2), 1152-1161.

Kuznetsova, M., C. Lee, and J. Aller (2005), Characterization of the proteinaceous matter in marine aerosols, *Mar. Chem.*, *96* (3-4), 359-377.

Lampert, W. (1978), Release of dissolved organic carbon by grazing zooplankton, *Limnol. Oceangr.*, *23* (4), 831-834.

Leck, C., and E.K. Bigg (2005), Biogenic particles in the surface microlayer and overlaying atmosphere in the central Arctic Ocean during summer, *Tellus Ser. B*, *57* (4), 305-316.

Leck, C., and E.K. Bigg (2008), Comparison of sources and nature of the tropical aerosol with the summer high Arctic aerosol, *Tellus*, *60B*, 118-126.

Meskhidze, N., and A. Nenes (2006), Phytoplankton and cloudiness in the Southern Ocean, *Science*, *314* (5804), 1419-1423.

Middlebrook, A.M., D.M. Murphy, and D.S. Thomson (1998), Observations of organic material in individual marine particles at Cape Grim during the First Aerosol Characterization Experiment (ACE 1), *J. Geophys. Res.-[Atmos.]*, *103* (D13), 16475-16483.

Moore, M.J.K., H. Furatani, G.C. Roberts, R.C. Moffet, M.K. Giles, B. Palenik, and K.A. Prather (2011), Effect of organic compounds on cloud condensation nuclei (CCN) activity of sea spray aerosol produced by bubble bursting, *Atmos. Environ.*, doi: 10.1016/j.atmosenv.2011.04.034.

Moore, R.H., E.D. Ingall, A. Sorooshian, and A. Nenes (2008), Molar mass, surface tension, and droplet growth kinetics of marine organics from measurements of CCN activity, *Geophys. Res. Lett.*, *35*, L07801, doi:10.1029/2008GL033350.

Neubauer, K.R., M.V. Johnston, and A.S. Wexler (1997), On-line analysis of aqueous aerosols by laser desorption ionization, *International Journal of Mass Spectrometry and Ion Processes*, *163* (1-2), 29-37.

Neubauer, K.R., M.V. Johnston, and A.S. Wexler (1998), Humidity effects on the mass spectra of single aerosol particles, *Atmos. Environ.*, *32* (14-15), 2521-2529.

O'Dowd, C.D., M.C. Facchini, F. Cavalli, D. Ceburnis, M. Mircea, S. Decesari, S. Fuzzi, Y.J. Yoon, and J.P. Putaud (2004), Biogenically driven organic contribution to marine aerosol, *Nature*, *431* (7009), 676-680.

Poschl, U. (2005), Atmospheric aerosols: Composition, transformation, climate and health effects, *Angewandte Chemie-International Edition*, *44* (46), 7520-7540.

Pyo, Y.J., M. Gierth, J.I. Schroeder, and M.H. Cho (2010), High-Affinity K(+) Transport in Arabidopsis: AtHAK5 and AKT1 Are Vital for Seedling Establishment and Postgermination Growth under Low-Potassium Conditions, *Plant Physiology*, *153* (2), 863-875.

Quinn, P.K., T.S. Bates, D.J. Coffman, and D.S. Covert (2008), Influence of particle size and chemistry on the cloud nucleating properties of aerosols, *Atmos. Chem. Phys.*, *8* (4), 1029-1042.

Rinaldi, M., S. Decesari, D. Finessi, L. Giulianelli, C. Carbone, S. Fuzzi, C.D. O'Dowd, D. Ceburnis, and M.C. Facchini (2010), Primary and secondary organic marine aerosol and oceanic biological activity: Recent results and new perspectives for future studies, *Advances in Meteorology*, doi:10.1155/2010/310682.

Russell, L.M., R. Bahadur, and P.J. Ziemann (2011), Identifying organic aerosol sources by comparing functional group composition in chamber and atmospheric particles, *PNAS*, doi:10.1073/pnas.1006461108.

Russell, L.M., L.N. Hawkins, A.A. Frossard, P.K. Quinn, and T.S. Bates (2010), Carbohydrate-like composition of submicron atmospheric particles and their production from ocean bubble bursting, *PNAS*, *107* (15), 6652-6657.

Sander, R., W.C. Keene, A.A.P. Pszenny, R. Arimoto, G.P. Ayers, E. Baboukas, J.M. Cainey, P.J. Crutzen, R.A. Duce, G. Honninger, B.J. Huebert, W. Maenhaut, N. Mihalopoulos, V.C. Turekian, and R. Van Dingenen (2003), Inorganic bromine in the marine boundary layer: a critical review, *Atmos. Chem. Phys.*, *3*, 1301-1336.

Silva, P.J., and K.A. Prather (2000), Interpretation of mass spectra from organic compounds in aerosol time-of-flight mass spectrometry, *Anal. Chem.*, *72* (15), 3553-3562.

Song, X.H., P.K. Hopke, D.P. Fergenson, and K.A. Prather (1999), Classification of single particles analyzed by ATOFMS using an artificial neural network, ART-2a, *Anal. Chem.*, *71* (4), 860-865.

Swietlicki, E., H.C. Hansson, K. Hameri, B. Svenningsson, A. Massling, G. McFiggans, P.H. McMurry, T. Petaja, P. Tunved, M. Gysel, D. Topping, E. Weingartner, U. Baltensperger, J. Rissler, A. Wiedensohler, and M. Kulmala (2008), Hygroscopic properties of submicrometer atmospheric aerosol particles measured with H-TDMA instruments in various environments - a review, *Tellus Ser. B*, *60* (3), 432-469.

Wells, M.L., and E.D. Goldberg (1991), Occurrence of Small Colloids in Sea-Water, *Nature*, *353* (6342), 342-344.

Wells, M.L., and E.D. Goldberg (1992), Marine Submicron Particles, *Mar. Chem.*, *40* (1-2), 5-18.

Wise, M.E., E.J. Freney, C.A. Tyree, J.O. Allen, S.T. Martin, L.M. Russell, and P.R. Buseck (2009), Hygroscopic behavior and liquid-layer composition of aerosol particles generated from natural and artificial seawater, *J. Geophys. Res.-[Atmos.], 114*, D03201, doi:10.1029/2008JD010449.

Woodcock, A.H., C.F. Kientzler, A.B. Arons, and D.C. Blanchard (1953), Giant condensation nuclei from bursting bubbles, *Nature*, *172* (4390), 1144-1145.

Xiao, H.S., J.L. Dong, L.Y. Wang, L.J. Zhao, F. Wang, and Y.H. Zhang (2008), Spatially resolved micro-Raman observation on the phase separation of effloresced sea salt droplets, *Environ. Sci. Tech., 42* (23), 8698-8702.

Zelenyuk, A., D. Imre, L.A. Cuadra-Rodriguez, and B. Ellison (2007), Measurements and interpretation of the effect of a soluble organic surfactant on the density, shape and water uptake of hygroscopic particles, *J. Aerosol Sci., 38*, 903-923.

Chapter 5

5. The Impact of Shipping, Agricultural, and Urban Emissions on the Single Particle Chemistry Observed Aboard the R/V Atlantis during CalNex

5.1 Synopsis

The CalNex field campaign was undertaken, in part, to obtain a better understanding of the regional impacts of different pollution sources in California. As part of this study, real-time shipboard measurements were made of the size-resolved single-particle mixing-state of sub- and super-micron particles along the California coast. Major differences were noted between Southern and Northern California; in Southern California, the particles were dominated by soot (up to ~89% by number), whereas organic carbon (OC) particles comprised the largest fraction of submicron number concentrations in the Sacramento area (up to ~67% by number). The mixing-state of these carbonaceous particle types varied during the cruise with sulfate being more prevalent on soot particles in Southern California due to the influence of shipping and port emissions, while contributions of secondary organic aerosol, including amines, and nitrate were more prevalent in Northern California and during time periods impacted by agricultural emissions (e.g. from the inland Riverside and Central Valley regions). These regional differences and changes in the mixing-state of carbonaceous particles have implications for particle heterogeneous reactivity, water uptake, and cloud nucleating

abilities, which should be taken into account when determining how to regulate particulate sources in California.

5.2 Introduction

Atmospheric aerosols contribute to air pollution, adverse effects on human health, and global climate change [*Poschl*, 2005]. In terms of health effects, particulate air pollution has been linked to cardiopulmonary disease [*Pope and Dockery*, 2006] and decreased lung function in children [*Gauderman et al.*, 2000]. Particles scatter and absorb solar and terrestrial radiation contributing to the aerosol direct effect [*IPCC*, 2007; *Poschl*, 2005] and also serve as nuclei for the formation of cloud droplets and ice crystals constituting the aerosol indirect effect [*IPCC*, 2007; *Lohmann and Feichter*, 2005; *Poschl*, 2005]. Aerosol particles also play a role in altering the lifetime [*Albrecht*, 1989] and radiative properties of clouds [*Twomey*, 1977], in addition to altering precipitation frequency and intensity [*Rosenfeld et al.*, 2008]. Despite these impacts, uncertainties remain regarding the role of aerosols on climate change and global radiative forcing [*IPCC*, 2007]. Policymakers have introduced numerous strategies to mitigate the impacts of particulate matter; however, a greater understanding is needed in order to properly regulate sources. The aim of the CalNex field campaign is to elucidate the link between aerosols, air pollution, and climate in order to guide policies regarding emission regulations in California.

To achieve this, it is essential to better understand the role of particle size and composition in shaping the health and climatic impacts of aerosols. Smaller particles have greater adverse health effects due to their ability to penetrate deeper into the

respiratory system while particle composition influences aerosol toxicity (e.g. through the contribution of metals and polycyclic aromatic hydrocarbons (PAHs)) [*Bernstein et al.*, 2004; *Fang et al.*, 2008; *Gauderman et al.*, 2000; *Pinkerton et al.*, 2004; *Pope and Dockery*, 2006; *Poschl*, 2005; *Sunderman*, 2001]. Particle size and chemical composition also influence both the aerosol direct and indirect effects. Particle size affects aerosol optical properties since light scattering efficiency is greatest for particle diameters of the same order of magnitude as solar and terrestrial radiation wavelengths [*Poschl*, 2005; *Quinn et al.*, 2005]; additionally, smaller particles are also less efficient as cloud nuclei [*Lohmann and Feichter*, 2005; *McFiggans et al.*, 2006; *Poschl*, 2005; *Quinn et al.*, 2008]. The mixing state of aerosol particles with secondary species also impacts the aerosol direct effect, particularly for black carbon (soot) [*Jacobson*, 2000; *Moffet and Prather*, 2009; *Schnaiter et al.*, 2005]. Particle chemistry also influences the cloud forming potential of aerosols, for example, high mass fractions of water insoluble material (e.g. hydrophobic organics) have been shown to decrease the ability of particles to act as nuclei for cloud droplets [*McFiggans et al.*, 2006; *Quinn et al.*, 2008]. In addition to understanding the physicochemical properties of freshly emitted particles from different sources, it is important to also note that particle size and composition evolve over time due to atmospheric processing (e.g. gas-particle partitioning, heterogeneous reactions, etc.) thereby altering the health and climatic impacts of particles [*Poschl*, 2005]. It is, thus, important to measure the physicochemical properties of both freshly emitted particles as well as particles that have been processed in the atmosphere to distinguish how sources as well as aging processes influence particle chemistry and size.

California is impacted by diverse particle sources including ships, vehicle exhaust, oil refineries, animal husbandry emissions, etc. The Ports of Los Angeles (LA) and Long Beach (LB) are the busiest container ports in the United States, contributing high levels of ship and port emissions (e.g. diesel truck emissions, oil refinery emissions) to Southern California. Locations in inland Southern California (e.g. Riverside) and the Sacramento and San Joaquin Valley areas in Northern California are impacted by dairy farm and agricultural emissions also leading to high mass concentrations of particulate matter that is namely secondary in nature [*Chen et al.*, 2007; *Chow et al.*, 2006a; *Docherty et al.*, 2008; *Grover et al.*, 2008; *Hughes et al.*, 2000; *Hughes et al.*, 2002; *Magliano et al.*, 1999; *Pastor et al.*, 2003; *Qin et al.*, 2012; *Sorooshian et al.*, 2008]. Assessing how these regional differences in particle sources in California impact the physicochemical properties of aerosols is a key step in fulfilling the goals of the CalNex field campaign.

Herein we present real-time measurements of single-particle composition and size using aerosol time-of-flight mass spectrometry (ATOFMS) during the CalNex campaign aboard the R/V Atlantis sampling platform. Single-particle mass spectrometry is well-suited for providing the high temporal resolution and mass spectral fingerprints necessary for distinguishing diverse particle sources as well as assessing the impact of atmospheric processing on particle size and chemistry [*Pratt and Prather*, 2011; *Sullivan and Prather*, 2005]. Atmospheric measurements were made off the California coast, targeting specific sources, including the Ports of LA and LB, continental outflow from Santa Monica, and emissions from Northern California including the inland, Sacramento area. This paper

describes the significant differences observed in single particle mixing-state and sources between these different regions. The implications of these findings are discussed.

5.3 Methods

Ambient aerosol measurements were made onboard the R/V Atlantis from May 14-June 8, 2010 as part of the CalNex 2010 field campaign (http://www.esrl.noaa.gov/csd/calnex/). The ship traveled from San Diego up to Sacramento, then back to the Port of San Francisco where the study ended; the cruise track is shown in Figure 5.1. The air in the sampling manifold was conditioned to 55 ± 5% relative humidity (RH) using a heated inlet [*Bates et al.*, 2004]. Meteorological and gas phase constituents were measured by the Pacific Marine Environmental Laboratory (PMEL) onboard the ship.

5.3.1 Aerosol Measurements: ATOFMS

The size-resolved chemical composition of individual aerosol particles from 0.2-3.0 µm aerodynamic diameter was measured in real-time using an aerosol time-of-flight mass spectrometer (ATOFMS). The operating principles of the ATOFMS have been described previously [*Gard et al.*, 1997; *Prather et al.*, 1994]. Briefly, particles are sampled through a converging nozzle inlet into a differentially pumped vacuum chamber causing particles to be accelerated to a size-dependent terminal velocity. Particles next enter the sizing region of the instrument consisting of two continuous wave (532 nm) lasers separated by a fixed distance. The time taken to traverse the laser beams is recorded giving the terminal velocity of the particle, which is used to calculate the aerodynamic diameter of the particle. The calculated particle velocity is also used to time

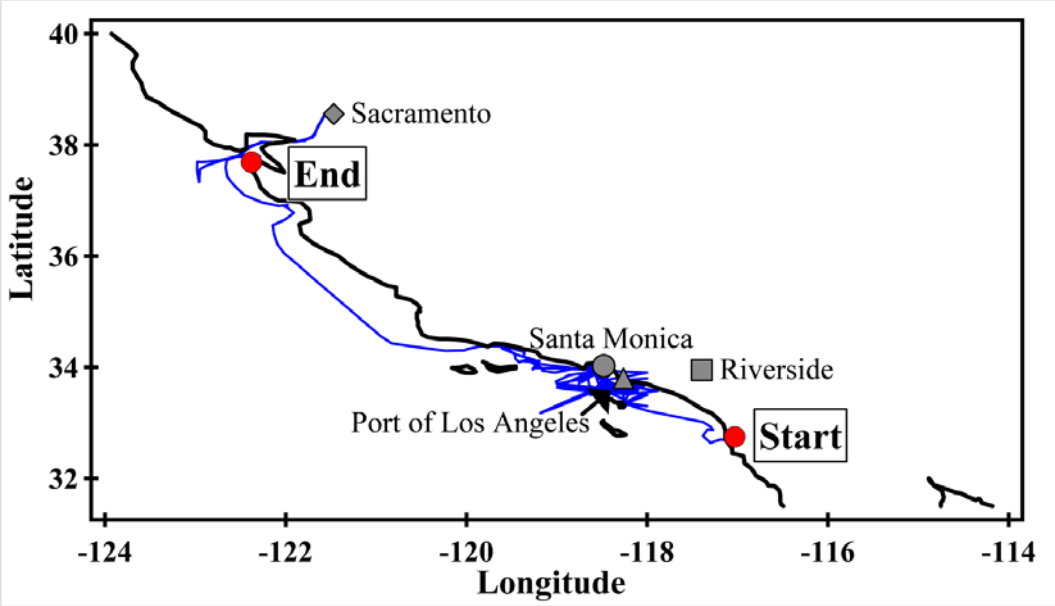

Figure 5.1: The cruise track for CalNex (blue line) is shown along the California coast. The Port of Los Angeles (grey triangle), the Santa Monica area (grey dot), Riverside (grey square) and the Sacramento area (grey diamond) are shown along with the start and end points of the cruise.

the firing of a Q-switched Nd:YAG laser operating at ~1.2 mJ laser power that simultaneously desorbs and ionizes compounds from individual particles creating positive and negative ions, which are analyzed in a dual polarity time-of-flight mass spectrometer. Dual-polarity spectra provide complementary information regarding the source (e.g. ships vs. sea salt) and age of the particle (e.g. fresh vs. reacted sea salt) [*Guazzotti et al.*, 2001; *Noble and Prather*, 1996].

The YAADA software toolkit was used to import ion peak lists into MATLAB v 6.5.1 (The MathWorks, Inc.) for processing of ATOFMS data [*Allen*, 2002]. The individual particle mass spectra were then analyzed using a clustering algorithm (ART-2a), which groups particles together based on mass spectral similarities [*Song et al.*, 1999]. Data were averaged into 1-hour time bins and separated into submicron (0.2-1.0 μm) and supermicron (1.0-3.0 μm) particles. Ship exhaust from the R/V Atlantis was filtered out by eliminating time periods when the sampling mast was pointed toward the exhaust stack at the rear of the ship. Data are presented in coordinated universal time (UTC) as day of year (DOY). Each ion peak assignment presented in this paper corresponds to the most likely ion produced at a given mass-to-charge (*m/z*). Particle types described herein are defined by characteristic ion peaks and/or possible sources and do not reflect all of the species present within a particular particle class.

5.4 Results

Temporal trends of single-particle measurements were analyzed to discern differences in particle chemistry between sources in Southern and Northern California. The temporal variability of the top sub- and supermicron particle types detected by

ATOFMS as well as the latitudinal position of the ship are shown in Figure 5.2. Several trends in single-particle mixing-state were identified based on differences in particle source, meteorological conditions, and aging processes. To illustrate this, six distinct time periods are identified by colored boxes in Figure 5.2; the time periods are defined as Riverside Transport (Period 1, boxed in red), Stagnant/Ports Transport (Period 2, boxed in black), Marine/Coastal Transport (Period 3, boxed in cyan), Ports of Los Angeles/Long Beach (LA/LB) (Period 4, boxed in green), Central Valley Transport (Period 5, boxed in orange), and Sacramento (Period 6, boxed in purple). The following sections provide a detailed comparison and discussion of the gas phase and meteorological conditions present, prevalent particle types and sources, the mixing state of carbonaceous particles, and the secondary particulate species present during each time period.

5.4.1 Characteristics of Each Period

During Periods 1-3, measurements were concentrated around Southern California and Santa Monica, in particular, while measurements during Period 4 were concentrated in the Ports of LA and LB and surrounding shipping lanes. During Period 5, measurements extended further north to the Santa Barbara region; Period 6 was completely in Northern California when the ship remained in the Deep Water Channel/Sacramento region for 3 days. Table 5.1 shows the corresponding dates and meteorological and gas phase measurements for each time period, while Figure 5.3 shows the 48-hour air mass back trajectories [*Draxler and Rolph*, 2011] for each time period to highlight differences in transport conditions. Periods 1, 5, and 6 had agricultural

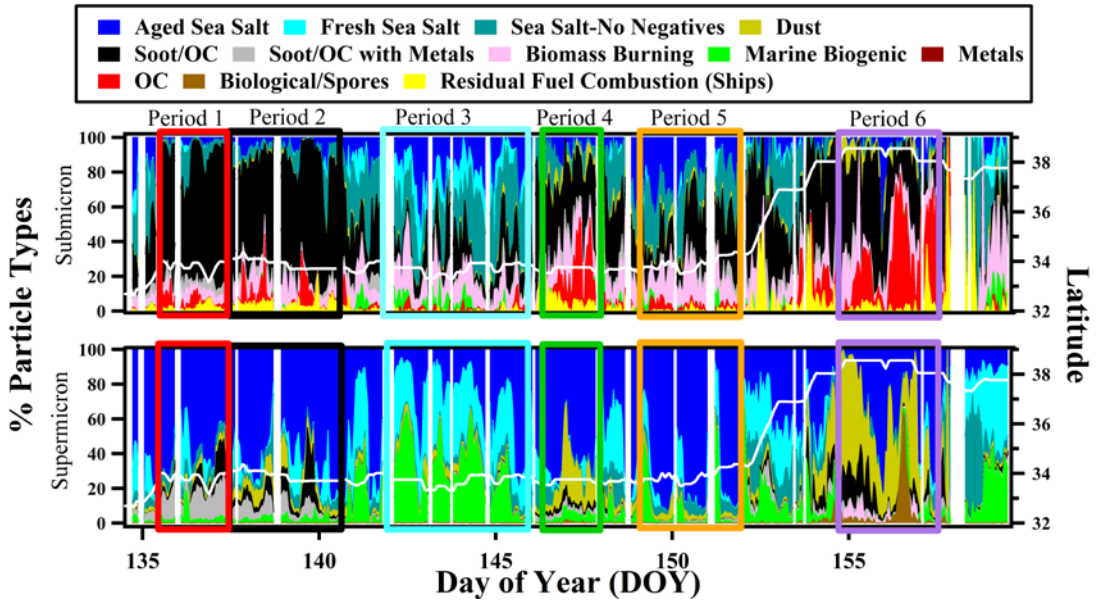

Figure 5.2: Hourly temporal profile of single-particle mixing state observed by ATOFMS as a function of day of year (DOY) and latitude (white line). The top and bottom panels show the single-particle chemistry for submicron particles (0.2-1.0 µm) and supermicron particles (1.0-3.0 µm), respectively. Colored boxes highlight 6 different periods when differences in particle composition were observed due to different meteorological conditions, gas phase concentrations, and aging processes.

Table 5.1: Average meteorological conditions (wind speed, wind direction), average gas-phase concentrations (radon, CO, NO_x, ozone, SO_2), latitudinal and longitudinal range, and DOY for measurements made during each of the 6 different time periods highlighted.

Period	Location/Air Mass	Day of Year (DOY)	Dates	Latitude	Longitude	Wind Speed (m/s)	RH	Air Temp (°C)	Radon (mBq/m^3)	SO_2 (ppbv)	Ozone (ppbv)	NO_x (ppbv)	CO (ppbv)
1	Riverside	135.5-137.37	5/15/2010 12:00-5/17/2010 9:00	33.14N to 34.02N	118.33W to 119.22W	2.93	88.59	13.21	2551.41	0.07	47.09	N/A	176.92
2	Stagnant/Ports	137.37-140.5	5/17/2010 9:00-5/20/2010 12:00	33.67N to 34.38N	118.22W to 119.69W	3.88	90.84	13.14	906.27	0.04	38.91	N/A	127.91
3	Marine/Coastal	142-146	5/22/2010 0:00-5/26/2010 0:00	33.31N to 33.95N	118.07W to 118.93W	5.18	72.36	13.93	1548.20	0.17	37.77	4.74	156.15
4	Port of Los Angeles	146.337-147.8747	5/26/2010 8:00-5/27/2010 21:00	33.53N to 33.77N	118.1W to 118.5W	2.40	72.72	16.04	735.81	3.36	29.42	18.13	147.00
5	Central Valley	149-151.87	5/29/2010 0:00-5/31/2010 21:00	33.5N to 34.4N	118.17W to 119.85W	3.29	83.47	15.21	3183.13	0.45	43.63	5.15	156.56
6	Sacramento Deep Water Channel	154.6253-157.6247	6/3/2010 15:00-6/6/2010 15:00	38.02N to 38.56N	121.55 W to 122.16W	4.53	69.36	20.86	1564.03	0.39	20.64	2.70	111.46

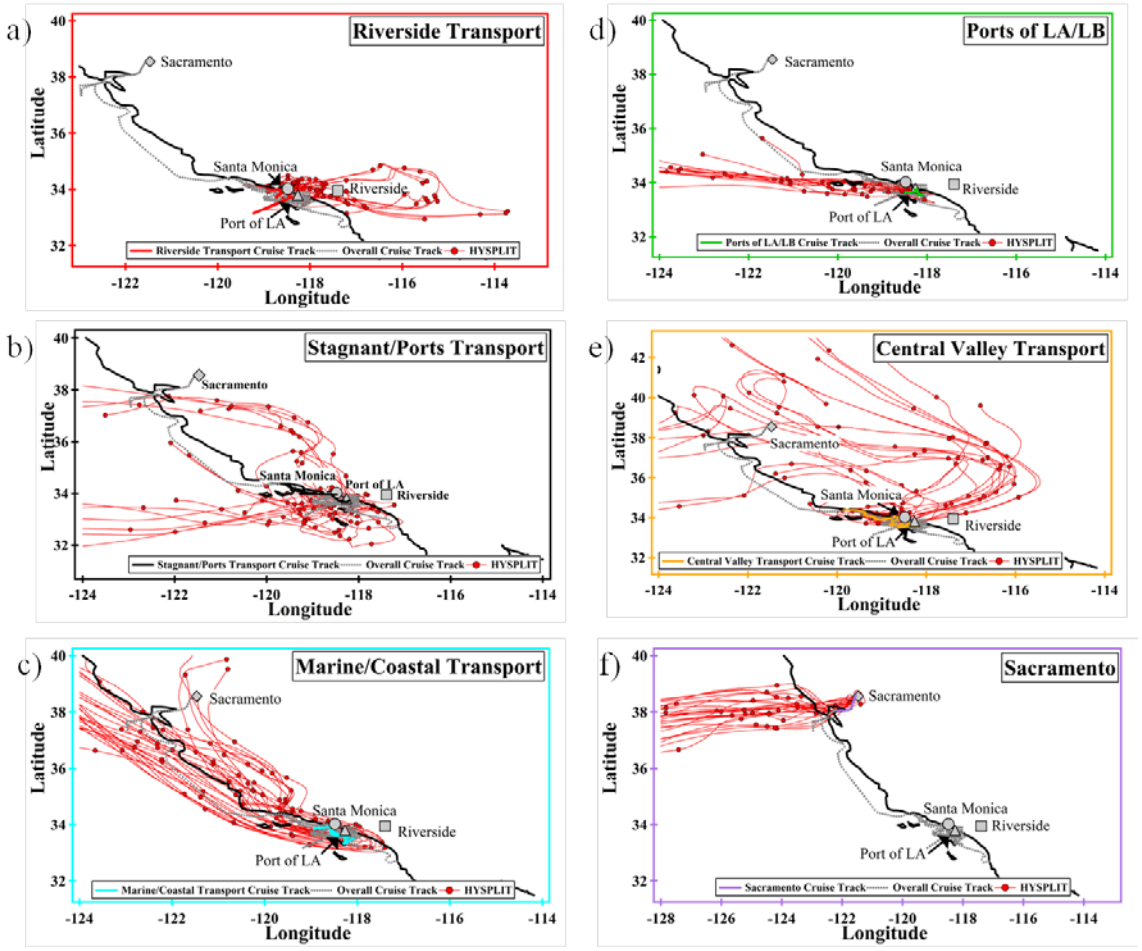

Figure 5.3: 48-hour HYSPLIT air mass back-trajectories at 500 m (red lines) shown during the cruise (grey dotted line) corresponding to (a) Period 1: Riverside Transport boxed in red, (b) Period 2: Stagnant/Ports Transport boxed in black, (c) Period 3: Marine/Coastal Transport boxed in cyan, (d) Period 4: Port of Los Angeles boxed in green, (e) Period 5: Central Valley Transport boxed in orange, and (f) Period 6: Sacramento boxed in purple. Red dots on the HYSPLIT trajectories denote 12 hour increments. The Port of Los Angeles (grey triangle), the Santa Monica area (grey dot), Riverside (grey square) and the Sacramento area (grey diamond) are also shown.

influence from Riverside or the Central Valley region, while Periods 2 and 4 were heavily influenced by emissions from the Ports of LA/LB, and Period 3 was influenced by oceanic emissions and serves as a background period.

5.4.1.1 Period 1: Riverside Transport

During Period 1, sampled air masses were transported from the inland, Riverside region before traversing the port and Santa Monica region (see Figure 5.3a); thus, Period 1 is characterized by influences from both port as well as agricultural emissions. Particulate matter in Riverside typically shows heavy signs of aging, characterized by high concentrations of secondary species such as nitrate, amines, ammonium, and secondary organics [*Hughes et al.*, 2000; *Hughes et al.*, 2002; *Liu et al.*, 2000; *Pastor et al.*, 2003; *Pratt et al.*, 2009; *Pratt and Prather*, 2009; *Qin et al.*, 2012]. Radon concentrations were high averaging ~2551 mBq/m^3, and the highest average $O_{3(g)}$ concentrations (~47 ppbv) were observed, confirming the heavily aged, continentally influenced air masses sampled during this period. Further, low temperatures averaging ~13.2°C and high RH averaging ~88.5% were observed suggesting that aqueous phase processing was dominant during this period.

5.4.1.2 Period 2: Stagnant/Ports Transport

Sampled air masses stagnated around the coast, port, and Santa Monica regions during Period 2 highlighting that local port emissions (e.g. emissions from vehicles, ships, etc.) were dominant. Both $O_{3(g)}$ and radon concentrations (~38.9 ppbv and ~906 mBq/m^3 on average, respectively) were lower during Period 2 than Period 1 suggesting that aerosols underwent less chemical aging than particles observed during Period 1.

Again, high RH (~90.8% on average) and low temperatures (~13.1°C on average) were observed suggesting that most aerosols underwent aqueous processing and exhibited favorable conditions for the condensation of semi-volatile compounds.

5.4.1.3 Period 3: Marine/Coastal Transport

During Period 3, most air masses followed a coastal/oceanic trajectory along the California coast. Wind speeds reached ~14.5 m/s, which enhances the production of fresh sea spray particles, comprised of both fresh sea salt and biogenically-derived organics, from bursting bubbles generated by breaking waves [*Blanchard and Woodcock*, 1957; *Monahan et al.*, 1983; *O'Dowd and De Leeuw*, 2007]. Thus, Period 3 is characterized by ocean-derived aerosol; however, this period is not representative of clean marine conditions based on the high radon concentrations (~1548 mBq/m^3 on average) and high particle number counts (~6347 cm^{-3} on average) [*Fitzgerald*, 1991; *Hawkins et al.*, 2010; *O'Dowd and De Leeuw*, 2007; *Twohy et al.*, 2005].

5.4.1.4 Period 4: Ports of LA/LB Transport

Period 4 was characterized by high $SO_{2(g)}$ and $NO_{x(g)}$ concentrations (~3.4 ppbv and ~18ppbv, respectively, on average) and low wind speeds (~2.4 m/s on average) and radon concentrations (~736 mBq/m^3 on average). Local port and shipping emissions dominated the particle chemistry during this period with little influence from other continental/transported sources.

5.4.1.5 Period 5: Central Valley Transport

Figure 5.3e shows air masses traveling across the Central Valley during Period 5. The highest Radon concentrations were measured during this time period averaging ~3183 mBq/m^3 and high average $O_{3(g)}$ concentrations (~43 ppbv) were also observed. Similar to Riverside, the Central Valley aerosol is characterized by high concentrations of secondary species, namely secondary organic aerosol and ammonium nitrate due to contributions from dairy farms and other agricultural emissions [*Chen et al.*, 2007; *Chow et al.*, 2006a; *Chow et al.*, 2006b]; hence, particulate matter observed during Period 5 is expected to be highly aged, similar to Period 1. However, higher temperature (~15.2°C on average) and lower RH conditions (~83% on average) were observed during Period 5 leading to less aqueous phase processing than was observed during Period 1.

5.4.1.6 Period 6: Sacramento

During Period 6, air masses were of oceanic origin, traveling over the San Francisco Bay area prior to arriving in the Sacramento region, which is within the Central Valley. Due to these unique meteorological conditions, local sources of pollution from the Central Valley were likely diluted when sampling in the Sacramento region took place. Diurnal temperature and RH profiles were observed ranging from ~16-30°C and ~24-93%, respectively; as such, diurnal profiles in particle chemistry were observed with aqueous phase processing occurring at night while secondary processing due to photochemistry occurred during the day. The lowest $O_{3(g)}$, $NO_{x(g)}$, and lowest $CO_{(g)}$ were observed along with high radon concentrations (~1564 mBq/m^3 on average) suggesting

that fewer anthropogenic emissions were detected compared to the previous periods in Southern California.

5.4.2 Observed Particle Types

5.4.2.1 Submicron Particle Chemistry

Particle composition was found to vary by latitude, as shown in Figure 5.2, and also Figure 5.4, which shows the size-resolved chemistry of particles detected during each period. Increased number fractions of soot particles (up to ~89% of submicron particles by number) were observed in Southern California, particularly during Periods 1, 2, and 4 when port and urban (e.g. vehicles) emissions were dominant. In addition to soot, particles from residual fuel combustion (e.g. emissions from ships and oil refineries) were also observed namely when port and shipping emissions influenced particle chemistry during Periods 2 and 4. This residual fuel combustion particle type represented at most ~25% of submicron particles and is characterized by ion peaks associated with transition metals found in residual fuel oil, notably vanadium ($^{51}V^{+}$, $^{67}VO^{+}$), nickel ($^{58,60}Ni^{+}$), and iron ($^{54,56}Fe^{+}$), in addition to sulfate ($^{97}HSO_4^{-}$) and, to a lesser extent, nitrate ($^{46}NO_2^{-}$, $^{62}NO_3^{-}$) (Figure 5.5a) [*Agrawal et al.*, 2008; *Ault et al.*, 2010; *Ault et al.*, 2009; *Corbett and Fischbeck*, 1997; *Healy et al.*, 2009; *Murphy et al.*, 2009]. During Period 4, additional industrial particle types were observed at the Ports of LA and LB, including metals concentrated in the submicron size mode, which most likely represent emissions from incineration [*Moffet et al.*, 2008a] and are the subject of a future paper (P. Weiss-Penzias et al., manuscript in preparation, 2012). Additionally, organic carbon (OC) represented a much higher fraction of the detected submicron particles during Period 4

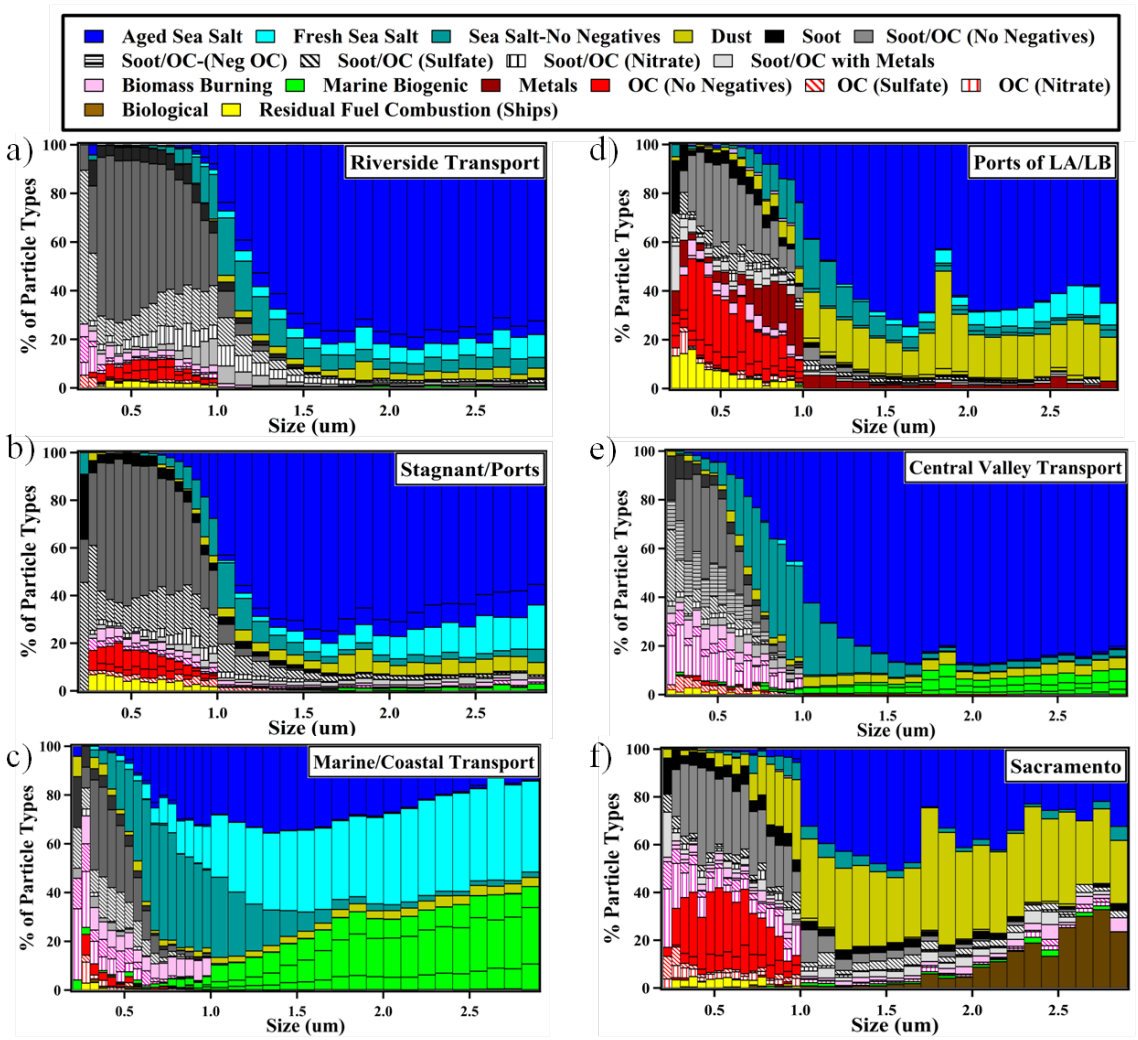

Figure 5.4: Fraction of particle types as a function of size observed during the 6 different time periods. Submicron particles (0.2-1.0 μm) are plotted in 0.05 μm bins while supermicron particles (1.0-3.0 μm) are plotted in 0.1 μm bins.

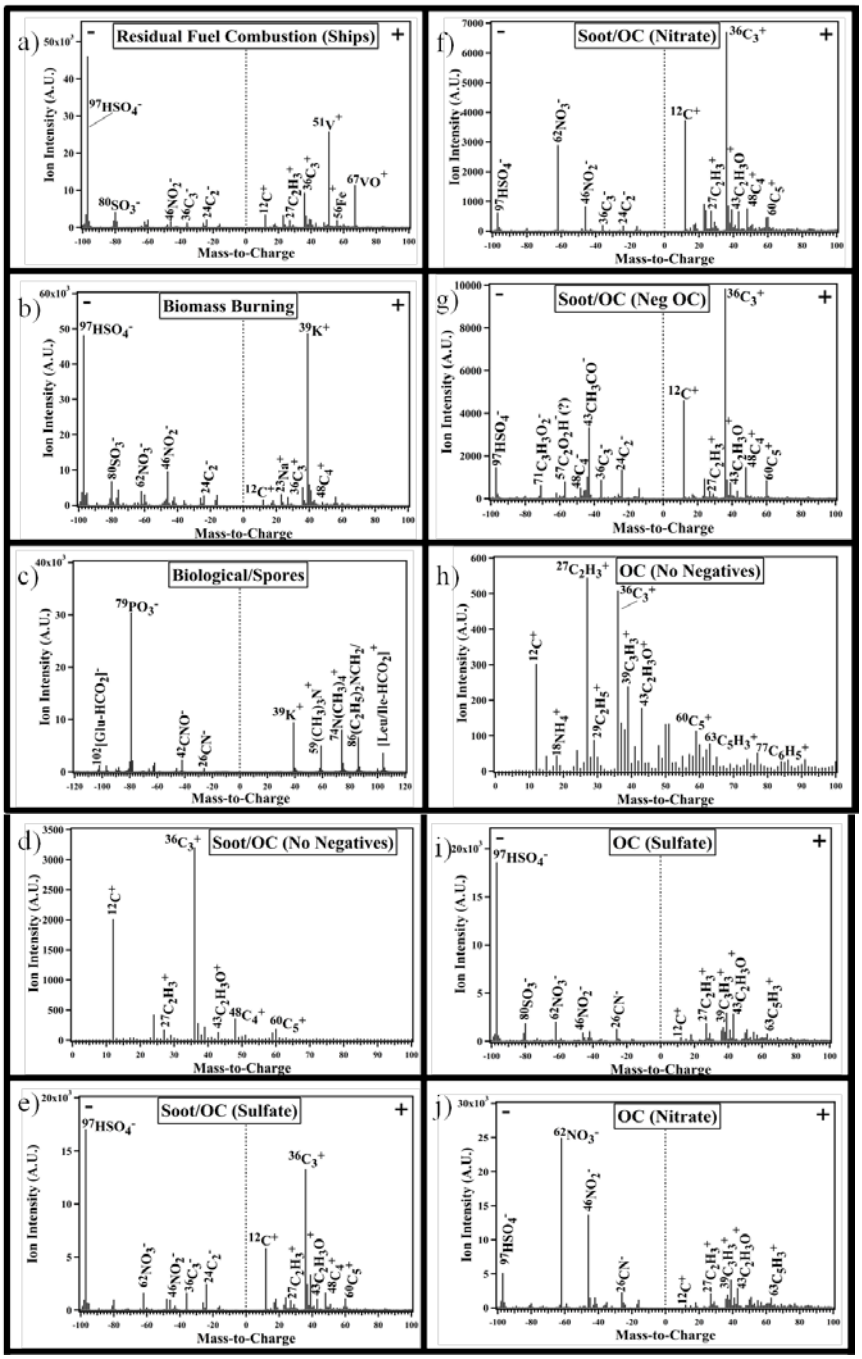

Figure 5.5: Representative mass spectra of (a) Residual Fuel Combustion from ships, (b) Biomass Burning, (c) Biological/Spores, (d) Soot/OC (No Negatives), (e) Soot/OC (Sulfate), (f) Soot/OC (Nitrate), (g) Soot/OC (Neg OC), (h) OC (No Negatives), (i) OC (Sulfate), (j) OC (Nitrate) particles are shown. For mass spectra containing both positive and negative ions, dashed lines separate negative ions (left side) and positive ions (right side).

(~12% of the total submicron particles detected on average) than the previous periods likely due to elevated vehicular and shipping emissions, which have been shown to contribute high mass concentrations of organic carbon to the aerosol burden [*Lack et al.*, 2009; *Murphy et al.*, 2009; *Russell et al.*, 2000; *Sodeman et al.*, 2005].

In contrast, soot and particles from residual fuel combustion made negligible contributions to the observed particle chemistry in Southern California during Marine and Central Valley Transport periods (Periods 3 and 5) and in the Sacramento region (Period 6). During Marine Transport conditions (Period 3), submicron particle chemistry was dominated by sea salt particles (up to ~57%) likely due to the production of fresh sea spray aerosol induced by high wind speeds. As shown in Figures 5.2 and 5.4, particles from biomass burning were elevated in the submicron mode, particularly during Periods 5 and 6, representing up to ~42% of submicron particles. Biomass burning particles are characterized by an intense potassium peak ($^{39}K^+$) in addition to carbonaceous peaks (both elemental and organic), organic nitrogen peaks ($^{26}CN^-$, $^{42}CNO^-$), ion peaks associated with potassium salts ($^{113}K_2Cl^+$, $^{213}K_3SO_4^+$, etc.), and secondary species such as sulfate and/or nitrate (Figure 5.5b) [*Pratt et al.*, 2010; *Qin and Prather*, 2006; *Silva et al.*, 1999]. Elevated biomass burning emissions detected during Periods 5 and 6 are likely emitted from crop burning, which has been found to contribute significantly to the Central Valley aerosol [*Chen et al.*, 2007; *Chow et al.*, 2006a; *Hays et al.*, 2005].

The key difference in particle chemistry observed in Northern California during Period 6 was the high percentage of submicron organic carbon (OC) particles detected, constituting up to ~67% of submicron particles by number; the high percentage of

organics was observed due to new particle formation (NPF) events. While the lower size limit of the nozzle-inlet ATOFMS (~0.2 μm) cannot be used to probe the chemistry of newly formed particles, ATOFMS measurements can provide insight into the composition of these particles as they grow to sizes detectable by the instrument [*Creamean et al.*, 2011]. Figure 5.6 shows particle number concentration as a function of diameter measured by a differential mobility particle sizer (DMPS). Several distinct events are highlighted in black boxes when high number concentrations of small particles (~0.02 μm) were observed followed by rapid growth to ~0.08-0.1 μm, which is indicative of NPF events [*Creamean et al.*, 2011; *Hegg and Baker*, 2009; *Kulmala*, 2003]. As shown in Figure 5.6, the percentage of submicron OC particles was clearly elevated as newly formed particles grew suggesting that organic species contribute to this growth in agreement with previous studies [*Creamean et al.*, 2011; *Kulmala*, 2003; *Smith et al.*, 2008; *Zhang et al.*, 2004]. The formation of new particles occurred under conditions of low RH and intense solar radiation; however, growth of these particles occurred as RH increased with many of the detected OC particles lacking negative ion spectra (~74% on average) indicating that an appreciable amount of particulate water was associated with these particles [*Neubauer et al.*, 1997; *Neubauer et al.*, 1998].

5.4.2.1 Supermicron Particle Chemistry

Aged sea salt dominated the supermicron particle chemistry during most periods representing up to ~72% of supermicron particles, as shown in Figures 5.2 and 5.4. Aged sea salt particles have undergone heterogeneous reactions with gas phase nitrogen oxides (e.g. $N_2O_{5(g)}$, $HNO_{3(g)}$), resulting in the displacement of chloride by particulate nitrate

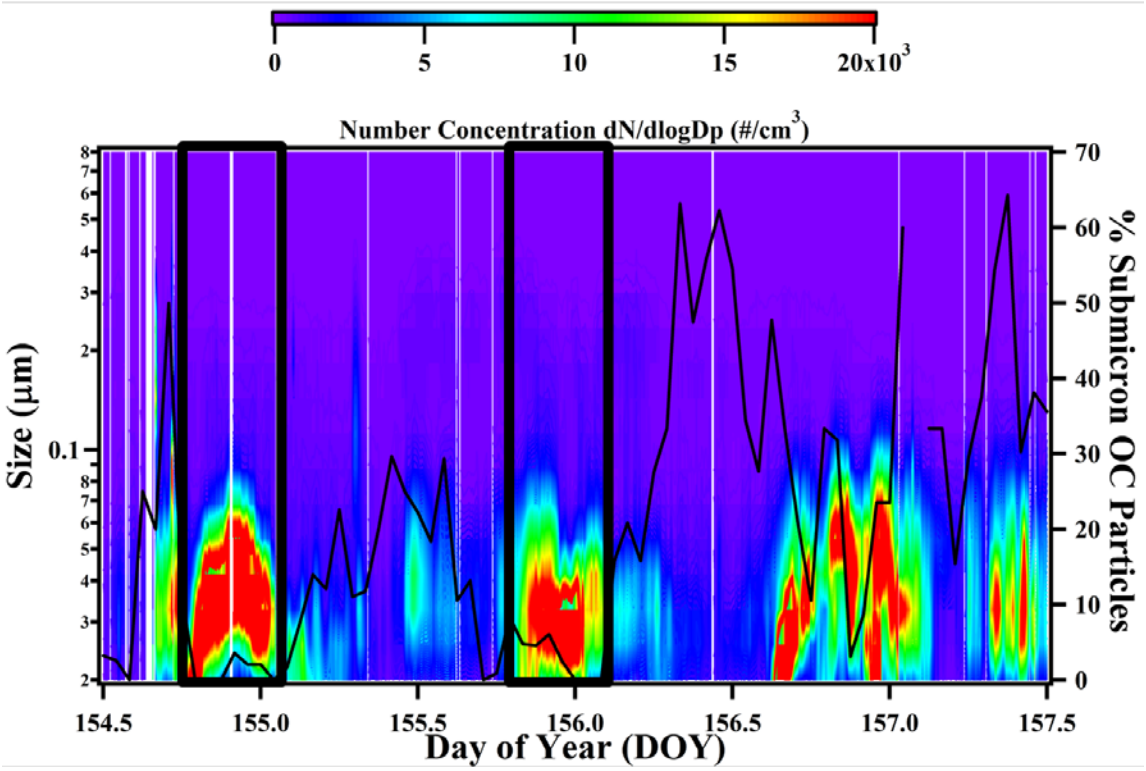

Figure 5.6: Size distributions of particle number concentrations as a function of size and DOY are shown on a log scale. The percentage of submicron OC particles (black line) is shown as a function of DOY. Time periods when new particle formation events were observed are shown in black boxes.

[*Behnke et al.*, 1991; *Chang et al.*, 2011; *Vogt et al.*, 1996]. During the Marine Transport period (Period 3), however, fresh sea salt and marine biogenic particle types dominated the supermicron particle chemistry representing ~33% and ~26% of supermicron particles on average, respectively. Marine biogenic particle types include Mg-type [*Gaston et al.*, 2011] and S-type particles (C.J. Gaston et al., manuscript in preparation, 2012), which represent primary, ocean-derived particle types associated with marine biological activity. The combined high wind speeds in addition to the presence of a strong red tide bloom leading to elevated biological activity along the Southern California coast (www.sccoos.org) explains the dominance of fresh sea salts and marine biogenic emissions during Period 3.

Marine particle types were negligible in the inland, Sacramento region during Period 6. Instead, dust particles were found to represent ~39% of supermicron particles on average, and biological particles were also found to represent up to ~64% of supermicron particles as shown in Figures 5.2 and 5.4f. Most of these biological particles were determined to be spores containing high concentrations of dipicolinic acid, a compound that is easily detected using laser/desorption ionization at 266 nm and serves as an ideal matrix for the detection of amino acids, which typically have low absorption cross sections at 266 nm [*Silva and Prather*, 2000; *Srivastava et al.*, 2005]. Consistent with previous measurements of spores using laser/desorption ionization at 266 nm, spores detected during CalNex contained $^{39}K^+$, $^{59}(CH_3)_3N^+$, $^{74}(CH_3)_4N^+$, *m/z* +86 due to either $(C_2H_5)_2NCH_2^+$ or the amino acids [leucine-HCO_2] and [isoleucine–HCO_2], *m/z* +104, which is yet to be identified, phosphate ($^{63}PO_2^-$, $^{79}PO_3^-$), organic nitrogen ($^{26}CN^-$, $^{42}CNO^-$

), and *m/z* -123, which is most likely due to dipicolinic acid-HCO_2 [*Srivastava et al.*, 2005] (see Figure 5.5c for representative mass spectrum). Spores have rarely been detected by ATOFMS in ambient environments and represent a very unique particle type most likely detected due to agricultural emissions from the Sacramento area.

5.4.3 Variations in the Mixing-State of Carbonaceous Particle Types

5.4.3.1 Soot Particle Mixing-State

In addition to probing overall trends in particle chemistry, observed differences in the mixing-state of soot-dominated particles as a function of time and latitude were also investigated as shown in Figure 5.7a. Soot particles are characterized by intense elemental carbon ion peaks ($^{12}C^+$, $^{36}C_3^+$, $^{48}C_4^+$,…C_n^+). Notably, most of the soot particles were typically mixed with low intensity organic peaks ($^{27}C_2H_3^+$, $^{43}C_2H_3O^+$, etc.), herein referred to as soot/OC particles [*Spencer and Prather*, 2006]. The mixing-state of soot/OC particles was found to vary based on the influence of port and/or agricultural emissions. Overall, the majority of soot/OC particles (~62% of soot particles on average) lacked negative ion spectra (see Figures 5.5d and 5.7a), with sizes peaking in number at ~0.5-0.6 μm and extending up into the supermicron size range (Figure 5.4). The lack of negative ion spectra and larger sizes suggests that these particles contained appreciable particulate water even at 55% RH and most likely had undergone cloud or fog processing [*Moffet et al.*, 2008b; *Neubauer et al.*, 1997; *Neubauer et al.*, 1998].

The most striking trend shown in Figure 5.7a is the high percentage of soot/OC (sulfate) particles detected in Southern California (representing up to ~60% of detected submicron soot particles for time periods 1-4) that decreased significantly as the ship

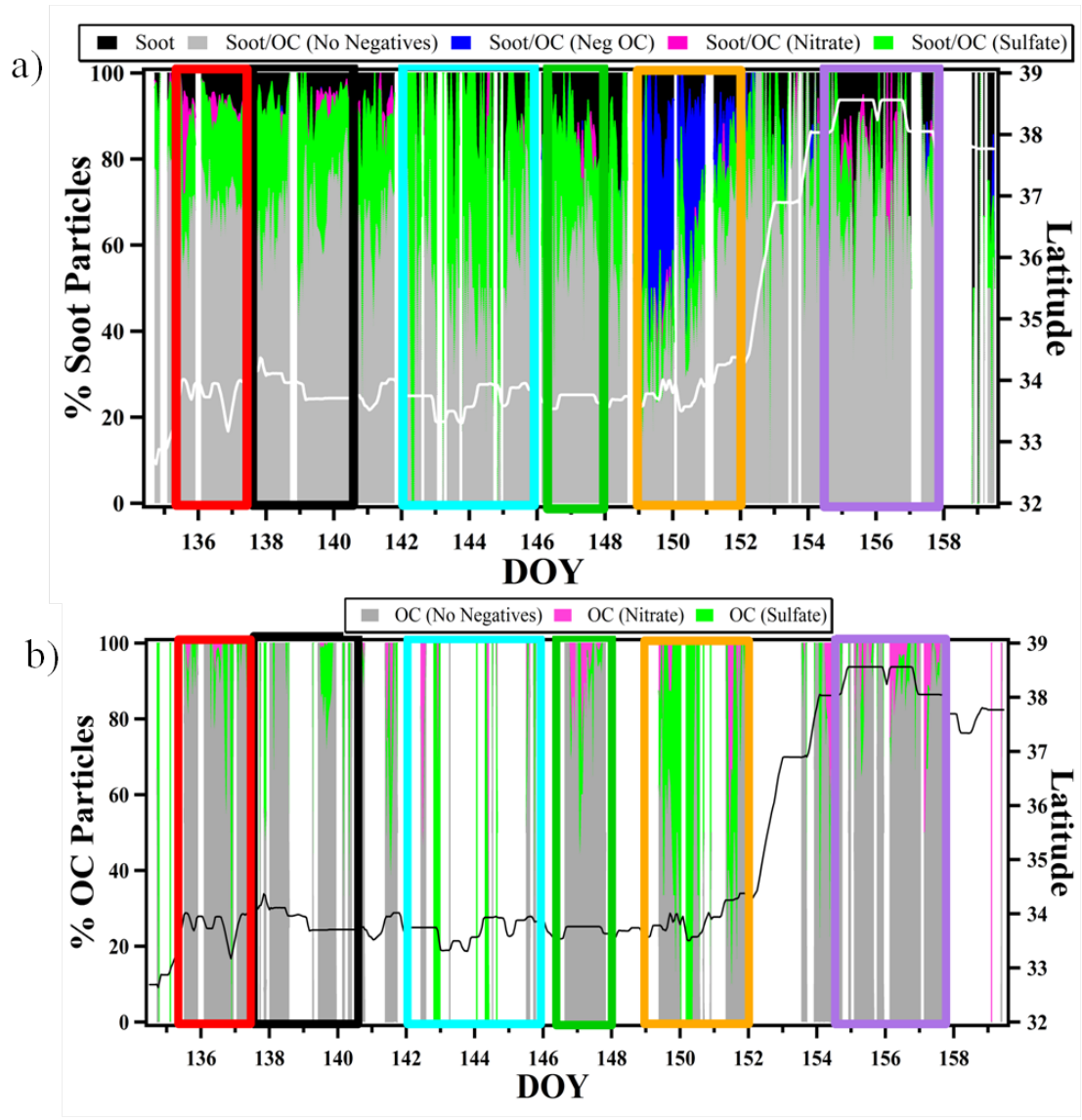

Figure 5.7: Hourly temporal trends in carbonaceous mixing-state. The top panel (a) shows hourly temporal trends for different soot particle types: Soot (black), Soot/OC (No Negatives) (grey), Soot/OC (Sulfate) (green), Soot/OC (Nitrate) (pink), and Soot/OC (Neg OC) (blue) as a function of latitude (white line). The bottom panel (b) shows hourly temporal trends for different organic particle types: OC (No Negatives) (grey), OC (Sulfate) (green), and OC (Nitrate) (pink) as a function of latitude (black line). The 6 different time periods are boxed.

moved north along the California coast. Soot/OC (sulfate) particles are characterized by intense sulfate peaks ($^{80}SO_3^-$, $^{97}HSO_4^-$) (see Figure 5.5e) and are typically considered to represent relatively fresh combustion emissions [*Moffet and Prather*, 2009]. However, during CalNex, soot/OC (sulfate) particles were typically found to peak at larger sizes than expected, ~0.55 μm on average, indicating that this particle type likely underwent aqueous phase processing as well. The highest percentage of soot/OC (sulfate) particles were observed during Periods 2-4 likely due to the prevalence of shipping and diesel truck emissions at the ports, which contain high levels of $SO_{2(g)}$ [*Agrawal et al.*, 2008; *Ault et al.*, 2010; *Corbett and Fischbeck*, 1997; *Corbett and Koehler*, 2003], and aqueous phase processing of soot particles leading to the formation of high amounts of particulate sulfate. Another potential source of elevated sulfate on soot particles, particularly during Marine Transport conditions (Period 3), is the presence of red tide blooms of *L. polyedrum*, a marine organism that has been shown to contribute biogenic sulfate to aerosols [*Gaston et al.*, 2010], in Southern Californian waters during CalNex (www.sccoos.org).

In addition to influence from port emissions, agricultural emissions were also found to impact soot mixing-state during Periods 1, 5, and 6. During periods of agricultural influence, soot/OC (nitrate) particles were also observed; these particles had similar positive ion markers to the soot/OC (sulfate) particles, but contain intense nitrate peaks ($^{46}NO_2^-$, $^{62}NO_3^-$) rather than sulfate (see Figure 5.5f). These particles are considered highly aged [*Moffet and Prather*, 2009] as confirmed by the fact that this particle type peaked at ~0.75 μm during the campaign and was found to extend into the

supermicron size mode (Figure 5.4); this particle type represented up to ~33% of soot particles.

In addition to soot/OC (nitrate) particles, unique soot/OC particles containing sulfate and intense ions at *m/z* -43, -57, and -71 (see Figure 5.5g) were detected during a period of agricultural influence (Central Valley Transport conditions) and have never been detected before by ATOFMS. Since organic peaks in soot/OC particles typically appear as positive ions, this particle type has been labeled Soot/OC (Neg OC). At this juncture, we speculate that this particle type represents a soot particle core heavily coated with secondary organic aerosol (SOA). Evidence for this speculation comes from the fact that this particle type peaks at a small size (~0.35 μm), as shown in Figure 5.4e, which could be due to the collapse of the soot particle core that can occur in the presence of heavy organic coatings [*Spencer and Prather*, 2006]. The unique organic markers likely correspond to $^{43}CH_3CO^-$, $^{57}C_2O_2H^-$, and $^{71}C_3H_3O_2^-$ [*McLafferty and Turecek*, 1993; *Silva et al.*, 1999; *Silva and Prather*, 2000] possibly due to contributions from levoglucason and/or methylglyoxal (*m/z* -71), glyoxal (*m/z* -57), and acetaldehyde (*m/z* -43) [*Silva et al.*, 1999; *Silva and Prather*, 2000]; however, additional field and laboratory measurements are required to confirm the identification of these ion peaks.

5.4.3.2 The Mixing-State of Organics

In addition to the mixing state of soot-containing particles, the mixing-state of OC particles was also investigated by examining their trends. These particles are distinguished from the soot/OC types described above in that these particles are not characterized by intense elemental carbon peaks characteristic of soot particles. Three

types of OC particles were identified during CalNex: OC (no negatives), OC (sulfate), and OC (nitrate). Temporal trends of the OC particle types are shown in Figure 5.7b. Most OC particles were found to lack negative ion spectra (~68% on average) (see Figure 5.5h) and peaked in the 0.5-0.6 μm size range, as shown in Figure 5.4, suggesting that these particles had undergone aqueous phase processing similar to soot particles. However, during Marine and Central Valley Transport conditions (Periods 3 and 5), OC particles containing intense sulfate peaks (see Figure 5.5i) were more common, representing ~58% of organic particles, likely due to photo-chemically produced sulfate. In addition to sulfate, OC particles with intense nitrate peaks (see Figure 5.5j) were also observed during Periods 3 and 5, representing ~15% of organic particles on average. Of note, OC (nitrate) particles peaked at a small particle size (~0.35 μm) and were found to peak at night rather than during the day; this is unexpected if OC (nitrate) particles are formed due to the condensation of photochemically-produced nitrate. Instead, these observations suggest possible contributions of organonitrates formed from reactions with nitrate radical at night [*Ng et al.*, 2008].

In addition to the OC types described above, OC particles detected during CalNex also frequently contained aromatic peaks ($^{51}C_4H_3^+$, $^{63}C_5H_3^+$, $^{77}C_6H_5^+$, etc) [*Silva and Prather*, 2000], which have been associated with vehicle exhaust [*Shields et al.*, 2007; *Sodeman et al.*, 2005; *Spencer et al.*, 2006; *Toner et al.*, 2008] and humic substances formed from biomass burning [*Holecek et al.*, 2007; *Mayol-Bracero et al.*, 2002; *Qin and Prather*, 2006]. Further, OC particles also contained ion peaks indicative of amines (e.g. $^{59}(CH_3)_3N^+$, $^{86}(C_2H_5)_2NCH_2^+$, $^{101}(C_2H_5)_3N^+$, $^{118}(C_2H_5)_3NOH^+$, etc.), which are semi-

volatile species that can partition onto pre-existing particles [*Angelino et al.*, 2001; *Pratt et al.*, 2009; *Schade and Crutzen*, 1995], and oxygenated organic markers (e.g. $^{43}C_2H_3O^+$) that indicate the presence of SOA [*Qin et al.*, 2012] (see Figure 5.5h). Ternary plots were used to examine the prevalence of these compounds on OC particles to further elucidate the mixing-state and sources of OC particles using the ion peaks $^{59}(CH_3)_3N^+$, $^{43}C_2H_3O^+$, and $^{77}C_6H_5^+$ as markers for amines, SOA/oxygenated organics, and aromatics, respectively (see Figure 5.8).

Amines were found to dominate the OC mixing-state during the first two periods with up to ~65% of OC particles containing amine markers, as shown in Figure 5.8. Dairy farm emissions from the Chino area in Southern California, in addition to favorable meteorological conditions (e.g. low temperatures and high RH), explain the dominance of amines during these two time periods [*Hughes et al.*, 2002; *Pastor et al.*, 2003; *Pratt et al.*, 2009; *Qin et al.*, 2012; *Schade and Crutzen*, 1995; *Sorooshian et al.*, 2008]. Further, up ~18% of organic carbon particles contained amines at the Ports of LA/LB during Period 4 even though inland transport conditions were not encountered suggesting that ports could contribute an industrial source of amines.

Interestingly, amines were not dominant during Central Valley Transport conditions (Period 5), as would be expected. Instead, oxygenated organics were dominant (see Figure 5.8e) likely due to contributions of photochemical-produced SOA. The high ozone concentrations measured during Period 5 supports the assignment of organics during Period 5 as being from secondary rather than primary sources [*Na et al.*, 2004; *Qin et al.*, 2012]. Oxygenated organics were also dominant during Marine

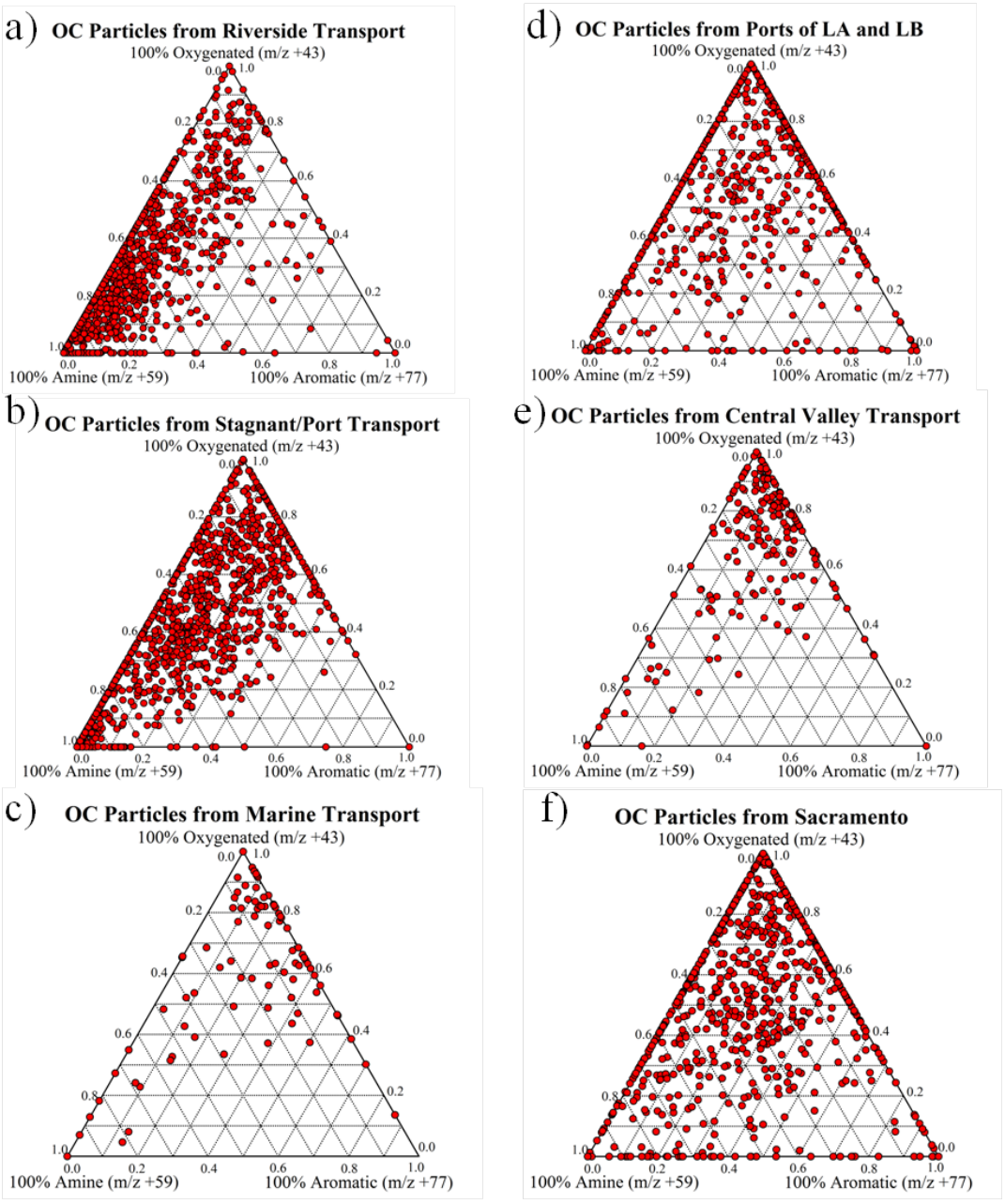

Figure 5.8: Ternary plots for individual OC particles observed for the 6 different time periods. The top corner of the ternary plots corresponds to OC particles containing only an oxygenated organic peak ($^{43}C_2H_3O^+$), the left bottom corner denotes OC particles containing only the amine peak ($^{59}(CH_3)_3N^+$), and the right bottom corner corresponds to OC particles containing only an aromatic peak ($^{77}C_6H_5^+$).

Transport conditions (Period 3), likely due to secondary contributions. However, another possibility for the detection of oxygenated organics during Period 3 is the presence of organics from marine biogenic sources, such as lipopolysaccharides, that contribute organics with a higher oxygen content than organics from anthropogenic sources [*Facchini et al.*, 2008; *Ovadnevaite et al.*, 2011; *Russell et al.*, 2011; *Russell et al.*, 2010].

Aromatics were more prevalent during periods 4 and 6 than any other periods. The increased frequency of aromatics in the Ports of LA and LB is likely due to increased emissions from diesel combustion by trucks [*Kasper et al.*, 2007; *Maricq*, 2007; *Shields et al.*, 2007; *Spencer et al.*, 2006] in addition to emissions from ships, which also contribute aromatics and high mass concentrations of organic aerosol [*Kasper et al.*, 2007; *Lack et al.*, 2009; *Murphy et al.*, 2009; *Russell et al.*, 2009]. Oxygenated organics and amines in Sacramento are likely from agricultural emissions [*Chow et al.*, 2006b; *Sorooshian et al.*, 2008] while the observed aromatics are likely humic substances derived from biomass burning [*Holecek et al.*, 2007; *Mayol-Bracero et al.*, 2002].

5.4.4 Contributions of Secondary Species

In addition to probing the secondary mixing-state of carbonaceous particle types, the prevalence of the secondary species ammonium, nitrate, and sulfate was examined for all particle types. Figure 5.9 shows a temporal of the average absolute peak area of sulfate ($^{97}HSO_4^-$), ammonium ($^{18}NH_4^+$), and nitrate ($^{46}NO_2^-$, $^{62}NO_3^-$, $^{30}NO^+/CH_3NH^+$) for submicron and supermicron particles as a function of latitude. The absolute peak area for a particular *m/z* can be related to the relative amount of the corresponding chemical species present on the particles [*Bhave et al.*, 2002; *Gross et al.*, 2000]. For submicron

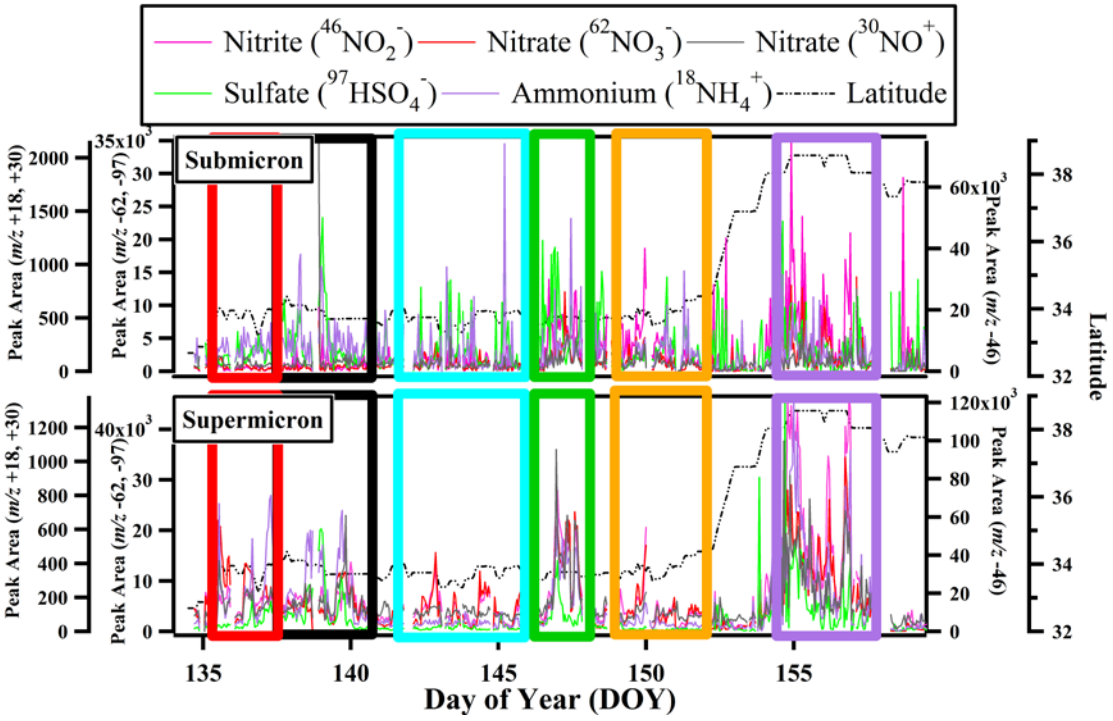

Figure 5.9: Hourly-averaged absolute ion peak areas for nitrate (red, pink, and grey lines), sulfate (green line), and ammonium (purple line) as a function of DOY and latitude (black line). The top panel shows ion peak areas for submicron particles while the bottom panel shows ion peak areas for supermicron particles.

particles, sulfate peak area was larger than nitrate until the ship began to head north, between periods 4 and 5. In Northern California, nitrate peak area, namely $^{46}NO_2^-$, was more intense than sulfate on submicron particles. The elevated submicron sulfate during Periods 1-4 was mainly internally mixed with soot/OC particles and is most likely due to elevated $SO_{2(g)}$ emissions from the Ports of LA and LB. Most submicron nitrate observed during Periods 5 and 6 was associated with submicron biomass burning, sea salt, and dust particles, which can acquire nitrate through heterogeneous reactions with nitric acid ($HNO_{3(g)}$) [*Krueger et al.*, 2003; *Shi et al.*, 2008; *Sullivan et al.*, 2007]. Ammonium was typically correlated with sulfate on submicron particles due to the condensation of ammonium sulfate and/or the titration of sulfate by ammonium.

In contrast, nitrate peaks were more intense than sulfate for supermicron particles due to contributions of dust and sea salt particles that had been heterogeneously reacted. Ammonium was typically associated with reacted dust particles due to the titration of heterogeneously acquired nitrate and sulfate on these particles [*Sullivan et al.*, 2007]. Interestingly, supermicron ammonium and the nitrate marker $^{30}NO^+/CH_3NH^+$ were found to be correlated namely during periods influenced by agricultural emissions from the Riverside and Central Valley regions. The correlation between ammonium and *m/z* +30, in particular, for supermicron particles is most likely due to the condensation of ammonium nitrate [*Hughes et al.*, 2002; *Liu et al.*, 2000; *Qin et al.*, 2012], which has been found to be a dominate contributor to the Riverside and Central Valley aerosol due to high concentrations of gas phase precursors from dairy farms [*Appel et al.*, 1978; *Chen et al.*, 2007; *Chow et al.*, 2006a; *Hughes et al.*, 2002; *Magliano et al.*, 1999; *Pratt and*

Prather, 2009; *Qin et al.*, 2012]. Further, the observed lower temperature and high RH observed during Periods 1 and 2 and at night during Period 6 also favor partitioning of ammonium nitrate to the particle phase during these time periods [*Appel et al.*, 1978; *Stelson and Seinfeld*, 1982].

5.5 Conclusions and Implications for California

The observed differences in mixing state observed along the Southern California coast and in Northern California during different transport conditions have significant implications for differences in regional air pollution as well as regional differences in aerosol climate forcing. Particle mixing-state was found to vary based on the influence of port, agricultural, and background emissions from the ocean. Soot particles were the most prevalent submicron particle type in Southern California; the mixing-state of soot particles detected in Southern California were impacted by shipping and vehicles emissions from the Ports of LA and LB, which contributed sulfate to soot particles. In Northern California and during periods influenced by agricultural emissions, nitrate and unique organic compounds contributed to the mixing-state of soot particles. The observed differences in soot mixing-state could significantly impact the absorbing and cloud nucleating properties of soot particles, particularly as soot particles are aged and accumulate soluble material or are oxidized to water soluble material [*Decesari et al.*, 2002; *Jacobson*, 2000; *Lammel and Novakov*, 1995; *Moffet and Prather*, 2009; *Schnaiter et al.*, 2005].

In contrast, organic carbon was the dominant submicron particle type in Northern California, due to NPF events. The mixing-state of organics was also found to vary

during different transport and meteorological conditions. Oxygenated organic compounds were frequently associated with particles during marine and Central Valley transport conditions, likely due contributions from SOA and, possibly, marine biogenics. Aromatics were found to contribute to organics due to distillate and gasoline combustion when port and vehicular emissions were dominant and in Sacramento likely due to contributions from biomass burning. In addition to exhibiting strong absorbing properties for UV wavelengths [*Hoffer et al.*, 2006; *Sun et al.*, 2007], aromatics also contribute to adverse health effects highlighting their atmospheric significance [*Bernstein et al.*, 2004]. Amines were also frequently observed when air masses were transported from Riverside likely due to the impact of dairy farm emissions and favorable meteorological conditions. The presence of amines is significant as they have been shown to contribute to aerosol hygroscopicity and cloud droplet formation, particularly through the formation of aminium salts [*Sorooshian et al.*, 2008]. Overall, we found that chemical properties of aerosol particles differ widely across California based on particle source and transport conditions. The observed differences in the particle types, soot and OC mixing-state, and aging processes due to differences in meteorological conditions will most likely result in regional differences in the health, optical, and cloud nucleating properties for the aerosol populations observed across California. This should be taken into account when determining which emissions sources to regulate in order to mitigate the adverse effects of aerosols on both human health and climate change.

5.6 Acknowledgements

The authors would like to thank Derek Coffman, Drew Hamilton, and the entire crew of the R/V Atlantis for assistance during the CalNex field campaign. Prof. Chris Cappa is acknowledged for assistance with filtering out ship exhaust time periods. Prof. Dan Cziczo is acknowledged for assistance prior to the CalNex campaign. We gratefully acknowledge the NOAA Air Resources Laboratory for the provision of the HYSPLIT transport model and READY website (http://ready.arl.noaa.gov/HYSPLIT.php) used in this publication. The authors also gratefully acknowledge the Southern California Coastal Ocean Observing System (SCCOOS) (www.sccoos.org/) for the provision of harmful algal bloom data used in this publication. The entire Prather group is acknowledged for helpful comments and discussion. C.J.G. was funded through the Aerosol Chemistry and Climate Institute at Pacific Northwest National Laboratory. This work was funded by the California Air Resources Board (CARB).

Chapter 5 is in preparation for submission to *Journal of Geophysical Research*: Gaston, C.J., Quinn, P.K., Bates, T.S., Prather, K.A. The impact of shipping, agriculatural, and urban emissions on single particle chemistry observed aboard the R/V Atlantis during CalNex. The dissertation author was the primary investigator and author of this paper.

5.7 References

Agrawal, H., Q.G.J. Malloy, W.A. Welch, J.W. Miller, and D.R. Cocker (2008), In-use gaseous and particulate matter emissions from a modern ocean going container vessel, *Atmos. Environ., 42* (21), 5504-5510.

Albrecht, B.A. (1989), Aerosols, cloud microphysics, and fractional cloudiness, *Science*, *245* (4923), 1227-1230.

Allen, J.O. (2002), YAADA software toolkit to analyze single-particle mass spectral data: Reference manual version 1.1, *Arizona State University*, http://www.yaada.org.

Angelino, S., D.T. Suess, and K.A. Prather (2001), Formation of aerosol particles from reactions of secondary and tertiary alkylamines: Characterization by aerosol time-of-flight mass spectrometry, *Environ. Sci. Tech., 35* (15), 3130-3138.

Appel, B.R., E.L. Kothny, E.R. Hoffer, G.M. Hidy, and J.J. Wesolowski (1978), Sulfate and nitrate data from the California Aerosol Characterization Experiment (ACHEX), *Environ. Sci. Tech., 12*, 418-425.

Ault, A.P., C.J. Gaston, Y. Wang, G. Dominguez, M.H. Thiemens, and K.A. Prather (2010), Characterization of the single particle mixing state of individual ship plume events measured at the Port of Los Angeles, *Environ. Sci. Tech., 44* (6), 1954-1961.

Ault, A.P., M.J. Moore, H. Furutani, and K.A. Prather (2009), Impact of emissions from the Los Angeles port region on San Diego air quality during regional transport events, *Environ. Sci. Tech., 43* (10), 3500-3506.

Authorities, A.A.o.P., North American Port Container Traffic, American Association of Port Authorities, 2006.

Bates, T.S., P.K. Quinn, D.J. Coffman, D.S. Covert, T.L. Miller, J.E. Johnson, G.R. Carmichael, I. Uno, S.A. Guazzotti, D.A. Sodeman, K.A. Prather, M. Rivera, L.M. Russell, and J.T. Merrill (2004), Marine boundary layer dust and pollutant transport associated with the passage of a frontal system over eastern Asia, *J. Geophys. Res.-[Atmos.], 109* (D19S19), doi:10.1029/2003JD004094.

Behnke, W., H.U. Kruger, V. Scheer, and C. Zetzsch (1991), Formation of Atomic Cl from Sea Spray Via Photolysis of Nitryl Chloride - Determination of the Sticking Coefficient of N_2O_5 on NaCl Aerosol, *J. Aerosol Sci., 22*, S609-S612.

Bernstein, J.A., N. Alexis, C. Barnes, I.L. Bernstein, J.A. Bernstein, A. Nel, D. Peden, D. Diaz-Sanchez, S.M. Tarlo, and P.B. Williams (2004), Health effects of air pollution, *Journal of Allergy and Clinical Immunology*, *114* (5), 1116-1123.

Bhave, P.V., J.O. Allen, B.D. Morrical, D.P. Fergenson, G.R. Cass, and K.A. Prather (2002), A field-based approach for determining ATOFMS instrument sensitivities to ammonium and nitrate, *Environ. Sci. Tech.*, *36* (22), 4868-4879.

Blanchard, D.C., and A.H. Woodcock (1957), Bubble formation and modification in the sea and its meteorological significance, *Tellus*, *9* (2), 145-158.

CARB, Final Regulation Order. Fuel Sulfur and Other Operational Requirments for Ocean-Going Vessels Within California Waters and 24 Nautical Miles of the California Baseline, California Air Resources Board: Sacramento, CA, 2009.

Chang, W.L., P.V. Bhave, S.S. Brown, N. Riemer, J. Stutz, and D. Dabdub (2011), Heterogeneous atmospheric chemistry, ambient measurements, and model calculations of N_2O_5: A review, *Aerosol Sci. Tech.*, *45* (6), 665-695.

Chen, L.W.A., J.G. Watson, J.C. Chow, and K.L. Magliano (2007), Quantifying $PM_{2.5}$ source contributions for the San Joaquin Valley with multivariate receptor models, *Environ. Sci. Tech.*, *41* (8), 2818-2826.

Chow, J.C., L.W.A. Chen, J.G. Watson, D.H. Lowenthal, K.A. Magliano, K. Turkiewicz, and D.E. Lehrman (2006a), $PM_{2.5}$ chemical composition and spatiotemporal variability during the California Regional PM_{10}/$PM_{2.5}$ Air Quality Study (CRPAQS), *J. Geophys. Res.-[Atmos.]*, *111* (D10), D10S04, doi:10.1029/2005JD006457.

Chow, J.C., J.G. Watson, D.H. Lowenthal, L.W.A. Chen, and K.L. Magliano (2006b), Particulate carbon measurements in California's San Joaquin Valley, *Chemosphere*, *62* (3), 337-348.

Corbett, J.J., and P. Fischbeck (1997), Emissions from ships, *Science*, *278* (5339), 823-824.

Corbett, J.J., and H.W. Koehler (2003), Updated emissions from ocean shipping, *J. Geophys. Res.-[Atmos.]*, *108* (D20), 4650, doi:10.1029/2003JD003751.

Creamean, J.M., A.P. Ault, J.E. Ten Hoeve, M.Z. Jacobson, G.C. Roberts, and K.A. Prather (2011), Measurements of aerosol chemistry during new particle formation events at a remote rural mountain site, *Environ. Sci. Tech.*, *45* (19), 8208-8216.

Decesari, S., M.C. Facchini, E. Matta, M. Mircea, S. Fuzzi, A.R. Chughtai, and D.M. Smith (2002), Water soluble organic compounds formed by oxidation of soot, *Atmos. Environ., 36* (11), 1827-1832.

Docherty, K.S., E.A. Stone, I.M. Ulbrich, P.F. DeCarlo, D.C. Snyder, J.J. Schauer, R.E. Peltier, R.J. Weber, S.M. Murphy, J.H. Seinfeld, B.D. Grover, D.J. Eatough, and J.L. Jimenez (2008), Apportionment of primary and secondary organic aerosols in Southern California during the 2005 Study of Organic Aerosols in Riverside (SOAR-1), *Environ. Sci. Tech., 42* (20), 7655-7662.

Draxler, R.R., and G.D. Rolph (2011), HYSPLIT (HYbrid Single-Particle Lagrangian Integrated Trajectory) Model access via NOAA ARL READY Website (http://ready.arl.noaa.gov/HYSPLIT.php), *NOAA Air Resources Laboratory*, Silver Spring, MD.

Facchini, M.C., M. Rinaldi, S. Decesari, C. Carbone, E. Finessi, M. Mircea, S. Fuzzi, D. Ceburnis, R. Flanagan, E.D. Nilsson, G. de Leeuw, M. Martino, J. Woeltjen, and C.D. O'Dowd (2008), Primary submicron marine aerosol dominated by insoluble organic colloids and aggregates, *Geophys. Res. Lett., 35*, L17814, doi:10.1029/2008GL034210.

Fang, S.C., E.A. Eisen, J.M. Cavallari, M.A. Mittleman, and D.C. Christiani (2008), Acute changes in vascular function among welders exposed to metal-rich particulate matter, *Epidemiology*, *19* (2), 217-225.

Fitzgerald, J.W. (1991), Marine aerosols: A review, *Atmos. Environ. A-Gen. Topics*, *25* (3-4), 533-545.

Gard, E., J.E. Mayer, B.D. Morrical, T. Dienes, D.P. Fergenson, and K.A. Prather (1997), Real-time analysis of individual atmospheric aerosol particles: Design and performance of a portable ATOFMS, *Anal. Chem., 69* (20), 4083-4091.

Gard, E.E., M.J. Kleeman, D.S. Gross, L.S. Hughes, J.O. Allen, B.D. Morrical, D.P. Fergenson, T. Dienes, M.E. Galli, R.J. Johnson, G.R. Cass, and K.A. Prather (1998), Direct observation of heterogeneous chemistry in the atmosphere, *Science*, *279* (5354), 1184-1187.

Gaston, C.J., H. Furutani, S.A. Guazzotti, K.R. Coffee, T.S. Bates, P.K. Quinn, L.I. Aluwihare, B.G. Mitchell, and K.A. Prather (2011), Unique ocean-derived particles serve as a proxy for changes in ocean chemistry, *J. Geophys. Res.-[Atmos.]*, *116*, D18310, doi:10.1029/2010JD015289.

Gaston, C.J., K.A. Pratt, X.Y. Qin, and K.A. Prather (2010), Real-time detection and mixing state of methanesulfonate in single particles at an inland urban location during a phytoplankton bloom, *Environ. Sci. Tech., 44* (5), 1566-1572.

Gauderman, W.J., R. McConnell, F. Gilliland, S. London, D. Thomas, E. Avol, H. Vora, K. Berhane, E.B. Rappaport, F. Lurmann, H.G. Margolis, and J. Peters (2000), Association between air pollution and lung function growth in southern California children, *American Journal of Respiratory and Critical Care Medicine*, *162* (4), 1383-1390.

Gross, D.S., M.E. Galli, P.J. Silva, and K.A. Prather (2000), Relative sensitivity factors for alkali metal and ammonium cations in single particle aerosol time-of-flight mass spectra, *Anal. Chem.*, *72* (2), 416-422.

Grover, B.D., N.L. Eatough, W.R. Woolwine, J.P. Cannon, D.J. Eatough, and R.W. Long (2008), Semi-continuous mass closure of the major components of fine particulate matter in Riverside, CA, *Atmos. Environ.*, *42*, 250-260.

Guazzotti, S.A., K.R. Coffee, and K.A. Prather (2001), Continuous measurements of size-resolved particle chemistry during INDOEX-Intensive Field Phase 99, *J. Geophys. Res.-[Atmos.]*, *106* (D22), 28607-28627.

Hawkins, L.N., L.M. Russell, D.S. Covert, P.K. Quinn, and T.S. Bates (2010), Carboxylic acids, sulfates, and organosulfates in processed continental organic aerosol over the southeast Pacific Ocean during VOCALS-REx 2008, *J. Geophys. Res.-[Atmos.]*, *115*, D13201, doi:10.1029/2009JD013276.

Hays, M.D., P.M. Fine, C.D. Geron, M.J. Kleeman, and B.K. Gullett (2005), Open burning of agricultural biomass: Physical and chemical properties of particle-phase emissions, *Atmos. Environ.*, *39* (36), 6747-6764.

Healy, R.M., I.P. O'Connor, S. Hellebust, A. Allanic, J.R. Sodeau, and J.C. Wenger (2009), Characterization of single particles from in-port ship emissions, *Atmos Environ*, *43*, 6408-6414.

Hegg, D.A., and M.B. Baker (2009), Nucleation in the atmosphere, *Reports on Progress in Physics*, *72* (5), doi:10.1088/0034-4885/72/5/056801.

Hoffer, A., A. Gelencser, P. Guyon, G. Kiss, O. Schmid, G.P. Frank, P. Artaxo, and M.O. Andreae (2006), Optical properties of humic-like substances (HULIS) in biomass-burning aerosols, *Atmos. Chem. Phys.*, *6*, 3563-3570.

Holecek, J.C., M.T. Spencer, and K.A. Prather (2007), Analysis of rainwater samples: Comparison of single particle residues with ambient particle chemistry from the northeast Pacific and Indian oceans, *J. Geophys. Res.-[Atmos.]*, *112* (D22), doi:10.1029/2006JD008269.

Hughes, L.S., J.O. Allen, P. Bhave, M.J. Kleeman, G.R. Cass, D.Y. Liu, D.F. Fergenson, B.D. Morrical, and K.A. Prather (2000), Evolution of atmospheric particles along

trajectories crossing the Los Angeles basin, *Environ. Sci. Tech.*, *34* (15), 3058-3068.

Hughes, L.S., J.O. Allen, L.G. Salmon, P.R. Mayo, R.J. Johnson, and G.R. Cass (2002), Evolution of nitrogen species air pollutants along trajectories crossing the Los Angeles area, *Environ. Sci. Tech.*, *36* (18), 3928-3935.

IPCC, Climate Change 2007: The Physical Science Basis. Contribution of Working Group I to the Fourth Assessment Report of the Intergovernmental Panel on Climate Change, Cambridge University Press, Cambridge, United Kingdom and New York, NY, USA, 2007.

Jacobson, M.Z. (2000), A physically-based treatment of elemental carbon optics: Implications for global direct forcing of aerosols, *Geophys. Res. Lett.*, *27* (2), 217-220.

Kasper, A., S. Aufdenblatten, A. Forss, M. Mohr, and H. Burtscher (2007), Particulate emissions from a low-speed marine diesel engine, *Aerosol Sci. Tech.*, *41* (1), 24-32.

Krueger, B.J., V.H. Grassian, A. Laskin, and J.P. Cowin (2003), The transformation of solid atmospheric particles into liquid droplets through heterogeneous chemistry: Laboratory insights into the processing of calcium containing mineral dust aerosol in the troposphere, *Geophys. Res. Lett.*, *30* (3), 1148,doi:10.1029/2002GL016563.

Kulmala, M. (2003), How particles nucleate and grow, *Science*, *302* (5647), 1000-1001.

Lack, D.A., J.J. Corbett, T. Onasch, B. Lerner, P. Massoli, P.K. Quinn, T.S. Bates, D.S. Covert, D. Coffman, B. Sierau, S. Herndon, J. Allan, T. Baynard, E. Lovejoy, A.R. Ravishankara, and E. Williams (2009), Particulate emissions from commercial shipping: Chemical, physical, and optical properties, *J. Geophys. Res.-[Atmos.]*, *114*, D00F04, doi:10.1029/2008JD011300.

Lammel, G., and T. Novakov (1995), Water Nucleation Properties of Carbon-Black and Diesel Soot Particles, *Atmos. Environ.*, *29* (7), 813-823.

Liu, D.-Y., K.A. Prather, and S.V. Herring (2000), Variations in the size and chemical composition of nitrate-containing particles in Riverside, CA, *Aerosol Sci. Tech.*, *33* (1-2), 71-86.

Lohmann, U., and J. Feichter (2005), Global indirect aerosol effects: A review, *Atmos. Chem. Phys.*, *5*, 715-737.

Magliano, K.L., V.M. Hughes, L.R. Chinkin, D.L. Coe, T.L. Haste, N. Kumar, and F.W. Lurmann (1999), Spatial and temporal variations in PM10 and PM2.5 source

contributions and comparison to emissions during the 1995 integrated monitoring study, *Atmos. Environ., 33* (29), 4757-4773.

Maricq, M.M. (2007), Chemical characterization of particulate emissions from diesel engines: A review, *J. Aerosol Sci., 38* (11), 1079-1118.

Mayol-Bracero, O.L., P. Guyon, B. Graham, G. Roberts, M.O. Andreae, S. Decesari, M.C. Facchini, S. Fuzzi, and P. Artaxo (2002), Water-soluble organic compounds in biomass burning aerosols over Amazonia - 2. Apportionment of the chemical composition and importance of the polyacidic fraction, *J. Geophys. Res.-[Atmos.], 107* (D20), 8091, doi:10.1029/2001JD000522.

McFiggans, G., P. Artaxo, U. Baltensperger, H. Coe, M.C. Facchini, G. Feingold, S. Fuzzi, M. Gysel, A. Laaksonen, U. Lohmann, T.F. Mentel, D.M. Murphy, C.D. O'Dowd, J.R. Snider, and E. Weingartner (2006), The effect of physical and chemical aerosol properties on warm cloud droplet activation, *Atmos. Chem. Phys., 6*, 2593-2649.

McLafferty, F.W., and F. Turecek, *Interpretation of Mass Spetra*, University Science Books, Sausalito, CA, 1993.

Moffet, R.C., Y. Desyaterik, R.J. Hopkins, A.V. Tivanski, M.K. Gilles, Y. Wang, V. Shutthanandan, L.T. Molina, R.G. Abraham, K.S. Johnson, V. Mugica, M.J. Molina, A. Laskin, and K.A. Prather (2008a), Characterization of aerosols containing Zn, Pb, and Cl from an industrial region of Mexico City, *Environ. Sci. Tech., 42* (19), 7091-7097.

Moffet, R.C., and K.A. Prather (2009), In-situ measurements of the mixing state and optical properties of soot with implications for radiative forcing estimates, *PNAS, 106* (29), 11872-11877.

Moffet, R.C., X. Qin, T. Rebotier, H. Furutani, and K.A. Prather (2008b), Chemically segregated optical and microphysical properties of ambient aerosols measured in a single-particle mass spectrometer, *J. Geophys. Res., 113* (D12213), D12213, doi:10.1029/2007JD009393.

Monahan, E.C., C.W. Fairall, K.L. Davidson, and P.J. Boyle (1983), Observed interrelations between 10m winds, ocean whitecaps and marine aerosols, *Quarterly Journal of the Royal Meteorological Society, 109* (460), 379-392.

Murphy, S.M.A., H.; Sorooshian, A.; Padro, L. T.; Gates, S.W. H.; Hersey, W. A.; Jung, H.; Miller, J. W.; Cocker, D. R., and A.J. Nenes, H. H.; Flagan, R. C.; Seinfeld, J. H. (2009), Comprehensive simultaneous shipboard and airborne characterization of exhaust from a modern container ship at sea., *Environ. Sci. Tech., 43* (13), 4626-4640.

Na, K., A.A. Sawant, C. Song, and D.R. Cocker (2004), Primary and secondary carbonaceous species in the atmosphere of Western Riverside County, California, *Atmos Environ, 38*, 1345-1355.

Neubauer, K.R., M.V. Johnston, and A.S. Wexler (1997), On-line analysis of aqueous aerosols by laser desorption ionization, *International Journal of Mass Spectrometry and Ion Processes*, *163* (1-2), 29-37.

Neubauer, K.R., M.V. Johnston, and A.S. Wexler (1998), Humidity effects on the mass spectra of single aerosol particles, *Atmos. Environ.*, *32* (14-15), 2521-2529.

Ng, N.L., A.J. Kwan, J.D. Surratt, A.W.H. Chan, P.S. Chhabra, A. Sorooshian, H.O.T. Pye, J.D. Crounse, P.O. Wennberg, R.C. Flagan, and J.H. Seinfeld (2008), Secondary organic aerosol (SOA) formation from reaction of isoprene with nitrate radicals (NO_3), *Atmos. Chem. Phys.*, *8* (14), 4117-4140.

Noble, C.A., and K.A. Prather (1996), Real-time measurement of correlated size and composition profiles of individual atmospheric aerosol particles, *Environ. Sci. Tech.*, *30* (9), 2667-2680.

O'Dowd, C.D., and G. De Leeuw (2007), Marine aerosol production: a review of the current knowledge, *Phil. Trans. A*, *365* (1856), 1753-1774.

Ovadnevaite, J., C. O'Dowd, M. Dall'Osto, D. Ceburnis, D.R. Worsnop, and H. Berresheim (2011), Detecting high contributions of primary organic matter to marine aerosol: A case study, *Geophys. Res. Lett.*, *38*, L02807, doi:10.1029/2010GL046083.

Pastor, S.H., J.O. Allen, L.S. Hughes, P. Bhave, G.R. Cass, and K.A. Prather (2003), Ambient single particle analysis in Riverside, California by aerosol time-of-flight mass spectrometry during the SCOS97-NARSTO, *Atmos. Environ.*, *37*, S239-S258.

Pinkerton, K.E., Y.M. Zhou, S.V. Teague, J.L. Peake, R.C. Walther, I.M. Kennedy, V.J. Leppert, and A.E. Aust (2004), Reduced lung cell proliferation following short-term exposure to ultrafine soot and iron particles in neonatal rats: Key to impaired lung growth? *Inhalation Toxicology*, *16*, 73-81.

Pope, C.A., and D.W. Dockery (2006), Health effects of fine particulate air pollution: Lines that connect, *Journal of the Air & Waste Management Association, 56* (6), 709-742.

Poschl, U. (2005), Atmospheric aerosols: Composition, transformation, climate and health effects, *Angewandte Chemie-International Edition*, *44* (46), 7520-7540.

Prather, K.A., T. Nordmeyer, and K. Salt (1994), Real-Time Characterization of Individual Aerosol-Particles Using Time-of-Flight Mass-Spectrometry, *Anal. Chem., 66* (9), 1403-1407.

Pratt, K.A., L.E. Hatch, and K.A. Prather (2009), Seasonal volatility dependence of ambient particle phase amines, *Environ. Sci. Tech., 43* (14), 5276-5281.

Pratt, K.A., A.J. Heymsfield, C.H. Twohy, S.M. Murphy, P.J. DeMott, J.G. Hudson, R. Subramanian, Z.E. Wang, J.H. Seinfeld, and K.A. Prather (2010), In Situ Chemical Characterization of Aged Biomass-Burning Aerosols Impacting Cold Wave Clouds, *J. Atmos. Sci., 67* (8), 2451-2468.

Pratt, K.A., and K.A. Prather (2009), Real-time, single-particle volatility, size, and chemical composition measurements of aged urban aerosols, *Environ. Sci. Tech., 43* (21), 8276-8282.

Pratt, K.A., and K.A. Prather (2011), Mass spectrometry of atmospheric aerosols—Recent developments and applications. Part II: On-line mass spectrometry techniques, *Mass Spectrometry Reviews*, DOI 10.1002/mas.20330.

Qin, X., K.A. Pratt, L.G. Shields, S.M. Toner, and K.A. Prather (2012), Seasonal comparisons of single-particle chemical mixing state in Riverside, CA, *Atmos. Environ., Submitted*.

Qin, X.Y., and K.A. Prather (2006), Impact of biomass emissions on particle chemistry during the California Regional Particulate Air Quality Study, *International Journal of Mass Spectrometry, 258* (1-3), 142-150.

Quinn, P.K., T.S. Bates, T. Baynard, A.D. Clarke, T.B. Onasch, W. Wang, M.J. Rood, E. Andrews, J. Allan, C.M. Carrico, D. Coffman, and D. Worsnop (2005), Impact of particulate organic matter on the relative humidity dependence of light scattering: A simplified parameterization, *Geophys. Res. Lett., 32* (22), L22809, doi:10.1029/2005GL024322.

Quinn, P.K., T.S. Bates, D.J. Coffman, and D.S. Covert (2008), Influence of particle size and chemistry on the cloud nucleating properties of aerosols, *Atmos. Chem. Phys., 8* (4), 1029-1042.

Roberts, G.C., P. Artaxo, J.C. Zhou, E. Swietlicki, and M.O. Andreae (2002), Sensitivity of CCN spectra on chemical and physical properties of aerosol: A case study from the Amazon Basin, *J. Geophys. Res.-[Atmos.], 107* (D20), 8070, doi:10.1029/2001JD000583.

Rosenfeld, D., U. Lohmann, G.B. Raga, C.D. O'Dowd, M. Kulmala, S. Fuzzi, A. Reissell, and M.O. Andreae (2008), Flood or drought: How do aerosols affect precipitation? *Science, 321* (5894), 1309-1313.

Russell, L.M., R. Bahadur, and P.J. Ziemann (2011), Identifying organic aerosol sources by comparing functional group composition in chamber and atmospheric particles, *PNAS*, doi:10.1073/pnas.1006461108.

Russell, L.M., L.N. Hawkins, A.A. Frossard, P.K. Quinn, and T.S. Bates (2010), Carbohydrate-like composition of submicron atmospheric particles and their production from ocean bubble bursting, *PNAS, 107* (15), 6652-6657.

Russell, L.M., K.J. Noone, R.J. Ferek, R.A. Pockalny, R.C. Flagan, and J.H. Seinfeld (2000), Combustion organic aerosol as cloud condensation nuclei in ship tracks, *American Meteorological Society*, 2591-2606.

Russell, L.M., S. Takahama, S. Liu, L.N. Hawkins, D.S. Covert, P.K. Quinn, and T.S. Bates (2009), Oxygenated fraction and mass of organic aerosol from direct emission and atmospheric processing measured on the R/V Ronald Brown during TEXAQS/GoMACCS 2006, *J. Geophys. Res.-[Atmos.], 114*, D00F05, doi:10.1029/2008JD011275.

Schade, G.W., and P.J. Crutzen (1995), Emission of aliphatic amines from animal husbandry and their reactions: Potential source of N_2O and HCN, *J. Atmos. Chem., 22* (3), 319-346.

Schnaiter, M., C. Linke, O. Mohler, K.H. Naumann, H. Saathoff, R. Wagner, U. Schurath, and B. Wehner (2005), Absorption amplification of black carbon internally mixed with secondary organic aerosol, *J. Geophys. Res.-[Atmos.], 110* (D19), D19204, doi:10.1029/2005JD006046.

Shi, Z., D. Zhang, M. Hayashi, H. Ogata, H. Ji, and W. Fujiie (2008), Influences of sulfate and nitrate on the hygroscopic behaviour of coarse dust particles, *Atmos. Environ., 42* (4), 822-827.

Shields, L.G., D.T. Suess, and K.A. Prather (2007), Determination of single particle mass spectral signatures from heavy-duty diesel vehicle emissions for PM2.5 source apportionment, *Atmos. Environ., 41* (18), 3841-3852.

Silva, P.J., D.Y. Liu, C.A. Noble, and K.A. Prather (1999), Size and chemical characterization of individual particles resulting from biomass burning of local Southern California species, *Environ. Sci. Tech., 33* (18), 3068-3076.

Silva, P.J., and K.A. Prather (2000), Interpretation of mass spectra from organic compounds in aerosol time-of-flight mass spectrometry, *Anal. Chem.*, *72* (15), 3553-3562.

Smith, J.N., M.J. Dunn, T.M. VanReken, K. Iida, M.R. Stolzenburg, P.H. McMurry, and L.G. Huey (2008), Chemical composition of atmospheric nanoparticles formed from nucleation in Tecamac, Mexico: Evidence for an important role for organic species in nanoparticle growth, *Geophys. Res. Lett.*, *35* (4), L04808, doi:10.1029/2007GL032523.

Sodeman, D.A., S.M. Toner, and K.A. Prather (2005), Determination of single particle mass spectral signatures from light-duty vehicle emissions, *Environ. Sci. Tech.*, *39* (12), 4569-4580.

Song, X.H., P.K. Hopke, D.P. Fergenson, and K.A. Prather (1999), Classification of single particles analyzed by ATOFMS using an artificial neural network, ART-2a, *Anal. Chem.*, *71* (4), 860-865.

Sorooshian, A., S.N. Murphy, S. Hersey, H. Gates, L.T. Padro, A. Nenes, F.J. Brechtel, H. Jonsson, R.C. Flagan, and J.H. Seinfeld (2008), Comprehensive airborne characterization of aerosol from a major bovine source, *Atmos. Chem. Phys.*, *8* (17), 5489-5520.

Spencer, M.T., and K.A. Prather (2006), Using ATOFMS to determine OC/EC mass fractions in particles, *Aerosol Sci. Tech.*, *40* (8), 585-594.

Spencer, M.T., L.G. Shields, D.A. Sodeman, S.M. Toner, and K.A. Prather (2006), Comparison of oil and fuel particle chemical signatures with particle emissions from heavy and light duty vehicles, *Atmos. Environ.*, *40* (27), 5224-5235.

Srivastava, A., M.E. Pitesky, P.T. Steele, H.J. Tobias, D.P. Fergenson, J.M. Horn, S.C. Russell, G.A. Czerwieniec, C.S. Lebrilla, E.E. Gard, and M. Frank (2005), Comprehensive assignment of mass spectral signatures from individual Bacillus atrophaeus spores in matrix-free laser desorption/ionization bioaerosol mass spectrometry, *Anal. Chem.*, *77* (10), 3315-3323.

Stelson, A.W., and J.H. Seinfeld (1982), Relative humidity and temperature dependence of the ammonium nitrate dissociation constant, *Atmos Environ*, *16* (5), 983-992.

Sullivan, R.C., S.A. Guazzotti, D.A. Sodeman, and K.A. Prather (2007), Direct observations of the atmospheric processing of Asian mineral dust, *Atmos. Chem. Phys.*, *7*, 1213-1236.

Sullivan, R.C., and K.A. Prather (2005), Recent advances in our understanding of atmospheric chemistry and climate made possible by on-line aerosol analysis instrumentation, *Anal. Chem., 77* (12), 3861-3885.

Sun, H.L., L. Biedermann, and T.C. Bond (2007), Color of brown carbon: A model for ultraviolet and visible light absorption by organic carbon aerosol, *Geophys. Res. Lett., 34* (17), L17813, doi:10.1029/2007GL029797.

Sunderman, F.W. (2001), Review: Nasal toxicity, carcinogenicity, and olfactory uptake of metals, *Annals of Clinical and Laboratory Science, 31* (1), 3-24.

Toner, S.M., L.G. Shields, D.A. Sodeman, and K.A. Prather (2008), Using mass spectral source signatures to apportion exhaust particles from gasoline and diesel powered vehicles in a freeway study using UF-ATOFMS, *Atmos. Environ., 42* (3), 568-581.

Twohy, C.H., M.D. Petters, J.R. Snider, B. Stevens, W. Tahnk, M. Wetzel, L. Russell, and F. Burnet (2005), Evaluation of the aerosol indirect effect in marine stratocumulus clouds: Droplet number, size, liquid water path, and radiative impact, *J. Geophys. Res.-[Atmos.], 110* (D8), doi:10.1029/2004JD005116.

Twomey, S. (1977), The influence of pollution on the shortwave albedo of clouds, *J. Atmos. Sci., 34* (7), 1149-1152.

Vogt, R., P.J. Crutzen, and R. Sander (1996), A mechanism for halogen release from sea-salt aerosol in the remote marine boundary layer, *Nature, 383* (6598), 327-330.

Zhang, Q., C.O. Stanier, M.R. Canagaratna, J.T. Jayne, D.R. Worsnop, S.N. Pandis, and J.L. Jimenez (2004), Insights into the chemistry of new particle formation and growth events in Pittsburgh based on aerosol mass spectrometry, *Environ. Sci. Tech., 38* (18), 4797-4809.

Chapter 6

6. Changes in the Single-Particle Composition of Ship Emissions in California: Impact of Stricter Regulations on Shipping Emissions

6.1 Synopsis

In California, ship emissions constitute a major source of particulate matter near the Ports of Los Angeles (LA) and Long Beach (LB), the busiest container ports in the USA. Ships typically combust high sulfur residual oil (RO) producing high concentrations of particulate sulfate and metals including vanadium, which impact human health and climate. To mitigate these effects, regulations were adopted in 2009 requiring ships to switch from RO to low sulfur marine distillate oil (MDO) or marine gas oil (MGO) within 24 miles of the California coast. To evaluate the efficacy of these new regulations, aerosol measurements made before and after the enactment of the regulations were compared, both at the source (Ports of LA and LB) and at a receptor site. These measurements revealed that the number of vanadium-containing particles emitted from ships has decreased by up to ~61% while the relative amount of submicron sulfate from ship emissions was found to decrease by a factor of ~2.5 resulting in a decline in the fraction of particles that can activate as cloud droplets. Decreases in the mass concentrations of particulate sulfate and vanadium at both the Ports of LA and LB and at the receptor site in San Diego corroborate the decline observed by the single-particle measurements. As shipping is expected to increase in the future, the observed changes in

the single-particle chemistry and mass concentrations of both sulfate and transition metals associated with ship emissions should be taken into account for future regulations.

6.2 Introduction

Atmospheric aerosols contribute to global climate change through direct interactions with solar and terrestrial radiation as well as indirect interactions by facilitating the formation of cloud droplets and ice crystals; additionally, aerosols contribute to air pollution and adverse effects on human health [*Poschl*, 2005]. Emissions from ocean-faring ships represent a large source of particulate matter (PM) to the atmosphere, producing ~1.2-1.6 Tg PM/yr [*Corbett and Koehler*, 2003; *Eyring et al.*, 2010], with most of these emissions occurring within 400 km of coastal regions [*Corbett and Fischbeck*, 1997; *Corbett et al.*, 1999]. Ship emissions significantly impact global climate directly through the production of pollutants such as black carbon (soot), ozone, and $CO_{2(g)}$, making ship emissions the highest source of pollution per ton of fuel consumed [*Corbett and Fischbeck*, 1997; *Eyring et al.*, 2010]. Additionally, ship emissions contribute indirectly to climate change by increasing cloud droplet number concentrations (CDNC) namely by producing ~5.5 Tg S/yr of $SO_{2(g)}$, which is converted to particulate sulfate and contributes significantly to cloud droplet formation [*Eyring et al.*, 2010; *Hobbs et al.*, 2000; *Hudson et al.*, 2000]. Many climatic effects are dependent on whether ships are combusting high sulfur residual oil (RO), which emits higher mass concentrations of particulate sulfate [*Hudson et al.*, 2000], or lower sulfur fuels such as marine distillate oil (MDO) or marine gas oil (MGO); due to the low cost, an estimated 70-80% of commercial ships combust RO [*Corbett and Fischbeck*, 1997]. Additional

CDNC from ship emissions influence the cloud microphysics of marine stratocumulus clouds resulting in increased cloud optical thickness, decreased cloud effective radius, increased cloud lifetime, and potentially leading to suppressed drizzle formation [*Albrecht*, 1989; *Hudson et al.*, 2000; *Radke et al.*, 1989; *Russell et al.*, 1999; *Twomey*, 1977]. Because oceans represent a dark surface with a low albedo and marine environments are characterized by low background particle concentrations, marine environments are extremely sensitive to aerosol perturbations of cloud properties from ship emissions; in fact, ~17-39% of the anthropogenic indirect effect has been attributed to the effect of ship emissions on clouds over the ocean [*Eyring et al.*, 2010; *Slingo*, 1990].

In addition to their impact on global climate, ship emissions have adverse impacts on human health. Particle number concentrations from ship emissions typically peak in the ultrafine size mode (< 0.1 μm) [*Murphy et al.*, 2009], which tends to have greater negative health effects due to the ability of smaller particles to penetrate deeper into the respiratory system [*Bernstein et al.*, 2004; *Gauderman et al.*, 2000; *Pope and Dockery*, 2006]. In addition to size, particle mixing-state determines the impacts of aerosols on human health. Ship PM contains black carbon, sulfate, organics, and transition metals, particularly Fe, V, and Ni with RO containing higher mass concentrations of these components [*Agrawal et al.*, 2008; *Ault et al.*, 2010; *Ault et al.*, 2009; *Healy et al.*, 2009; *Murphy et al.*, 2009]; V and Ni have been shown to have a synergistic, negative impact on the heart and lungs [*Campen et al.*, 2001; *Dye et al.*, 1999] while Fe and soot have synergistic, adverse impacts on lung function and growth [*Pinkerton et al.*, 2004].

Overall, the physicochemical properties of ship emissions are thought to contribute to ~60,000 premature deaths annually, particularly near major ports [*Corbett et al.*, 2007].

In California, ship emissions are of particular concern due to the presence of several ports including the Ports of Los Angeles (LA) and Long Beach (LB), which, combined, make up the busiest container port in the United States [*Authorities*, 2006]. In light of recent literature highlighting the deleterious effects of emissions from RO combustion, new regulations were adopted in 2009 requiring ships to combust low sulfur marine fuel instead of RO as they come within 24 nautical miles of the California coast [*CARB*, 2009]. A recent study by *Lack et al.* [2011] found that as ships switched from RO to MDO or MGO, mass concentrations of particulate non-refractory organics and sulfate decreased as did the percentage of particles able to form cloud droplets. In addition, understanding how the mixing-state of PM from ship emissions has changed is crucial because the mixing-state influences the heterogeneous reactivity, cloud forming potential, and hygroscopicity of individual particles [*Poschl*, 2005]. The goal of this paper is to examine how recent changes in California regulations regarding ship emissions have impacted both mass concentrations and the single-particle chemistry of particles both freshly emitted from ships as well as ship emissions that have been subsequently processed in the atmosphere during transport to a receptor site by examining four studies spanning from 2006-2011. The implications of these findings are discussed.

6.3 Methods

6.3.1 Ambient Measurements

Ambient measurements of freshly emitted ship plumes were made at the Southern California Marine Institute (SCMI) located on Terminal Island at the Ports of LA and LB from November 16-26, 2007 as part of the Los Angeles Basin Mobile Lab Study-part II [*Ault et al.*, 2010] and again from May 10-16, 2011; measurements made in 2007 are herein referred to as SCMI 2007 and those made in 2011 are referred to as SCMI 2011. Ambient measurements were also made in 2006 from August 17-October 3 and in 2009 from August 9-October 2 at the end of the Scripps Institution of Oceanography (SIO) pier in La Jolla, California, which is ~300 m from shore and ~8 m above the Pacific Ocean. More details on the 2006 campaign can be found in *Ault et al.* [2009]. Measurements from the SIO Pier study in 2006 and the SCMI study in 2007 were made prior to the passage of the new regulations requiring ships to burn MDO or MGO within 24 miles of the California coast, while measurements made at the SIO Pier in 2009 and at SCMI in 2011 were made after the passage of the new regulations.

6.3.2 Cloud Condensation Nuclei Data

Number counts of particles that can act as cloud condensation nuclei (N_{CCN}) were measured on the SIO Pier in 2006 using a prototype continuous-flow streamwise thermal-gradient cloud condensation nuclei counter (CCNc) [*Roberts and Nenes*, 2005] held at a supersaturation of ~0.4%. The supersaturation of the CCNc is a function of the column temperature gradient (dT), which was calibrated using $(NH_4)_2SO_4$ (Aldrich, 99.999%). Total particle concentrations (N_{CN}) were measured using a scanning mobility particle

sizer (SMPS, TSI, model 3081 differential mobility analyzer and TSI, model 3010 condensation particle counter) with a time resolution of 5 minutes, which were subsequently compared to CCN counts providing a measure of the fraction of total particles that could nucleate particles at the given supersaturation ($fCCN_{0.4\%}$):

$$fCCN_{0.4\%} = \frac{N_{CCN}}{N_{CN}} \quad (1)$$

CCN measurements were also made on the SIO Pier in 2009 using a commercial CCNc (Droplet Measurement Technologies), which scans through supersaturations from 0.1-1.0%. For the purpose of this paper, only measurements of N_{CCN} made at 0.4% supersaturation are compared. An SMPS was also used in 2009, and total particle concentration measurements were made using a condensation particle counter (CPC) (TSI, model 3010) in 2009. Activation diameters (D_{act}) were subsequently determined from fCCN and size distributions obtained from the SMPS [*Furutani et al.*, 2008].

6.3.3 Particulate Mass Concentration Data

Particulate mass concentrations for particles with aerodynamic diameters of≤ 2.5 μm ($PM_{2.5}$), and mass concentrations of individual chemical species on particles in the same size range are measured continuously throughout California as part of the Environmental Protection Agency (EPA) Interagency Monitoring of PROtected Visual Environments (IMPROVE) [*Malm et al.*, 2004] and CARB Air Quality (AQ) monitoring networks. Mass concentrations of sulfate and vanadium are of particular interest for this analysis. $PM_{2.5}$ and particulate sulfate and vanadium concentrations were available every 3-6 days. During SCMI 2007 and SCMI 2011, $PM_{2.5}$ data was collected in Los Angeles on Terminal Island within the Ports of LA and LB while mass concentrations of sulfate

and vanadium were obtained from a site in downtown LA ~37.6 km from SCMI. During the Pier 2006 and 2009 campaigns, mass concentrations were obtained from a site in El Cajon ~30.6 km from the SIO Pier.

6.3.4 Aerosol time-of-flight Mass Spectrometry

The size-resolved chemical composition of individual aerosols was measured in real-time using an aerosol time-of-flight mass spectrometer (ATOFMS) [*Gard et al.*, 1997; *Prather et al.*, 1994; *Su et al.*, 2004]. Two different instruments were used during these studies. The ultrafine (UF)-ATOFMS detects particles from 100-1000 nm aerodynamic diameter (Da) and was used during SCMI 2007 and SCMI 2011. The converging nozzle inlet ATOFMS, which detects aerosol particles in the size range of 0.2-3.0 μm D_a, was used to make measurements on the end of the SIO pier in 2006 and 2009. The operating principles of the ATOFMS have been described previously [*Gard et al.*, 1997]. Briefly, particles are sampled at atmospheric pressure through the sampling inlet (e.g. converging nozzle or aerodynamic lens inlet) into a differentially pumped vacuum chamber causing particles to be accelerated to a size-dependent terminal velocity, which is measured in the sizing region of the instrument consisting of two continuous wave lasers (532 nm) separated at a fixed distance. The time taken to traverse the laser beams is recorded and is converted to D_a using calibrations from polystyrene latex spheres of known sizes. The particle velocity is also used to time the firing of a Q-switched Nd:YAG laser that simultaneously desorbs and ionizes compounds from individual particles creating positive and negative ions, which are analyzed in a dual polarity time-of-flight mass spectrometer. Dual-polarity spectra provide complementary

information regarding the source (e.g. ships vs. sea salt) and age of the particle (e.g. fresh vs. reacted sea salt) [*Guazzotti et al.*, 2001; *Noble and Prather*, 1996]. Ambient particles were dried with a silica gel diffusion drier for both sets of measurements at the SIO pier to decrease the particulate water content, which suppresses the intensity and frequency of negative ion spectra [*Neubauer et al.*, 1997; *Neubauer et al.*, 1998].

6.3.5 Data Analysis

The YAADA software toolkit was used to import ion peak lists into MATLAB (The MathWorks, Inc.) for processing of ATOFMS data [*Allen*, 2002]. An adaptive neural network (ART-2a), was used to cluster together particles with similar mass spectral peaks and intensities [*Fergenson et al.*, 2001; *Gard et al.*, 1998; *Guazzotti et al.*, 2001; *Song et al.*, 1999]. Data were averaged into 1-hour time bins for measurements made during the pier studies, which were long-term field studies (e.g. lasting ~ 3 months each), while 10-min time bins were used for SCMI 2007 and SCMI 2011, which were short-term field studies (e.g. lasting ~6-10 days each). Each ion peak assignment presented in this paper corresponds to the most likely ion produced at a given mass-to-charge (*m/z*). Particle types described in this paper are defined by characteristic ion peaks and/or possible sources and do not reflect all of the compounds present within a particular particle class.

6.4 Results and Discussion

6.4.1 Single-Particle Measurements of Ship Plumes

This section aims to show a decline in particles produced by ships combusting high sulfur RO at the Ports of LA and LB by comparing measurements during SCMI

2007 before the regulations were enacted and during SCMI 2011 after the regulations were enacted. Particles emitted by ships combusting high sulfur RO are primarily classified as organic carbon (OC)-V type particles by ATOFMS and are characterized by vanadium ion markers ($^{51}V^{+}$, $^{67}VO^{+}$), iron ($^{56}Fe^{+}$), and nickel ($^{58,60}Ni^{+}$). Additionally, these particles may contain elemental carbon (EC) peaks ($^{12}C_1$, $^{24}C_2^{+}$, $^{36}C_3^{+}$…C_n^{+}), lower intensity OC peaks ($^{27}C_2H_3^{+}$, $^{37}C_3H^{+}$, etc.), and sulfate and sulfuric acid peaks ($^{80}SO_3^{-}$, $^{97}HSO_4^{-}$, $^{195}H_2SO_4HSO_4^{-}$) (see Figure 6.1) [*Ault et al.*, 2010; *Ault et al.*, 2009]. This particle type is typically concentrated in the smallest submicron size bins detected by the instrument; aging of these particles causes them to grow by acquisition of particulate water and nitrate [*Ault et al.*, 2010; *Ault et al.*, 2009].

A comparison of the size distribution and number fraction of V-containing particles for individual ship plumes measured during SCMI 2007 and SCMI 2011 is shown in Figure 6.2. The identification of ship plume emissions was made using concurrent measurements of particle number concentrations and gas phase measurements of $SO_{2(g)}$ as mentioned in *Ault et al.* [2010]. Ship plumes were characterized by the dramatic increase in particle number concentrations and $SO_{2(g)}$ lasting ~10-40 minutes. These observations are consistent with previous measurements of ship emissions [*Ault et al.*, 2010; *Corbett and Fischbeck*, 1997; *Corbett and Koehler*, 2003]. For SCMI 2007, two different ship plumes are compared, one in which a container vessel was burning RO and the other from a vessel burning MDO or MGO [*Ault et al.*, 2010]. The plume identified during SCMI 2011 was from a ship burning MDO or MGO. Higher overall number fractions of OC-V particles were emitted by the ship combusting high sulfur RO

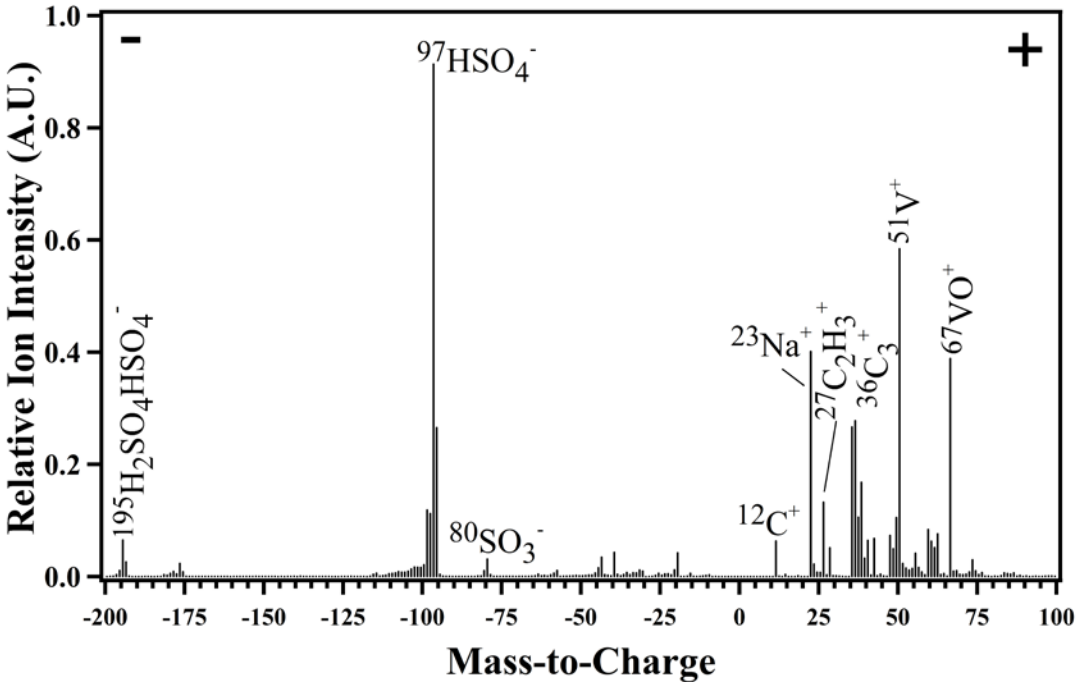

Figure 6.1: Representative mass spectrum of the OC-V-sulfate particle type characteristic of shipping combusting high sulfur residual fuel. Reproduced with permission from Ault et al., 2010. Copyright 2010 American Chemical Society.

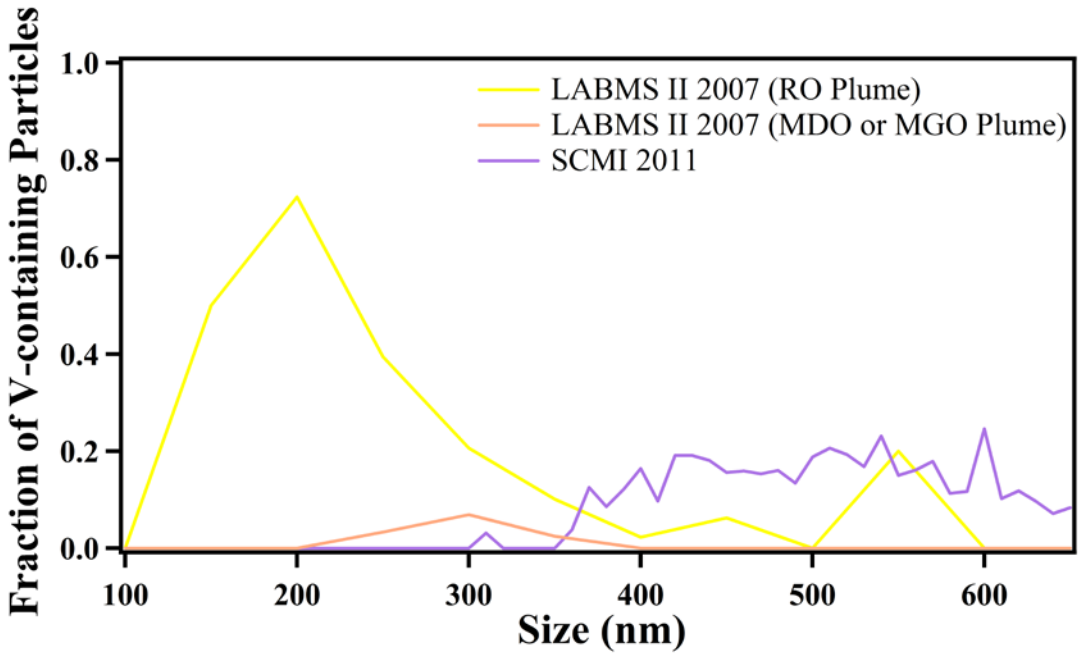

Figure 6.2: Observed number fractions of V-containing particles emitted from a ship combusting low sulfur MDO or MGO emitted during SCMI 2007 (orange), a ship combusting high sulfur RO emitted during SCMI 2007 (yellow), and from a ship plume observed during SCMI 2011 (purple). Particle types are plotted as a function of size in 50 nm size bins.

during SCMI 2007 with OC-V particles representing ~72% of the observed particles within the 200-250 nm size bin. In contrast, emissions from both the distillate fuel plume during SCMI 2007 and from the plume observed during SCMI 2011 contained lower number fractions of OC-V particles (~7% for the distillate fuel plume during SCMI 2007 and ~20% for the plume observed during SCMI 2011) that extended out to larger sizes peaking above ~300 nm. OC-V particles observed in distillate fuel plumes during SCMI 2007 were determined to represent a background particle type with contributions from oil refineries [*Singh et al.*, 2002] and chemically aged ship emissions [*Ault et al.*, 2010]; the chemically aged/background nature of this particle type explains the fact that these particles extend out to larger sizes [*Ault et al.*, 2010]. Although the number fraction of OC-V particles was higher during SCMI 2011 than in the distillate fuel plume observed during SCMI 2007, it is likely that most of the OC-V particles observed during SCMI 2011 also represent a background particle type rather than a freshly emitted particle type.

Changes in the single-particle mixing-state of individual ship plumes between the two years were also examined in further detail in Figure 6.3, which shows a subtraction plot of mass spectra derived from particles measured in a RO burning ship plume during SCMI 2007 (top) and a marine distillate burning plume from SCMI 2011 (bottom). The peak area of a particular *m/z* can be related to the relative amount of a specific chemical species on each particle type [*Bhave et al.*, 2002; *Gross et al.*, 2000] meaning that differences in the ion peaks shown in Figure 6.3 represent changes in the chemistry of particles between the two campaigns. Particles detected in ship plumes during SCMI 2007 contained larger ion peak areas of vanadium, elemental carbon, organic carbon,

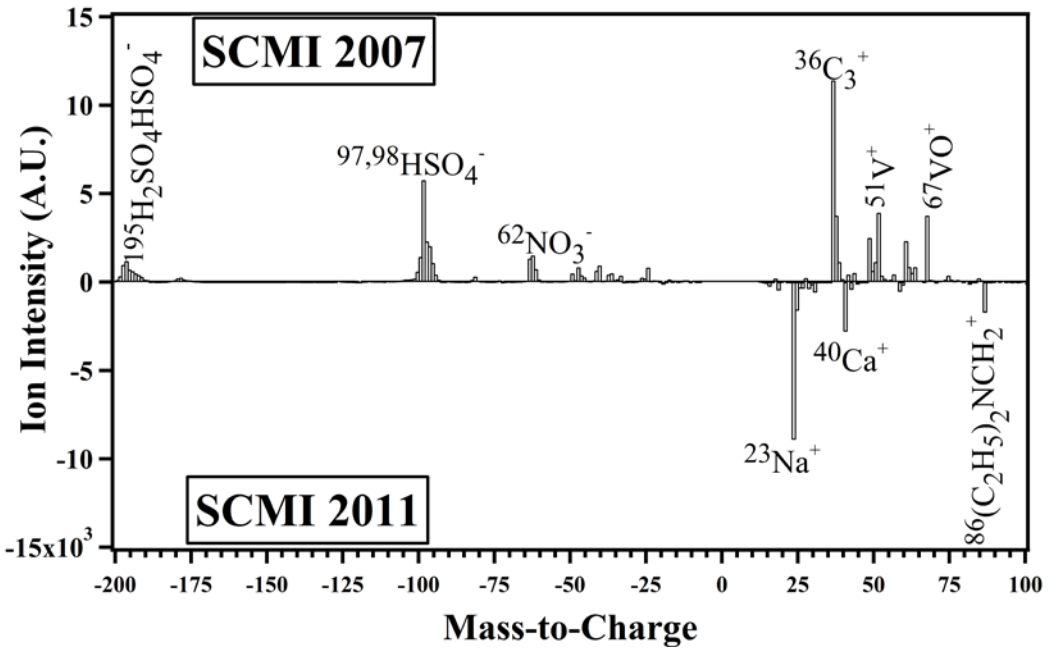

Figure 6.3: Subtraction plot of mass spectra produced by particles observed in ship plumes during SCMI 2007 (top) and SCMI 2011 (bottom).

sulfate, and sulfuric acid peaks ($^{177}HSO_4SO_3^-$, $^{195}H_2SO_4HSO_4^-$). Increased vanadium, sulfate, and sulfuric acid peaks during SCMI 2007 are likely due to the higher heavy metal and sulfur content of the RO fuel combusted; additionally, organic carbon detected during SCMI 2007 is likely due to the presence of lubricating oil and asphaltenes in high sulfur RO [2010; *Corbett and Fischbeck*, 1997; *Kasper et al.*, 2007; *Murphy et al.*, 2009]. The higher sulfuric acid content of the particles could also be due to the increased presence of vanadium in the particles, which has been suggested to catalyze the formation of sulfuric acid from $SO_{2(g)}$ [*Ault et al.*, 2010]. Overall, the heavy metal, organic carbon, and sulfate content of aerosols in fresh ship plumes observed at the Port of LA have declined due to changes in regulations requiring ships to combust lower sulfur MDO or MGO as they approach the California coast.

6.4.2 Overall Decline in Emissions from High Sulfur RO Combustion Observed at the Port of LA

In addition to probing differences in the particle chemistry of individual ship plumes, differences in the overall number fraction of V-containing particles were also observed between SCMI 2007 and SCMI 2011. Figure 6.4a uses box and whisker plots to show the percentage of all particles from SCMI 2007 and SCMI 2011 that were identified as V-containing; box top and bottom represent the 75th and 25th percentiles, respectively, and the whiskers represent the 90th and 10th percentiles. The percentages of V-containing particles in the 10th percentiles were considerably lower during SCMI 2011 than SCMI 2007 (~0.6% vs. 4%, respectively) while the 90th percentiles also peaked at a lower percentage for SCMI 2011 than SCMI 2007 (~9% vs. ~13%, respectively). The

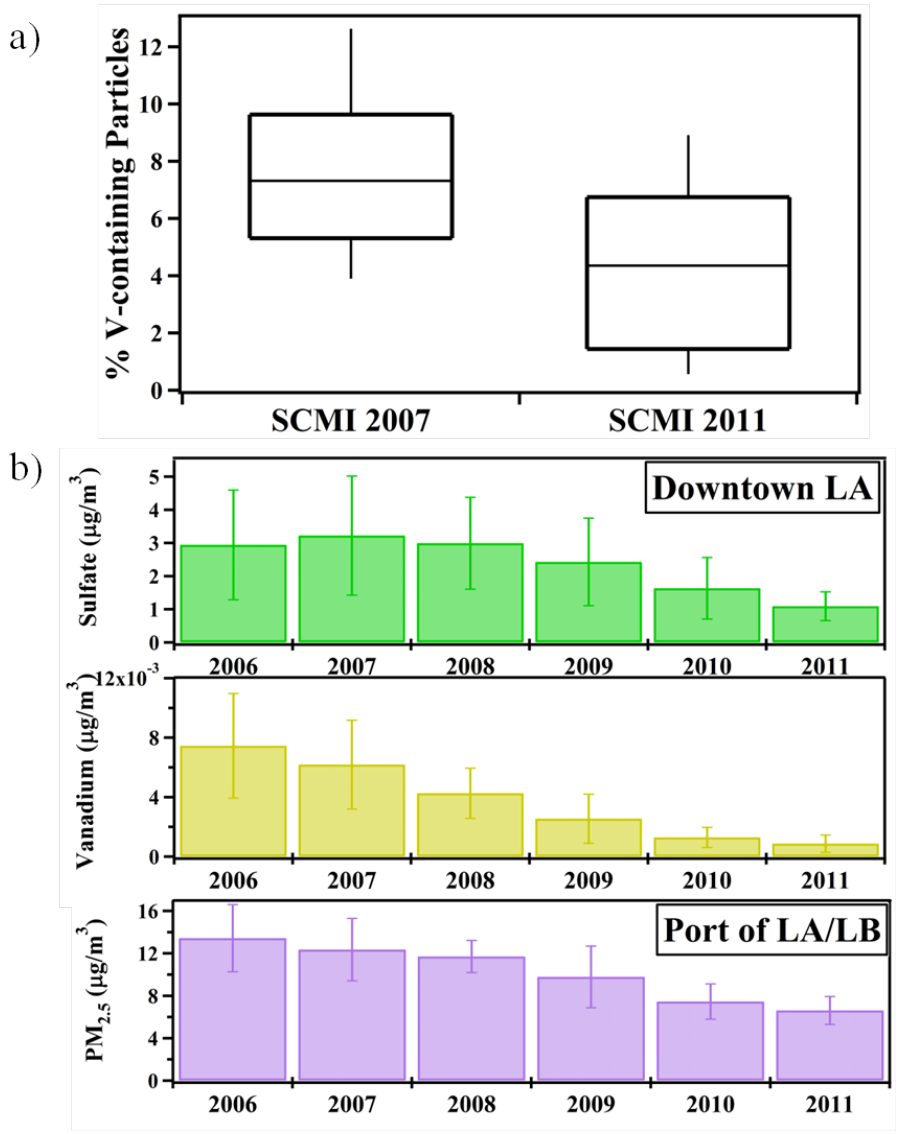

Figure 6.4: (a) Box and whisker plots depicting the percentage of V-containing particles observed during SCMI 2007 and SCMI 2011. The top and bottom of the box represent the 25th and 75th percentiles, respectively, while the middle band represents the median of the percentage of V-containing particles. The bottom and top whiskers represent the 10th and 90th percentiles, respectively. (b) Average annual mass concentration data of $PM_{2.5}$ sulfate (top panel), vanadium (middle panel), and total mass concentrations (bottom panel) collected in 2006-2011 during the SCMI 2007 and SCMI 2011 campaigns are shown while standard deviations are shown as error bars.

median percentage of V-containing particles was lower in 2011 compared to 2007, ~4.3% vs. 7.3%, representing an overall decrease in V-containing particles of ~41% between the two years. Despite the presence of other sources of V-containing particles (e.g. oil refineries), new regulations on ship fuel appear to have led to a decrease in the V-containing particle type due to changes in the particle composition of ship emissions.

Mass concentration data collected from monitoring sites in the LA region provide further support for the observed single-particle measurements showing a decline in particle types associated with high sulfur RO combustion. Figure 6.4b shows annual average mass concentrations of vanadium and sulfate on $PM_{2.5}$ obtained from a monitoring site in Downtown LA in addition to total $PM_{2.5}$ mass concentrations obtained from a site located at the Port of LA. Average vanadium mass concentrations were found to decrease from ~6.2 ng/m^3 in 2007 to ~0.9 ng/m^3 in 2011 representing an overall decline in vanadium mass concentrations of ~86%, while average sulfate mass concentrations were found to decrease from ~3.2 $\mu g/m^3$ in 2007 to ~1.1 $\mu g/m^3$ in 2011 representing an overall decline in sulfate mass concentrations of ~66%. These results agree with the single-particle results showing an overall decline in V-containing particles observed between these two studies and the decline in sulfate observed on particles from ship plumes. It should be noted, however, that mass concentration data was only available through May, 2011 and, thus, additional mass concentration results from 2011 are needed to make a more comprehensive comparison between the two years. Total $PM_{2.5}$ mass concentrations also decreased from ~12.4 $\mu g/m^3$ on average in 2007 to ~6.6 $\mu g/m^3$ in 2011 representing an overall decrease of ~47% between the two years.

Although the observed decreases in mass concentrations could be due to differences in meteorological conditions and the number of ships encountered during both years, the previous two sections of this manuscript have provided compelling evidence for a sharp decline in vanadium, sulfate, and overall PM mass, from both a single-particle and a bulk perspective, in the Ports of LA and LB associated with the enactment of regulations on shipping emissions in California. However, in order to probe the full efficacy of these regulations, changes in particle chemistry must also be shown at receptor sites that are frequented by emissions transported from the Ports of LA and LB. The following sections present evidence for a decline in particles associated with high sulfur RO combustion at a receptor site in San Diego as a consequence of recent regulations on ship emissions; the long-term and climatic implications of these findings are also probed.

6.4.3 Inter-Annual Comparison of Changes in the Single-Particle Chemistry and Particulate Mass Concentrations of Transported Port Emissions at a Receptor Site

Ship emissions transported from the Ports of LA and LB were measured at a receptor site (SIO Pier, La Jolla, CA) from August-October, 2006, and from August-October 2009; the first of these studies being conducted before regulations were enacted, and the second after regulations were enacted. The SIO Pier site is frequently impacted by emissions from the Ports of LA and LB, which occurred during ~32% of the time during the campaign in 2006 [*Ault et al.*, 2009] and ~47% of the time during the campaign in 2009, providing an opportunity to compare the physicochemical properties of transported emissions both before and after the new regulations were enacted. During

both Pier studies, 3 main air mass transport conditions were observed: transport from the Ports of LA and LB, transport from the ocean (oceanic), and inland transport (continental). An example of each of these transport conditions were selected for both years and the size-resolved chemistry of particles detected during each of these 3 time periods is shown in Figure 6.5. The end goal was to make inter-annual comparisons of particle chemistry during periods when ship emissions were transported from the Ports of LA and LB with periods when oceanic and continental emissions were sampled. Table 6.1 shows the times representative of each transport condition during both years. Characteristic 48-hour air mass back-trajectories observed during each of the three transport conditions for both years are shown in Figure 6.6 using the HYSPLIT model [*Draxler and Rolph*, 2011]. Air masses originating from the ports are shown in the first column with trajectories traversing the ports located at ~33.79°N and 118.26°W. Air masses characterized as oceanic had not touched the continent in over 48 hours, while those characterized as continental originated from the inland, desert region of California and/or had undergone long-range transport across the continent. Continental air masses were typically associated with high wind speeds resulting in less time for atmospheric processing to occur before the air masses were sampled. In 2006, transport events contained more V-containing particles compared to non-transport events [*Ault et al.*, 2009] but not in 2009. Up to ~18% of the detected particles in the smallest size bins were classified as V-containing during Port conditions in 2006. In contrast, the fraction of V-containing particles was low (~3-5% of the total particles detected per size bin) for both years during oceanic and continental transport conditions and in 2009 when emissions were transported from the Ports of LA and LB. Additionally, a higher number

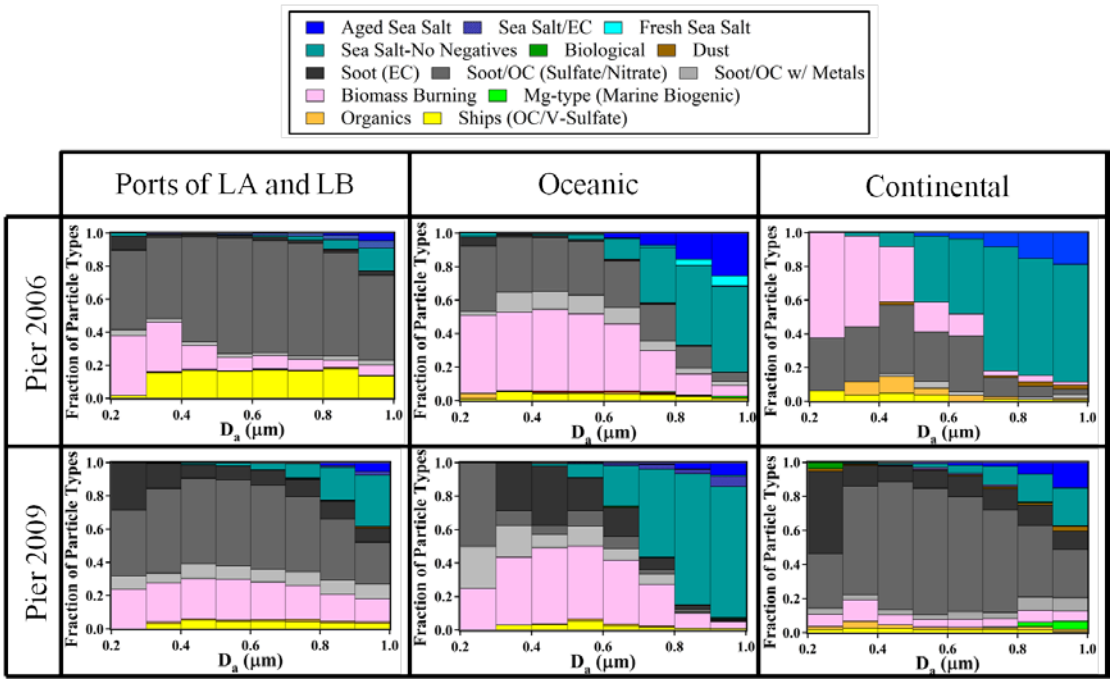

Figure 6.5: Fraction of submicron particle types observed during different transport conditions: transport from the Ports of LA and LB (left column), oceanic (middle column), and continental (right column) measured on the SIO Pier in 2006 (top row) and 2009 (bottom row). Particle types are plotted as a function of size in 0.1 μm size bins.

Table 6.1: Time periods of Port of Los Angeles, oceanic, and continental transport conditions examined for 2006 and 2009.

Transport Condition	Date (PDT)
Ports of LA and LB 2006	9/12/06 0:00 - 9/13/06 0:00
Oceanic 2006	9/14/06 7:00 - 9/15/06 23:00
Continental 2006	9/17/06 16:00 - 9/18/06 1:00
Ports of LA and LB 2009	9/27/09 2:00 - 9/29/09 2:00
Oceanic 2009	9/29/09 14:00 - 9/30/09 0:00
Continental 2009	9/23/09 8:00 - 9/24/09 2:00

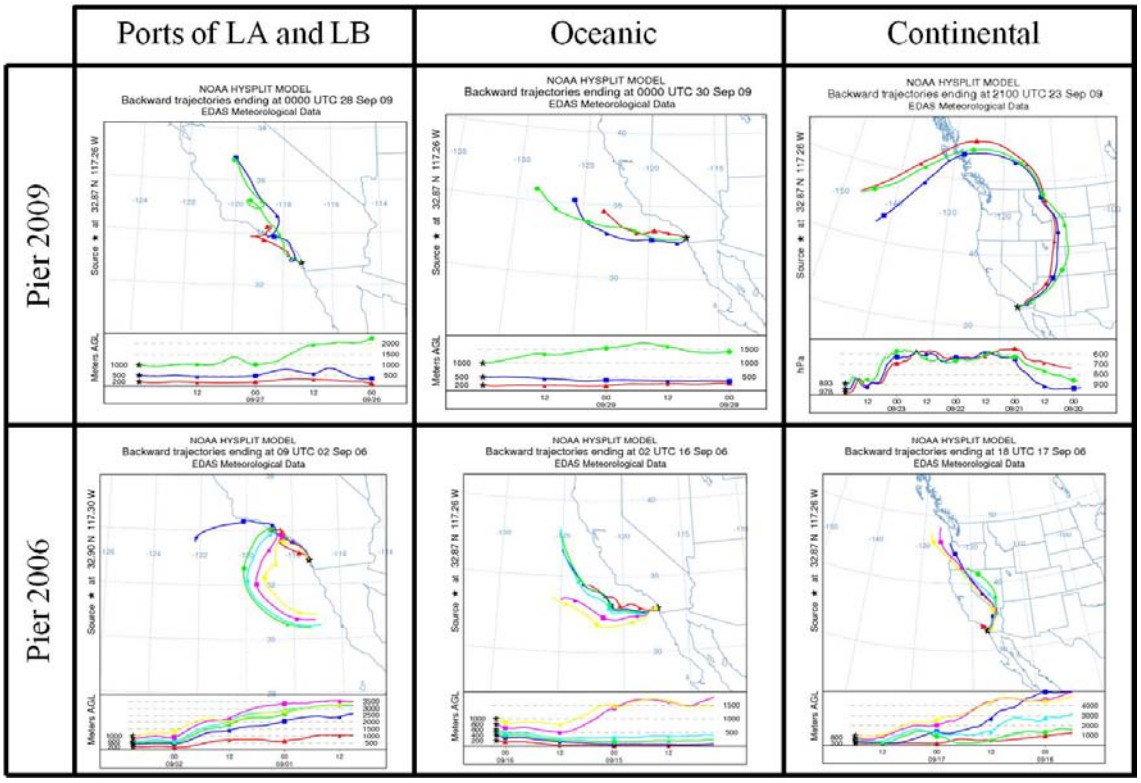

Figure 6.6: 48-hour air mass back-trajectories representative of transport from the Ports of LA and LB (left column), oceanic transport (middle column), and continental transport (right column) from the SIO Pier in 2009 (top row) and 2006 (bottom row).

fraction of fresh soot and soot/OC (sulfate/nitrate) particles were observed in 2009 when emissions were transported from the port consistent with previous observations of soot rather than OC-V-sulfate particles from the combustion of MDO or MGO [*Ault et al.*, 2010; *Shields et al.*, 2007; *Spencer et al.*, 2006]. This suggests that V-containing particles observed in 2009 were likely background types emitted from ships out in the open ocean (e.g. beyond the 24 nautical mile limit imposed by the new regulations) with few contributions of this particle type from the Ports of LA and LB.

Finally, differences in emissions observed during all port transport times were also probed. Figure 6.7a shows box and whisker plots of the percentage of V-containing particles observed during all transport events on the SIO Pier in 2006 and 2009 (see Figure 6.8 for box and whisker plots of V-containing particles during each individual transport event). The percentages of V-containing particles showed a much narrower distribution in 2009 with the 90th percentiles peaking at a lower percentage for emissions transported from the Ports of LA and LB in 2009 than 2006 (~6% vs. ~12.4%, respectively). The median percentage of V-containing particles during transport events was lower in 2009 compared to 2006, ~2% vs. ~5.3% representing an overall decrease in V-containing particles of ~61% between the two years. In addition to a decline in V-containing particles, sulfate ion peak areas were on average a factor ~2.5 lower on all submicron particles in 2009 than 2006 during transport conditions.

Mass concentration data from a site near the SIO Pier confirms the decrease in both vanadium and sulfate, which were found to decrease by ~67% and ~29%, respectively, in 2009 compared to 2006 (see Figure 6.7b). Additionally, atmospheric

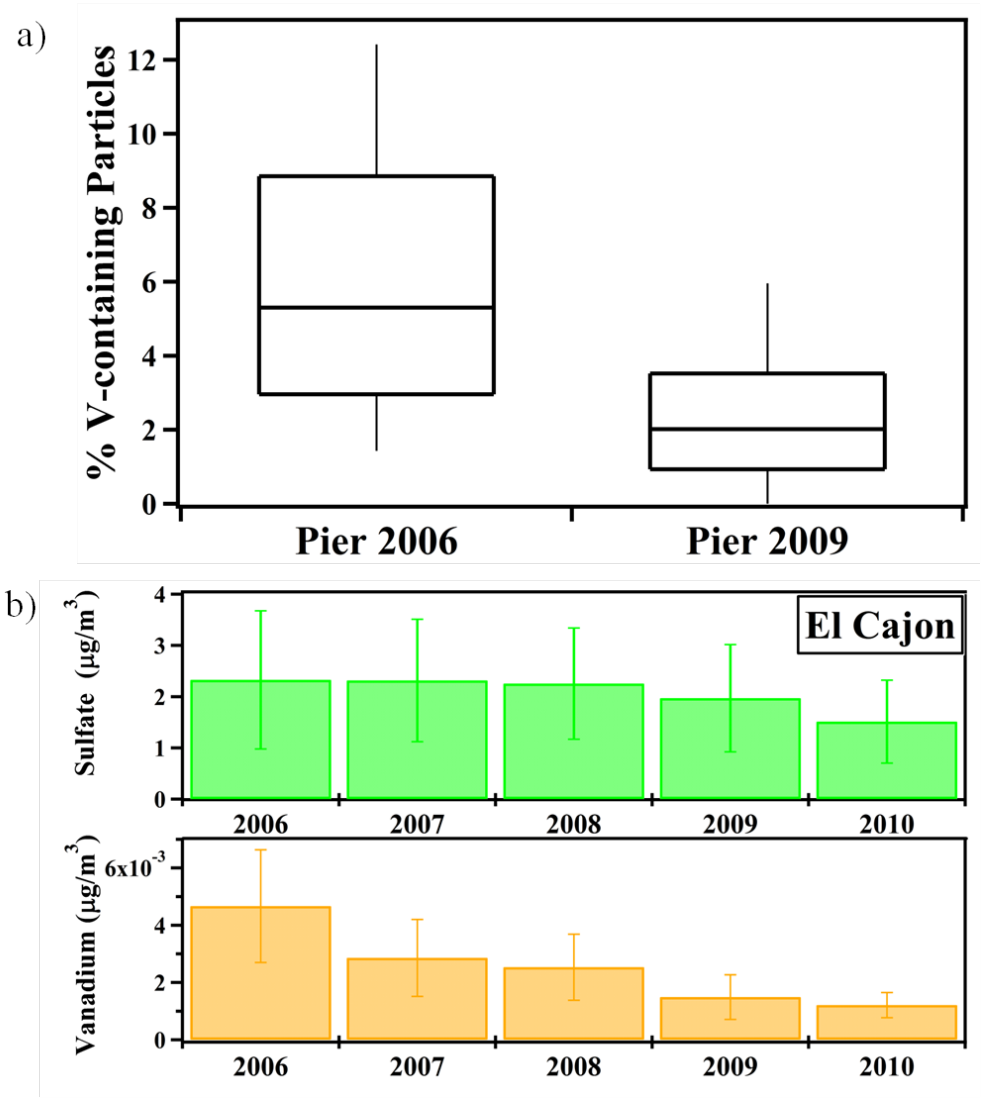

Figure 6.7: (a) Box and whisker plots depicting the percentage of V-containing particles observed during measurements made on the SIO Pier in 2006 and 2009 during all events when emissions were transported from the Ports of LA and LB. The top and bottom of the box represent the 25th and 75th percentiles, respectively, while the middle band represents the median of the percentage of V-containing particles. The bottom and top whiskers represent the 10th and 90th percentiles, respectively. (b) Average annual mass concentration data of $PM_{2.5}$ sulfate (top panel) and vanadium (bottom panel) collected in 2006-2010 during the Pier 2006 and Pier 2009 campaigns are presented while standard deviations are shown as error bars.

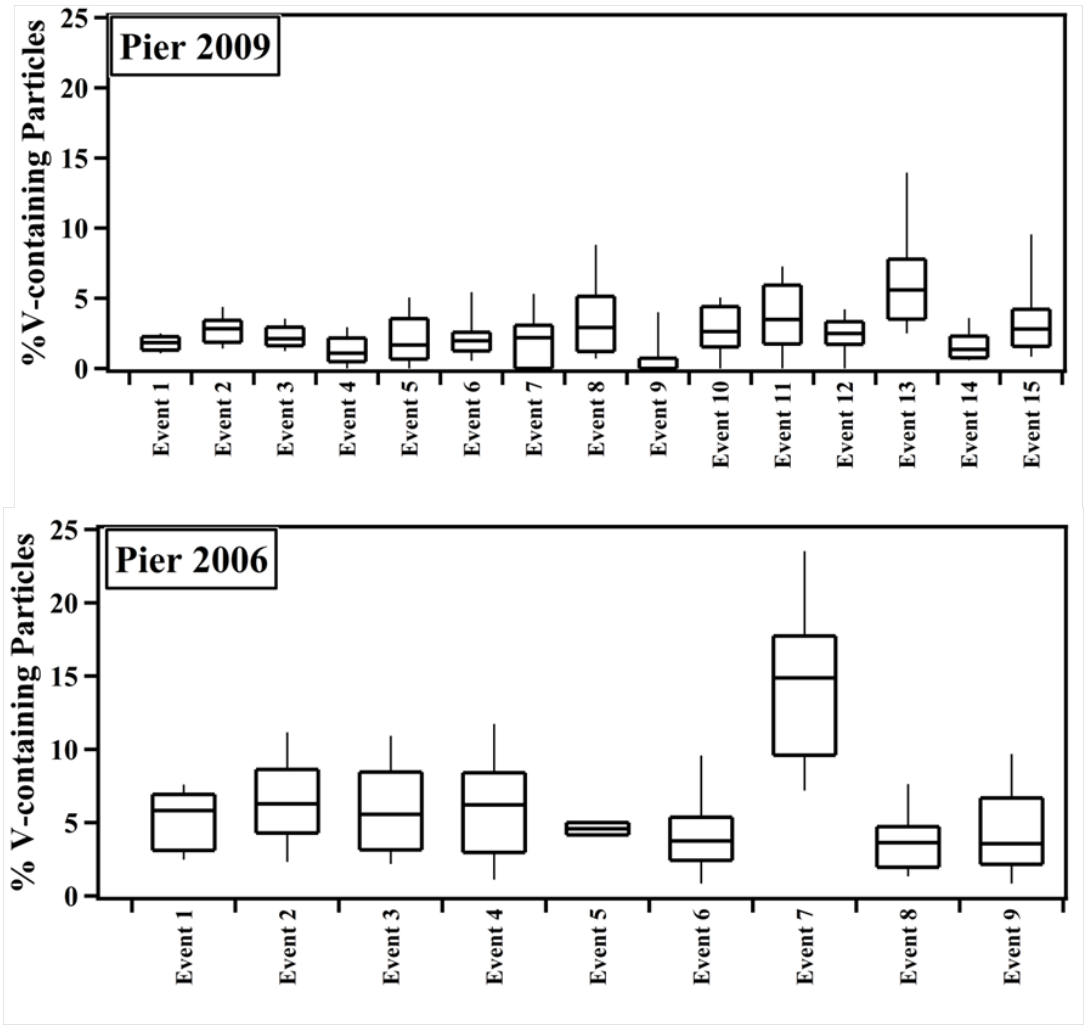

Figure 6.8: Box and whisker plots depicting the percentage of V-containing particles observed during measurements made on the SIO Pier in 2006 and 2009 individual events when emissions were transported from the Ports of LA and LB. The top and bottom of the box represent the 25th and 75th percentiles, respectively, while the band near the middle represents the 50th percentile of the percentage of V-containing particles. The bottom and top whiskers represent the 10th and 90th percentiles, respectively.

processing (e.g. cloud processing) likely contributed additional particulate sulfate to the sampled aerosol at the pier possibly underestimating the decline in sulfate between the two years due to changes in shipping emissions; this is supported by the fact that the RH was elevated during both campaigns (average RH was 86% in 2006 and 79% in 2009). However, the results suggest that despite the fact that emissions from the Ports of LA and LB were transported more frequently to the SIO Pier in 2009 than 2006, fewer emissions produced from RO combustion were observed in 2009 due to changes in shipping emissions along the California coast.

6.4.4 Inter-Annual Comparison of fCCN during Transport Events

Measurements of CCN concentrations made at the Pier in 2006 and 2009 were compared to further probe the implications of the observed changes in the chemistry of transported ship emissions. fCCN and D_{act} were compared when emissions were transported from the Ports of LA and LB for both 2006 and 2009. Transported particles had slightly higher fCCN values in 2006 than in 2009 by ~ 15% (median values of 0.63 ± 0.13 in 2006 and 0.53 ± 0.18 in 2009) and lower D_{act} values (83.4 ± 9.1 nm in 2006 and 89.2 ± 8.0 nm in 2009 on average) than 2009 by ~ 9%. It should be noted that previous measurements of ship emissions have shown much lower fCCN values of ~0.1-0.12 [*Hobbs et al.*, 2000; *Hudson et al.*, 2000] because the measurements presented here are for particles that have been transported and subsequently aged and/or cloud processed while previous measurements were for fresh ship emissions. We note that these differences in the fCCN and D_{act} are small and within error of each other most likely due to aging and/or cloud processing during transport that contributes soluble material to

transported port emissions making differences in fCCN and D_{act} smaller than predicted. Despite these small differences, the fCCN and D_{act} values reported herein are still noteworthy as they represent, to the best of our knowledge, the first reported changes of the cloud nucleating properties of ship emissions transported to a receptor cite due to the recent fuel regulations. The most likely explanation for these differences is the decline in particulate sulfate, in agreement with recent measurements, which measured a decline in both non-refractory particulate sulfate and fCCN as ships switched to low sulfur MDO or MGO while approaching the California coast [*Lack et al.*, 2011; *Lack et al.*, 2009].

6.4.5 Atmospheric Implications

Since the passage of the new regulations in 2009, the measured particle chemistry of fresh ship plumes, fresh port emissions, and transported port emissions showed that V-containing particles and particulate mass concentrations of vanadium have decreased. In addition, particulate sulfate has decreased resulting in lower values of fCCN at a receptor site. Recent measurements have highlighted changes in bulk particle composition and fCCN in ship plumes upon switching to low sulfur MDO or MGO close to the California coast [*Lack et al.*, 2011]; however, the results presented herein are the first to show the long-term impact of recent regulations on shipping emissions in California and the impact of these regulations on the single-particle chemistry at a receptor site. The observed decline in the vanadium and sulfate content of ship emissions are expected to mitigate some of the health and climatic impacts that ship emissions have in California; these improvements should be monitored on a long-term basis through epidemiological and air

quality studies that can serve as a case study for other regions contemplating regulations on shipping emissions in coastal waters.

6.5 Acknowledgements

The authors would like to thank Christian McDonald for use of the SIO Pier during the 2006 and 2009 campaigns and with assistance in setup. Prof. Daniel Cziczo is acknowledged for use of the DMT CCNc instrument during the SIO Pier measurements in 2009. We gratefully acknowledge the NOAA Air Resources Laboratory for the provision of the HYSPLIT transport model and READY website (http://ready.arl.noaa.gov/HYSPLIT.php) used in this publication. Prof. V. Ramanathan and Dr. Craig Corrigan are acknowledged for providing the aethalometer used during SCMI 2007. The Southern California Marine Institute, specifically Dr. Richard Peiper and Carrie Wolfe, hosted the sampling in 2007 and 2011. Greg Roberts is acknowledged for use of the prototype CCNc instrument. C. J. Gaston was funded through the Aerosol Chemistry and Climate Institute at Pacific Northwest National Laboratory. A. P. Ault was funded by a Department of Energy Global Change Education Program graduate research environmental fellowship and a grant from the San Diego Unified Port District. The SCMI 2011 campaign and M.D. Zauscher were funded by the U.S. Environmental Protection Agency PM Center Grant # R832415. This work was funded by the California Air Resources Board (CARB).

Chapter 6 is in preparation for submission to *Environmental Science & Technology*: Gaston, C.J., Ault, A.P., Zaucher, M.D., Furutani, H., Cahill, J.F., Collins, D.B., Suski, K.J., Prather, K.A. Changes in the single-particle composition of ship

emissions in California: Impact of stricter regulations on shipping emissions. The dissertation author was the primary investigator and author of this paper.

6.6 References

Agrawal, H., Q.G.J. Malloy, W.A. Welch, J.W. Miller, and D.R. Cocker (2008), In-use gaseous and particulate matter emissions from a modern ocean going container vessel, *Atmos. Environ., 42* (21), 5504-5510.

Albrecht, B.A. (1989), Aerosols, cloud microphysics, and fractional cloudiness, *Science, 245* (4923), 1227-1230.

Allen, J.O. (2002), YAADA software toolkit to analyze single-particle mass spectral data: Reference manual version 1.1, *Arizona State University*, http://www.yaada.org.

Ault, A.P., C.J. Gaston, Y. Wang, G. Dominguez, M.H. Thiemens, and K.A. Prather (2010), Characterization of the single particle mixing state of individual ship plume events measured at the Port of Los Angeles, *Environ. Sci. Tech., 44* (6), 1954-1961.

Ault, A.P., M.J. Moore, H. Furutani, and K.A. Prather (2009), Impact of emissions from the Los Angeles port region on San Diego air quality during regional transport events, *Environ. Sci. Tech., 43* (10), 3500-3506.

Authorities, A.A.o.P., North American Port Container Traffic, American Association of Port Authorities, 2006.

Bernstein, J.A., N. Alexis, C. Barnes, I.L. Bernstein, J.A. Bernstein, A. Nel, D. Peden, D. Diaz-Sanchez, S.M. Tarlo, and P.B. Williams (2004), Health effects of air pollution, *Journal of Allergy and Clinical Immunology, 114* (5), 1116-1123.

Bhave, P.V., J.O. Allen, B.D. Morrical, D.P. Fergenson, G.R. Cass, and K.A. Prather (2002), A field-based approach for determining ATOFMS instrument sensitivities to ammonium and nitrate, *Environ. Sci. Tech., 36* (22), 4868-4879.

Campen, M.J., J.P. Nolan, M.C.J. Schladweiler, U.P. Kodavanti, P.A. Evansky, D.L. Costa, and W.P. Watkinson (2001), Cardiovascular and thermoregulatory effects of inhaled PM-associated transition metals: A potential interaction between nickel and vanadium sulfate, *Toxicological Sciences, 64* (2), 243-252.

CARB, Final Regulation Order. Fuel Sulfur and Other Operational Requirments for Ocean-Going Vessels Within California Waters and 24 Nautical Miles of the California Baseline, California Air Resources Board: Sacramento, CA, 2009.

Corbett, J.J., and P. Fischbeck (1997), Emissions from ships, *Science, 278* (5339), 823-824.

Corbett, J.J., P.S. Fishbeck, and S.N. Pandis (1999), Global nitrogen and sulphur inventories for oceangoing ships, *J. Geophys. Res.*, *104* (3), 3457-3470.

Corbett, J.J., and H.W. Koehler (2003), Updated emissions from ocean shipping, *J. Geophys. Res.-[Atmos.]*, *108* (D20), 4650, doi:10.1029/2003JD003751.

Corbett, J.J., J.J. Winebrake, E.H. Green, P. Kasibhatla, V. Eyring, and A. Lauer (2007), Mortality from ship emissions: A global assessment, *Environ. Sci. Tech.*, *41* (24), 8512-8518.

Draxler, R.R., and G.D. Rolph (2011), HYSPLIT (HYbrid Single-Particle Lagrangian Integrated Trajectory) Model access via NOAA ARL READY Website (http://ready.arl.noaa.gov/HYSPLIT.php), *NOAA Air Resources Laboratory*, Silver Spring, MD.

Dye, J.A., K.B. Adler, J.H. Richards, and K.L. Dreher (1999), Role of soluble metals in oil fly ash-induced airway epithelial injury and cytokine gene expression, *Am. J. Physiol.*, *277*, L498-L510.

Eyring, V., I.S.A. Isaksen, T. Berntsen, W.J. Collins, J.J. Corbett, O. Endresen, R.G. Grainger, J. Moldanova, H. Schlager, and D.S. Stevenson (2010), Transport impacts on atmosphere and climate: Shipping, *Atmos Environ*, *44*, 4735-4771.

Fergenson, D.P., X.H. Song, Z. Ramadan, J.O. Allen, L.S. Hughes, G.R. Cass, P.K. Hopke, and K.A. Prather (2001), Quantification of ATOFMS data by multivariate methods, *Anal. Chem.*, *73* (15), 3535-3541.

Furutani, H., M. Dall'osto, G.C. Roberts, and K.A. Prather (2008), Assessment of the relative importance of atmospheric aging on CCN activity derived from field observations, *Atmos. Environ.*, *42* (13), 3130-3142.

Gard, E., J.E. Mayer, B.D. Morrical, T. Dienes, D.P. Fergenson, and K.A. Prather (1997), Real-time analysis of individual atmospheric aerosol particles: Design and performance of a portable ATOFMS, *Anal. Chem.*, *69* (20), 4083-4091.

Gard, E.E., M.J. Kleeman, D.S. Gross, L.S. Hughes, J.O. Allen, B.D. Morrical, D.P. Fergenson, T. Dienes, M.E. Galli, R.J. Johnson, G.R. Cass, and K.A. Prather (1998), Direct observation of heterogeneous chemistry in the atmosphere, *Science*, *279* (5354), 1184-1187.

Gauderman, W.J., R. McConnell, F. Gilliland, S. London, D. Thomas, E. Avol, H. Vora, K. Berhane, E.B. Rappaport, F. Lurmann, H.G. Margolis, and J. Peters (2000), Association between air pollution and lung function growth in southern California children, *American Journal of Respiratory and Critical Care Medicine*, *162* (4), 1383-1390.

Gross, D.S., M.E. Galli, P.J. Silva, and K.A. Prather (2000), Relative sensitivity factors for alkali metal and ammonium cations in single particle aerosol time-of-flight mass spectra, *Anal. Chem., 72* (2), 416-422.

Guazzotti, S.A., K.R. Coffee, and K.A. Prather (2001), Continuous measurements of size-resolved particle chemistry during INDOEX-Intensive Field Phase 99, *J. Geophys. Res.-[Atmos.], 106* (D22), 28607-28627.

Healy, R.M., I.P. O'Connor, S. Hellebust, A. Allanic, J.R. Sodeau, and J.C. Wenger (2009), Characterization of single particles from in-port ship emissions, *Atmos Environ, 43*, 6408-6414.

Hobbs, P.V., T.J. Garrett, R.J. Ferek, S.R. Strader, D.A. Hegg, G.M. Frick, W.A. Hoppel, R.F. Gasparovic, L.M. Russell, D.W. Johnson, C.D. O'Dowd, P.A. Durkee, K.E. Nielsen, and G. Innis (2000), Emissions from ships with respect to their effects on clouds, *Journal of Atmospheric Sciences, 57*, 2570-2590.

Hudson, J.G., T.J. Garrett, P.V. Hobbs, S.R. Strader, Y. Xie, and S.S. Yum (2000), Cloud condensation nuclei and ship tracks, *Journal of Atmospheric Sciences, 57*, 2696-2706.

Kasper, A., S. Aufdenblatten, A. Forss, M. Mohr, and H. Burtscher (2007), Particulate emissions from a low-speed marine diesel engine, *Aerosol Sci. Tech., 41* (1), 24-32.

Lack, D.A., C.D. Cappa, J. Langridge, R. Bahreini, G. Buffaloe, C. Brock, K. Cerully, D. Coffman, K. Hayden, J. Holloway, B. Lerner, P. Massoli, S.-M. Li, R. McLaren, A.M. Middlebrook, R. Moore, A. Nenes, I. Nuaaman, T.B. Onasch, J. Peischl, A. Perring, P.K. Quinn, T. Ryerson, J.P. Schwartz, R. Spackman, S.C. Wofsy, D. Worsnop, B. Xiang, and E. Williams (2011), Impact of fuel quality regulation and speed reductions on shipping emissions: Implications for climate and air quality, *Environ. Sci. Tech., 45* (20), 9052-9060.

Lack, D.A., J.J. Corbett, T. Onasch, B. Lerner, P. Massoli, P.K. Quinn, T.S. Bates, D.S. Covert, D. Coffman, B. Sierau, S. Herndon, J. Allan, T. Baynard, E. Lovejoy, A.R. Ravishankara, and E. Williams (2009), Particulate emissions from commercial shipping: Chemical, physical, and optical properties, *J. Geophys. Res.-[Atmos.], 114*, D00F04, doi:10.1029/2008JD011300.

Malm, W.C., B.A. Schichtel, M.L. Pitchford, L.L. Ashbaugh, and R.A. Eldred (2004), Spatial and monthly trends in speciated fine particle concentration in the United States, *J. Geophys. Res., 109* (D03306), doi:10.1029/2003JD003739.

Murphy, S.M.A., H.; Sorooshian, A.; Padro, L. T.; Gates, S.W. H.; Hersey, W. A.; Jung, H.; Miller, J. W.; Cocker, D. R., and A.J. Nenes, H. H.; Flagan, R. C.; Seinfeld, J.

H. (2009), Comprehensive simultaneous shipboard and airborne characterization of exhaust from a modern container ship at sea., *Environ. Sci. Tech.*, *43* (13), 4626-4640.

Neubauer, K.R., M.V. Johnston, and A.S. Wexler (1997), On-line analysis of aqueous aerosols by laser desorption ionization, *International Journal of Mass Spectrometry and Ion Processes*, *163* (1-2), 29-37.

Neubauer, K.R., M.V. Johnston, and A.S. Wexler (1998), Humidity effects on the mass spectra of single aerosol particles, *Atmos. Environ.*, *32* (14-15), 2521-2529.

Noble, C.A., and K.A. Prather (1996), Real-time measurement of correlated size and composition profiles of individual atmospheric aerosol particles, *Environ. Sci. Tech.*, *30* (9), 2667-2680.

Petroleum products--Fuels (Class F) Specifications of Marine Fuels, edited by I.S. Organization, Geneva, 2010.

Pinkerton, K.E., Y.M. Zhou, S.V. Teague, J.L. Peake, R.C. Walther, I.M. Kennedy, V.J. Leppert, and A.E. Aust (2004), Reduced lung cell proliferation following short-term exposure to ultrafine soot and iron particles in neonatal rats: Key to impaired lung growth? *Inhalation Toxicology*, *16*, 73-81.

Pope, C.A., and D.W. Dockery (2006), Health effects of fine particulate air pollution: Lines that connect, *Journal of the Air & Waste Management Association*, *56* (6), 709-742.

Poschl, U. (2005), Atmospheric aerosols: Composition, transformation, climate and health effects, *Angewandte Chemie-International Edition*, *44* (46), 7520-7540.

Prather, K.A., T. Nordmeyer, and K. Salt (1994), Real-Time Characterization of Individual Aerosol-Particles Using Time-of-Flight Mass-Spectrometry, *Anal. Chem.*, *66* (9), 1403-1407.

Radke, L.F., J.A. Coakley, and M.D. King (1989), Direct and Remote-Sensing Observations of the Effects of Ships on Clouds, *Science*, *246* (4934), 1146-1149.

Roberts, G.C., and A. Nenes (2005), A continuous-flow streamwise thermal-gradient CCN chamber for atmospheric measurements, *Aerosol Sci. Tech.*, *39* (3), 206-221.

Russell, L.M., J.H. Seinfeld, R.C. Flagan, R.J. Ferek, D.A. Hegg, P.V. Hobbs, W. Wobrock, A.I. Flossmann, C.D. O'Dowd, K.E. Nielsen, and P.A. Durkee (1999), Aerosol dynamics in ship tracks, *J. Geophys. Res.-[Atmos.]*, *104* (D24), 31077-31095.

Shields, L.G., D.T. Suess, and K.A. Prather (2007), Determination of single particle mass spectral signatures from heavy-duty diesel vehicle emissions for PM2.5 source apportionment, *Atmos. Environ., 41* (18), 3841-3852.

Singh, M., P.A. Jaques, and C. Sioutas (2002), Size distribution and diurnal characteristics of particle-bound metals in source and receptor sites of the Los Angeles Basin, *Atmos. Environ., 36* (10), 1675-1689.

Slingo, A. (1990), Sensitivity of the Earth's radiation budget to changes in low clouds, *Nature, 343* (6253), 49-51.

Song, X.H., P.K. Hopke, D.P. Fergenson, and K.A. Prather (1999), Classification of single particles analyzed by ATOFMS using an artificial neural network, ART-2a, *Anal. Chem., 71* (4), 860-865.

Spencer, M.T., L.G. Shields, D.A. Sodeman, S.M. Toner, and K.A. Prather (2006), Comparison of oil and fuel particle chemical signatures with particle emissions from heavy and light duty vehicles, *Atmos. Environ., 40* (27), 5224-5235.

Su, Y.X., M.F. Sipin, H. Furutani, and K.A. Prather (2004), Development and characterization of an aerosol time-of-flight mass spectrometer with increased detection efficiency, *Anal. Chem., 76* (3), 712-719.

Twomey, S. (1977), The influence of pollution on the shortwave albedo of clouds, *J. Atmos. Sci., 34* (7), 1149-1152.

Chapter 7

7. Real-Time Detection and Mixing State of Methanesulfonate in Single Particles at an Inland Urban Location during a Phytoplankton Bloom

7.1 Synopsis

Dimethyl sulfide (DMS), produced by oceanic phytoplankton, is oxidized to form methanesulfonic acid (MSA) and sulfate, which influence particle chemistry and hygroscopicity. Unlike sulfate, MSA has no known anthropogenic sources making it a useful tracer for ocean-derived biogenic sulfur. Despite numerous observations of MSA, predominately in marine environments, the production pathways of MSA have remained elusive highlighting the need for additional measurements, particularly at inland locations. During the Study of Organic Aerosols in Riverside, CA from July-August 2005 (SOAR-1), MSA was detected in submicron and supermicron particles using real-time, single-particle mass spectrometry. MSA was detected due to blooms of DMS-producing organisms along the California coast. The detection of MSA depended on both the origin of the sampled air mass as well as the concentration of oceanic chlorophyll present. MSA was mainly mixed with coastally emitted particle types implying that partitioning of MSA occurred before transport to Riverside. Importantly, particles containing vanadium had elevated levels of MSA compared to particles not containing vanadium, suggesting a possible catalytic role of vanadium in MSA formation. This study demonstrates how anthropogenic, metal-containing aerosols can

enhance the atmospheric processing of biogenic emissions, which need to be considered when modeling coastal as well as urban locations.

7.2 Introduction

Aerosols contribute significantly to climate change by directly scattering and absorbing incoming solar radiation and acting as cloud condensation nuclei (CCN) [*Poschl*, 2005]. Sulfate is an aerosol species of particular climatic importance from a scattering perspective in addition to enhancing the cloud forming potential of aerosols [*Kiehl and Briegleb*, 1993]. In Riverside, CA, sulfate comprises up to 13-20% of the mass of particles ranging in size from 0.1-2.5 μm [*Singh et al.*, 2002]. Sulfate derives from sulfur dioxide (SO_2) oxidation forming sulfuric acid (H_2SO_4), which condenses onto particles; sources of sulfate include both anthropogenic [*Barnes et al.*, 2006] and biogenic sources with the most important biogenic sulfate source being the oxidation of dimethyl sulfide (DMS) [*Bates et al.*, 1992]. DMS is produced from the enzymatic cleavage of dimethylsulphoniopropionate (DMSP), a compound produced by oceanic phytoplankton [*Bates et al.*, 1992; *Charlson et al.*, 1987]. A simplified reaction scheme of DMS oxidation adopted from Hopkins et al. (2008) and von Glasow and Crutzen (2004) is shown below [*Hopkins et al.*, 2008; *von Glasow and Crutzen*, 2004].

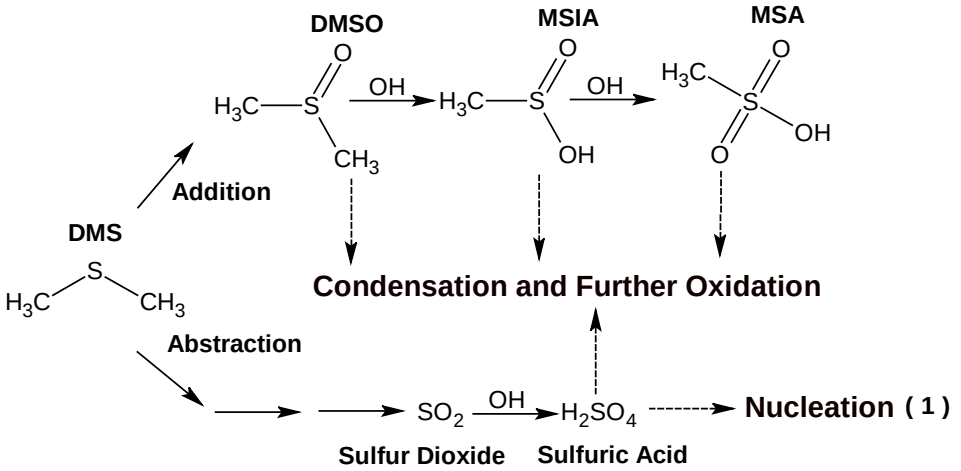

Sulfate formation from DMS primarily derives from the OH-abstraction path [*Barnes et al.*, 2006; *Hopkins et al.*, 2008] leading to sulfate formation on pre-existing particles or the homogeneous nucleation of particles, which act as a new source of CCN potentially increasing cloud droplet number [*Hopkins et al.*, 2008; *Kreidenweis and Seinfeld*, 1988]. Organosulfur compounds such as dimethyl sulfoxide (DMSO), methanesulfinic acid (MSIA), and methanesulfonic acid (MSA), as well as other products, are also produced from DMS oxidation via the OH-addition pathway. DMSO primarily condenses onto pre-existing particles and droplets where oxidation to form the intermediate MSIA and the more stable product, MSA, takes place; aqueous phase processing enhances the kinetics of these oxidation processes [*Bardouki et al.*, 2002; *Barnes et al.*, 2006; *Hopkins et al.*, 2008]. MSA can also be oxidized in the condensed phase leading to the formation of additional sulfate; however, this is slower and less efficient than the abstraction pathway [*Bardouki et al.*, 2002; *Barnes et al.*, 2006]. Since condensation and aqueous phase processing is favored over nucleation, organosulfur compounds are not known to act as a new source of CCN [*Barnes et al.*, 2006; *Hopkins et al.*, 2008; *Kreidenweis and Seinfeld*, 1988]. Because of the opposing influence that

different sulfur compounds can have on cloud droplet number, it is important to distinguish between these species to understand their formation and evolution in atmospheric aerosols.

Previous measurements of DMS oxidation products, primarily sulfate and MSA, typically used off-line bulk analysis techniques. These measurements revealed that particle mass concentrations of both sulfate and MSA peak during the summer, and the ratio of the two species depend on factors such as temperature, presence of clouds, presence of NO_x, and contribution of anthropogenic sulfate [*Ganor et al.*, 2000; *Hopkins et al.*, 2008; *Kouvarakis and Mihalopoulos*, 2002; *Watts et al.*, 1990]. Because sulfate has anthropogenic and biogenic sources, MSA is also measured alone as an indicator of biogenic sulfur. Using on-line instrumentation, Phinney et al. (2006) and Zorn et al. (2008) quantified MSA at sea using an aerosol mass spectrometer (AMS) showing diurnal trends in particulate MSA concentrations and correlations with oceanic biological activity demonstrating the importance of real-time measurements [*Phinney et al.*, 2006; *Zorn et al.*, 2008]. Single particle observations of the mixing state of MSA-containing particles have primarily shown MSA to be in the form of sodium and ammonium salts [*Hopkins et al.*, 2008; *Kolaitis et al.*, 1989]. While each of these studies has contributed significantly to our understanding of the conditions when MSA formation occurs, the impacts of intense oceanic blooms on MSA and sulfate concentrations at inland locations remains unexplored. A number of important questions exist with regards to MSA in inland urban locations: (i) how much of a contribution does biogenic sulfur make to urban aerosols during periods of high biological oceanic activity?, (ii) what degree of

interaction occurs between ocean-derived biogenic emissions and anthropogenic aerosols?, and (iii) how is MSA distributed within individual particles? The goal of this paper is to shed further light on these questions by performing real-time, single-particle measurements of MSA-containing aerosols at an inland, urban environment.

During the summer of 2005 as part of the Study of Organic Aerosols in Riverside, CA (SOAR-1), real-time mass spectrometry measurements detected individual ambient aerosols with MSA. Furthermore, co-located AMS measurements corroborated the presence of organosulfur species (MSA) during SOAR-1 [*Huffman et al.*, 2009]. The summer Riverside aerosol showed the largest impacts from the ocean when daily westerly winds transported coastal emissions across the Los Angeles (LA) Basin to Riverside [*Qin et al.*, 2009]. In the summer of 2005, intense blooms of *L. polyedrum* prevailed off the coast of southern California [*Mayali et al.*, 2008]. Because dinoflagellate species of phytoplankton such as *L. polyedrum* are known to produce high concentrations of DMSP and DMSO [*Hatton and Wilson*, 2007], SOAR-1 was influenced by anomalously high concentrations of ocean-derived biogenic sulfur. Single-particle, size-resolved chemistry and diurnal trends of MSA are used herein to elucidate the influence of elevated ocean-derived biological activity on aerosol chemistry at an inland urban location.

7.3 Methods

During SOAR-1, ambient measurements were made on the University of California, Riverside campus, approximately 60 miles inland from the Pacific Ocean from July 30-August 15, 2005 (http://cires.colorado.edu/jimenez-

group/Field/Riverside05/). Meteorological parameters including wind direction, wind speed, and relative humidity (RH) were measured at the site. Chlorophyll data, which serves as a proxy for oceanic biological activity, was obtained from the Southern California Coastal Ocean Observing System (SCCOOS) (www.sccoos.org) from the Newport Beach station at approximately 33.6ºN, 117.9°W. Data was also obtained from the Scripps Institution of Oceanography (SIO) Pier at 32.87ºN, 117.3°W to supplement data from the Newport Beach station by illustrating the high levels of biological activity off the California coast from a historical perspective since this station has measured chlorophyll for roughly 20 years. Data from the Newport Beach station is used for direct comparison of chlorophyll concentrations with the detection of MSA based on the air mass back trajectories, which indicate that the air masses travelled closer to this station than the SIO Pier station before reaching Riverside, thus providing a more accurate proxy of biological activity. Surface chlorophyll concentrations were measured twice a week at the SIO Pier, and concentrations at ~3 m depth were measured every 4 minutes using automated sensors at both the SIO Pier and the Newport Beach station. All data are presented in Pacific Standard Time (PST), one hour behind local time.

The size-resolved chemical composition of individual aerosols was obtained in real-time using an aerosol time-of-flight mass spectrometer (ATOFMS) with a size range of 0.2-3.0 μm. The ATOFMS has been described in detail elsewhere [*Gard et al.*, 1997]. Briefly, particles are sampled through a converging nozzle where they enter a differentially pumped vacuum region causing the particles to be accelerated to their terminal velocity. The particles next enter a light scattering region consisting of two

continuous-wave lasers (532 nm) located at a fixed distance from one another. The time required to traverse these two lasers is correlated to the terminal velocity of the particle; the velocity is converted to an aerodynamic diameter by calibrating with polystyrene latex spheres of a known size. A 266 nm Nd:YAG laser desorbs and ionizes species from individual particles producing both positive and negative ions that are analyzed in a dual-polarity time-of-flight mass spectrometer.

A software toolkit, YAADA, was used to import ion peak lists into MATLAB (The MathWorks) allowing for the analysis of ATOFMS data [*Allen*, 2002]. Searches for MSA-containing particles, characterized by an intense peak at *m/z* -95 ($CH_3SO_3^-$) [*Neubauer et al.*, 1996; *Silva and Prather*, 2000], were performed by selecting a peak area of 300 or above for *m/z* -95. Fresh sea salt particles produce $NaCl_2^-$ cluster ions at *m/z* -93, -95, and -97 [*Guazzotti et al.*, 2001], which could interfere with the assignment of *m/z* -95 to MSA. However, almost all of the detected sea salt particles (>99%) were aged as indicated by the strong presence of nitrate and sulfate that heterogeneously displaced chloride [*Gard et al.*, 1998] allowing for the unambiguous assignment of *m/z* -95 to MSA. The measured particle mass spectra were then analyzed using a clustering algorithm (ART-2a), which groups particles together based on mass spectral similarities [*Song et al.*, 1999]. ART-2a was run separately for submicron (0.2-1.0 μm) and supermicron (1.0-3.0 μm) particles. Using ART-2a with a vigilance factor of 0.8, over 90% of MSA-containing particles and over 80% of non-MSA-containing particles were classified into 50 distinct clusters, providing a representative view of the aerosol composition during the study. Naming schemes for the particle types presented in this

paper are based on previous work [*Pastor et al.*, 2003; *Pratt and Prather*, 2009; *Qin et al.*, 2009]. Peak identifications within this paper correspond to the most probable ions for a given *m/z* ratio. The particle types observed were aged organic carbon (Aged OC), aged sea salt, amines, Ca-containing, dust, elemental carbon (EC), elemental carbon mixed with organic carbon (ECOC), ECOC and EC mixed with inorganic species (Inorganic ECOC and Inorganic EC, respectively), biomass burning (K-combustion), NH_4-containing, vanadium from combustion sources (OC-V-sulfate), and polycyclic aromatic hydrocarbons (PAH).

7.4 Results and Discussion

7.4.1 Temporal Trends of MSA-containing Particles and Biological Activity

ATOFMS measurements during SOAR-1 indicate that up to ~67% of the submicron (0.2-1.0 μm) and up to ~33% of supermicron (1.0-3.0 μm) particles by number contained MSA. The average negative ion mass spectrum for a representative MSA-containing particle type, shown in Figure 7.1, clearly shows a distinct ion marker at *m/z* -95 indicative of MSA. In Figure 7.2a, the fractions of all submicron and supermicron particles containing MSA and chlorophyll concentrations taken from the Newport Beach station at 3 m depth from July 30-August 15, 2005 are shown. The inset in Figure 7.2a shows 48-hour HYSPLIT air mass back-trajectories [*Draxler and Rolph,* 2003] representative of those occurring over the duration of the study in addition to the locations of the two automated stations collecting chlorophyll data. A comparison of the data collected at the two automated stations can be found in Figure 7.3. The chlorophyll

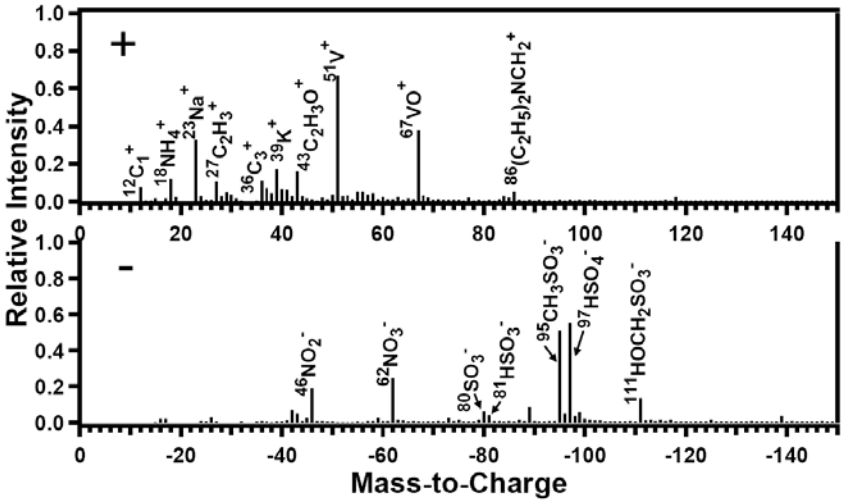

Figure 7.1: Average positive and negative ion mass spectra for the OC-V-sulfate particle type containing MSA (*m/z* -95) during SOAR-1.

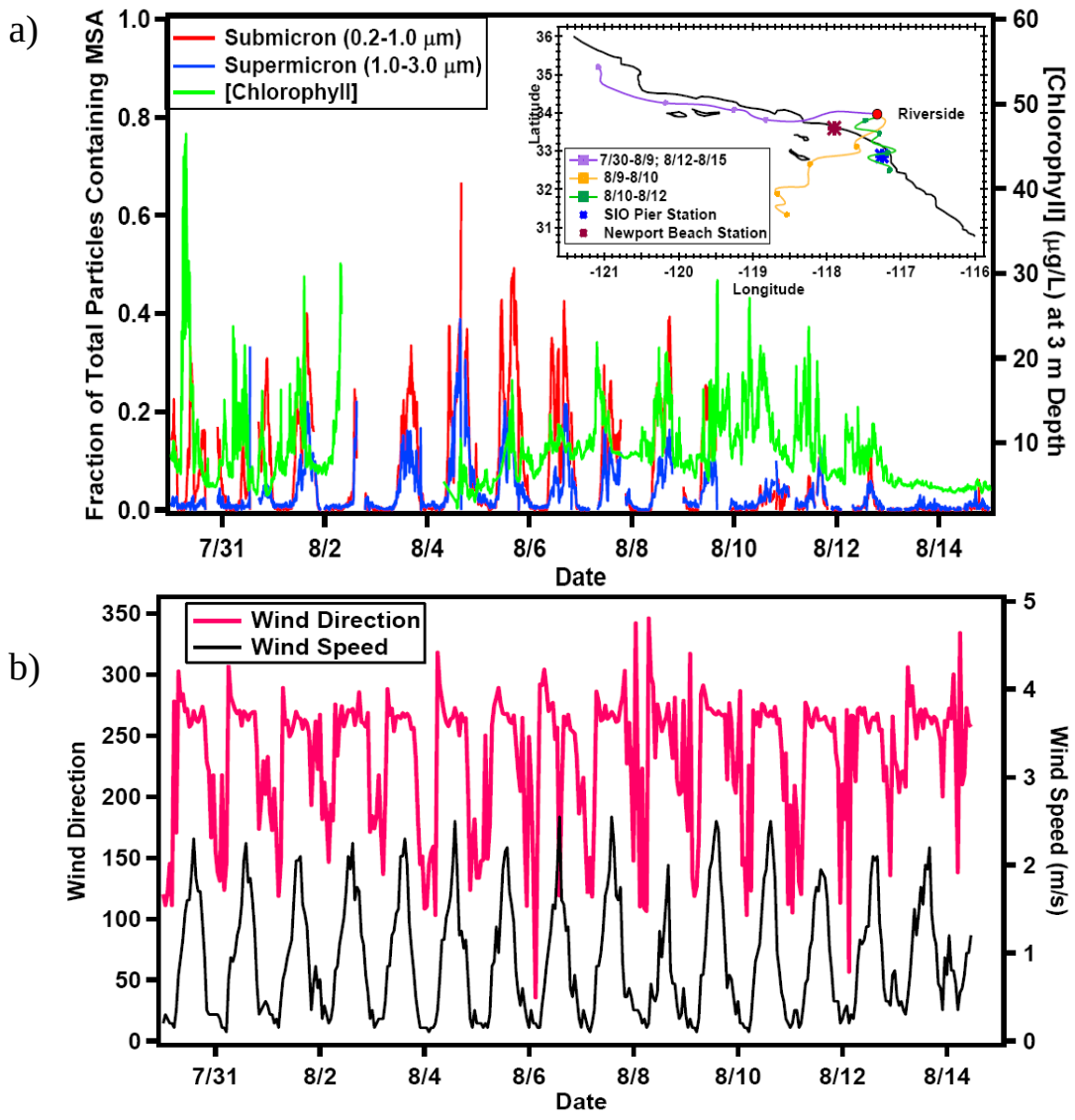

Figure 7.2: (a) Time series showing the fraction of MSA-containing submicron (red line) and supermicron (blue line) particles during SOAR-1 and chlorophyll concentrations (green line) taken from the Newport Beach station (33.6ºN, 117.9°W) at 3 m depth. Gaps in chlorophyll data occur from August 2-4. Inset shows typical HYSPLIT 48 hour back-trajectories for air masses arriving to the sampling site during different time periods in addition to the locations of the automated chlorophyll stations. Each trajectory is taken at 500 m altitude, and each point on the trajectory corresponds to a 12-hour increment. (b) Time series showing the corresponding wind speed (black line) and direction (pink line).

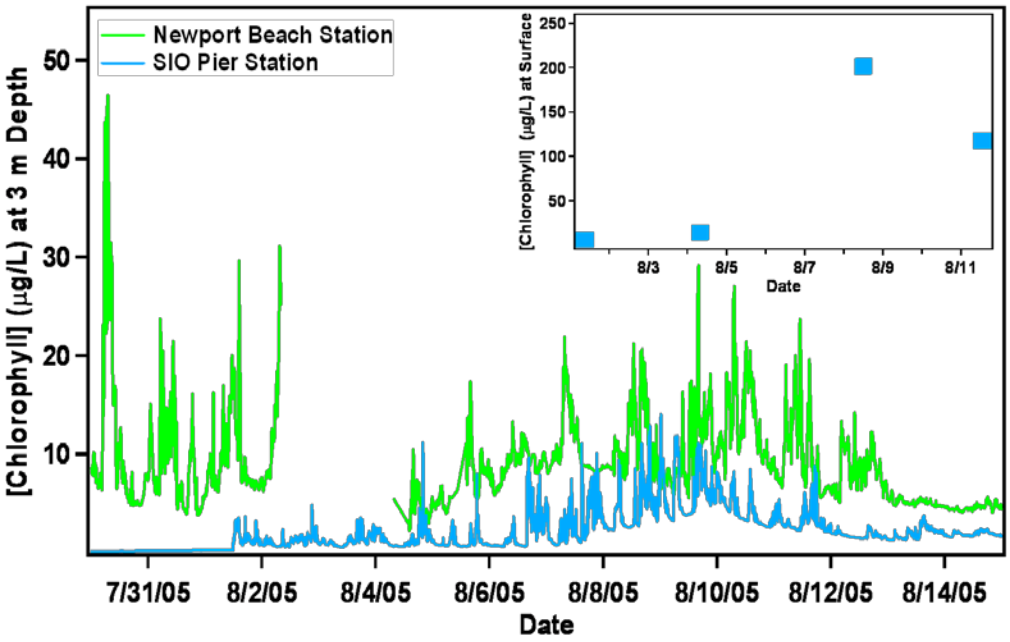

Figure 7.3: Chlorophyll data at 3 m depth from the Newport Beach (33.6ºN, 117.9°W) and SIO Pier (32.87ºN, 117.3°W) automated stations. Inset is chlorophyll data measured at the surface of the SIO Pier.

concentrations taken at 3 m depth for both stations are comparable showing similarities in diurnal trends and similar magnitudes of chlorophyll concentrations. Inset in this figure is the surface chlorophyll data taken at the SIO Pier. The chlorophyll measurements show elevated concentrations and a diurnal pattern consistent with the presence of a phytoplankton bloom. Although the SIO Pier station has two depths of chlorophyll data and a longer continuous data set, the data from the Newport Beach station was primarily used in this paper due to the fact that the air masses travelled closer to this station than the SIO Pier station before reaching the sampling site as seen in Figure 7.2. Chlorophyll data from the SIO Pier station provided a historical context to base our assertion that high levels of biological oceanic activity occurred during SOAR-1. Three main air mass trajectory patterns were observed with transport times estimated from HYSPLIT ranging from ~8 hours to longer than a day [*Draxler and Rolph*, 2003; *Qin et al.*, 2009]: (i) "Coastal" occurred between July 30-August 9 and resumed August 12-15 with sampled air masses originating from the Pacific Ocean northwest of LA traversing near the Newport Beach station before arriving to Riverside, (ii) "Open Ocean" occurred August 9-10 and originated further from the coast toward the open ocean, and (iii) "Inland/Stagnant" occurred August 10-12 with limited oceanic transport resulting in an observed decrease in the fraction of MSA-containing particles on August 10 as shown in Figure 7.2a. Additionally, Figure 7.2b shows the corresponding wind speed and direction during this time period. Comparison of the time series in Figure 7.2a and 7.2b shows a strong diurnal trend with fractions of MSA-containing particles increasing ~6-8 hours following the onset of westerly winds and increased wind speed during coastal transport conditions, as verified by HYSPLIT air mass back trajectories (e.g. 7/30-8/9 as shown in

Figure 7.2a). Day-to-day variations can be explained, in part, by changes in meteorological conditions.

In addition to meteorology, oceanic biological activity also influenced the observed fractions of MSA-containing particles. On August 12, the air masses follow the "Coastal" trajectories; however, in contrast to July 30-August 9, the fractions of MSA remained low (Figure 7.2a). This is attributed to an observed decrease in oceanic chlorophyll concentrations to ≤ 5 μg/L (Figure 7.2a), which followed the end of the major phytoplankton bloom on August 11 [*Mayali et al.*, 2008]. Prior to this, diurnal spikes in both the fraction of MSA-containing particles and chlorophyll concentrations were observed with daily chlorophyll concentrations typically reaching up to ~25-30 μg/L. Similar spikes in chlorophyll were observed from the same depth at the SIO Pier in La Jolla, CA. At the same time, surface chlorophyll concentrations measured twice per week at the SIO Pier reached as high as ~200 μg/L. Analysis of 18 years of surface chlorophyll measured at the SIO Pier yields an average of 2.5 μg/L with a maximum of 218.95 μg/L [*Kim et al.,* 2009] indicating that anomalously high levels of biological activity were occurring off the coast of California during SOAR-1 resulting in the detection of large number fractions of MSA-containing particles, as shown herein. Furthermore, we speculate that some of the MSA detected in Riverside could oxidize completely impacting sulfate levels at locations further inland; however, no measurements were made at these locations. The contribution of biogenic sulfur during summer has been established for several coastal locations [*Ganor et al.*, 2000; *Kouvarakis and Mihalopoulos*, 2002; *Watts et al.*, 1990]; however, these are the first real-

time, single-particle measurements of MSA at an inland location during a period of intense biological activity establishing how oceanic biological activity could impact both MSA and, potentially, sulfate levels at an inland urban location in California under the proper meteorological conditions. This is significant due to the interest in sorting out the major sources of sulfate in California and determining the relative proportions from anthropogenic sources (i.e. ships, heavy duty diesel vehicles) versus biogenic sources (i.e. oceanic biological activity).

7.4.2 Temporal Trends of MSA-containing Particles and Biological Activity

Riverside is impacted by local sources including vehicle exhaust and nearby Chino dairy farms, which contribute to ammonium, nitrate, carbonaceous, and amine concentrations, in addition to transported particle types from the LA coast, which provide a source of ocean-derived aerosol species and additional sources of combustion aerosols [*Hughes et al.*, 2000; *Pastor et al.*, 2003; *Pratt and Prather*, 2009]. To gain further insight into the sources and processes contributing to the presence of MSA, we examined the mixing state of MSA-containing particles. The size-resolved, single-particle mixing state of MSA-containing particles is illustrated in Figure 7.4 for submicron and supermicron particles. While Figure 7.4 classifies MSA-containing particles into general particle types based on the most prevalent ion peaks, it is important to note that ~76% and ~45% of MSA-containing submicron particles, by number, were internally mixed with ammonium and sodium, respectively, and ~83% and ~71% of MSA-containing supermicron particles, by number, were internally mixed with ammonium and sodium, respectively. The prevalence of these two species with MSA is expected based on

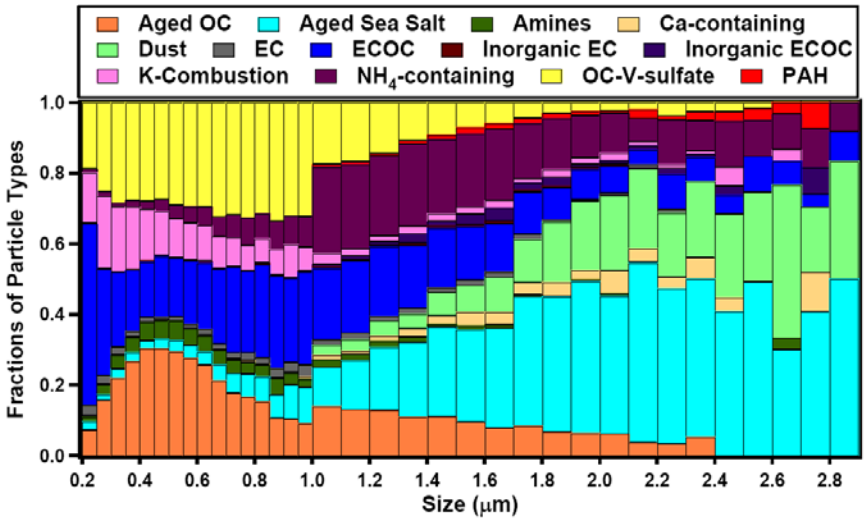

Figure 7.4: MSA-containing particle types plotted as a function of size. Submicron (0.2-1.0 μm) particles are plotted in 0.05 μm bins while supermicron (1.0-3.0 μm) particles are plotted in 0.1 μm bins.

previous measurements of the mixing state of MSA-containing particles [*Hopkins et al.*, 2008; *Kolaitis et al.*, 1989]. Additionally, ~87% of MSA-containing submicron and ~82% of MSA-containing supermicron particles contained sulfate (*m/z* -97 (HSO_4^-)), which is expected since DMS and, to a lesser extent, MSA oxidation also produces sulfate [*Bardouki et al.*, 2002; *Barnes et al.*, 2006]. In sum, ~25% of all submicron and ~22% of all supermicron particles, by number, contained sulfate. However, since ATOFMS measurements cannot distinguish biogenic and anthropogenic sulfate contributions to *m/z* -97, the relative contribution of biogenic sulfate cannot be inferred herein. MSA was mixed primarily with transported and aged particle types, and a higher percentage of submicron particles contained MSA (up to 67%) in comparison to the supermicron particles (up to 33%) as shown in Figure 7.5 likely due to the enhanced particle surface area in this size range. MSA and its organosulfur precursors are condensable species that contribute to particle growth rather than nucleation [*Barnes et al.*, 2006; *Kreidenweis and Seinfeld*, 1988]. MSA has typically been measured as sodium or ammonium salts associated with smaller aerosol particles (diameter > 2 μm) [*Kolaitis et al.*, 1989]. Because the measurements shown in this manuscript have shown a wide variation in the mixing-state of particles containing MSA, the size distribution of MSA-containing particles was examined and compared to the size distribution of the total hit particles during SOAR-1 (Figure 7.5). The particle detection efficiency of the ATOFMS depends on particle size. This is namely due to the transmission efficiency of the nozzle inlet, which creates a sharp peak at 1.7 μm [*Allen et al.*, 2000; *Qin et al.*, 2006]. Ambient number concentrations of aerosols; however, display an opposing trend with higher number concentrations at smaller particle sizes [*Seinfeld and Pandis*, 2006].

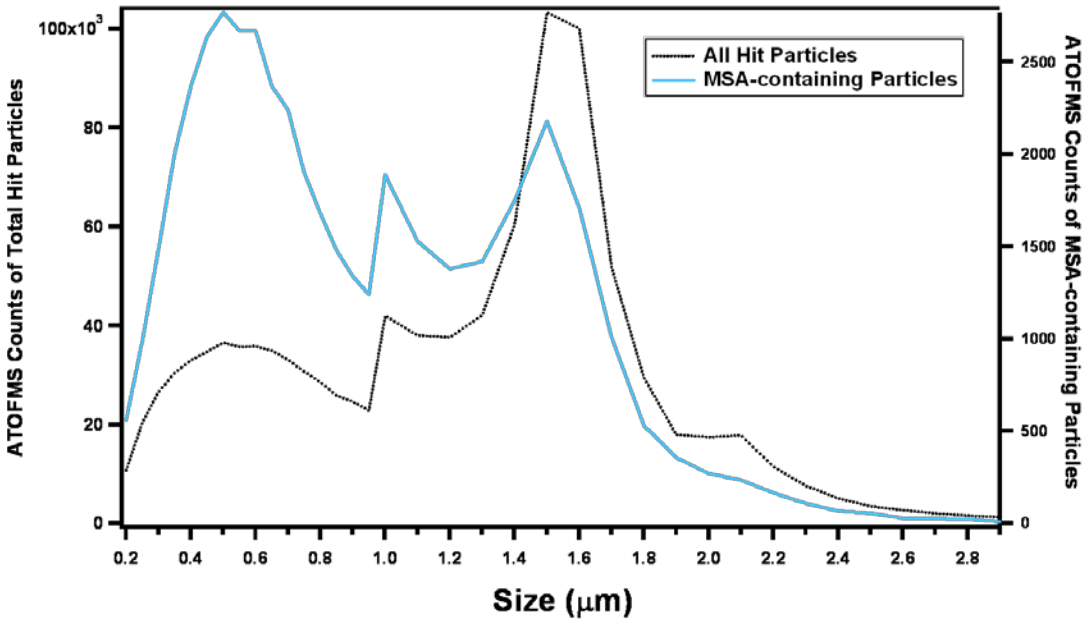

Figure 7.5: Size distributions of all hit particles (black line) during SOAR-1 and only MSA-containing particles (blue line).

These two opposing factors result in a bimodal size distribution as seen in Figure 7.5, which is a representative size distribution of hit particles obtained from the ATOFMS. Comparison of the size distribution of the total hit particles and the size distribution of MSA-containing particles shows a relative enrichment of MSA on submicron particles.

Comparison of MSA-containing particles with all observed particle types for SOAR-1 revealed that some particle types contained little to no MSA while large fractions of other particle types contained MSA. No MSA was detected on submicron dust, and only ~3% of the total observed supermicron dust contained MSA, which is expected since dust is locally produced unlike MSA [*Hughes et al.*, 2000]. Interestingly, only small fractions of the measured carbonaceous particle types (e.g. Aged OC, EC, and ECOC) were found to contain MSA. It is possible that the accumulation of secondary species particularly OC, which was the most commonly observed carbonaceous particle type, on pre-existing particles during transport from the LA coast to Riverside could potentially mask the detection of MSA [*Hughes et al.*, 2000; *Pratt and Prather*, 2009]. Certain particle types, however, were found to be enriched in MSA: approximately 37% and ~20% of the total observed OC-V-sulfate submicron and supermicron particles, respectively, and ~33% of aged sea salt submicron particles contained MSA. The OC-V-sulfate particle type is associated with residual fuel combustion primarily from ships [*Ault et al.*, 2009a; *Ault et al.*, 2009b; *Isakson et al.*, 2001]. OC-V-sulfate particles and aged sea salt are both coastally emitted along with DMS, which suggests that DMS oxidation products primarily partitioned onto coastal particle types that then underwent

aging as they were transported inland. Therefore, MSA is a useful marker for segregating transported versus locally generated particles.

7.4.3 Correlation of MSA with Other Species

During SOAR-1, MSA-containing particles were typically associated with fog processing markers (see Figure 7.1) at *m/z* -81 (HSO_3^-) and -111 ($HOCH_2SO_3^-$), which are the ion markers for the organosulfur compound hydroxymethanesulfonate (HMS) [*Neubauer et al.*, 1996; *Qin and Prather*, 2006; *Whiteaker and Prather*, 2003]. Figure 7.6 illustrates the temporal trends observed for submicron MSA, V, sulfate, and HMS-containing particles and RH. The correlation between V and MSA-containing particles (R^2 = 0.57) can be attributed to the fact that they were both coastally emitted as well as the potential catalytic role of vanadium in enhancing MSA on particles described in the next section. Submicron particles containing MSA and sulfate were also correlated (R^2 = 0.68) potentially implying a common source for both species. The correlation between MSA and HMS was very strong (R^2 = 0.84), which suggests the important role of aqueous phase chemistry in MSA formation [*Bardouki et al.*, 2002] as well as the hygroscopic nature of MSA [*Barnes et al.*, 2006]. Previous studies have shown HMS tracking RH during stagnant fog events [*Whiteaker and Prather*, 2003]; however, HMS was not correlated with RH during this study suggesting that the formation of HMS was not due to local increases in RH. HMS was instead correlated with MSA suggesting that MSA-containing particles had undergone aqueous phase processing either coastally or during transport to Riverside.

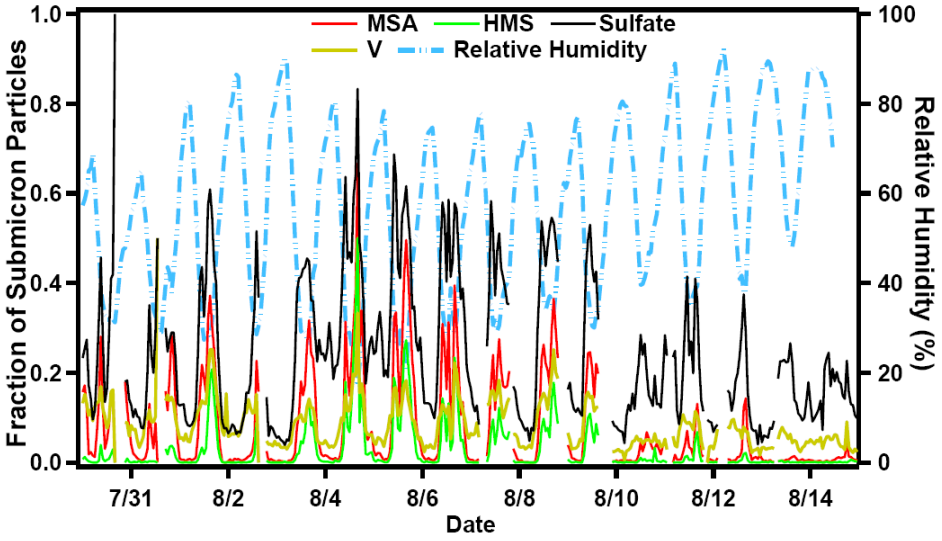

Figure 7.6: Temporal profile of ATOFMS counts of submicron MSA- (red line), HMS- (green line), sulfate- (black line) and V- (brown line) containing particles. Relative humidity (RH) is also shown (dashed blue line).

7.4.4 Role of Vandium in MSA Formation

Vanadium is one of the most common metals observed in Riverside, particularly during coastal transport conditions [*Pratt and Prather*, 2009; *Singh et al.*, 2002]. Vanadium is used to catalyze the oxidation of sulfur species such as S(IV) [*Dunn et al.*, 1999] and DMS [*Sahle-Demessie and Devulapelli*, 2008] under industrial conditions. To better understand the observed correlation between vanadium and MSA-containing particles described above, the relationship between MSA and vanadium was further investigated. MSA-containing particles were grouped by particle type and subdivided into particles with and without V by segregating particles containing *m/z* +51 (V^+) and +67 (VO^+). ATOFMS utilizes laser desorption/ionization corresponding to an energy input of 4.7eV/photon (at 266nm) [*Lide*, 2009] producing ~9.4eV for a two photon ionization. This energy input makes this technique very sensitive to trace metals since the ionization potential of metals is low [*Carson et al.*, 1995; *Gross et al.*, 2000; *Lide*, 2009]. Because of this sensitivity, a true distinction between particles mixed with V and those without V can be made. Figure 7.7 shows representative spectra from one particular particle type (aged sea salt) mixed with vanadium (Figure 7.7a) and without vanadium (Figure 7.7b). The amount of MSA on each particle type containing V and those not containing V was compared by averaging ion peak areas. The peak area of a particular *m/z* can be related to the relative amount of a specific chemical species on each particle type [*Bhave et al.*, 2002; *Gross et al.*, 2000]; Figure 7.8 shows a comparison for the major particle types detected during the study. During the laser desorption/ionization process, variations in ion intensity can occur depending on the chemical matrix of the

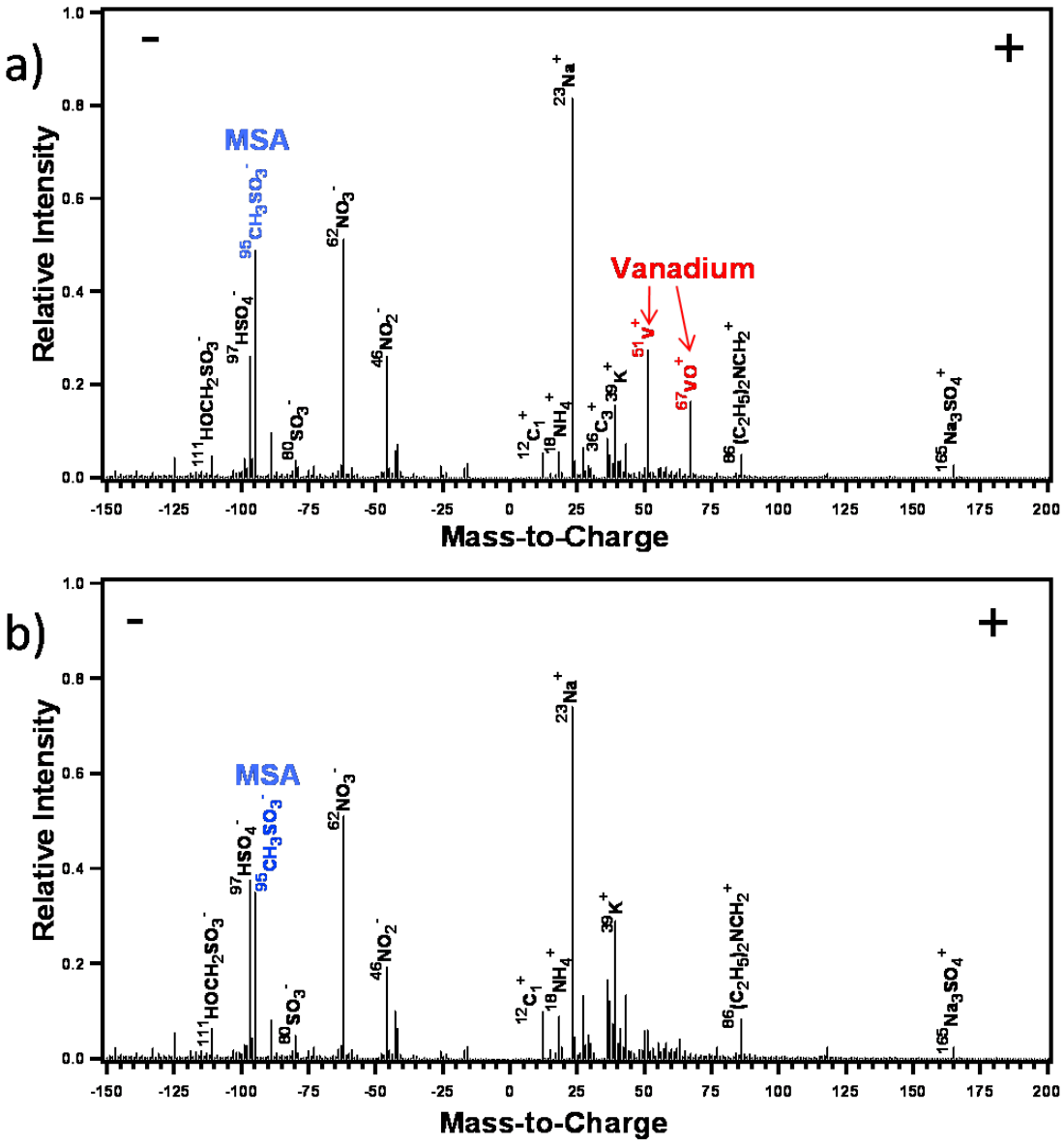

Figure 7.7: Representative average aged sea salt positive and negative ion mass spectra of particles (a) mixed with and (b) without V.

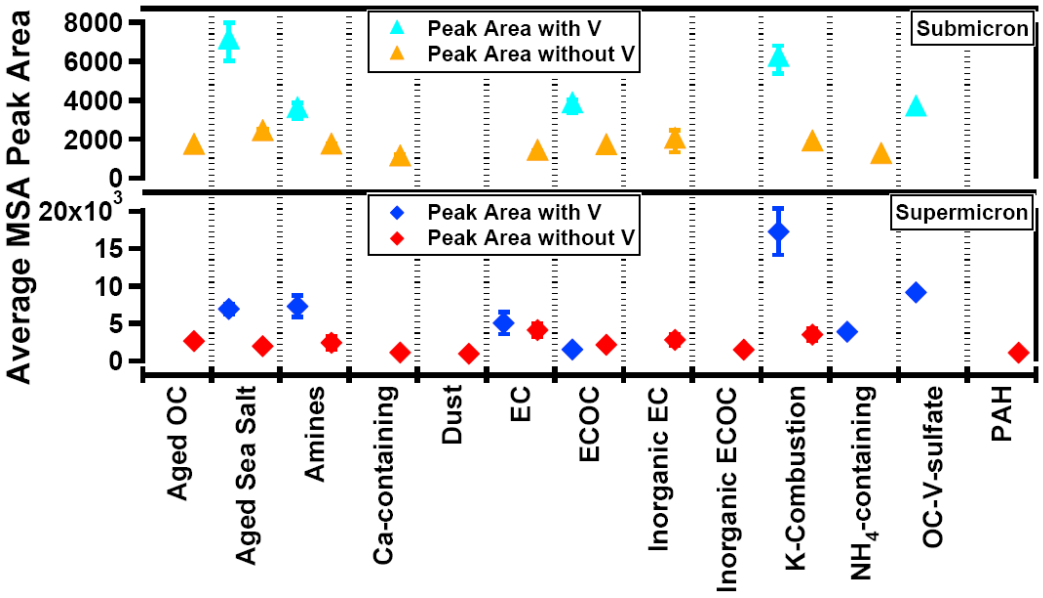

Figure 7.8: Average peak area of MSA (*m/z* -95) for MSA-containing submicron particle types mixed with V (light blue triangles) and submicron particles containing no V (orange triangles) are shown in the top panel. The average peak area of MSA on supermicron particles containing V (dark blue diamonds) and containing no V (red diamonds) are shown in the bottom panel. The vertical bars correspond to 95% confidence intervals associated with the peak areas.

particle [*Bhave et al.*, 2002]. It is important to note that the particles shown in Figure 7.8 have been separated into different matrices, based on general particle type, and the MSA ion intensities are only compared for the same chemical matrix. Furthermore, vanadium represents a small mass fraction of the total particle mass [*Ault et al.*, 2009b] so its presence or absence has a negligible effect on the overall chemical matrix. As shown in Figure 7.8, the peak area of MSA found on particles types that contained vanadium was, in general, ~3 times larger when compared to similar matrix particles not containing vanadium adding strong support that vanadium is acting as a catalyst for the formation of MSA. Another factor that must be considered is that the increased amount of MSA on particles internally mixed with vanadium could be solely due to the fact that both species were emitted along the coast leading to increased time for MSA formation to occur on these particles during transport to Riverside. However, if this were the case, then it would be expected that other coastally emitted particle types such as aged sea salt would also have higher amounts of MSA present regardless of whether it was internally mixed with vanadium or not. As shown in Figure 7.8, only the particles types, including aged sea salt, internally mixed with vanadium had higher amounts of MSA. This shows that transport time is not the only factor leading to enriched MSA in particles. Residual fuel also contains high levels of iron [2005], which is known to catalyze sulfur oxidation in the aqueous phase [*Alexander et al.*, 2009]. Because the ionization potential for vanadium is much lower (6.75 eV for V vs. 7.90 eV for Fe) [*Lide*, 2009] and hence the ATOFMS sensitivity for vanadium is higher than for iron, the possibility that iron is actually present and playing a role in catalyzing MSA formation rather than vanadium cannot be ruled out. However, these results show that different particle types emitted by

specific anthropogenic sources, in this case residual fuel burning from ships, enhance MSA and, potentially, sulfate production in atmospheric particles.

7.4.5 Atmospheric Implications

These measurements reveal how high biological oceanic activity can impact aerosol chemistry in an inland, urban environment. Periods when high levels of oceanic biological activity were observed correlated with high levels of MSA at an inland location, particularly on particles containing vanadium. Past measurements have primarily examined the influence of MSA on aerosols in clean marine environments. Our measurements, however, show that MSA can also condense onto anthropogenic particle types as well as sea salt. Future studies at multiple sampling locations spaced along a trajectory from the LA coast to inland locations should be conducted to further investigate how the mixing-state of MSA-containing particles evolves in urban locations. Previous ATOFMS studies have demonstrated the evolution of particle mixing-state within the LA Basin; however, time periods influenced by high levels of oceanic biological activity were not investigated [*Hughes et al.*, 2000].

This study shows how anthropogenic aerosols can influence the atmospheric processing of biogenically emitted sulfur species. Enhanced production of MSA has been observed for reactions between $MSIA_{(aq)}$ and Fe(III) [*Key et al.*, 2008]; however, little is known about the ability of anthropogenic emissions to influence the processing of ambient biogenic sulfur emissions. This study demonstrates the catalytic abilities of vanadium to enhance MSA formation; vanadium has also been shown to enhance the conversion of anthropogenically produced SO_2 to sulfate in a recent single-particle study

[*Ault et al.*, 2009a]. Typically, biogenic and anthropogenic sources are considered separately when describing aerosol and air pollution chemistry; however, this study highlights the importance of including anthropogenic aerosols from sources such as ships when estimating the production of MSA and sulfate in coastal and urban environments. Finally, both MSA and sulfate strongly influence particle hygroscopicity meaning that the enhanced production of either of these species by anthropogenic particle types could have significant implications for cloud droplet formation in both marine and inland environments.

7.5 Acknowledgements

The authors would like to acknowledge Paul Ziemann (UC Riverside), Ken Docherty (CU, Boulder), the UC Riverside Air Pollution Research Center, and the entire Prather group, particularly Laura Shields, for assistance during the SOAR-1 field campaign. The authors also thank Meagan McKay and the Goldstein group (UC Berkeley) for providing wind direction, wind speed, and relative humidity data. This work was supported by the California Air Resources Board (CARB 04-336). K. Pratt has been funded in part by an NSF Graduate Research Fellowship (2006-2009) and an EPA STAR Graduate Fellowship (2005-2006). The EPA has not officially endorsed this publication, and the views expressed herein may not reflect the views of the EPA. The authors gratefully acknowledge the NOAA Air Resources Laboratory (ARL) for the provision of the HYSPLIT transport and dispersion model and/or READY website (http://www.arl.noaa.gov/ready.html) used in this publication. The authors also gratefully acknowledge the Southern California Coastal Ocean Observing System

(SCCOOS) (www.sccoos.org/) for the provision of chlorophyll data used in this publication.

7.6 References

Petroleum products--Fuels (Class F) Specifications of Marine Fuels, edited by I.S. Organization, Geneva, 2005.

Alexander, B., R.J. Park, D.J. Jacob, and S. Gong (2009), Transition metal-catalyzed oxidation of atmospheric sulfur: Global implications for the sulfur budget, *J. Geophys. Res.*, *114* (D02309), doi:10.1029/2008JD010486.

Allen, J.O. (2002), YAADA software toolkit to analyze single-particle mass spectral data: Reference manual version 1.1, *Arizona State University*, http://www.yaada.org.

Allen, J.O., D.P. Fergenson, E.E. Gard, L.S. Hughes, B.D. Morrical, M.J. Kleeman, D.S. Gross, M.E. Galli, K.A. Prather, and G.R. Cass (2000), Particle detection efficiencies of aerosol time of flight mass spectrometers under ambient sampling conditions, *Environ. Sci. Tech.*, *34* (1), 211-217.

Ault, A.P., C.J. Gaston, Y. Wang, G. Dominguez, M.H. Thiemens, and K.A. Prather (2010), Characterization of the single particle mixing state of individual ship plume events measured at the port of Los Angeles, *Environ. Sci. Technol.*, *44* (6), 1954-1961.

Ault, A.P., M.J. Moore, H. Furutani, and K.A. Prather (2009), Impact of emissions from the Los Angeles port region on San Diego air quality during regional transport events, *Environ. Sci. Tech.*, *43* (10), 3500-3506.

Bardouki, H., M.B. da Rosa, N. Mihalopoulos, W.U. Palm, and C. Zetzsch (2002), Kinetics and mechanism of the oxidation of dimethylsulfoxide (DMSO) and methanesulfinate (MSI^-) by OH radicals in aqueous medium, *Atmos. Environ.*, *36* (29), 4627-4634.

Barnes, I., J. Hjorth, and N. Mihalopoulos (2006), Dimethyl sulfide and dimethyl sulfoxide and their oxidation in the atmosphere, *Chem. Rev.*, *106* (3), 940-975.

Bates, T.S., B.K. Lamb, A. Guenther, J. Dignon, and R.E. Stoiber (1992), Sulfur emissions to the atmosphere from natural sources, *J. Atmos. Chem.*, *14* (1-4), 315-337.

Bhave, P.V., J.O. Allen, B.D. Morrical, D.P. Fergenson, G.R. Cass, and K.A. Prather (2002), A field-based approach for determining ATOFMS instrument sensitivities to ammonium and nitrate, *Environ. Sci. Tech.*, *36* (22), 4868-4879.

Carson, P.G., K.R. Neubauer, M.V. Johnston, and A.S. Wexler (1995), On-line chemical analysis of aerosols by rapid single-particle mass spectrometry, *J. Aerosol Sci.*, *4* (26), 535-545.

Charlson, R.J., J.E. Lovelock, M.O. Andreae, and S.G. Warren (1987), Oceanic phytoplankton, atmospheric sulfur, cloud albedo and climate, *Nature*, *326* (6114), 655-661.

Draxler, R.R., and G.D. Rolph (2003), HYSPLIT (HYbrid Single-Particle Lagrangian Integrated Trajectory) model access via NOAA ARL READY Website (http://www.arl.noaa.gov/ready/hysplit4.html), *NOAA Air Resources Laboratory*, Silver Spring, MD.

Dunn, J.P., H.G. Stenger, and I.E. Wachs (1999), Oxidation of sulfur dioxide over supported vanadia catalysts: Molecular structure-reactivity relationships and reaction kinetics, *Catal. Today*, *51* (2), 301-318.

Ganor, E., H.A. Foner, H.G. Bingemer, R. Udisti, and I. Setter (2000), Biogenic sulphate generation in the Mediterranean Sea and its contribution to the sulphate anomaly in the aerosol over Israel and the Eastern Mediterranean, *Atmos. Environ.*, *34* (20), 3453-3462.

Gard, E., J.E. Mayer, B.D. Morrical, T. Dienes, D.P. Fergenson, and K.A. Prather (1997), Real-time analysis of individual atmospheric aerosol particles: Design and performance of a portable ATOFMS, *Anal. Chem.*, *69* (20), 4083-4091.

Gard, E.E., M.J. Kleeman, D.S. Gross, L.S. Hughes, J.O. Allen, B.D. Morrical, D.P. Fergenson, T. Dienes, M.E. Galli, R.J. Johnson, G.R. Cass, and K.A. Prather (1998), Direct observation of heterogeneous chemistry in the atmosphere, *Science*, *279* (5354), 1184-1187.

Gross, D.S., M.E. Galli, P.J. Silva, and K.A. Prather (2000), Relative sensitivity factors for alkali metal and ammonium cations in single particle aerosol time-of-flight mass spectra, *Anal. Chem.*, *72* (2), 416-422.

Guazzotti, S.A., K.R. Coffee, and K.A. Prather (2001), Continuous measurements of size-resolved particle chemistry during INDOEX-Intensive Field Phase 99, *J. Geophys. Res.-[Atmos.]*, *106* (D22), 28607-28627.

Hatton, A.D., and S.T. Wilson (2007), Particulate dimethylsulphoxide and dimethylsulphoniopropionate in phytoplankton cultures and Scottish coastal waters, *Aquat. Sci.*, *69* (3), 330-340.

Hopkins, R.J., Y. Desyaterik, A.V. Tivanski, R.A. Zaveri, C.M. Berkowitz, T. Tyliszczak, M.K. Gilles, and A. Laskin (2008), Chemical speciation of sulfur in marine cloud droplets and particles: Analysis of individual particles from the marine boundary layer over the California Current, *J. Geophys. Res.-[Atmos.]*, *113* (D4), D04209, doi:10.1029/2007JD008954.

Huffman, J.A., K.S. Docherty, A.C. Aiken, M.J. Cubison, I.M. Ulbrich, P.F. DeCarlo, D. Sueper, J.T. Jayne, D.R. Worsnop, P.J. Ziemann, and J.L. Jimenez (2009), Chemically-resolved aerosol volatility measurements from two megacity field studies, *Atmos. Chem. Phys.*, *9*, 7161-7182.

Hughes, L.S., J.O. Allen, P. Bhave, M.J. Kleeman, G.R. Cass, D.Y. Liu, D.F. Fergenson, B.D. Morrical, and K.A. Prather (2000), Evolution of atmospheric particles along trajectories crossing the Los Angeles basin, *Environ. Sci. Tech.*, *34* (15), 3058-3068.

Isakson, J., T.A. Persson, and E.S. Lindgren (2001), Identification and assessment of ship emissions and their effects in the harbour of G(o)over-circleteborg, Sweden, *Atmos. Environ.*, *35* (21), 3659-3666.

Key, J.M., N. Paulk, and A.M. Johansen (2008), Photochemistry of iron in simulated crustal aerosols with dimethyl sulfide oxidation products, *Environ. Sci. Tech.*, *42* (1), 133-139.

Kiehl, J.T., and B.P. Briegleb (1993), The relative roles of sulfate aerosols and greenhouse gases in climate forcing, *Science*, *260* (5106), 311-314.

Kim, H.-J., A.J. Miller, J. McGowan, and M.L. Carter (2009), Coastal phytoplankton blooms in the Southern California Bight, *Progress in Oceanography*, *82*, 137-147.

Kolaitis, L.N., F.J. Bruynseels, R.E.V. Grieken, and M.O. Andreae (1989), Determination of methanesulfonic acid and non-sea-salt sulfate in single marine aerosol particles, *Environ. Sci. Tech.*, *23*, 236-240.

Kouvarakis, G., and N. Mihalopoulos (2002), Seasonal variation of dimethylsulfide in the gas phase and of methanesulfonate and non-sea-salt sulfate in the aerosols phase in the Eastern Mediterranean atmosphere, *Atmos. Environ.*, *36* (6), 929-938.

Kreidenweis, S.M., and J.H. Seinfeld (1988), Nucleation of sulfuric acid-water and methanesulfonic acid-water solution particles: Implications for the atmospheric chemistry of organosulfur species, *Atmos. Environ.*, *22* (2), 283-296.

Lide, D.R., Ed., *CRC Handbook of Chemistry and Physics*, CRC Press/Taylor and Francis, Boca Raton, FL, 2009.

Mayali, X., P.J.S. Franks, and F. Azam (2008a), Cultivation and ecosystem role of a marine Roseobacter clade-affiliated cluster bacterium, *Appl. Environ. Microbiol.*, *74* (9), 2595-2603.

Mayali, X., P.J.S. Franks, and F. Azarn (2008b), Cultivation and ecosystem role of a marine Roseobacter clade-affiliated cluster bacterium, *Applied and Environmental Microbiology*, *74* (9), 2595-2603.

Neubauer, K.R., S.T. Sum, M.V. Johnston, and A.S. Wexler (1996), Sulfur speciation in individual aerosol particles, *J. Geophys. Res.-[Atmos.]*, *101* (D13), 18701-18707.

Pastor, S.H., J.O. Allen, L.S. Hughes, P. Bhave, G.R. Cass, and K.A. Prather (2003), Ambient single particle analysis in Riverside, California by aerosol time-of-flight mass spectrometry during the SCOS97-NARSTO, *Atmos. Environ.*, *37*, S239-S258.

Phinney, L., W.R. Leaitch, U. Lohmann, H. Boudries, D.R. Worsnop, J.T. Jayne, D. Toom-Sauntry, M. Wadleigh, S. Sharma, and N. Shantz (2006), Characterization of the aerosol over the sub-arctic north east Pacific Ocean, *Deep-Sea Res. Pt. II*, *53* (20-22), 2410-2433.

Poschl, U. (2005), Atmospheric aerosols: Composition, transformation, climate and health effects, *Angewandte Chemie-International Edition*, *44* (46), 7520-7540.

Pratt, K.A., and K.A. Prather (2009), Real-time, single-particle volatility, size, and chemical composition measurements of aged urban aerosols, *Environ. Sci. Tech.*, *43* (21), 8276-8282.

Qin, X., L.G. Shields, S.M. Toner, K.A. Pratt, and K.A. Prather (2009), Seasonal comparisons of the single particle mixing state in Riverside, CA during the SOAR 2005 campaign, *Aerosol Sci. Technol., In Preparation*.

Qin, X.Y., P.V. Bhave, and K.A. Prather (2006), Comparison of two methods for obtaining quantitative mass concentrations from aerosol time-of-flight mass spectrometry measurements, *Anal. Chem.*, *78* (17), 6169-6178.

Qin, X.Y., and K.A. Prather (2006), Impact of biomass emissions on particle chemistry during the California Regional Particulate Air Quality Study, *International Journal of Mass Spectrometry*, *258* (1-3), 142-150.

Sahle-Demessie, E., and V.G. Devulapelli (2008), Vapor phase oxidation of dimethyl sulfide with ozone over V_2O_5/TiO_2 catalyst, *Applied Catalysis B: Environmental*, *84* (3-4), 408-419.

Seinfeld, J.H., and S.N. Pandis, *Atmospheric Chemistry and Physics*, John Wiley & Sons, Inc., Hoboken, New Jersey, 2006.

Silva, P.J., and K.A. Prather (2000), Interpretation of mass spectra from organic compounds in aerosol time-of-flight mass spectrometry, *Anal. Chem.*, *72* (15), 3553-3562.

Singh, M., P.A. Jaques, and C. Sioutas (2002), Size distribution and diurnal characteristics of particle-bound metals in source and receptor sites of the Los Angeles Basin, *Atmos. Environ.*, *36* (10), 1675-1689.

Song, X.H., P.K. Hopke, D.P. Fergenson, and K.A. Prather (1999), Classification of single particles analyzed by ATOFMS using an artificial neural network, ART-2a, *Anal. Chem.*, *71* (4), 860-865.

von Glasow, R., and P.J. Crutzen (2004), Model study of multiphase DMS oxidation with a focus on halogens, *Atmos. Chem. Phys.*, *4*, 589-608.

Watts, S.F., P. Brimblecombe, and A.J. Watson (1990), Methanesulfonic acid, dimethyl sulfoxide and dimethyl sulfone in aerosols, *Atmospheric Environment Part a-General Topics*, *24* (2), 353-359.

Whiteaker, J.R., and K.A. Prather (2003), Hydroxymethanesulfonate as a tracer for fog processing of individual aerosol particles, *Atmos. Environ.*, *37* (8), 1033-1043.

Zorn, S.R., F. Drewnick, M. Schott, T. Hoffmann, and S. Borrmann (2008), Characterization of the South Atlantic marine boundary layer aerosol using an aerodyne aerosol mass spectrometer, *Atmos. Chem. Phys.*, *8* (16), 4711-4728.

Chapter 8

8. Conclusions and Future Directions

8.1 Synopsis

This dissertation presents insights into the single-particle mixing-state of marine aerosols from both natural (e.g. sea spray) and anthropogenic (e.g. ships) sources from measurements made during several shipboard campaigns including the Indian Ocean Experiment (INDOEX) and CalNex, coastal ground-based measurements including those made at the Scripps Pier, and from laboratory experiments. Section 8.2 provides a brief summary and discussion of these results while Section 8.3 discusses several on-going projects and future directions that can be taken from the work presented in this dissertation.

8.2 Conclusions

Aerosols influence global climate directly by scattering and absorbing incoming solar radiation and indirectly by initiating cloud droplet and ice crystal formation [*Forster et al.*, 2007; *Poschl*, 2005]; the radiative impact of aerosols on global climate is uncertain and represents the greatest challenge in our ability to accurately forecast future temperature rises due to climate change [*Forster et al.*, 2007]. Particle size and composition play crucial roles in shaping aerosol-cloud interactions, which pose the greatest amount of uncertainty in terms of global radiative forcing [*Forster et al.*, 2007]. The physicochemical properties of marine aerosols, including sea spray and anthropogenic emissions, are of particular interest since oceans cover over 70% of the

Earth's surface. Further, marine stratocumulus clouds contribute greatly to global radiative cooling with some estimates showing that this cooling can exceed the warming produced by a doubling of $CO_{2(g)}$ [*Slingo*, 1990; *Stevens et al.*, 2003]. Measuring and discerning differences in both particle size and composition attributed to changes in oceanic biological activity, emissions from anthropogenic sources, and rapid changes due to atmospheric processing such as heterogeneous reactions is challenging yet necessary to unravel complex aerosol-cloud-climate interactions. The results presented herein in this dissertation utilize aerosol time-of-flight mass spectrometry (ATOFMS) to make real-time measurements of the size-resolved composition of individual marine particles in order to address this challenge.

As discussed in Chapter 1.4.3, recent publications have highlighted the enrichment of biogenically-derived organic material in marine aerosol compared to bulk seawater [*Blanchard*, 1964; *Duce and Hoffman*, 1976]. However, one question that has remained relatively unexplored is how much of this organic material is externally or internally mixed from sea salt. *O'Dowd et al.* [2004] hypothesized that the manner in which submicron organic material is mixed with sea spray aerosol will greatly impact the cloud droplet number concentration that can potentially be formed over the ocean during periods of high biological activity. Chapter 2 of this dissertation shows evidence for ocean-derived particles that are externally mixed from sea salt particles and have strong real-time correlations with proxies for biological activity, particularly atmospheric dimethyl sulfide (DMS). To the best of our knowledge, this is the first time such real-time correlations between ambient sea spray particles and proxies for oceanic biological

activity have been reported. These unique particles were found to contain internal mixtures of Mg^{2+} and/or Ca^{2+}, K^{+}, and organic carbon, and are referred to in this work as Mg-type particles; the detection of these particles provide the first evidence that inorganic ions are also enriched in sea spray at the single-particle level during periods of elevated biological activity. Although these particles were found to be characterized by inorganic ion peaks (e.g. $^{24}Mg^{+}$), it is likely that these particles contain a significant amount of organic material and provide evidence for an externally mixed population of organic-enriched sea spray aerosols produced from biogenic organic material. Further evidence for this stems from the fact that these Mg-type particles were found to be enriched in smaller sizes compared to sea salt particles much like marine organics, which have also been found to be enriched in the smallest size modes [*Facchini et al.*, 2008; *O'Dowd et al.*, 2004; *Oppo et al.*, 1999]. Since these Mg-type particles represent an externally mixed aerosol population, these particles could possibly add to particle concentrations potentially increasing cloud droplet number concentrations (CDNC), which would impact cloud formation and microphysics in the marine environment.

In addition to biogenically-derived organic material, biological activity has been proposed to change the chemical composition of marine aerosols through secondary oxidation involving the gaseous compound DMS [*Barnes et al.*, 2006; *Bates et al.*, 1992; *Charlson et al.*, 1987]; yet, much remains unknown regarding the marine sulfur cycle, and how it affects the physicochemical properties of sea spray aerosol. As noted in Chapter 3, novel sulfur ions ($^{32}S^{+}$, $^{64}S_2^{+}$, etc.) were detected in sea spray particles in regions of elevated biological activity only at night. These ions were not associated with

DMS oxidation products such as MSA ($^{95}CH_3SO_3^-$) and sulfates ($^{64}SO_2^-$, $^{81}HSO_3^-$, $^{97}HSO_4^-$) or other sulfur oxides such as hydroxymethanesulfonate ($^{111}CH_3SO_4^-$), which form negative ion spectra [*Gaston et al.*, 2010; *Silva and Prather*, 2000], suggesting that these ions are formed from a novel production pathway involving the marine sulfur cycle. Further, these sulfur ions were found both as external mixtures and as internal mixtures with sea spray particles (e.g. sea salt and Mg-type particles); bubbling experiments successfully reproduced these spectra suggesting that these ions are associated with particles that are directly ejected from the ocean and not with secondary formation processes. Comparison with sulfur-containing standards showed that these ions are most likely produced from elemental sulfur. Certain marine bacteria oxidize sulfide and thiosulfate to sulfate forming elemental sulfur globules as an intermediate [*Brune*, 1989; *Prange et al.*, 1999]. These globules are in the 1-3 μm size range, which is similar to the size range of particles containing elemental sulfur ions described in Chapter 3 of this dissertation; hence, these globules are the most likely source of the particulate, elemental sulfur detected by ATOFMS. Although unusually large sulfur-containing particles have been detected in the marine environment before [*Mouri et al.*, 1995], the composition of these particles was assumed to be sulfate derived from DMS oxidation; hence, the results presented in Chapter 3 represent the first time that particulate, elemental sulfur from a marine biogenic source has been detected in the marine environment. Further, these results are the first to suggest that particulate, biogenic sulfur can be contributed from primary rather than secondary sources. Since gaseous elemental sulfur has been detected in trace quantities in the marine environment [*Atlas*, 1991], the results shown in Chapter 3 suggest that once ejected in the atmosphere, these novel sulfur particles could possibly

contribute elemental sulfur to the gas phase wherein this sulfur would be oxidized to ultimately form sulfate, possibly contributing new particles to the marine environment capable of nucleating cloud droplets.

Chapters 2 and 3 have primarily focused on results from ambient measurements from shipboard and coastal studies of sea spray aerosols. However, additional laboratory experiments are necessary to thoroughly investigate differences in the single-particle chemistry of marine aerosols due to changes in biological activity. Chapter 4 of this dissertation shows results from laboratory studies characterizing sea spray aerosol generated from bubble bursting. These experiments monitored changes in the size-resolved composition of sea spray generated from artificial seawater as biogenically-derived organics, produced from filtered phytoplankton cells, as well as whole phytoplankton cells themselves were added to the solutions. The resulting composition shifted from a dominantly inorganic composition, namely salts, to high number concentrations of organic material internally mixed with inorganic ions (e.g. Mg^{2+}, Ca^{2+}, K^{+}) in addition to the detection of sea salt internally mixed with organic carbon as dissolved organic material (DOM) was added to the artificial seawater solutions. These results confirm the hypothesis in Chapter 2 that Mg-type particles represent marine organic material that is associated with trace, inorganic ions; these associations are in agreement with current theories regarding the formation of marine microgels from the bridging of acidic polymers with divalent cations [*Chin et al.*, 1998; *Orellana et al.*, 2007; *Verdugo et al.*, 2004; *Verdugo et al.*, 2008]. Specific organic compounds associated with sea spray particles generated from bubbling artificial seawater and DOM

included alkanes ($^{27}C_2H_3^+$, $^{29}C_2H_5^+$, $^{41}C_3H_5^+$, etc.), oxygenated organics ($^{43}C_2H_3O^+$, $^{45}CH_2O^+$, etc.), organic peaks that are most likely due to polysaccharides ($^{59}CH_3COO^-$ and $^{71}C_3H_3OO^-$) [*Silva et al.*, 1999], amines ($^{86}(C_2H_5)_2NCH_2^+$), organic nitrogen ($^{26}CN^-$, $^{42}CNO^-$), and humic substances ($^{91}C_7H_7^+$) [*Angelino et al.*, 2001; *Silva and Prather*, 2000]. The addition of phytoplankton cells produced similar particle types to those produced from adding DOM to artificial seawater; however, the addition of Synechococcus produced K-phosphate particles that were concentrated in the supermicron size mode. Further, these particles were found to take up Rb^+, which can displace intracellular K^+, suggesting that K-phosphate represents intact bioaerosols [*Epstein et al.*, 1963; *Pyo et al.*, 2010]. Particles generated from the addition of organic material and phytoplankton cells to artificial seawater were comparable to those generated by bubbling natural seawater and to particles observed in ambient measurements from previous studies. These experiments serve as a basis for assigning a marine, biogenic source to ambient particles that are measured in the marine environment. Further, the diversity in single-particle mixing-state shown in Chapter 4 has atmospheric implications for the role of oceanic biological activity in shaping aerosol-cloud-climate interactions since differences in composition at the single-particle level influence heterogeneous reactions, water uptake, and the ability to nucleate the formation of cloud droplets and ice crystals.

In addition to natural sources, anthropogenic emissions also contribute to the marine environment. Differences in anthropogenic contributions to the marine environment along the California coast were probed during shipboard measurements

made as part of the CalNex field campaign that started in San Diego traversing up the coast to Sacramento then ending at the Port of San Francisco; several point sources of emissions were targeted, namely the Ports of Los Angeles and Long Beach, ocean-going ships, continental outflow from Santa Monica, and agricultural emissions from Sacramento. As shown in Chapter 5, latitudinal gradients in particle mixing-state were observed with soot particles dominating the submicron particle chemistry in Southern California while particulate organics prevailed in the Sacramento region, particularly after the occurrence of new particle formation events. Most soot particles were internally mixed with organic carbon with a high fraction of these particles lacking negative ion spectra, indicating the presence of particulate water [*Moffet et al.*, 2008b; *Neubauer et al.*, 1997; *Neubauer et al.*, 1998]. Latitudinal gradients in the mixing-state of carbonaceous particle types were also observed with a high fraction of soot particles containing sulfate in Southern California particularly when air masses were transported from coastal regions most likely due to high emissions of $SO_{2(g)}$ from the port regions and from ships. During periods of inland transport from Riverside, CA, soot particles were internally mixed with nitrate while high number concentrations of amines were observed; however, during periods of transport from the Central Valley, soot particles containing unique organic peaks were observed that have never been detected before, in addition to organic carbon internally mixed with nitrate. Organics were observed in Sacramento after nucleation events suggesting that these organics contribute to particle growth following new particle formation events. Overall, these results highlight differences in single-particle mixing-state attributed to differences in the source as well as the secondary processing of anthropogenic emissions, which impact the optical and cloud nucleating properties of

anthropogenic emissions contributing to the California coast. The latitudinal differences in soot mixing-state is particularly important since these differences have been shown to strongly impact the warming potential of soot particles [*Jacobson*, 2000; *Moffet and Prather*, 2009].

In addition to emissions from continental outflow, ship emissions in California were also investigated. Ships produce the largest amount of pollutants per ton of fuel combusted; the climatic and human health impacts from these pollutants is highly dependent on the type of fuel that is combusted [*Corbett and Fischbeck*, 1997; *Eyring et al.*, 2010]. Ships typically combust high sulfur residual fuel producing high number and mass concentrations of toxic heavy metals (e.g. V, Ni), organics, and sulfate [*Agrawal et al.*, 2008; *Ault et al.*, 2010; *Lack et al.*, 2009]. Further, ship emissions impact the microphysical and radiative impacts of clouds in the marine environment [*Eyring et al.*, 2010; *Hobbs et al.*, 2000; *Hudson et al.*, 2000; *Russell et al.*, 2000; *Russell et al.*, 1999]. In an effort to curb high sulfate and high metal-containing emissions resulting from combusting high sulfur residual fuel oil, regulations were passed in 2009 requiring ships to switch from high sulfur residual fuel to low sulfur marine distillate fuel within 24 miles of approaching the California coast [*CARB*, 2009]. To assess the impact of these regulations on the single-particle mixing-state of ship emissions, Chapter 6 explored ATOFMS measurements of ship emissions at the source and after transport prior to and after the regulations were enacted by using results from measurements made at the Scripps Pier in 2006 and 2009, measurements during CalNex, and ground-based measurements at the Ports of Los Angeles and Long Beach in 2007. Vanadium-

containing particles, characteristic of emissions from residual fuel combustion [*Ault et al.*, 2010; *Ault et al.*, 2009], were found to decrease while increased number concentrations of soot particles were observed in freshly emitted ship emissions as a result of the new regulations. The mixing-state of vanadium-containing particles was probed; both sulfate and organics were found to decrease after the new regulations were passed, which is in agreement with recent measurements by *Lack et al.* [2011] who observed a decrease in both components when marine distillate fuel was combusted. The decrease in organic carbon associated with ship emissions could be due to decreased amounts of lubricating oil needed to combust marine distillate fuel and/or the decreased amounts of asphaltenes, which are high mass, low volatility organic compounds, associated with marine distillate fuel. As a result of the decreased amount of sulfate and increased soot particles, the propensity for ship emissions to nucleate cloud droplets were found to decrease after the new regulations were passed suggesting that one climatic effect of the new regulations will be a decreased impact of ship emissions on the radiative properties of clouds. Since shipping emissions are expected to rapidly increase over the next 50 years, particularly in the Arctic Ocean as sea ice continues to melt in this region [*Eyring et al.*, 2005], the observed changes in particle mixing-state as a result of the recent regulations in California should be taken into account when determining future regulations both in California as well as in other areas of the world where ship emissions contribute heavily to the aerosol burden.

Chapters 2-6 have probed the impact of biological activity and anthropogenic emissions and secondary processing on the single-particle mixing-state of marine

aerosols separately; however, it is likely that anthropogenic and marine biogenic emissions can influence the atmospheric processing of each other in important, yet poorly understood ways. In order to address this issue, results shown in Chapter 7 probe the ability of anthropogenic emissions to alter the processing of marine biogenic emissions from DMS oxidation products. During the Study of Organic Aerosols in Riverside, CA (SOAR), local and transported anthropogenic emissions were detected in Riverside, CA, which is an inland, polluted region of California. During the study, oceanic biological activity was highly elevated due to a red tide bloom of *L. polyedrum*, a dinoflagellate known to produce high quantities of DMS [*Hatton and Wilson*, 2007], prevailed along the California coast. As a result, internal mixtures of anthropogenic particle types, such as amines, ship emissions, biomass burning, etc., and the DMS oxidation product methanesulfonic acid (MSA) were detected on individual particles for the first time. The detection of MSA was found to track both meteorological conditions as well as chlorophyll *a* concentrations. Further, MSA was found to track the chemical marker for fog processing, hydroxymethanesulfonate (HMS, $^{111}CH_3SO_4^-$) [*Qin and Prather*, 2006; *Whiteaker and Prather*, 2003], confirming the role of aqueous phase chemistry in the formation of MSA [*Bardouki et al.*, 2002]. Most notably, particles internally mixed with vanadium, typically observed in particles from residual fuel combustion, were found to have elevated levels of MSA, even in aged sea salt particles. These results suggest that vanadium could be catalyzing the oxidation of biogenic sulfur resulting in elevated levels of MSA formation. Transition metals have been found to catalyze sulfur oxidation during aqueous phase processing in cloud droplets [*Alexander et al.*, 2009; *Deguillaume et al.*, 2005]; however, this is the first ambient evidence suggesting that anthropogenic,

metal-containing particles can affect the secondary processing of marine biogenic emissions.

8.3 Current Work and Future directions

The work presented in this dissertation has resulted in several on-going projects as well as well as inspired several spin-off projects that will build upon the results shown in this work. Several examples of on-going current work and future projects are discussed below.

During CalNex, several periods were encountered where ATOFMS measurements detected freshly emitted sea spray particles concurrently with gas phase measurements of anthropogenic, reactive gases. The combination of these two observations led to unique observations of heterogeneous reactions on sea spray particles in the polluted, marine environment. The reactive gas $N_2O_{5(g)}$ was measured by Steve Brown and Nick Wagner using Cavity Ring-Down Spectroscopy (CaRDS) [*Brown et al.*, 2002]. $N_2O_{5(g)}$ is a nighttime NO_x-reservoir species that reacts heterogeneously leading to the formation of particulate nitrate [*Vogt and Finlayson-Pitts*, 1994]. The reaction has garnered significant attention as the reactive uptake of $N_2O_{5(g)}$ is thought to decrease global NO_x concentrations by ~50% annually [*Dentener and Crutzen*, 1993], which influences the production of tropospheric ozone and the lifetime of methane, two key greenhouse gases [*Forster et al.*, 2007; *Shindell et al.*, 2009]. When the reaction occurs in the presence of chlorine-containing particles, $ClNO_{2(g)}$ is formed, which is photolyzed during the day to produce Cl radicals that can alter the production of tropospheric ozone [*Finlayson-Pitts et al.*, 1989; *Folkers et al.*, 2003; *Keene et al.*, 1990; *Vogt et al.*, 1996]. The most notable

reaction known to produce $ClNO_{2(g)}$ is that between $N_2O_{5(g)}$ and sea salt, where NaCl is fresh, unreacted sea salt and $NaNO_3$ is reacted sea salt:

$$N_2O_{5(g)} \longleftrightarrow N_2O_{5(aq)} \quad (1)$$

$$NaCl_{(aq)} + N_2O_{5(aq)} \longrightarrow NaNO_{3(aq)} + ClNO_{2(aq)} \quad (2)$$

$$ClNO_{2(aq)} \longleftrightarrow ClNO_{2(g)} \quad (3)$$

Measurements of $ClNO_{2(g)}$ were performed during CalNex by Joel Thornton and Theran Riedel using chemical ionization mass spectrometry [*Kercher et al.*, 2009]; both $ClNO_{2(g)}$ and $N_2O_{5(g)}$ were used for comparison to single-particle measurements of sea spray aerosol. It should be noted that heterogeneous reactions with both nitric acid ($HNO_{3(g)}$) and $N_2O_{5(g)}$ lead to the formation of particulate nitrate. Nitric acid can react with particles during any time of the day; however, reaction with $N_2O_{5(g)}$ can only occur at night. Further, *only* the heterogeneous reaction of $N_2O_{5(g)}$ results in the formation of $ClNO_{2(g)}$; therefore, comparisons between particulate nitrate and $ClNO_{2(g)}$ can be used to assess the heterogeneous reactions uptake of $N_2O_{5(g)}$ that leads to the formation of nitrate on ambient particles.

The particle age of sea spray (e.g. sea salt, Mg-type marine biogenic [*Gaston et al.*, 2011]) was probed using ATOFMS by determining temporal changes in the ion peak intensities of nitrate, nitrite, and chloride. Figure 8.1 shows representative mass spectra of freshly emitted and reacted sea salt and Mg-type particles. Fresh and reacted particles are differentiated by the accumulation of nitrite ($^{46}NO_2^-$) and nitrate ($^{62}NO_3^-$) ion peaks

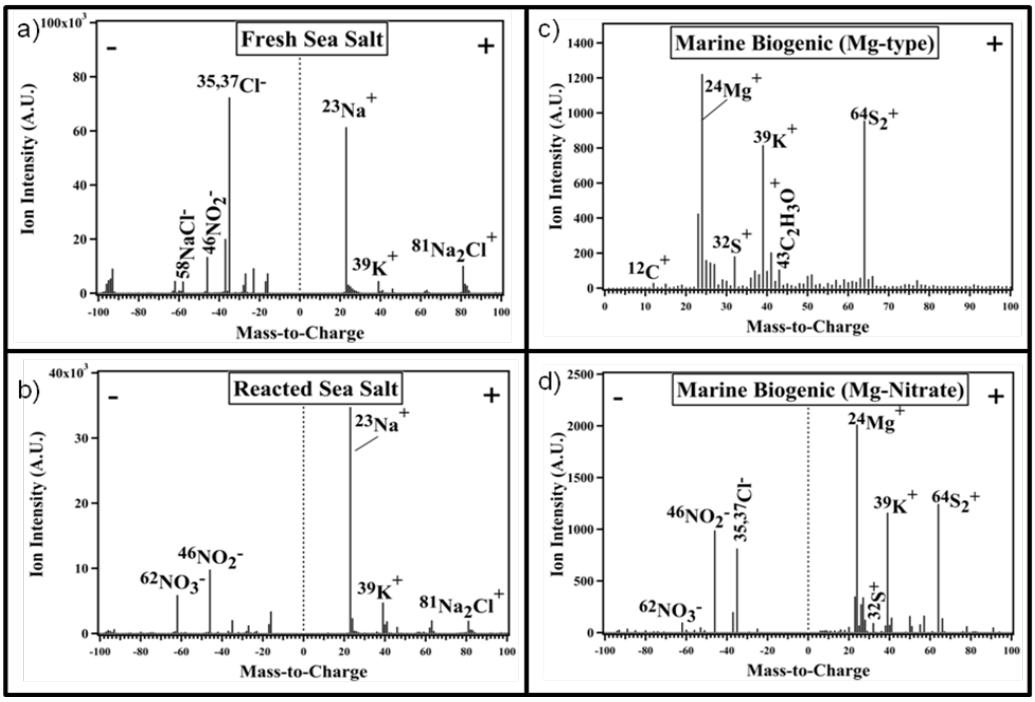

Figure 8.1: Representative mass spectra of (a) fresh sea salt, (b) reacted sea salt, (c) Mg-type, and (d) reacted Mg-type particles. Dashed lines in the spectra are used to delineate positive and negative ion peaks.

and, particularly in the case of sea salt, the loss of chloride ($^{35,37}Cl^-$) [*Gard et al.*, 1998; *Gaston et al.*, 2011; *Guazzotti et al.*, 2001]. As shown in Figure 8.1, freshly emitted Mg-type particles typically lack negative ion spectra therefore the observed loss of particulate chloride was not as pronounced as it was for sea salt particles. Measurements of gas-phase compounds and particulate ion peak areas from ATOFMS measurements were all analyzed at 1-min time resolution and are presented in Greenwich Mean Time (GMT), which is 7 hours ahead of local time (PDT). Measurements from May 21-31, 2010 were probed since these days contained the highest number concentrations of sea spray particles and because these days did not include measurements from the inland, Sacramento region. Figure 8.2 shows the temporal trends observed between gas-phase $N_2O_{5(g)}$ and $ClNO_{2(g)}$, and the ion peak area of nitrite and nitrate on sea salt particles for May 21-31, 2010. In general, the formation of particulate nitrite and nitrate tracks $N_2O_{5(g)}$ and the formation of $ClNO_{2(g)}$, although a few spikes in particulate nitrite and nitrate are observed during the daytime when $N_2O_{5(g)}$ and $ClNO_{2(g)}$ are photolyzed; these daytime peaks in nitrate and nitrite are most likely due to heterogeneous reactions with $HNO_{3(g)}$ instead of $N_2O_{5(g)}$.

Many of the time periods examined were impacted by rapid shifts in air masses namely due to the ship moving in and out of polluted marine environments leading to abrupt changes in the chloride and nitrate content of sea spray particles due to changes in transport conditions rather than due to chemical processing of marine aerosols. May 24 was found to best represent the chemical processing of sea spray aerosol with minimal

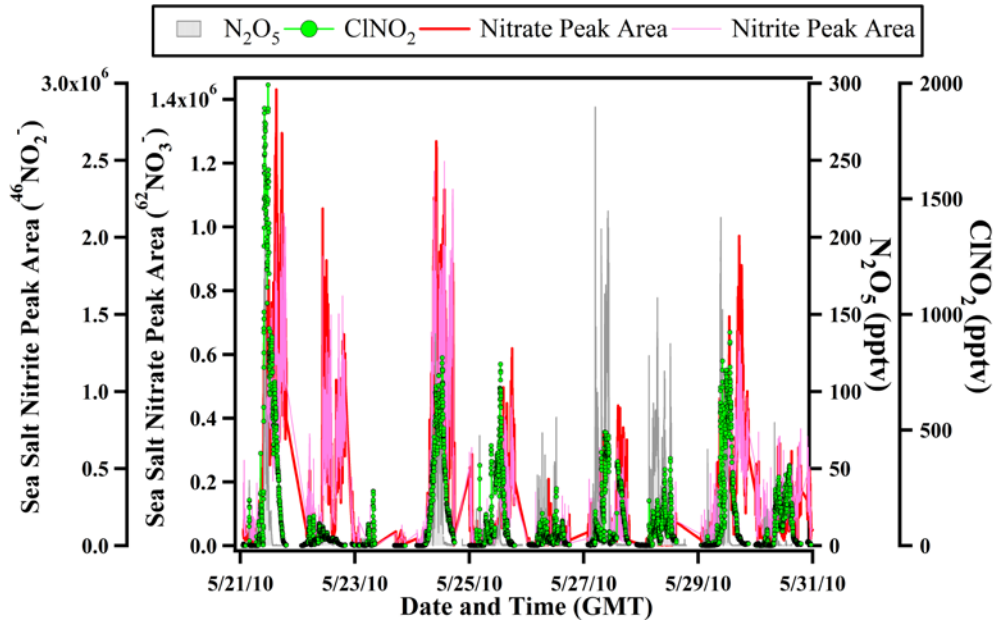

Figure 8.2: 1-minute temporal trends of particulate nitrite (pink line), particulate nitrate (red line), $ClNO_{2(g)}$ (green dots), and $N_2O_{5(g)}$ (shaded grey lines).

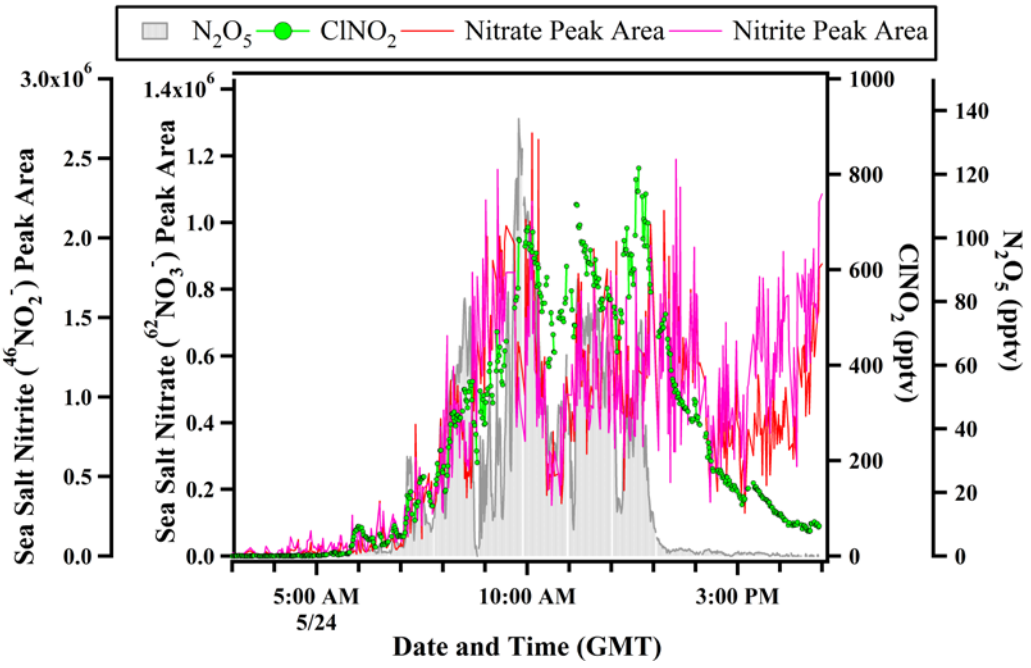

Figure 8.3: 1-minute temporal trends of particulate nitrite (pink line), particulate nitrate (red line), $ClNO_{2(g)}$ (green dots), and $N_2O_{5(g)}$ (shaded grey lines) for May 24, 2010.

interference from changes in air masses. Figure 8.3 shows increases in particulate nitrite and nitrate on sea spray particles concurrent with the production of $ClNO_{2(g)}$. Strong correlations between particulate nitrite or nitrate and the production of $ClNO_{2(g)}$ are shown in Figure 8.4 for both sea salt and Mg-type particles providing evidence that the reactive uptake of $N_2O_{5(g)}$ is occurring on both particle types leading to the accumulation of particulate nitrate. As noted in Figure 8.4, a strong size dependence was not observed for the reaction under these particular conditions. It should be noted that on May 24, particle surface area was dominated by supermicron rather than submicron particles, which could explain the lack of a size dependence. Figure 8.5 shows the ratio of chloride to nitrate for sea salt particles as a function of the production of $ClNO_{2(g)}$. The strong correlation confirms the heterogeneous displacement of chloride and subsequent formation of particulate nitrate and $ClNO_{2(g)}$ as the uptake of $N_2O_{5(g)}$ proceeds.

The presented results are promising for using real-time, single-particle measurements of aerosol mixing-state and on-line gas-phase measurements to understand heterogeneous reactions in the ambient atmosphere. Current parameterizations of this reaction in the marine environment in chemical transport models typically focus on NaCl particles while ignoring the effect of trace salts and marine biogenic particles [*Chang et al.*, 2011; *Evans and Jacob*, 2005]; the work shown suggests that these particle types need to be included in these models in order to adequately parameterize this reaction. Additional work is currently underway to understand how particulate nitrite and nitrate peak areas evolve as the reaction progresses. Also, additional particle types are being probed to determine the propensity for $N_2O_{5(g)}$ uptake to occur on other particle types

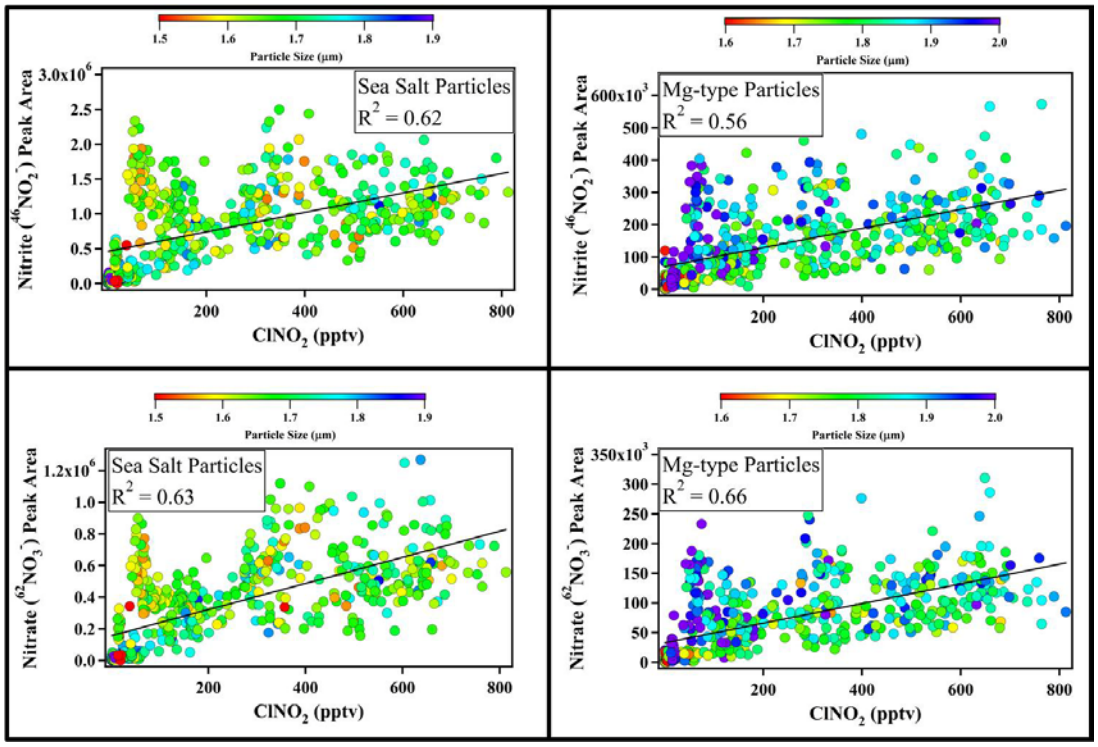

Figure 8.4: Correlations between particulate nitrite and $ClNO_{2(g)}$ (top panel) and particulate nitrate and $ClNO_{2(g)}$ (bottom panel) for sea salt (left panel) and Mg-type (right panel) particles for May 24, 2010.

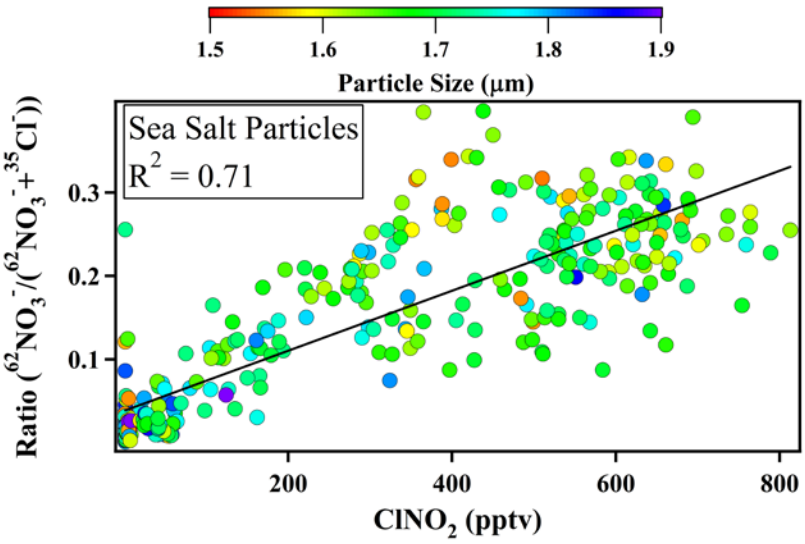

Figure 8.5: Correlation plot of the normalized ratio of nitrate:chloride on sea salt particles and $ClNO_{2(g)}$ for May 24, 2010.

such as dust, biomass burning, etc. Preliminary results from dust particles show a lack of reactive uptake of $N_2O_{5(g)}$, which could be due to the presence of nitrate that has accumulated on dust prior to reaction with $N_2O_{5(g)}$ that is suppressing the reaction [*Mentel et al.*, 1999; *Wahner et al.*, 1998]. This analysis will be added to the manuscript, which is currently in preparation, prior to submission to an appropriate journal, most likely *Journal of Geophysical Research*.

Other work that I have completed that is not shown in this dissertation includes laboratory measurements of the size-resolved composition of dust particles and the resulting cloud nucleating potential of these particles. These measurements complimented ambient aircraft measurements made during the Ice in Clouds Experiment-Layers (ICE-L) by Dr. Kerri Pratt. The results of one of these measurements were published in a manuscript detailing the detection of playa salts in orographic wave clouds [*Pratt et al.*, 2010]. Also not included in this dissertation is work I did in collaboration with Brian Palenik and an undergraduate student, Rudy Urbano. We collaborated to sample and characterize bioaerosols detected in the atmosphere at the end of the SIO Pier. Bioaerosols were characterized through molecular techniques to assess both the viability of the bioaerosols found as well as to determine the contributions of different bacteria and fungi. This work resulted in a first author publication for Rudy [*Urbano et al.*, 2011].

Continuation of laboratory investigations of sea spray aerosols is also underway. An NSF-sponsored Center for Aerosol Impacts on Climate and the Environment (CAICE) has been established and is currently focused on understanding changes in sea

spray aerosol chemistry associated with changes in biological activity, heterogeneous reactions, etc. One of the main goals is to incorporate multiple, complimentary measurements of sea spray aerosols, including electron microscopy, in order to fully understand the impact of each of these variables on the mixing-state. I have assisted in some of these studies by providing ambient data representative of background marine conditions for comparison to laboratory measurements. Since my postdoctoral position with Prof. Joel Thornton will involve examining heterogeneous reactions of $N_2O_{5(g)}$, I hope that my involvement with this center will continue beyond my graduate studies.

Additional collaborations are also underway for data collected during the CalNex field campaign. Abrupt increases in particulate mercury observed during CalNex by Prof. Peter Weiss at UC Santa Cruz were found to coincide with ATOFMS measurements of incineration particles [*Moffet et al.*, 2008a]. The results of these measurements are the focus of a future manuscript in preparation. I am also collaborating with Prof. Chris Cappa at UC Davis to understand the role of soot mixing-state on aerosol optical properties observed during CalNex. The results of this collaboration are currently in a manuscript that is in preparation and will be submitted to *Science*. I am also involved with collaborations on several other data sets including measurements that Andy Ault and myself made in Riverside, CA as part of the Los Angeles Basin Mobile Study (LABMS) during the summer of 2007. Jessie Creamean from the Prather group has incorporated these measurements into a manuscript that will be submitted to *Atmospheric Environment*. I also participated in measurements of biomass burning aerosol during the 2007 San Diego wildfires. Melanie Zauscher currently has a manuscript in preparation

highlighting the effect of atmospheric processing on changes in the single-particle mixing-state of biomass burning aerosol that will be submitted to either *Atmospheric Environment* or *Environmental Science and Technology*.

To conclude, the results presented in this dissertation have provided significant insight regarding the role of oceanic biological activity, anthropogenic emissions, and subsequent atmospheric processing on marine particle chemistry. These results can be expanded upon by coupling these changes in the physicochemical properties of marine aerosols with changes in aerosol optical properties and the propensity of these particles to form cloud droplets. Further insight into how biogenically-derived marine organics can impact the heterogeneous reactivity of sea spray particles should be investigated using controlled laboratory experiments such as those currently underway by members of CAICE. These results will no doubt expand our understanding of both air-sea interactions as well as how anthropogenic emissions can influence the processing of marine-derived particles.

8.4 Acknowledgements

Matthew Ruppel is acknowledged for helping edit this chapter.

8.5 References

Agrawal, H., Q.G.J. Malloy, W.A. Welch, J.W. Miller, and D.R. Cocker (2008), In-use gaseous and particulate matter emissions from a modern ocean going container vessel, *Atmos. Environ., 42* (21), 5504-5510.

Alexander, B., R.J. Park, D.J. Jacob, and S. Gong (2009), Transition metal-catalyzed oxidation of atmospheric sulfur: Global implications for the sulfur budget, *J. Geophys. Res., 114* (D02309), doi:10.1029/2008JD010486.

Angelino, S., D.T. Suess, and K.A. Prather (2001), Formation of aerosol particles from reactions of secondary and tertiary alkylamines: Characterization by aerosol time-of-flight mass spectrometry, *Environ. Sci. Tech., 35* (15), 3130-3138.

Atlas, E. (1991), Observation of possible elemental sulfur in the marine atmosphere and speculation on its origin, *Atmos. Environ., 25A* (12), 2701-2705.

Ault, A.P., C.J. Gaston, Y. Wang, G. Dominguez, M.H. Thiemens, and K.A. Prather (2010), Characterization of the single particle mixing state of individual ship plume events measured at the Port of Los Angeles, *Environ. Sci. Tech., 44* (6), 1954-1961.

Ault, A.P., M.J. Moore, H. Furutani, and K.A. Prather (2009), Impact of emissions from the Los Angeles port region on San Diego air quality during regional transport events, *Environ. Sci. Tech., 43* (10), 3500-3506.

Bardouki, H., M.B. da Rosa, N. Mihalopoulos, W.U. Palm, and C. Zetzsch (2002), Kinetics and mechanism of the oxidation of dimethylsulfoxide (DMSO) and methanesulfinate (MSI^-) by OH radicals in aqueous medium, *Atmos. Environ., 36* (29), 4627-4634.

Barnes, I., J. Hjorth, and N. Mihalopoulos (2006), Dimethyl sulfide and dimethyl sulfoxide and their oxidation in the atmosphere, *Chem. Rev., 106* (3), 940-975.

Bates, T.S., B.K. Lamb, A. Guenther, J. Dignon, and R.E. Stoiber (1992), Sulfur emissions to the atmosphere from natural sources, *J. Atmos. Chem., 14* (1-4), 315-337.

Blanchard, D.C. (1964), Sea-to-air transport of surface active material, *Science, 146* (364), 396-397.

Brown, S.S., H. Stark, S.J. Ciciora, R.J. McLaughlin, and A.R. Ravishankara (2002), Simultaneous in situ detection of atmospheric NO_3 and N_2O_5 via cavity ring-down spectroscopy, *Review of Scientific Instruments, 73* (9), 3291-3301.

Brune, D.C. (1989), Sulfur oxidation by phototrophic bacteria, *Biochimica et Biophysica Acta*, *975*, 189-221.

CARB, Final Regulation Order. Fuel Sulfur and Other Operational Requirments for Ocean-Going Vessels Within California Waters and 24 Nautical Miles of the California Baseline, California Air Resources Board: Sacramento, CA, 2009.

Chang, W.L., P.V. Bhave, S.S. Brown, N. Riemer, J. Stutz, and D. Dabdub (2011), Heterogeneous atmospheric chemistry, ambient measurements, and model calculations of N_2O_5: A review, *Aerosol Sci. Tech.*, *45* (6), 665-695.

Charlson, R.J., J.E. Lovelock, M.O. Andreae, and S.G. Warren (1987), Oceanic phytoplankton, atmospheric sulfur, cloud albedo and climate, *Nature*, *326* (6114), 655-661.

Chin, W.C., M.V. Orellana, and P. Verdugo (1998), Spontaneous assembly of marine dissolved organic matter into polymer gels, *Nature*, *391* (6667), 568-572.

Corbett, J.J., and P. Fischbeck (1997), Emissions from ships, *Science*, *278* (5339), 823-824.

Deguillaume, L., M. Leriche, K. Desboeufs, G. Mailhot, C. George, and N. Chaumerliac (2005), Transition metals in atmospheric liquid phases: Sources, reactivity, and sensitive parameters, *Chem. Rev.*, *105* (9), 3388-3431.

Dentener, F.J., and P.J. Crutzen (1993), Reaction of N_2O_5 on tropospheric aerosols: Impact on the global distributions of NO_x, O_3, and OH, *J. Geophys. Res.*, *98* (D4), 7149-7163.

Duce, R.A., and E.J. Hoffman (1976), Chemical fractionation at the air-sea interface, *Ann. Rev. Earth Planet. Sci.*, *4*, 187-228.

Epstein, E., O.E. Elzam, and D.W. Rains (1963), Resolution of dual mechanisms of potassium absorption by barley roots, *PNAS*, *49* (5), 684-692.

Evans, M.J., and D. Jacob (2005), Impact of new laboratory studies of N_2O_5 hydrolysis on global model budgets of tropospheric nitrogen oxides, ozone, and OH, *Geophys. Res. Lett.*, *32*, L09813, doi:10.1029/2005GL022469.

Eyring, V., I.S.A. Isaksen, T. Berntsen, W.J. Collins, J.J. Corbett, O. Endresen, R.G. Grainger, J. Moldanova, H. Schlager, and D.S. Stevenson (2010), Transport impacts on atmosphere and climate: Shipping, *Atmos Environ*, *44*, 4735-4771.

Eyring, V., H.W. Kohler, A. Lauer, and B. Lemper (2005), Emissions from international shipping: 2. Impact of future technologies on scenarios until 2050, *J. Geophys. Res.-[Atmos.], 110* (D17), D17306, doi:10.1029/2004JD005620.

Facchini, M.C., M. Rinaldi, S. Decesari, C. Carbone, E. Finessi, M. Mircea, S. Fuzzi, D. Ceburnis, R. Flanagan, E.D. Nilsson, G. de Leeuw, M. Martino, J. Woeltjen, and C.D. O'Dowd (2008), Primary submicron marine aerosol dominated by insoluble organic colloids and aggregates, *Geophys. Res. Lett., 35*, L17814, doi:10.1029/2008GL034210.

Finlayson-Pitts, B.J., M.J. Ezell, and J.N. Pitts Jr. (1989), Formation of chemically active chlorine compounds by reactions of atmospheric NaCl particles with gaseous N_2O_5 and $ClONO_2$, *Nature*, *337*, 241-244.

Folkers, M., T.F. Mentel, and A. Wahner (2003), Influence of an organic coating on the reactivity of aqueous aerosols probed by the heterogeneous hydrolysis of N_2O_5, *Geophys. Res. Lett., 30* (12), 1644, doi:10.1029/2003GL017168.

Forster, P., V. Ramaswamy, P. Artaxo, T. Berntsen, R. Betts, D.W. Fahey, J. Haywood, J. Lean, D.C. Lowe, G. Myhre, J. Nganga, R. Prinn, G. Raga, M. Schulz, and R. Van Dorland, Changes in Atmospheric Constituents and in Radiative Forcing, in *Climate Change 2007: The Physical Science Basis. Contribution of Working Group I to the Fourth Assessment Report of the Intergovernmental Panel on Climate Change*, edited by S. Solomon, D. Qin, M. Manning, Z. Chen, M. Marquis, K.B. Averyt, M. Tignor, and H.L. Miller, Cambridge University Press, Cambridge, United Kingdom and New York, NY, USA, 2007.

Gard, E.E., M.J. Kleeman, D.S. Gross, L.S. Hughes, J.O. Allen, B.D. Morrical, D.P. Fergenson, T. Dienes, M.E. Galli, R.J. Johnson, G.R. Cass, and K.A. Prather (1998), Direct observation of heterogeneous chemistry in the atmosphere, *Science*, *279* (5354), 1184-1187.

Gaston, C.J., H. Furutani, S.A. Guazzotti, K.R. Coffee, T.S. Bates, P.K. Quinn, L.I. Aluwihare, B.G. Mitchell, and K.A. Prather (2011), Unique ocean-derived particles serve as a proxy for changes in ocean chemistry, *J. Geophys. Res.-[Atmos.], 116*, D18310, doi:10.1029/2010JD015289.

Gaston, C.J., K.A. Pratt, X.Y. Qin, and K.A. Prather (2010), Real-time detection and mixing state of methanesulfonate in single particles at an inland urban location during a phytoplankton bloom, *Environ. Sci. Tech., 44* (5), 1566-1572.

Guazzotti, S.A., K.R. Coffee, and K.A. Prather (2001), Continuous measurements of size-resolved particle chemistry during INDOEX-Intensive Field Phase 99, *J. Geophys. Res.-[Atmos.], 106* (D22), 28607-28627.

Hatton, A.D., and S.T. Wilson (2007), Particulate dimethylsulphoxide and dimethylsulphoniopropionate in phytoplankton cultures and Scottish coastal waters, *Aquat. Sci.*, *69* (3), 330-340.

Hobbs, P.V., T.J. Garrett, R.J. Ferek, S.R. Strader, D.A. Hegg, G.M. Frick, W.A. Hoppel, R.F. Gasparovic, L.M. Russell, D.W. Johnson, C.D. O'Dowd, P.A. Durkee, K.E. Nielsen, and G. Innis (2000), Emissions from ships with respect to their effects on clouds, *Journal of Atmospheric Sciences*, *57*, 2570-2590.

Hudson, J.G., T.J. Garrett, P.V. Hobbs, S.R. Strader, Y. Xie, and S.S. Yum (2000), Cloud condensation nuclei and ship tracks, *Journal of Atmospheric Sciences*, *57*, 2696-2706.

Jacobson, M.Z. (2000), A physically-based treatment of elemental carbon optics: Implications for global direct forcing of aerosols, *Geophys. Res. Lett.*, *27* (2), 217-220.

Keene, W.C., A.A.P. Pszenny, D.J. Jacob, R.A. Duce, J.N. Galloway, J.J. Schultz-Tokos, H. Sievering, and J.F. Boatman (1990), The geochemical cycling of reactive chlorine through the marine troposphere, *Glob. Biogeochem. Cy.*, *4* (4), 407-430.

Kercher, J.P., T.P. Riedel, and J.A. Thornton (2009), Chlorine activation by N_2O_5: simultaneous, in situ detection of $ClNO_2$ and N_2O_5 by chemical ionization mass spectrometry, *Atmos. Meas. Tech.*, *2* (1), 193-204.

Lack, D.A., J.J. Corbett, T. Onasch, B. Lerner, P. Massoli, P.K. Quinn, T.S. Bates, D.S. Covert, D. Coffman, B. Sierau, S. Herndon, J. Allan, T. Baynard, E. Lovejoy, A.R. Ravishankara, and E. Williams (2009), Particulate emissions from commercial shipping: Chemical, physical, and optical properties, *J. Geophys. Res.-[Atmos.]*, *114*, D00F04, doi:10.1029/2008JD011300.

Mentel, T.F., M. Sohn, and A. Wahner (1999), Nitrate effect in the heterogeneous hydrolysis of dinitrogen pentoxide on aqueous aerosols, *Phys. Chem. Chem. Phys.*, *1*, 5451-5457.

Moffet, R.C., Y. Desyaterik, R.J. Hopkins, A.V. Tivanski, M.K. Gilles, Y. Wang, V. Shutthanandan, L.T. Molina, R.G. Abraham, K.S. Johnson, V. Mugica, M.J. Molina, A. Laskin, and K.A. Prather (2008a), Characterization of aerosols containing Zn, Pb, and Cl from an industrial region of Mexico City, *Environ. Sci. Tech.*, *42* (19), 7091-7097.

Moffet, R.C., and K.A. Prather (2009), In-situ measurements of the mixing state and optical properties of soot with implications for radiative forcing estimates, *PNAS*, *106* (29), 11872-11877.

Moffet, R.C., X. Qin, T. Rebotier, H. Furutani, and K.A. Prather (2008b), Chemically segregated optical and microphysical properties of ambient aerosols measured in a single-particle mass spectrometer, *J. Geophys. Res.*, *113* (D12213), D12213, doi:10.1029/2007JD009393.

Mouri, H., K. Okada, and S. Takahashi (1995), Giant sulfur-dominant particles in remote marine boundary layer, *Geophys. Res. Lett.*, *22* (5), 595-598.

Neubauer, K.R., M.V. Johnston, and A.S. Wexler (1997), On-line analysis of aqueous aerosols by laser desorption ionization, *International Journal of Mass Spectrometry and Ion Processes*, *163* (1-2), 29-37.

Neubauer, K.R., M.V. Johnston, and A.S. Wexler (1998), Humidity effects on the mass spectra of single aerosol particles, *Atmos. Environ.*, *32* (14-15), 2521-2529.

O'Dowd, C.D., M.C. Facchini, F. Cavalli, D. Ceburnis, M. Mircea, S. Decesari, S. Fuzzi, Y.J. Yoon, and J.P. Putaud (2004), Biogenically driven organic contribution to marine aerosol, *Nature*, *431* (7009), 676-680.

Oppo, C., S. Bellandi, N.D. Innocenti, A.M. Stortini, G. Loglio, E. Schiavuta, and R. Cini (1999), Surfactant components of marine organic matter as agents for biogeochemical fractionation and pollutant transport via marine aerosols, *Mar. Chem.*, *63* (3-4), 235-253.

Orellana, M.V., T.W. Peterson, A.H. Diercks, S. Donohoe, P. Verdugo, and G. van den Engh (2007), Marine microgels: Optical and proteomic fingerprints, *Mar. Chem.*, *105*, 229-239.

Poschl, U. (2005), Atmospheric aerosols: Composition, transformation, climate and health effects, *Angewandte Chemie-International Edition*, *44* (46), 7520-7540.

Prange, A., I. Arzberger, C. Engemann, H. Modrow, O. Schumann, H.G. Truper, R. Steudel, C. Dahl, and J. Hormes (1999), In situ analysis of sulfur in the sulfur globules of phototrophic sulfur bacteria by X-ray absorption near edge spectroscopy, *Biochimica et Biophysica Acta*, *1428*, 446-454.

Pratt, K.A., C.H. Twohy, S.M. Murphy, R.C. Moffet, A.J. Heymsfield, C.J. Gaston, P.J. DeMott, P.R. Field, T.R. Henn, D.C. Rogers, M.K. Gilles, J.H. Seinfeld, and K.A. Prather (2010), Observation of playa salts as nuclei in orographic wave clouds, *J. Geophys. Res.-[Atmos.]*, *115*, D15301, doi:10.1029/2009JD013606.

Pyo, Y.J., M. Gierth, J.I. Schroeder, and M.H. Cho (2010), High-Affinity K(+) Transport in Arabidopsis: AtHAK5 and AKT1 Are Vital for Seedling Establishment and Postgermination Growth under Low-Potassium Conditions, *Plant Physiology*, *153* (2), 863-875.

Qin, X.Y., and K.A. Prather (2006), Impact of biomass emissions on particle chemistry during the California Regional Particulate Air Quality Study, *International Journal of Mass Spectrometry, 258* (1-3), 142-150.

Russell, L.M., K.J. Noone, R.J. Ferek, R.A. Pockalny, R.C. Flagan, and J.H. Seinfeld (2000), Combustion organic aerosol as cloud condensation nuclei in ship tracks, *American Meteorological Society*, 2591-2606.

Russell, L.M., J.H. Seinfeld, R.C. Flagan, R.J. Ferek, D.A. Hegg, P.V. Hobbs, W. Wobrock, A.I. Flossmann, C.D. O'Dowd, K.E. Nielsen, and P.A. Durkee (1999), Aerosol dynamics in ship tracks, *J. Geophys. Res.-[Atmos.]*, *104* (D24), 31077-31095.

Shindell, D.T., G. Faluvegi, D.M. Koch, G.A. Schmidt, N. Unger, and S.E. Bauer (2009), Improved attribution of climate forcing to emissions, *Science, 326* (5953), 716-718.

Silva, P.J., D.Y. Liu, C.A. Noble, and K.A. Prather (1999), Size and chemical characterization of individual particles resulting from biomass burning of local Southern California species, *Environ. Sci. Tech., 33* (18), 3068-3076.

Silva, P.J., and K.A. Prather (2000), Interpretation of mass spectra from organic compounds in aerosol time-of-flight mass spectrometry, *Anal. Chem.*, *72* (15), 3553-3562.

Slingo, A. (1990), Sensitivity of the Earth's radiation budget to changes in low clouds, *Nature, 343* (6253), 49-51.

Stevens, B., D. Lenschow, G. Vali, H. Gerber, A.R. Bandy, B. Blomquist, J.-L. Brenguier, C.S. Bretherton, F. Burnet, T. Campos, S. Chai, I. Faloona, D. Friesen, S. Haimov, K. Laursen, D.K. Lilly, S.M. Loehrer, S.P. Malinowski, B. Morley, M.D. Petters, D.C. Rogers, L.M. Russell, V. Savic-Jovcic, J.R. Snider, D. Straub, M.J. Szumowski, H. Takagi, D. Thornton, M. Tschudi, C. Twohy, M. Wetzel, and M.C. van Zanten (2003), Dynamics and chemistry of marine stratocumulus: DYCOMS-II, *American Meteorological Society*, 579-593.

Urbano, R., B. Palenik, C.J. Gaston, and K.A. Prather (2011), Detection and phylogenetic analysis of coastal bioaerosols using culture dependent and independent techniques, *Biogeosciences, 8*, 301-309.

Verdugo, P., A.L. Alldredge, F. Azam, D.L. Kirchman, U. Passow, and P.H. Santschi (2004), The oceanic gel phase: a bridge in the DOM-POM continuum, *Mar. Chem., 92* (1-4), 67-85.

Verdugo, P., M.V. Orellana, W.C. Chin, T.W. Peterson, G. van den Engh, R. Benner, and J.I. Hedges (2008), Marine biopolymer self-assembly: implications for carbon cycling in the ocean, *Faraday Discuss.*, *139*, 393-398.

Vogt, R., P.J. Crutzen, and R. Sander (1996), A mechanism for halogen release from sea-salt aerosol in the remote marine boundary layer, *Nature*, *383* (6598), 327-330.

Vogt, R., and B.J. Finlayson-Pitts (1994), Tropospheric HONO and reactions of oxides of nitrogen with NaCl, *Geophys. Res. Lett.*, *21* (21), 2291-2294.

Wahner, A., T.F. Mentel, M. Sohn, and J. Stier (1998), Heterogeneous reaction of N_2O_5 on sodium nitrate aerosol, *J. Geophys. Res.-[Atmos.]*, *103* (D23), 31103-31112.

Whiteaker, J.R., and K.A. Prather (2003), Hydroxymethanesulfonate as a tracer for fog processing of individual aerosol particles, *Atmos. Environ.*, *37* (8), 1033-1043.